Modulation thérapeutique de l'autophagie dans les lymphomes anaplasiques à grandes cellules ALK positif

Sylvie Giuriato

UNIVERSITÉ TOULOUSE III PAUL SABATIER

Université de Toulouse

HABILITATION À DIRIGER DES RECHERCHES

Modulation thérapeutique de l'autophagie dans les lymphomes anaplasiques à grandes cellules ALK positif

Présentée par le

Dr Sylvie GIURIATO

Ecole doctorale et spécialité :
Biologie Santé Biotechnologies, Cancérologie

Unité de recherche :
Centre de Recherches en Cancérologie de Toulouse – Inserm UMR 1037

Jury :
Pr Estelle Espinos, Présidente
Dr Patrick Auberger, Rapporteur
Dr Serge Roche, Rapporteur
Dr Stéphan Vagner, Rapporteur
Dr Stéphane Manenti, Examinateur

Soutenue le 24 mai 2016

REMERCIEMENTS

Je remercie les membres du jury : les Drs Patrick Auberger, Serge Roche, Stéphan Vagner, Stéphane Manenti et Estelle Espinos, pour avoir accepté de juger ce travail ainsi que pour la discussion, agréable, enrichissante, et parfois inattendue que nous avons eue.

Je remercie mes multiples encadrant(e)s de DEA, de thèse et de post-docs, pour les nombreux conseils qu'ils m'ont donnés, ainsi que pour leur intérêt constant pour ma carrière.

Je remercie tous les collègues et collaborateurs rencontrés dans les différents laboratoires et pays pour le partage scientifique, l'entre-aide, et l'amitié qui nous ont liés.

Je remercie l'ensemble des étudiants que j'ai eu le plaisir d'encadrer, et tout particulièrement Melle Julie Frentzel, ma première étudiante en thèse, qui a partagé avec moi le même enthousiasme à étudier l'autophagie dans les lymphomes anaplasiques à grandes cellules ALK positif.

Enfin, je dédie ce manuscrit d'HDR à mon beau-frère, Franck Raibaut.

TABLE DES MATIÈRES

TABLE DES ILLUSTRATIONS

Préambule

Ma formation de recherche s'est effectuée dans plusieurs laboratoires, en France et à l'étranger. J'ai tout d'abord réalisé ma thèse de 1996 à 1999, dans l'équipe dirigée par le Dr Bernard Payrastre, à l'ex-unité Inserm 326 dirigée par le Pr Chap. Il s'agissait d'étudier, dans les plaquettes sanguines humaines, le rôle des enzymes SHIP1 et SHIP2, deux inositol 5-phosphatases impliquées dans le métabolisme des phosphoinositides et notamment dans la biosynthèse du second messager lipidique PI(3,4)P_2. Je bénéficiais alors d'un financement européen Biomed 2, qui m'a également permis de poursuivre, pour un an, mes travaux sur SHIP2 dans le cadre d'un premier stage post-doctoral dans le laboratoire de notre plus proche collaborateur, le Dr Christophe Erneux, à l'IRIBHM de Bruxelles. Ce travail a mis au jour les propriétés anti-tumorales de la protéine SHIP2 lors de sa surexpression dans la lignée cellulaire K562. Mon intérêt croissant pour les mécanismes d'oncogenèse a alors motivé mon départ pour l'université de Stanford, en Californie, pour rejoindre le jeune laboratoire du Dr Dean Felsher qui s'intéressait, grâce au développement de différents modèles murins conditionnels de tumeurs réversibles, à la compréhension du phénomène d' « addiction oncogénique ». Durant ce stage post-doctoral de trois ans (2001-2004), j'ai mis en évidence le rôle clé de l'angiogenèse dans la survenue de rechutes tumorales après inactivation de l'oncogène MYC.

À mon retour en France, à Toulouse, dans l'équipe dirigée par le Pr Georges Delsol, j'ai proposé de développer, sur les bases de mon savoir-faire acquis aux Etats-Unis, des modèles cellulaires et murins conditionnels pour l'expression de l'oncogène ALK (pour Anaplastic Lymphoma Kinase), ceci afin de compléter la grande spécialisation de mon laboratoire d'accueil sur l'étude des lymphomes anaplasiques à grandes cellules (LAGC) ALK positifs. Ces différents modèles ont été et sont toujours utilisés pour de nombreux travaux de l'équipe, portant ainsi à huit le nombre de publications scientifiques se rapportant à ces modèles. L'ensemble de ces recherches et résultats ont permis mon recrutement à l'INSERM, en 2008, en tant que CR1.

Plus récemment, j'ai souhaité développer un nouvel axe de recherche, toujours sur les LAGC ALK positifs, et me suis focalisée sur l'autophagie, un processus intracellulaire d'autodigestion, dont l'importance en cancérologie allait croissant. Grâce aux financements de l'Agence Nationale pour la Recherche (ANR-Jeune Chercheur Jeune Chercheuse, 2012-2015) et des Ligues Régionales et Nationales contre le Cancer (2011-2016), j'ai initié ces recherches avec le recrutement de Melle Géraldine Mitou (post-doctorante) puis de Melle Julie Frentzel (doctorante dont la soutenance est prévue en octobre prochain). Ainsi, ces deux étudiantes ont travaillé de concert pour démontrer les propriétés cytoprotectrices de l'autophagie dans des cellules de LAGC soumises à une thérapie ciblant l'oncogène ALK.

Au cours de ces mêmes années (2012-2015), le réseau européen de recherche sur les maladies dépendantes de l'oncogène ALK (ERIA) a pu se structurer sous l'impulsion forte du Dr Suzanne Turner (Université de Cambridge). Cette structure m'a permis d'élargir mes connaissances sur ces pathologies, d'étoffer mon réseau de collaboration et aussi de recruter prochainement un étudiant (Mr Domenico Sorrentino) dans le cadre d'un programme Marie-Curie ITN « ALKATRAS » (Coordonnateur : Dr S. Turner). En continuité avec ma thématique actuelle, son sujet de thèse portera sur la modulation thérapeutique de l'autophagie dans les tumeurs ALK-positives. Nous envisageons, pour cela, de travailler ensemble, une année, dans le laboratoire « leader » sur le développement de vaccins anti-ALK : celui du Dr Roberto Chiarle au Children's Hospital de Boston, USA. En effet, ce projet de recherche, qui sera présenté en fin de manuscrit, associe nos compétences sur les tumeurs ALK-positives, l'autophagie et l'immunothérapie des cancers (par approche vaccinale) dans le but de proposer une meilleure prise en charge des patients.

Pour la rédaction de ce manuscrit d'habilitation à diriger les recherches, il m'est apparu difficile de développer tous les aspects cités ci-dessus de ma carrière, le risque étant de dresser un catalogue au détriment d'une homogénéité dans le propos. Par conséquent, j'ai préféré privilégier la cohérence thématique en me focalisant uniquement sur mes travaux sur les LAGC ALK positifs, depuis la création des modèles cellulaires et murins conditionnels, leurs caractérisations et leur utilisation pour étudier les mécanismes de lymphomagenèse (angiogenèse) et, plus récemment, sur mon orientation vers l'étude du rôle, de la régulation et de la modulation thérapeutique de l'autophagie dans ces lymphomes. Ce manuscrit comprend donc une rétrospective sur mes activités de recherche depuis douze ans, suivie d'une présentation de mes projets futurs.

DIPLÔME

RÉPUBLIQUE FRANÇAISE
Ministère de l'Éducation Nationale, de la Recherche et de la Technologie
ACADÉMIE DE TOULOUSE

UNIVERSITÉ PAUL SABATIER
TOULOUSE III

ATTESTATION
DOCTORAT DE L'UNIVERSITÉ PAUL SABATIER

Arrêté du 30 mars 1992

Le Secrétaire Général de l'Université Paul Sabatier de Toulouse, soussigné, certifie que :

M **ademoiselle GIURIATO SYLVIE**

Né(e) le 17 Octobre 72

à TOULOUSE

a présenté en soutenance, le 4 Octobre 99

devant ladite Université

[X] une thèse [ ] un ensemble de travaux

Intitulé :

ROLE ET REGULATION DES 5-PHOSPHATASES DE LA FAMILLE SHIP DANS LES PLAQUETTES SANGUINES HUMAINES

Après délibération, le jury a prononcé l'admission de :

M **ademoiselle GIURIATO SYLVIE**

au titre de **DOCTEUR DE L'UNIVERSITÉ PAUL SABATIER**

spécialité

BIOCHIMIE

mention TRES HONORABLE AVEC FELICITATIONS DU JURY

Fait à Toulouse, le 12/10/99

UNIVERSITE PAUL SABATIER TOULOUSE

Pour le Secrétaire Général
et par délégation :
L'Attaché Principal d'Administration Scolaire et Universitaire,
Chef de la Division de la Scolarité

Lina DOUARD

Il ne peut être délivré de duplicata de la présente attestation. Il appartient à l'intéressé d'en établir des copies qu'il fait certifier conformes à l'original.

LABORIE TOULOUSE BALMA 85002/124583

RAPPORT SUR LA SOUTENANCE DE THESE DE MADEMOISELLE Sylvie GIURIATO

****

Les travaux scientifiques ont été exposés de façon remarquable, claire, synthétique, avec à l'appui une excellente iconographie. La discussion avec le jury a révélé sa parfaite connaissance du sujet et une grande maturité.

Le jury a été unanime pour accorder les Félicitations sur la base de l'originalité du travail, déjà publié à un excellent niveau (J. Biol.Chem.), de la qualité du document écrit et de de l'excellente prestation de la candidate.

Fait à Toulouse, le 5 octobre 1999

H. CHAP

S. Levy-Toledano

B. Payrastre

C. Gauthier

G. TAUC

E. VIVIER

Université PAUL SABATIER III
Pour copie conforme
07 JAN. 2000
Scolarité

CURRICULUM VITÆ

Sylvie GIURIATO
CR1, INSERM
Date de naissance : 17 Octobre 1972, à Toulouse.
Situation de famille : Vie maritale, trois enfants.

Addresse professionnelle :

Centre de Recherches en Cancérologie de Toulouse (CRCT)
UMR1037 INSERM-UPS-ERL5294 CNRS
Equipe 7: Biologie des ARNs dans les cancers hématologiques
Oncopole de Toulouse, Entrée C, 2 avenue Hubert Curien, CS53717
31037 TOULOUSE Cedex 1 - FRANCE
Tél : 0582741667. Mail : sylvie.giuriato@inserm.fr

Parcours universitaire

-Doctorat ès Sciences de la Vie (soutenu le 04 Octobre 1999), Mention très honorable et félicitations du Jury, Université Paul Sabatier, Toulouse, 1996-1999.
-Ingénieur de l'Ecole Polytechnique Universitaire de Nice (ex. Magistère de Pharmacologie) option DEA de Pharmacologie et Biologie Cellulaires et Moléculaires, 1992-1996.
-Diplôme d'Etude Universitaire Générale " Sciences de la Vie et de la Terre ". Université de Nice Sophia Antipolis, 1990-1992.

Parcours professionnel et situation actuelle

-Depuis 2008: CR1 INSERM U.1037, Centre de Recherches en Cancérologie de Toulouse (CRCT).
-Post-doctorant, Université Paul Sabatier, Toulouse, 2004-2008.
-Post-doctorant, Université de Stanford, Californie, USA, 2001-2004.
-Post-doctorant, IRIBHM, Bruxelles, 1999-2001.

Sociétés savantes

- Membre du CFATG (Club Francophone de l'AuTophaGie)
- Membre ERIA (European Research Initiative on ALK-related malignancies)
- Membre du consortium ALKATRAS (Responsable Working Package Enseignement)
- Membre American Association for Cancer Research (AACR)

Reviewer pour

-Autophagy, Blood, Oncotarget, PloS One, Human Gene Therapy.

Expertises

- Agence nationale de la Recherche (ANR)
- Fonds national de la recherche scientifique (Belgique) (FNRS)
- Programme « Emergence » (Cancéropôle PACA)
- Swiss National Science Foundation (SNSF)

Organisation de congrès internationaux

-Co-organisation avec le Dr S. Manenti (CRCT, Toulouse) d'un symposium « Autophagie et Cancer » à Toulouse le 15 septembre 2014.
http://www.canceropole-gso.org/?p=calendrier&id=1136&mod=evenement_consulter/

-Co-organisation avec le Dr I. Vergne (IPBS, Toulouse) des « International Autophagy Conference » à Toulouse du 16 au 18 septembre 2014.
http://cfatg.org/international-autophagy-conferences/

Présentations orales (Sélections / Invitations)

2007 : Presqu'île de Gien, CHO meeting. *Reversible tumorigenesis upon ALK oncogene inactivation.*

2008 : Toulouse, IPBS, Pr P. Lutz's lab. *Reversible tumorigenesis upon ALK oncogene inactivation.*

2009 : Limoges, Cancéropôle GSO ; Club imaging *in vivo*. *Development of a murine model expressing the TPM3-ALK oncogene and the luciferase.*

2009 : Limoges, Cancéropôle GSO ; Hematology and Cancer Session. *Development of a conditional model for ALK-induced lymphomagenesis.*

2010 : Salzburg, 1st Meeting of the European ALCL Study Group (ERIA). *Development of a conditional model for ALK-induced lymphomagenesis.*

2011 : Chatenay-Malabry, INSERM U984, Pr P. Codogno's lab. *Angiogenesis and autophagy in ALK positive lymphoma.*

2011 : Paris, SFH meeting. *Angiogenesis and autophagy in ALK positive lymphoma.*

2013 : Heidelberg, 4th ERIA Meeting. *Autophagy : new therapeutic target in ALK positive lymphoma?*

2014 : Bordeaux, INSERM U916, Dr M. Mergny's lab. *Autophagy : new therapeutic target in ALK positive lymphoma?*

2015 : Paris, Gustave Roussy Institute, Pr L. Brugières's lab. *Autophagy: new therapeutic target in ALK-positive Anaplastic Large Cell Lymphoma?*

2015 : Bern, Institute of Pathology, Dr M. Tschan's lab. *miRNA-mediated control of autophagy in Crizotinib-treated ALK-positive Anaplastic Large Cell Lymphoma.*

2015 : Varèse, 5th CAYA-NHL symposium. *Targeting autophagy enhances the anti-tumoral action of Crizotinib in ALK-positive anaplastic large cell lymphoma.*

ANIMATION DES ACTIVITÉS DE RECHERCHE ET D'ENSEIGNEMENT

Encadrements d'étudiants

1998-99 : Co-encadrement (50%) avec le Dr B. Payrastre d'un étudiant en DEA, Mr S. Bodin.

2002-04 : Encadrement (100%) et formation à la recherche en laboratoire d'un médecin pédiatre-oncologiste, le Dr Karen Rabin, Université de Stanford.

2005 : Encadrement (100%) de Melle Louise Weidler, étudiante en 2ème année de BTS de biochimie.

2004-05 : Encadrement (100%) de Melle Emile Bousquet, étudiante en Master 1ère année.

2005-06 : Encadrement (100%) de Melle Anissa Edir, étudiante en Master 1ère année.

2007-08 : Encadrement (100%) de Melle Marianne Foisseau, étudiante ingénieur en biotechnologie, École supérieure de biotechnologie Strasbourg (ESBS).

2007-08 : Encadrement (80%) de Melle Emile Dejean, étudiante en Master 2nde année.

2010 : Encadrement (100%) de Melle Sarah Bettini pour un stage estival pré-master 1ère année.

2011 : Encadrement (100%) de Melle Hafida Sellou pour un stage estival pré-master 1ère année.

2012-2015 : Encadrement (100%) de Melle Géraldine Mitou, étudiante en post-doctorat, sur le rôle de l'autophagie dans les lymphomes ALK positifs.

2013 : Encadrement (100%) en CDD (6 mois) de Melle Julie Frentzel, ingénieur de l'école supérieure de biotechnologie Strasbourg (ESBS), sur le rôle de l'autophagie dans les lymphomes ALK positifs.

2013-2016 : Doctorat (90%) (co-direction avec le Dr F. Meggetto) de Melle Julie Frentzel. Rôle et régulation de l'autophagie dans les lymphomes anaplasiques à grandes cellules ALK positifs. Soutenance prévue en octobre 2016.

2015-2016 : Co-encadrement (30%) avec Melle Julie Frentzel de Mr Romain Duclerq, étudiant en Master 1ère année.

A venir, 2016-2019 : Doctorat (100% souhaité) de Mr Domenico Sorrentino. Modulation thérapeutique de l'autophagie dans les tumeurs dépendantes de l'oncogène ALK.

Activités d'enseignement

Avril 2013 : Enseignement en U.E. MASTER 1/Mention PCIP, Méthodologie en anatomopathologie et en histologie. Applications aux modèles animaux. Toulouse, 2h, titre : « Un exemple de souris transgénique pour l'étude du cancer: la souris conditionnelle ALK ».

2013-2016 : Enseignement en U.E. MASTER 2, Microenvironnement tumoral, métastases et angiogenèse. Toulouse, 2h, titre : « Autophagie et Cancer ».

2014-2016 : Enseignement en U.E. MASTER 2, BBRT - SCMV, Parcours Immunologie-Cancérologie. Nantes, 2h, titre : « Autophagie et Cancer ».

Participation à des comités de thèse

Membre de trois comités de thèse (Université Paul Sabatier, Toulouse) :

2014-2015 : Melle Aïcha Bah.

2015-2016 : Mr Abdulrahman Mujalli.

2015-2016 : Melle Hripsimé Nahapetyan.

Responsabilités collectives

2011-2014 : Comité d'animation scientifique du CRCT : organisation de séminaires mensuels intra-CRCT, de conférences invitées, de demi-journées ou journées thématiques, des « retraites scientifiques » du CRCT.

2011-2012 : Comité scientifique de préparation à l'aménagement du CREFRE : Centre Régional d'Exploration Fonctionnelle et de Ressources Expérimentales, sur le site du CRCT : Centre de Recherches en Cancérologie de Toulouse.

Financements et Prix

2012-2015 : Agence nationale de la Recherche, Programme Jeune Chercheur (ANR-JCJC), 317000 euros. Projet « ALK-phagie ». Autophagie : nouvelle cible thérapeutique des tumeurs ALK positives.

2014-2015 : Fondation ARC, 25000 euros. Projet portant sur la « Régulation post transcriptionnelle de l'autophagie: nouvelle approche thérapeutique dans les lymphomes ALK positifs ».

2011-2012 : La Ligue régionale contre le cancer, 25000 euros. Projet portant sur l'« Autophagie : nouvelle cible thérapeutique des tumeurs ALK positives. »

2006-2008 : Financement post-doctoral par la Fondation de France.

2006 : 1er prix : « Thérapie ciblée des cancers ». Journée Cancéropôle, Toulouse.

2004-2006 : Financement post-doctoral par l'Association pour la Recherche sur le Cancer.

2002-2004 : Financement post-doctoral par la « Lymphoma Research Foundation ».

Collaborations scientifiques

2004-2010 : Collaboration avec le Dr D. Felsher (Université de Stanford, Californie, USA), pour le développement de modèles murins conditionnels de lymphomes ALK positifs et sur leur utilisation pour l'étude des mécanismes d'addiction oncogénique.

2010-2011 : Collaboration avec le Dr J. Cavaillé (CNRS UMR 5099, Toulouse) dans le cadre de l'étude sur la régulation du VEGF par le micro-ARN 16.

2010-2011 : Collaboration avec le Dr H. Prats (Inserm U1037, Toulouse) dans le cadre de l'étude sur l'angiogenèse dans les tumeurs ALK-positives.

2010-2011 : Collaboration avec le Dr P. Lebouteiller (Inserm U1043, Toulouse) pour valider *in vivo* les propriétés anti-angiogéniques et anti-tumorales de l'anticorps anti-CD160.

2010-2011 : Collaboration avec le Dr F. Gaits (Inserm U1037, Toulouse) pour valider *in vivo* les propriétés anti-tumorales d'un inhibiteur de la petite protéine G Rac.

2011-présent : Collaboration avec le Dr P. Codogno (Hôpital Necker Enfants Malades, Inserm U1151, Paris) pour l'étude de l'autophagie dans les lymphomes ALK positifs.

2014-présent : Collaboration avec le Dr M. Tschan (Institut de Pathologie, Université de Bern, Suisse) pour l'étude de la régulation de l'autophagie par les microARNs dans les lymphomes ALK positifs.

2015-présent : Collaboration avec le Dr R. Chiarle (Harvard Medical School, Boston Children's Hospital) pour étudier le rôle de l'autophagie dans les thérapies ciblées et les vaccins anti-tumoraux ciblant les tumeurs dépendantes de l'oncogène ALK (lymphome et cancer du poumon).

Expert-consultant

Reviewer pour

-Autophagy, Blood, Oncotarget, PloS One, Human Gene Therapy.

Expertises

- Agence nationale de la Recherche (ANR, France)
- Fonds national de la recherche scientifique (FNRS, Belgique)
- Programme « Emergence » (Cancéropôle PACA, France)
- Swiss National Science Foundation (SNSF, Suisse)

Sociétés savantes

- Membre du CFATG (Club Francophone de l'AuTophaGie)
- Membre ERIA (European Research Initiative on ALK-related malignancies)
- Membre du consortium ALKATRAS (Responsable du « Working Package » Enseignement)
- Membre American Association for Cancer Research (AACR)

PRODUCTION SCIENTIFIQUE

Bibliométrie

Données personnelles disponibles sur :

ResearcherID http://www.researcherid.com/rid/A-9113-2010
Google Scholar https://goo.gl/OpouUm

Liste des publications scientifiques

-Articles:

1. Mitou G, Frentzel J, Desquesnes A, Le Gonidec S, AlSaati T, Beau I, Lamant L, Meggetto F, Espinos E, Codogno P, Brousset P, **Giuriato S**. Targeting autophagy enhances the anti-tumoral action of crizotinib in ALK-positive anaplastic large cell lymphoma. **Oncotarget. 2015** Oct 6;6(30):30149-64.

2. C.Hoareau-Aveilla, T.Valentin, C.Daugrois, C.Quelen, G.Mitou, S.Quentin, J.Jia, S.Spicuglia, P.Ferrier, M.Ceccon, **S.Giuriato**, C.Gambacorti-Passerini, P.Brousset, L.Lamant and F.Meggetto. *Reversal of microRNA-150 silencing disadvantages Crizotinib-resistant NPM-ALK-positive cell growth.* **J Clin Invest. 2015** Sep;125(9):3505-18.

3. Dejean E, Foisseau M, Lagarrigue F, Lamant L, Prade N, Marfak A, Delsol G, **Giuriato S**, Gaits-Iacovoni F, Meggetto F. *ALK+ALCLs induce cutaneous, HMGB-1-dependent IL-8/CXCL8 production by keratinocytes through NF-κB activation.* **Blood. 2012,** May 17;119(20):4698-707.

4. E. Dejean, M.H Renalier, M. Foisseau, X. Agirre, N. Joseph, G.R. de Paiva, T. Al Saati, J. Soulier, C. Desjobert, L. Lamant, F. Prósper, DW. Felsher, J. Cavaillé, H. Prats, G. Delsol, **S. Giuriato*** and F. Meggetto*. *Hypoxia-microRNA-16 down-regulation induces VEGF expression in Anaplastic lymphoma kinase (ALK)-positive anaplastic large-cell lymphomas.* **Leukeamia, 2011**, Dec;25(12):1882-90. *Co-senior auteurs.

5. Colomba, A., **Giuriato, S.**, Dejean, E., Thornber, K., Delsol, G., Tronchère, H., Meggetto, F., Payrastre, B. and Gaits-Iacovoni, F. Inhibition of Rac controls NPM-ALK-dependent lymphoma development and dissemination. **Blood Cancer Journal**, **2011**, June 3; 1: 1-7.

6. Chabot S, Jabrane-Ferrat N, Bigot K, Tabiasco J, Provost A, Golzio M, Noman MZ, Giustiniani J, Bellard E, Brayer S, Aguerre-Girr M, Meggetto F, **Giuriato S**, Malecaze F, Galiacy S, Jaïs JP, Chose O, Kadouche J, Chouaib S, Teissié J, Abitbol M, Bensussan A, Le Bouteiller P. A novel antiangiogenic and vascular normalization therapy targeted against human CD160 receptor**. J Exp Med. 2011**, May 9;208(5):973-86.

7. **Giuriato, S**., Foisseau, M., Dejean, E., Felsher, D.W., Al Saati, T., Demur, C., Ragab, A., Kruczynski, A., Schiff, C., Delsol, G., Meggetto, F. Conditional TPM3-ALK and NPM-ALK transgenic mice develop reversible ALK-positive early B cell lymphoma/leukemia. **Blood**, **2010**. 115(20): p. 4061-70.

Those mouse models were cited in Science-Business eXchange : *Mouse models of anaplastic lymphoma kinase (ALK)-induced B cell leukemia and lymphoma.* 2010, 3 (18) p16; doi:10.1038/scibx.2010.571 Distillery: Techniques-Disease models.
http://www.nature.com/scibx/journal/v3/n18/full/scibx.2010.571.html

8. Tran, P.T., Fan, A.C., Bendapudi, P.K., Koh, S., Komatsubara, K., Chen, J., Horng, G., Bellovin, D.I., **Giuriato, S.**, Wang, C.S., Whitsett, J.A., and Felsher, D.W. *Combined Inactivation of MYC and K-Ras oncogenes reverses tumorigenesis in lung adenocarcinomas and lymphomas.* **PLoS ONE, 2008**, 3, e2125.

9. **Giuriato, S.**, Faumont, N., Bousquet, E., Foisseau, M., Bibonne A., Moreau, M., Al Saati, T., Felsher, D.W., Delsol, G. and Meggetto, F. *Development of a conditional bioluminescent transplant model for TPM3-ALK- induced tumorigenesis as a tool to validate ALK-dependent cancer targeted therapy.* **Cancer Biol Ther, 2007**, 6, pp 1318-23.

10. Lamant, L., De Reynies, A., Duplantier, MM., Rickman, D.S., Sabourdy, F., **Giuriato, S.**, Brugieres, L., Gaulard, P., Espinos, E. and Delsol, G. *Gene expression profiling of systemic anaplastic large cell lymphoma reveals differences depending on ALK status and two distinct morphological ALK+ subtypes.* **Blood**, **2007**, 109, pp2156-64.

11. **Giuriato, S.**, Ryeom S., Fan, A.C., Bachireddy, P., Lynch, R.C., Rioth, M.J., Riggelen, J., Kopelman, A.M., Passegué, E., Tang, F., Folkman, J. and Felsher, D.W. *Sustained regression of tumors upon MYC inactivation requires p53 or thrombospondin-1 to reverse the angiogenic switch.* **PNAS**, **2006,** 103, pp 16266-71.

12. Passegué, E., Wagers, A.J., **Giuriato S.**, Anderson, W.C. and Weissman, I.L. *Global analysis of proliferation and cell cycle gene expression in the regulation of hematopoietic stem and progenitor cell fates.* **J. Exp. Med., 2005,** 202, pp 1599-611.

13. Sander, S., Bullinger, L., Karlsson, A., **Giuriato, S.**, Hernandez-Boussard, T., Felsher, D.W and Pollack, J.R. *Comparative genomic hybridization on mouse cDNA microarrays and its application to a murine lymphoma model.* **Oncogene, 2005,** 24, pp 6101-7.

14. **Giuriato, S.**, Pesesse, X., Bodin, S., Sasaki, T., Viala, C., Marion, E., Penninger, J., Schurmans, S., Erneux, C. and Payrastre, B. *SH2 domain containing inositol 5-phosphatases 1 and 2 in blood platelets: interaction and respective role in the control of phosphatidylinositol 3,4,5-trisphosphate level.* **Biochem. J., 2003,** 376, pp 199-207.

15. Karlsson, A., **Giuriato, S.**, Tang, F., Fung-Weier, J., Levan, G. and Felsher, D.W. *Genomically complex lymphomas undergo sustained tumor regression upon MYC inactivation unless they acquirenovel chromosomal translocations*. **Blood**, **2003,** 101, pp2797-803.

16. Niebuhr, K., **Giuriato, S**., Pedron, T., Philpott, D.J., Gaits, F., Sable, J., Sheetz, M.P., Parsot, C., Sansonetti, P.J. and Payrastre B. *Conversion of PtdIns(4,5)P_2 into PtdIns(5)P by the Shigella flexneri effector IpgD reorganizes host cell morphology.* **EMBO J., 2002,** 21, pp5069-78.

17. **Giuriato, S.**, Blero, D., Robaye, B., Bryuns, C., Payrastre, B. and Erneux, C. *SHIP2 overexpression strongly reduces the proliferation rate of K562 erythroleukemia cell line*. **Biochem. Biophys. Res. Commun., 2002,** 296, pp 106-10.

18. Bodin, S., **Giuriato, S**., Ragab, J., Humbel, B.M., Viala, C., Vieu, C., Chap, H. and Payrastre, B. *Production of phosphatidylinositol(3,4,5)trisphosphate and phosphatidic acid in platelet rafts : Evidence for a critical role of cholesterol-enriched domains in human platelet activation.* **Biochemistry, 2001,** 40, pp 15290-9.

19. Pesesse, X., Dewaste, V., DeSmedt, F., Laffargue, M., **Giuriato, S.**, Payrastre, B. and Erneux, C. *The src homology 2 domain containing inositol 5-phosphatase SHIP2 is recruited to the epidermal growth factor (EGF) receptor and dephosphorylates phosphatidylinositol 3,4,5-trisphosphate in EGF-stimulated COS-7 cells.* **J. Biol. Chem.**, **2001,** 276, pp 28348-55.

20. **Giuriato, S.**, Bodin, S., Erneux, C., Woscholski, R., Plantavid, M., Chap, H. and Payrastre, B. *Pp60 c-src associates with the Src-homology-2-containing inositol 5-phosphatase SHIP1 and is involved in its tyrosine phosphorylation downstream □IIb□3 integrin in human platelets.* **Biochem. J, 2000,** 348, pp 107-12.

21. Schmid-Alliana, A., Menou, L., Manie, S., Schmid-Automarchi, H., Millet, M.A., **Giuriato, S**., Ferrua, B. and Rossi, B. *Microtubule integrity regulates src-like and extracellular signal-regulated kinase activities in human pro-monocytic cells. Importance for interleukin-1 production.* **J. Biol. Chem**., **1998,** 273, pp 3394-400.

22. **Giuriato, S**., Payrastre, B., Drayer, L.A., Plantavid, M., Woscholski, R., Parker, P., Erneux, C. and Chap, H. *Tyrosine phosphorylation and relocation of SHIP are integrin-mediated in thrombin-stimulated human blood platelets.* **J. Biol. Chem.**, **1997,** 272, pp 26857-63.

-Liste des revues:

1. **Giuriato S**, Turner SD. *Twenty years of modelling NPM-ALK-induced lymphomagenesis.* **Front Biosci**, **2015**, Jun 1;7:236-47.

2. Espinos, E., Duplantier, M.M., **Giuriato, S**., Allouche, M., Sabourdy, F., Delsol, G. and Lamant, L. *Anaplastic lymphoma kinase et lymphomes : aspects physiopathologiques et cliniques.* **Hématologie, 2005,** 11, 265-76.

3. **Giuriato, S.**, Rabin, K., Fan, A. C., Shachaf, C. M., and Felsher, D. W. *Conditional animal models: a strategy to define when oncogenes will be effective targets to treat cancer*. **Semin Cancer Biol, 2004,** 14, pp 3-11.

4. **Giuriato, S.** and Felsher, D.W. *How cancers escape their oncogene habit.* **Cell Cycle**, **2003,** 2, pp 329-32.

5. Missy, K., **Giuriato, S.**, Bodin, S., Plantavid, M. and Payrastre B. *L'intégrine □IIb□3 dans les plaquettes sanguines: un rôle dans la transduction des signaux.* **Médecine/sciences**, **2001,** 17, pp155-61.

6. Payrastre B., Missy, K., **Giuriato, S.**, Bodin, S., Plantavid, M. and Gratacap, M.P. *Phosphoinositides: key players in cell signalling, in time and space.* **Cellular signalling**, **2001,** 13, pp 377-87.

7. **Giuriato, S**., Payrastre, B., Gratacap, M.P., Chap, H. and Erneux, C. *Des ITIM du lymphocyte aux intégrines de la plaquette : SHIP, une protéine à la croisée des chemins ?* **Médecine/sciences**, **1998,** 14, pp 698-703.

- Chapitres de livre:

1. Delsol, G., Espinos, E., **Giuriato, S.** , Brousset, P., Lamant, L. and Meggetto, F. **(2010)** *Anaplastic large cell lymphoma* **The Lymphoid Neoplasms**, Ian T. Magrath (Third Edition), Hodder Arnold edition, pp655-64.

2. Erneux, C., **Giuriato, S.** and Pesesse, X. **(2002)** *The inositol polyphosphate 5-phosphatases.* **Encyclopedia of Molecular Medicine**, John Wiley & Sons, pp1755-8.

Licences/Offres de technologie

1. Giuriato, S. and Meggetto, F. *Conditionnal bioluminescent TPM3-ALK cell line*. Technology offer, Migratech database, Inserm Transfert.
https://migratech.inserm-transfert.fr/srv/tech/2/0vue2.asp?n=512

2. Giuriato, S. and Meggetto, F. *Conditionnal TPM3-ALK transgenic mice*. Technology offer, Migratech database, Inserm Transfert.
https://migratech.inserm-transfert.fr/srv/tech/2/0vue2.asp?n=467

3. Felsher, D.W., Giuriato, S. and Karlsson A.E. (2004) *MYC inactivation causes tumor regression in absence of novel chromosomal translocations.* Stanford Office of Technology Licensing, Reference S04-165.
http://stanfordtech.stanford.edu/4DCGI/docket?docket=04-165.

SYNTHÈSE DES TRAVAUX DE RECHERCHE

Au cours de ces douze dernières années, je me suis attachée à développer des modèles cellulaires et murins conditionnels pour l'expression des oncogènes NPM-ALK et TPM3-ALK, dans le but de mimer la pathologie humaine des lymphomes anaplasiques à grandes cellules (LAGC) ALK positif, de mieux comprendre la biologie de ces tumeurs et de tester de nouvelles thérapies.

Après une présentation générale et non exhaustive de la pathologie humaine, de l'oncogène ALK et des thérapies actuelles (chapitre A), cette synthèse de mes travaux de recherche sera divisée en trois grandes parties : (i) le développement et la caractérisation des modèles murins conditionnels de lymphome ALK+ (chapitre B); (ii) le rôle de l'angiogenèse dans le développement tumoral (chapitre C); (iii) le rôle de l'autophagie dans la réponse thérapeutique (chapitre D).

Enfin, en continuité avec ces derniers travaux de recherche, mes projets portant sur une modulation thérapeutique de l'autophagie pour améliorer le traitement des LAGC ALK positifs seront exposés (Projets de recherche).

A/ Présentation générale des lymphomes anaplasiques à grandes cellules (LAGC), de l'oncogène ALK et des thérapies actuelles

A-1/ Qu'est-ce qu'un lymphome ?

Un lymphome est un cancer du système lymphatique. Il en existe deux grandes familles : les lymphomes hodgkiniens (LH), qui représentent environ 20% de l'ensemble des lymphomes et les lymphomes non hodgkiniens (LNH), qui comptent pour la majorité des lymphomes (environ 80%). Ils se différencient essentiellement par la présence (LH) ou l'absence (LNH) de cellules caractéristiques sur le plan morphologique, appelées cellules de Reed-Sternberg, décrites pour la première fois en 1832 par le Dr Thomas Hodgkin.

Les lymphocytes B ou T cancéreux, qui constituent un lymphome, peuvent s'accumuler dans les ganglions lymphatiques (lymphomes ganglionnaires) et/ou dans le tissu lymphoïde que l'on trouve dans la plupart des organes (lymphomes extra-ganglionnaires). Les LH sont de phénotype B ; les LNH peuvent être de phénotype B ou T. Le LH est une maladie le plus souvent localisée, alors que le LNH est plus disséminé. Les LH sont de meilleur pronostic que les LNH.

Le diagnostic d'un lymphome est établi par la conjonction de nombreux paramètres : examens cliniques (ganglions volumineux, fièvre, perte de poids) ; imagerie médicale (scanner) pour visualiser et mesurer la taille des ganglions lymphatiques touchés par la maladie ainsi que pour identifier les organes atteints ; examens sanguins et biopsies d'un ou plusieurs ganglions situés au niveau de la zone présumée de la tumeur. Cette biopsie est

essentielle pour confirmer le diagnostic d'un lymphome, pour connaître son type précis (sur la base de différents marqueurs) et pour orienter son traitement.

A-2/ Présentation des LAGC ALK positifs

Les LAGC ALK positifs sont des lymphomes non hodgkiniens, de type T périphériques, qui représentent 10 à 15% des lymphomes de l'enfant et l'adolescent (pic à 10 ans), et 3% des lymphomes de l'adulte (pic après 60 ans). [1–3] Ce lymphome se développe principalement au niveau des ganglions lymphatiques (infiltration fréquente des ganglions intra-abdominaux ou médiastinaux au diagnostic), et s'accompagne (dans 40 à 68% des cas) d'atteintes extra-ganglionnaires au niveau des tissus mous, des os, de la peau, des poumons, du foie [4], et plus rarement, du cerveau. [5]

Sur le plan génétique, les LAGC ALK positifs se caractérisent par des translocations chromosomiques, impliquant invariablement le gène ALK (Anaplastic Lymphoma Kinase) en position 2p23 et un gène codant pour un partenaire de translocation variable. Dès les années 1980, la translocation t(2,5)(p23 ;q35) a été associée aux LAGC [6] et c'est le Dr Steve Morris, en 1994, qui identifie les deux gènes réarrangés : le gène codant pour la nucléophosmine (NPM) et le gène codant pour un nouveau récepteur à activité tyrosine kinase, qu'il nomme ALK pour Anaplastic Lymphoma Kinase.[7] Cette translocation conduit à la biosynthèse de la protéine de fusion oncogénique NPM-ALK. Depuis, d'autres réarrangements géniques ont été décrits, portant à dix le nombre total connu à ce jour d'oncogène de fusion ALK retrouvé dans les LAGC ALK positifs. [8] Notons que les formes NPM-ALK et TPM3-ALK (cloné en 1999 par le Pr L. Lamant au laboratoire [9]) constituent les deux formes majoritaires retrouvées chez les patients (Tableau 1).

Sur le plan immunophénotypique, ces lymphomes se caractérisent invariablement par une positivité pour les marqueurs ALK et CD30. Notons que la découverte des oncogènes de fusion ALK a été déterminante pour le diagnostic des LAGC ALK positifs et pour leur classification comme entité clinicopathologique à part entière.[10] Les LAGC ALK+ sont classiquement de phénotype T ou nul car ils expriment fortement (>75% des cas) des marqueurs cytotoxiques T (granzyme B, perforine) mais faiblement (< 30% des cas) des marqueurs T (Tableau 2) [11–13]. Notamment, les gènes du T-cell receptor (TCR) sont classiquement réarrangés mais ne conduisent pas à la production d'un TCR fonctionnel.[14–17]

Partenaire de fusion	Translocation	Fréquence (%)	Références
NPM1	t(2;5)(p23;q35)	75-80	*Morris et al., 1994* [7]
ALO17	t(2;17)(p23;q23)	<1	*Cools et al., 2002* [18]
TFG	t(2;3)(p23;q21)	2	*Hernandez et al., 1999* [19]
MSN	t(2;X)(p32;q11-12)	<1	*Tort et al., 2001* [20]
TPM3	t(1;2)(q25;p23)	12-18	*Lamant et al., 1999* [9]
TMP4	t(2;19)(p23;p13)	<1	*Meech et al., 2001* [21]
ATIC	inv(2)(p23;q35)	2	*Colleoni et al., 2000* [22]
MYH9	t(2;22)(p23;q11.2)	<1	*Lamant et al., 2003* [23]
CLTC1	t(2;17)(p23;q23)	2	*Touriol et al., 2000* [24]
TRAF1	t(2;9) (p23.2;q33.2)	<1	*Feldman et al., 2013* [25]

Tableau 1 : Translocations chromosomiques et partenaires de fusion retrouvés dans les LAGC ALK positif. NPM1, Nucleophosmin ; ALO17, ALK lymphoma oligomerization partner on chromosome 17 ; TFG, TRK-fused gene; MSN, Moesin; TPM3, Tropomyosin 3 ; TPM4, Tropomyosin 4 ; ATIC, 5-aminoimidazole-4-carboxamide ribonucleotide transformylase/IMP cyclohydrolase; MYH9, Non-muscle myosin heavy chain; CLTC1, Clathrin heavy chain-like 1 ; TRAF1, TNF receptor-associated factor 1. *Adapté d'après Roskoski et al, Pharmaco Research, 2013.*[8]

Immunophénotype	LAGC ALK$^+$ (%)
CD30	100
ALK	100
CD2	22
CD3	11,5
CD4	46
CD8	8
CD5	36
TIA1	54
Granzyme B, Perforine	>75
CD45	48
CD56	4-7
EMA	60-70
PAX5	0

Tableau 2 : Caractéristiques immunophénotypiques des LAGC ALK positif.
D'après la thèse du Dr Camille Daugrois, « Lymphomes anaplasiques à grandes cellules ALK positif : signature prognostique des rechutes précoces », soutenue le 19 octobre 2015, Université Paul Sabatier Toulouse III.

Sur le plan cytologique, ces lymphomes se caractérisent par la présence de cellules de grande taille, à cytoplasme abondant avec un noyau en forme de fer à cheval, appelées « hallmark cells ». Elles sont toujours observées dans les LAGC ALK positif, mais présentes en quantité variable selon les cinq sous-types morphologiques (forme commune, variant à petites cellules, variant lymphohistiocytaire, forme mixte, et variant « Hodgkin-like ») décrits plus en détail et illustrés dans d'excellentes revues.[13,26]

Enfin, l'origine cellulaire des LAGC ALK positifs n'est pas encore clairement définie. Deux hypothèses sont actuellement débattues : la plus ancienne propose qu'un lymphocyte T mature périphérique soit la cellule d'origine; la seconde, plus récente, propose une cellule souche hématopiétique ou un progéniteur thymique précoce.

*En faveur du premier cas de figure, il a été montré que la sur-expression de NPM-ALK dans des lymphocytes T primaires CD4+ matures permettait de récapituler fidèlement *in vitro* le phénotype des LAGC ALK positifs (larges cellules, expression de CD30, ALK signaling).[27] De plus, une étude *in vivo* montre que la sur-expression de NPM-ALK dans des lymphocytes T matures, en l'absence de compétition polyclonale, permet le développement de lymphomes T périphériques ALK positif.[28]

*En faveur de la seconde hypothèse, il a été récemment démontré dans une étude visant à identifier la cellule souche cancéreuse des LAGC ALK positif que celle-ci présentait un profil d'expression génique caractéristique d'un progéniteur thymique précoce.[29] En continuité avec ce travail, les auteurs ont récemment proposé une origine thymique des LAGC ALK positif, nécessitant une expression transitoire du TCR (T-Cell Receptor) pour « émigrer » du thymus et permettre le développement tumoral en périphérie.[17] Appuyant cette hypothèse, le transcrit NPM-ALK a été retrouvé dans quelques échantillons de sang de cordon d'une population saine, suggérant que la translocation t(2 ;5) ait lieu dans des cellules hématopoïétiques primitives.[30] Enfin, notons que l'incidence de la maladie (qui se développe principalement chez les enfants et les jeunes adultes) conforte cette hypothèse, du fait de l'involution thymique à l'âge adulte.[16]

Ainsi, le modèle proposé par le Dr Suzanne Turner (Figure 1), qui semble réconcilier ces deux hypothèses, est le suivant : les cellules souches hématopoiétiques ou thymiques précoces NPM-ALK positive pourraient réarranger leur TCR (de façon aberrante, du fait de l'expression de l'oncogène ALK) [13,17]. L'expression du TCR serait ensuite réprimée [14,15], ce qui permettrait la survie et la migration de ces cellules vers la périphérie.[17] En accord avec ce modèle, un événement secondaire, tel une réaction inflammatoire causée par une piqure d'insecte [31], pourrait permettre le développement tumoral en périphérie de ces lymphomes « T ou nul » cytotoxiques NPM-ALK positifs.[16]

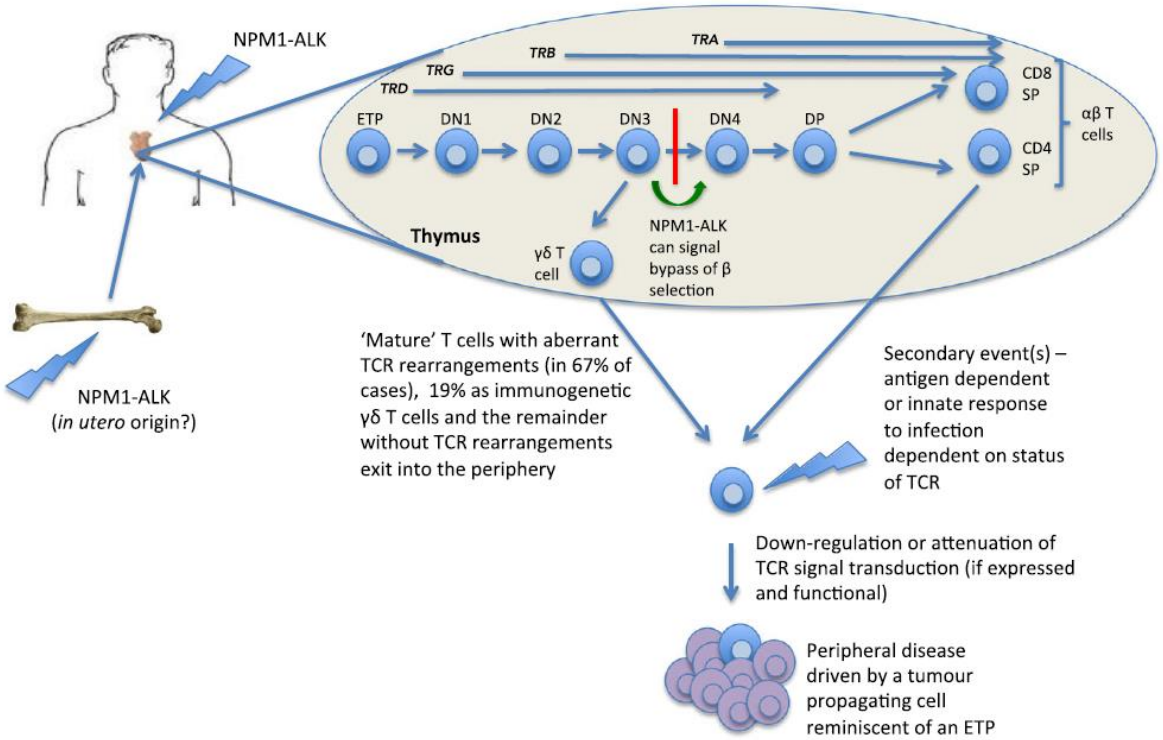

Figure 1: Origine cellulaire primitive des LAGC ALK positif et développement tumoral en périphérie. Dans ce modèle, l'expression de NPM-ALK dans une cellule souche hématopoiétique ou dans un progéniteur thymique précoce permettrait la survie cellulaire malgré un réarrangement aberrant du TCR. Un événement secondaire, tel une réponse inflammatoire à une piqûre d'insecte, pourrait alors conduire à l'expansion clonale et au développement tumoral en périphérie. TCR, T cell receptor ; ETP, Early thymic progenitor. *D'après Turner et al., Br J Haematol., 2016.*[16]

A-3/ Oncogène de fusion ALK et transduction du signal oncogénique

À ce jour, dix translocations chromosomiques ont été retrouvées dans les LAGC ALK positifs (Tableau 1). Elles associent la partie 5' du gène partenaire à la partie 3' du gène ALK, et codent ainsi pour une protéine de fusion constituée du domaine N-terminal du partenaire (porteur en général d'un domaine d'oligomérisation) et du domaine C-terminal de ALK, porteur du domaine à activité tyrosine kinase (Figure 2).

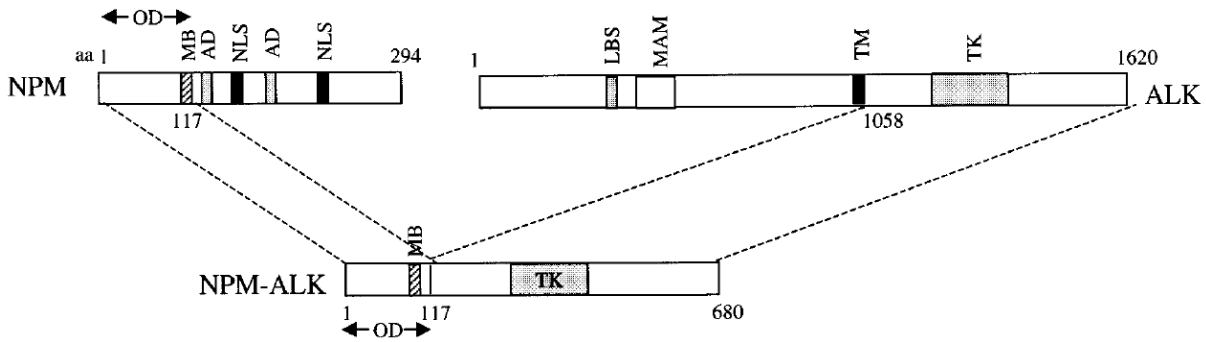

Figure 2 : Représentation schématique de la protéine de fusion NPM-ALK, issue de la translocation chromosomique t(2;5)(p23;q35). *D'après Duyster et al., Oncogene, 2001.*[32]

Le partenaire de translocation va ainsi permettre l'homodimérisation de la protéine de fusion, entraînant sa trans-phosphorylation sur résidu tyrosine et l'activation constitutive de la kinase ALK, ce qui lui confère ses propriétés oncogéniques. L'oncogène de fusion ALK, de par son activité catalytique, est capable de phosphoryler et d'activer en aval de nombreuses protéines de la signalisation impliquées dans la prolifération, la survie et la migration cellulaires. Parmi les grandes voies transductrices du signal oncogénique, sont activées par l'oncogène ALK les voies JAK/STAT3 [33,34] ; PI3Kinase/Akt/mTor [35,36]; Ras/MAPKinase [37,38] ; PLCγ [39] et Src [40]. D'excellentes revues décrivent ces voies en détail.[41–43]

A-4/ Thérapies actuelles des patients atteints de LAGC ALK positifs

Une des particularités des LAGC ALK positifs est leur grande chimio-sensibilité, lors des traitements de première ligne ou lors du traitement des rechutes, qui surviennent classiquement dans 25 à 35% des cas, quelles que soient les combinaisons de drogues utilisées et les durées de traitement.[44]

*Traitement de première ligne :
Il n'existe pas à ce jour de consensus pour le traitement des LAGC. Le traitement de première ligne, chez les adultes (>60ans), est une polychimiothérapie à base d'anthracycline comme la combinaison CHOP. Celle-ci associe quatre drogues : *le Cyclophosphamide (agent alkylant entraînant des dommages à l'ADN) ; *l'Hydroxydaunorubicine (aussi appelée doxorubicine ou adriamycine) (agent intercalant et anti-prolifératif par inhibition de la topoisomérase II) ; *l'Oncovin (vincristine) (inhibiteur de la duplication cellulaire par interaction avec la tubuline) ; *la Prednisone (agent anti-inflammatoire et lympholytique). Chez les enfants, le traitement est plus intense mais sur une plus courte durée. L'essai clinique ALCL99 a été déterminant pour démontrer que l'addition de Méthotrexate (agent de la classe des anti-métabolites) était essentielle pour éviter des rechutes méningées et que l'addition de Vinblastine en cours de chimiothérapie et en consolidation (pour 1 an) permettait de retarder l'apparition des rechutes. [45,46] À l'issue de ces chimiothérapies, il a été observé que 25 à 35% des patients (tout âge confondu) rechutent ou progressent sous traitement. [44,47] Une étude très récente suggère que l'addition prolongée (sur 2 ans) de Vinblastine pourrait réduire le nombre de rechute après l'arrêt du traitement.[48]

*Traitement des rechutes :
-pour les patients adultes chimiosensibles en rechute, une chimiothérapie à haute dose suivie d'une autogreffe des cellules souches est largement utilisée. Ceci permet de repousser encore la maladie avec 50 à 60% de chance de survie pour les patients ainsi traités.[16]
-pour les patients adultes réfractaires à la chimiothérapie ou en rechute, mais inéligibles pour une greffe des cellules souches, le pronostic reste très mauvais, ce qui ouvre la porte pour de nouvelles thérapies (voir ci-dessous l'utilisation de Crizotinib).

-pour les enfants et jeunes adultes, le traitement des rechutes se fait par chimiothérapie à haute dose suivie d'une autogreffe (ou allogreffe) ou par perfusion hebdomadaire de vinblastine. L'utilisation du Crizotinib chez des patients jeunes a également été décrite récemment (voir ci-dessous).

*Thérapies ciblant l'oncogène ALK:
Les protocoles thérapeutiques chez l'enfant ou l'adulte atteint de LAGC (notamment les patients réfractaires ou en rechute après chimiothérapie) sont sur le point de changer, notamment avec le développement de thérapies ciblant directement l'oncogène ALK.

Le Crizotinib (PF-02341066, Xalkori™) est un inhibiteur à double spécificité, ciblant les kinases mesenchymal-epithelial transition factor (c-MET) et ALK, développé par Pfizer (Figure 3 et Tableau 3). Il s'agit d'une aminopyridine, qui en se logeant dans la poche nucléotidique de la kinase ALK, bloque la fixation d'adenosine triphosphate (ATP).[49] Ainsi, l'autophosphorylation de la kinase ne se fait pas, ce qui la rend inactive. Ce sont les travaux de Christensen et al. qui ont démontré l'action inhibitrice du Crizotinib dans des lignées de LAGC ALK positif, en bloquant la phosphorylation de ALK et l'activation des voies de signalisation en aval, induisant ainsi un arrêt du cycle cellulaire et la mort par apoptose. L'utilisation de modèles précliniques (xénogreffes murines de lignée de Karpas-299 de LAGC ALK positif) a également validé l'efficacité *in vivo* du Crizotinib, qui induit la régression tumorale complète quand administré oralement à 100mg/kg/jour.[50]

La première utilisation du Crizotinib pour deux patients adultes atteints de LAGC ALK positif, en rechute après traitement chimiothérapeutique, a été décrite en 2011 par l'équipe du Pr Carlo Gambacorti-Passerini.[51] Cette étude a ensuite été étendue à un total de neuf patients, ce qui a permis, pour sept d'entre eux, d'atteindre une réponse complète après traitement, toujours observée après plus de 40 mois.[52] Pour les enfants et jeunes adultes, le Crizotinib a été utilisé chez huit patients en rechute ou réfractaires à la chimiothérapie de première ligne. Ceci a permis d'atteindre pour sept d'entre eux, une réponse complète.[53]

Diverses mutations de la kinase ALK, conférant une résistance au Crizotinib, ont été retrouvées à la fois chez deux patients adultes, inclus dans l'étude du Pr Gambacorti-Passerini et dans des lignées cellulaires de LAGC maintenues en présence de doses croissantes de Crizotinib.[52,54] Le développement d'inhibiteurs de l'oncogène ALK de nouvelles générations (Figure 3 et Tableau 3) a donc été entrepris pour proposer une alternative thérapeutique face à ces résistances.[55,56]

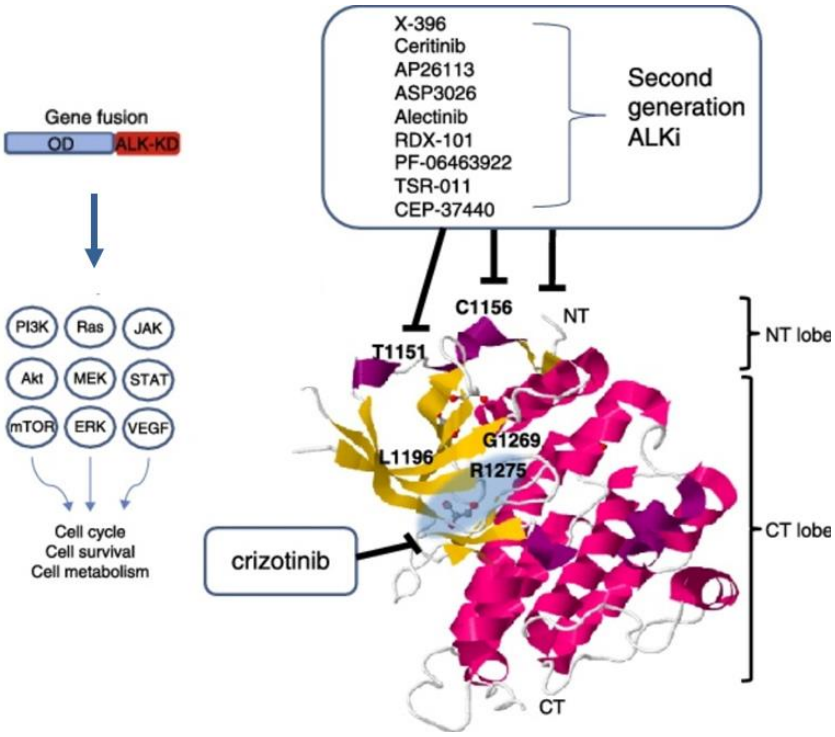

Figure 3: Inhibiteurs de la tyrosine kinase ALK. Dix inhibiteurs sont actuellement en cours d'essai clinique. Ils bloquent le site de fixation à l'ATP (oval bleu). Certaines résistances au Crizotinib, déjà décrites, peuvent être contournées par des inhibiteurs de seconde génération. *Adapté de Crescenzo et al., Curr Opin Pharmacol, 2015.*[55]

Drug	General chemical structure	Chemical formula	IC50
Crizotinib/PF-02341066 (Pfizer)	Aminopyridine	$C_{21}H_{22}Cl_2FN_5O$	ALK: 24 nM c-Met: 12 nM ROS1: 11 nM
X-396 (Xcovery)	6-Aminopyridazine	$C_{25}H_{25}Cl_2FN_6O_3$	ALK: <0.4 nM MET:0.74 nM
Ceritinib/LDK378 (Zykadia, Novartis)	2,4-Diaminopyridine	$C_{28}H_{36}ClN_5O_3S$	ALK: 0.2 nM IGF1R: >8 nM InsR: >7 nM
AP26113 (Ariad Pharmaceutical)	2,4-Diaminopyridine	$C_{26}H_{34}ClN_6O_2P$	ALK: 0.62 nM ROS1:1.9 nM EGFR: 15 nM
ASP3026 (Astellas pharma)	2,4-Diaminopyridine	$C_{29}H_{40}N_8O_3S$	ALK: 3.5 nM
Alectinib/RO5424802/CH5424802 (Chugai Pharmaceutical)	Tetracyclic ketone	$C_{30}H_{34}N_4O_2$	ALK: 1.9 nM
Entrectinib/RXDX-101/NMS-E628 (Neviano)	Aza-diaza indazole	$C_{31}H_{34}F_2N_6O_2$	ALK: 12 nM TrKA: 1 nM TrkB: 2 nM TrkC: 5 nM ROS1: 7 nM
PF-06463922 (Pfizer)	Macrocyclic 2-aminopyridine	$C_{25}H_{30}N_6O_2$	ALK: <0.07 nM ROS1: <0.02 nM
TSR-011 (Tesaro)	Structure undisclosed	NA	ALK: 0.7 nM TrKA: 0.5 nM TrkB: 1.5 nM TrkC: 2.4 nM
CEP-37440 (Teva)	2,4-Diaminopyridine	$C_{30}H_{38}ClN_7O_3$	ALK: 3.5 nM FAK: 2.3 nM

Tableau 3 : Caractéristiques principales des inhibiteurs de ALK.
D'après Crescenzo et al., Curr Opin Pharmacol, 2015.[55]

Notons également que les thérapies futures s'orientent vers des combinaisons thérapeutiques, par exemple une association d'inhibiteur tyrosine kinase (ITK) ciblant ALK avec les chimiothérapies décrites précédemment, ou bien l'utilisation d'un ITK ciblant ALK avec l'inhibition une voie oncogénique « de relais », impliquée dans la survie des cellules tumorales [44]. C'est dans ce contexte que s'inscrivent mes travaux sur le rôle de l'angiogenèse [57] et de l'autophagie [58] dans les LAGC ALK positif.

Ainsi, en 2004, date à laquelle je débutais dans le domaine des lymphomes anaplasiques à grandes cellules ALK positif, très peu de modèles murins avaient été développés, seules les grandes voies de signalisation activées par l'oncogène ALK avaient été décrites et aucun inhibiteur ciblant ALK n'était disponible. Ma contribution scientifique a été de démontrer, grâce au développement de modèles murins conditionnels de lymphomes ALK positif, que ceux-ci présentent une addiction pour leur oncogène de fusion (chapitre B); que l'angiogenèse, et notamment le VEGF (régulé en partie par le microARN 16), participe au développement tumoral (chapitre C) et représente donc une cible thérapeutique potentielle; et enfin que l'autophagie, activée sous traitement Crizotinib, peut être manipulée pour améliorer la thérapie (chapitre D).

B/ Développement et caractérisation de modèles murins conditionnels de lymphome ALK positif. Démonstration de l'addiction de ces lymphomes pour l'oncogène ALK (2004-2008 ; Inserm U563, Dir : Pr G. Delsol).

B-1/Introduction

J'ai rejoint l'équipe dirigée par le Pr Georges Delsol en 2004. Mon projet post-doctoral était de développer, sur les bases de mon expérience acquise aux Etats-Unis (2001-2004)[59–62], des modèles cellulaires et murins conditionnels pour l'expression de l'oncogène ALK (Anaplastic Lymphoma Kinase), ceci afin de compléter la grande spécialisation de mon laboratoire d'accueil sur l'étude des lymphomes anaplasiques à grandes cellules (LAGC) ALK positif. Cet objectif était visé à l'époque par de nombreux autres groupes de recherche car de tels modèles étaient très attendus pour une meilleure compréhension, sur le plan fondamental, de la pathologie et pour disposer de modèles précliniques pour l'évaluation de nouvelles thérapies anti-ALK. En 2004, seules deux publications rapportaient le développement de modèles transgéniques de lymphomes NPM-ALK positif. Il s'agissait (i) des travaux du Dr Suzanne Turner, dont la stratégie a été d'utiliser le promoteur « pan-hematopoiétique » *vav*, pour permettre à l'oncogène NPM-ALK de « choisir », en quelque sorte, sa lignée préférentielle de lymphomagenèse. Le phénotype observé a été le développement de lymphomes B et de plasmacytomes [63,64]; (ii) des travaux du Dr

Roberto Chiarle, dont la stratégie a été d'utiliser le promoteur CD4 pour diriger l'expression de NPM-ALK dans les lymphocytes T. Deux fondateurs ont été obtenus (N1 et N16) développant respectivement un lymphome B de type plasmacytome et un lymphome T thymique.[65]

Aucun de ces modèles ne permettant l'expression réversible de l'oncogène ALK, j'ai proposé d'utiliser le système d'expression régulée par la tétracycline (système Tet Off) pour développer des modèles murins conditionnels pour l'expression des oncogènes NPM-ALK et TPM3-ALK (ce dernier oncogène ayant été cloné dans mon laboratoire d'accueil [9]), afin de permettre non seulement l'étude du développement tumoral mais aussi de la régression après inactivation de l'oncogène.

B-2/ Résultats

B-2-1) Le système tétracycline :

Le système tétracycline permet de contrôler, temporellement, l'expression de gènes. [66,67] Il repose sur l'interaction, conditionnée par la tétracycline, du facteur de transcription tTA (pour *tetracycline-dependent transactivating protein*) avec son promoteur (Tet-O pour *tetracycline response element)*, en aval duquel le transgène d'intérêt a été préalablement inséré. En l'absence de doxycycline (analogue plus stable de la tétracycline), la protéine tTA se fixe au promoteur Tet-O et induit l'expression du transgène. L'addition de doxycycline induit un changement conformationnel de la protéine tTA et stoppe l'expression génique. Ce système permet de contrôler le moment précis ainsi que la durée d'induction du transgène. Cette propriété unique d'expression réversible a été largement utilisée en cancérologie et a mis en évidence le phénomène d' « addiction oncogénique ». J'ai souligné l'intérêt du système d'expression régulée par la tétracycline en répertoriant, dans deux revues successives et complémentaires, les premiers modèles animaux de tumeurs conditionnelles et en précisant les mécanismes connus et/ou proposés de régression et de rechute tumorale.[59,60]

B-2-2) Lignées cellulaires conditionnelles pour l'expression des oncogènes NPM-ALK et TPM3-ALK et modèles de transplantation en souris nude:

Les oncogènes NPM-ALK et TPM3-ALK ont été clonés dans le vecteur d'expression bidirectionnel régulé par la tétracycline et codant pour la luciférase. Les constructions ont été validées *in vitro* par transfection stable dans des fibroblastes embryonnaires murins (cellules MEFs Tet OFF). La transplantation sous-cutanée des clones stables sélectionnés dans des souris *nude* induit la formation de tumeurs fibroblastiques ALK-positive, réversibles par addition de doxycycline (Figure 4).

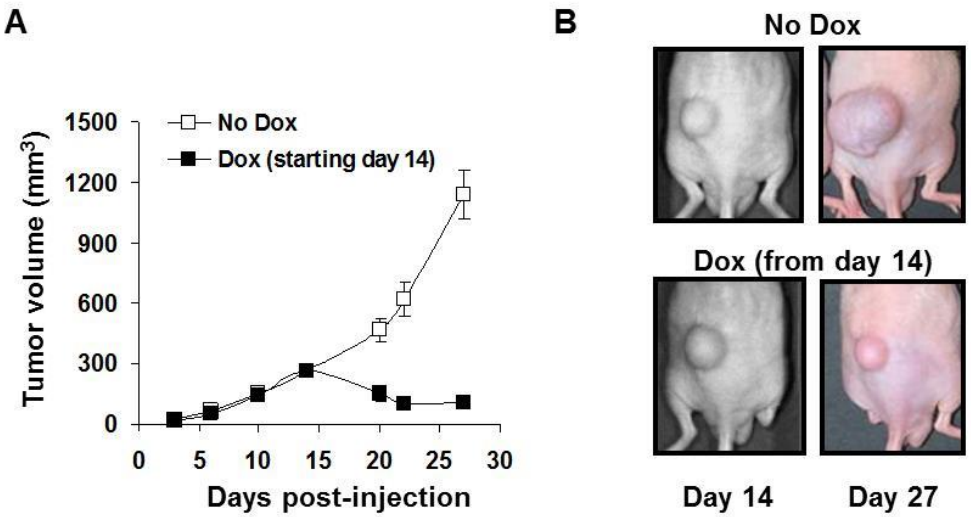

Figure 4: Réversibilité des tumeurs fibroblastiques TPM3-ALK positive par inactivation de l'oncogène (traitement à la doxycycline). A) Des cellules MEFs stables pour l'expression deTPM3-ALK ont été injectées en sous-cutanée dans des souris *nude*. Le traitement à la doxycycline (100μg/ml dans l'eau de boisson des animaux et une injection hebdomadaire intrapéritonéale (100μl d'une solution à 100μg/ml)), initié 14 jours après inoculation, induit la régression tumorale. Le volume tumoral a été calculé à partir de mesures réalisées au pied à coulisse. B) Photographies aux jours 14 et 27 de la progression des tumeurs sous-cutanées de souris non traitées (No Dox) ou traitées à la doxycycline (Dox), comme indiqué au point A.

Du fait de l'expression concomitante de l'oncogène ALK et de la luciférase, le développement tumoral peut être suivi par imagerie de bioluminescence. Cette propriété est particulièrement utile pour tester l'efficacité d'inhibiteurs de l'oncogène ALK. Pour preuve de principe, des souris *nude* ayant développé des tumeurs sous-cutanées ALK-positive ont été traitées avec de l'herbimycine A (inhibiteur général de tyrosine kinases, car le Crizotinib n'était pas encore commercialisé), déjà décrit *in vitro* comme inhibant la tyrosine kinase ALK.[68] Dans ce cas, le développement tumoral est inhibé et le signal bioluminescent associé à la tumeur est fortement diminué (Figure 5).

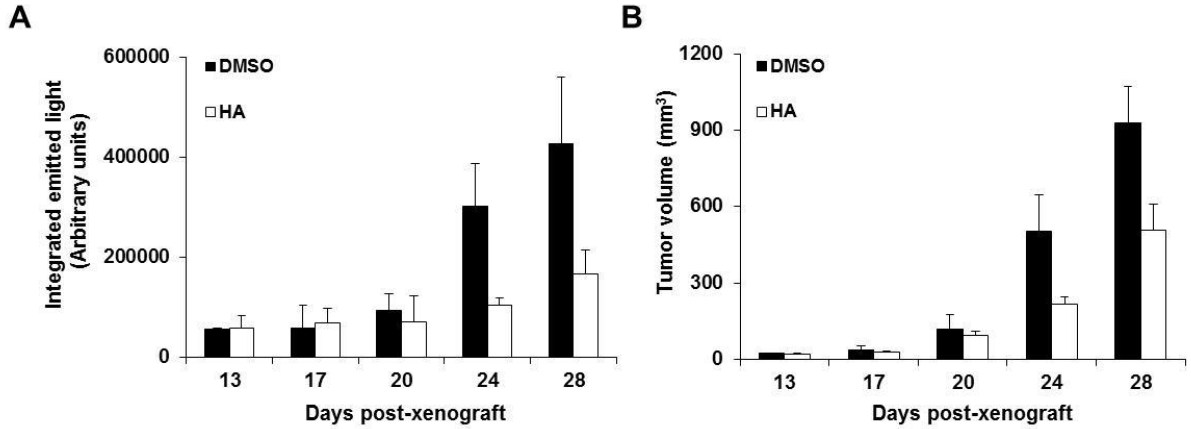

Figure 5: Le traitement à l'Herbimycin A (inhibiteur général de tyrosine kinase) réduit la croissance des tumeurs fibroblastiques TPM3-ALK positive. Des cellules MEFs stables pour l'expression de TPM3-ALK ont été injectées en sous-cutanée dans des souris *nude*. Le traitement à l'Herbimycin A (HA) (3 injections hebdomadaires intrapéritonéales (20μg /150μl) pendant 1 mois, initiées le lendemain des inoculations) ralentit le développement tumoral, comme visualisé par imagerie de bioluminescence (panel A) ou mesuré au pied à coulisse (panel B).

Ces travaux ont démontré que ce modèle de transplantation dans des souris *nude* de fibroblastes conditionnels pour l'expression de l'oncogène ALK et de la luciférase peut être utilisé comme outil pour valider des thérapies ciblant l'oncogène ALK.[69] Les cellules MEF NPM-ALK et MEF TPM3-ALK, ainsi que le modèle de transplantation dans la souris *nude*, ont fait l'objet d'une offre de technologie déposée à Inserm-Transfert.

B-2-3) Souris transgéniques conditionnelles pour l'expression de NPM-ALK et de TPM3-ALK :

L'obtention de ces modèles transgéniques conditionnels a nécessité le croisement de deux types de souris : des souris permettant le ciblage d'expression de ces oncogènes dans la lignée lymphoïde (Souris EμSRα-tTA) et des souris transgéniques pour NPM-ALK ou TPM3-ALK (Figure 6A). Les souris EμSRα-tTA m'ont été données par le Dr D. Felsher [70], chez qui j'avais effectué un stage post-doctoral antérieur à mon retour à Toulouse. Ce promoteur/enhancer EμSRα ayant déjà été décrit comme permettant l'expression génique dans un progéniteur lymphoïde précoce, je l'ai utilisé dans le but de diriger l'expression de l'oncogène ALK dans la lignée lymphoïde T, comme cela avait été décrit antérieurement pour de nombreux autres oncogènes : N-Ras [71], pim-1 [72], L-myc [73], c-myc [70], Tel-Jak2 [74] et Tax [75].

J'ai donc coordonné la décongélation des embryons au Centre de Distribution, Typage et Archivage animal d'Orléans (CDTA-CNRS) et la réimplantation de cette lignée au service de transgenèse de l'animalerie de l'IFR30 Toulouse. Les souris transgéniques NPM-ALK ou TPM3-ALK ont été produites au service de transgenèse de notre institut à partir des vecteurs d'expression bidirectionnelle (oncogène ALK et luciférase), régulés par la tétracycline, construits et validés, *in vitro* et *in vivo*, comme indiqué dans le paragraphe précédent.

Macroscopiquement, les souris double transgéniques conditionnelles présentent, suite à l'expression des oncogènes NPM-ALK et TPM3-ALK, une lymphadénopathie généralisée associée à une splénomégalie (Figure 6C-D). Des études en immunohistochimie et cytométrie de flux ont permis d'établir que les souris développent une leucémie et un lymphome B ALK positifs (Figure 6E) qui, rapidement (4 semaines) conduisent au décès des souris (Figure 6F). Ces deux hémopathies sont constituées de larges cellules de phénotype pro-B et pré-B précoce. Parallèlement, nous avons noté une expression inattendue de l'oncogène ALK dans les kératinocytes, à l'origine de lésions cutanées de type kératoacanthomes (Figure 6B-C). Ce résultat est à rapprocher de ceux décrits par Kwon et al. en 2005, qui ont observé un phénotype cutané (hyperkératose et alopécie) avec un fort infiltrat de lymphocytes T CD4 positif activés, ainsi qu'une lymphadénopathie et splénomégalie dans un modèle murin conditionnel pour l'expression de la protéine Tax (facteur de transactivation essentiel du virus HTLV-1), sous le contrôle du promoteur/enhancer EμSRα [75]. Il est donc très probable qu'une fuite du promoteur EμSRα dans les kératinocytes soit responsable de ces lésions cutanées.

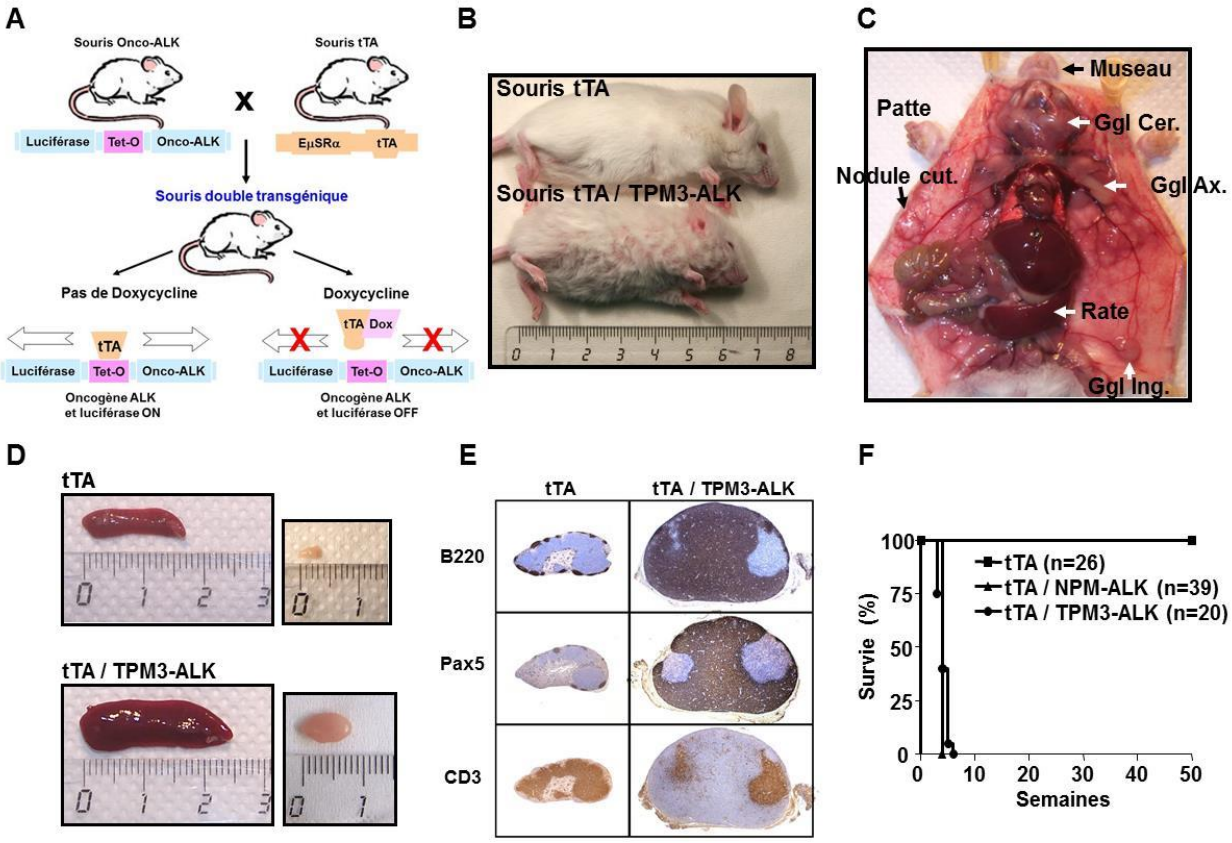

Figure 6: Analyse des modèles murins de lymphome ALK positif. A) Représentation schématique des croisements murins permettant l'obtention de souris double transgéniques conditionnelles pour l'expression de l'oncogène ALK (NPM-ALK ou TPM3-ALK) dans la lignée lymphoïde. En absence de doxycycline, le facteur de transactivation tTA permet l'expression de l'oncogène ALK et de la luciférase. En présence de doxycycline, ces expressions sont éteintes. B) Photographies comparatives d'une souris tTA et d'une souris double transgénique tTA/TPM3-ALK, montrant le défaut de croissance et le phénotype cutané anormal des souris tTA/TPM3-ALK. C) Nécropsie d'une souris tTA/TPM3-ALK montrant l'hypertrophie des ganglions lymphatiques (Cervicaux, Axillaires, Inguinaux) et de la rate ainsi que les lésions cutanées (museau, pattes et nodules cutanés). D) Photographies comparatives de la taille de la rate et des ganglions lymphatiques axillaires. E) Comparaison des marquages immunohistochimiques sur coupes sériées de ganglions prélevés sur des souris tTA ou tTA/TPM3-ALK, montrant le phénotype lymphoïde B (B220+, Pax5+) des cellules tumorales. Les zones négatives correspondent à des lymphocytes T résiduels (CD3+). F) Courbes de survie (Kaplan-Meier) des souris tTA, tTA/NPM-ALK et tTA/TPM3-ALK.

Un des résultats majeurs de notre étude a été de démontrer que les deux pathologies lymphoïdes et cutanées de notre modèle murin sont entièrement dépendantes de l'oncogène ALK, puisqu'elles régressent, suite à l'arrêt de son expression par la doxycycline (Figure 7B, D, F, H et J), ou suite à son inactivation fonctionnelle par un inhibiteur spécifique de la phosphorylation de ALK (Crizotinib), et ce, même à un stade très avancé de la maladie. Les tumeurs ALK positives présentent donc une addiction pour cet oncogène.

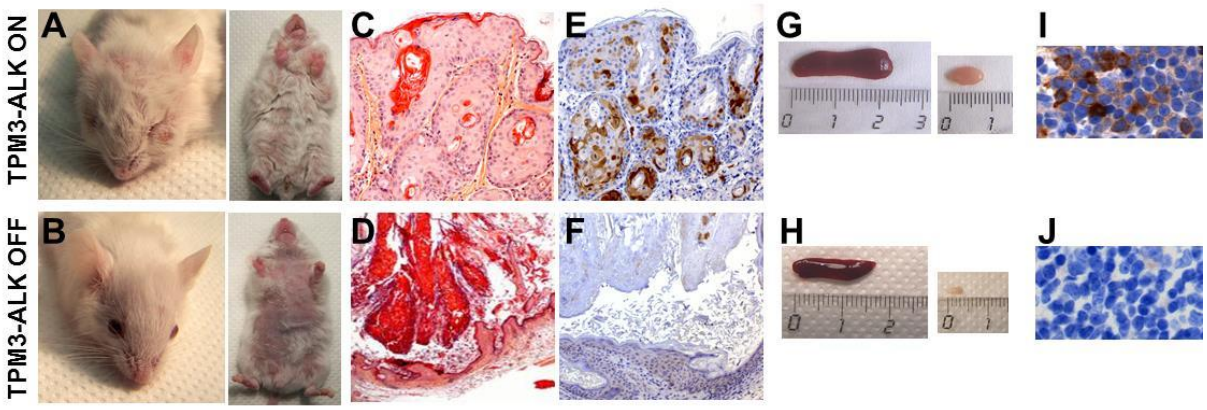

Figure 7: Réversibilité des pathologies cutanées et lymphoïdes après inactivation de l'oncogène ALK. Des souris double transgéniques, âgées de trois semaines et démontrant les mêmes signes extérieurs de maladie (kératoacanthome, défaut de croissance, large abdomen et inactivité) ont été soit non traitées (A, C, E, G, I), soit traitées 10 jours à la doxycycline (100µg/ml) (eau de boisson et une injection intrapéritoneale (100µl)) (B, D, F, H, J). Les photographies et analyses immunohistochimiques ont été réalisées à l'issue de ce traitement. Les souris traitées montrent une disparition des lésions cutanées (*B, D versus A, C*), le retour à une taille normale des organes lymphoïdes secondaires (H versus G), l'absence d'expression de ALK dans les kératinocytes (F versus E) et les ganglions (J versus I).

B.3/ Conclusion

Nos travaux montrent que l'expression de l'oncogène ALK sous la dépendance d'un promoteur/enhancer décrit pour être actif dans les progéniteurs lymphoïdes (EµSRα) conduit au développement de lymphome ALK positif de phénotype B. Ainsi, la prévalence d'expression dans la lignée lymphoïde B (par rapport à la lignée T) est retrouvée dans nos modèles murins ce qui souligne la difficulté, commune à de nombreux groupes [64,76], à développer un modèle animal mimant fidèlement la pathologie humaine (phénotype T ou nul). Ainsi, comme discuté dans la revue que je signe avec le Dr Suzanne Turner [76] (Cf. pages 109-122), trois problématiques majeures ont été constatées de par l'analyse de l'ensemble des modèles murins développés à ce jour dans le but de reproduire des LAGC ALK positif: (i) le choix du promoteur (et donc le ciblage cellulaire) s'est avéré particulièrement difficile en regard de la méconnaissance, dans l'ontogénie T, de la cellule cancéreuse initiatrice des LAGC ALK positif. Dans ce contexte, une avancée considérable résulte des travaux récents du Dr Suzanne Turner, comme expliqué précédemment dans le paragraphe A-2 (pages 34-35); (ii) l'expression ectopique de l'oncogène NPM-ALK est initiée à partir du site aléatoire d'intégration du transgène et il est probable que le niveau d'expression de l'oncogène NPM-ALK dans les modèles murins (chimériques et transgéniques) puisse avoir un impact sur le phénotype tumoral.[64,77,78] ; (iii) la transgenèse additive laisse intacte les deux allèles de chacun des partenaires de translocation (homozygotie des gènes NPM et ALK). Notons qu'aujourd'hui des solutions d'avenir existent, grâce notamment aux systèmes TALENs et CRISPR/Cas9, qui ont déjà été utilisés respectivement pour créer *de novo*, exactement au locus attendu, la translocation NPM-ALK dans deux lignées cellulaires (Jurkat

et RPE-1) [79], et pour développer très récemment un modèle murin de cancer du poumon EML4-ALK positif.[80]

En ce qui concerne les modèles murins transgéniques conditionnels de lymphome ALK positif, développés durant mon stage post-doctoral à Toulouse, ils ont donné la preuve de concept *in vivo* que l'inactivation ciblée de l'oncogène ALK permettait la régression tumorale.[81] Ainsi, cette démonstration de l'addiction des lymphomes pour l'oncogène ALK a été en parfait accord avec le développement concomitant de thérapies ciblées. Ces modèles sont également des « outils » de premier choix pour étudier les mécanismes moléculaires associés au développement des pathologies tumorales dépendantes de l'oncogène ALK, comme abordé dans le chapitre C suivant.

C/ Rôle de l'angiogenèse et régulation du VEGF dans les LAGC ALK positif (2008-2011 ; Inserm U563, Dir : Pr G. Delsol / Inserm U1037, Dir : Pr P. Brousset)

Les propriétés oncogéniques des protéines de fusion NPM-ALK et TPM3-ALK reposent sur leur activité tyrosine kinase incontrôlée. Les signaux initiés par l'oncogène ALK ont été extensivement étudiés ces dernières années. Ainsi, de nombreuses cascades de signalisation, mises en évidence essentiellement dans des lignées humaines de lymphome anaplasique ALK positif et confirmées dans différents modèles murins, participent à la transformation cellulaire, en augmentant la prolifération, la survie et la motilité cellulaires. De façon très schématique, les signaux médiés par l'oncogène ALK impliquent l'activation d'une série d'acteurs et de voies de signalisation clés incluant JAK/STAT3, PI3K/Akt/mTor, RAS/ERK, PLCγ et Src.

Dans ce contexte, et au vu de la forte vascularisation des souris transgéniques conditionnelles NPM-ALK et TPM3-ALK, j'ai émis l'hypothèse que l'angiogenèse pouvait participer au développement tumoral. Je me suis donc intéressée très tôt au VEGF et à sa régulation dans les LAGC ALK positif.

C-1/ Introduction

L'importance de l'angiogenèse dans le développement des tumeurs solides a été proposée, pour la première fois, par le Pr J. Folkman en 1971 [82]. L'implication de l'angiogenèse dans les cancers hématopoïétiques a été étudiée plus tardivement. Au commencement de notre étude, seuls quelques travaux décrivaient une participation de l'angiogenèse au développement d'hémopathies malignes.[83,84] Une expression accrue de VEGF avait été démontrée dans des lymphomes non-Hodgkiniens, et ceci était associé à la progression tumorale et à un mauvais pronostic.[85]

Concernant la régulation des taux de VEGF, elle était connue pour se faire à plusieurs niveaux au cours de sa biogenèse, incluant la transcription, la stabilisation de l'ARNm, les épissages alternatifs ainsi que la traduction en protéine.[86,87] Sa régulation, au niveau post-transcriptionnel, par des microARN (miARN), notamment miR-15 et miR-16, venait juste d'être publiée au début de nos recherches sur un lien éventuel entre oncogène ALK et angiogenèse.[88]

Dans ce contexte, pour suivre l'impulsion donnée par notre nouveau chef d'équipe, le Pr Pierre Brousset, intéressé par la biologie des ARNs dans les hémopathies malignes, nous avons étudié l'angiogenèse observée dans nos modèles de LAGC ALK positif en regard de la littérature sur les miARN et de leur profil d'expression dans cette pathologie. Très brièvement, les miARN sont de petits ARN non codants, simple-brin d'environ 22 nucléotides qui participent à la régulation post-transcriptionnelle de l'expression des gènes par le mécanisme d'interférence ARN (ARNi) ou ARN silencing.[89] Ces miARN, en se fixant sur la région 3' non traduite de leurs ARN messagers (ARNm) cibles, entrainent la répression traductionnelle ou la dégradation de ces transcrits. Une dérégulation de l'expression d'un miARN d'intérêt (sur ou sous-expression) peut donc entrainer une modulation d'expression de ses gènes cibles.

C-2/ Résultats

En utilisant les différents modèles développés au laboratoire et décrits dans le chapitre B précédent : les lignées murines (MEF TPM3-ALK), les modèles de transplantation en souris *nude*, les modèles transgéniques conditionnels de lymphome NPM-ALK et TPM3-ALK positif, ainsi que nos sérothèques et tumorothèques humaines et murines, nous avons observé les résultats majeurs suivants :

*la régulation positive des taux de VEGF suite à l'expression de l'oncogène ALK (dosage sérique ELISA), Figure 8A et B.

*la régulation négative des taux de miR-16 suite à l'expression de l'oncogène ALK (RT-qPCR), Figure 8C et D.

*une interaction directe entre miR-16 et la région 3' de l'ARN messager du VEGF (test luciférase sur des cellules MEF TPM3-ALK sur-exprimant miR-16 et une construction permettant l'expression contrôlée de la luciférase par l'extrémité 3' de l'ARN messager du VEGF (pRL-VEGF 3'UTR)), Figure 9A. Cette interaction est déstabilisée par surexpression soit d'un « locked nuclear acid » (LNA) anti-sens pour miR-16 ; soit d'un inhibiteur anti-miR-16, Figure 9B.

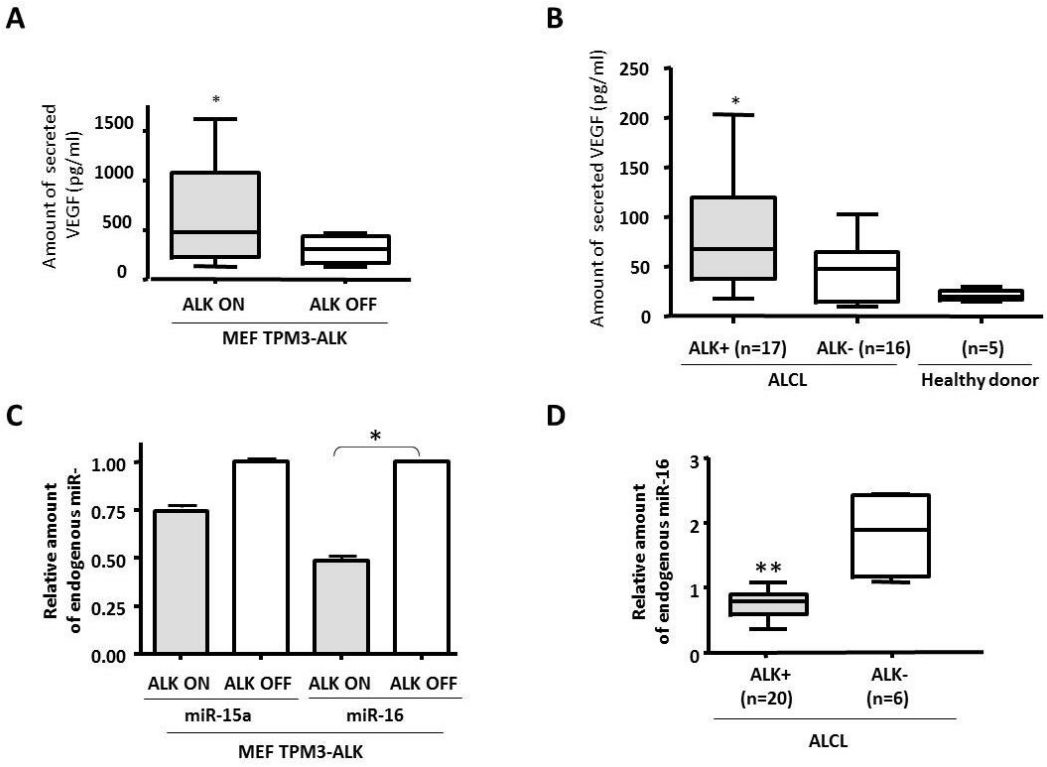

Figure 8: Régulation, dépendante de l'oncogène ALK, des taux de VEGF secrété et de miR-16 endogène dans les tumeurs murines et humaines. A et B) Le VEGF secrété dans le milieu de culture des cellules MEF TPM3-ALK et dans le sérum de patients atteints de LAGC (ALK positif et ALK négatif) a été déterminé par test ELISA. C et D) Les taux de miR-16 endogène, selon l'expression de TPM3-ALK, dans les cellules MEF TPM3-ALK et dans les biopsies de patients atteints de LAGC (ALK positif et ALK négatif) ont été déterminés par RT-qPCR.

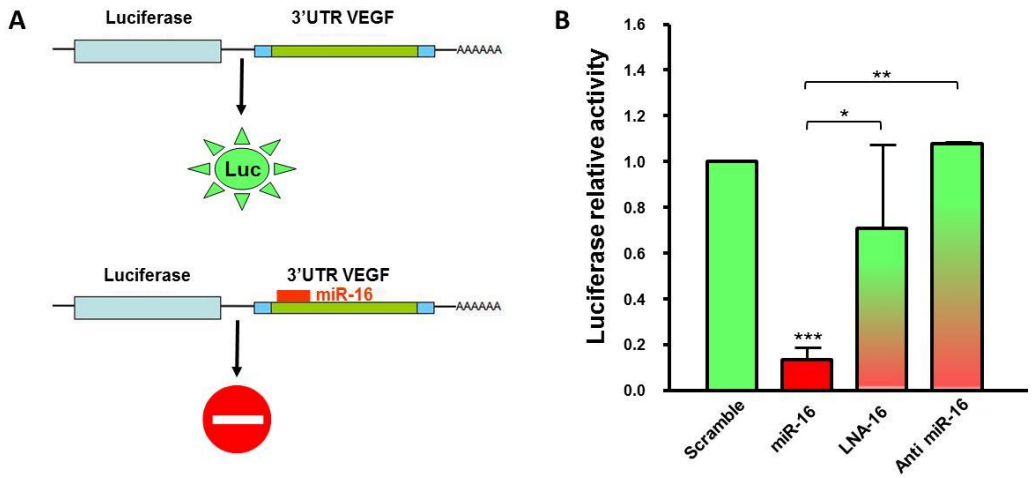

Figure 9: Liaison de miR-16 sur la région 3'UTR de l'ARN messager codant pour le VEGF. A) Représentation schématique du test de liaison de miR-16 sur la partie 3'UTR de l'ARNm du VEGF, en utilisant un système rapporteur d'activité luciférase. B) La construction pRL-VEGF 3'UTR a été co-transfectée avec miR-16 en présence ou absence d'un antisens LNA-16 ou d'un inhibiteur de miR-16. L'activité luciférase a été mesurée au luminomètre, 48h après transfection.

*un défaut d'angiogenèse et de croissance tumorale *in vivo* par sur-expression de miR-16 dans les cellules MEF TPM3-ALK, préalablement à leur transplantation sous-cutanée en souris *nude* (mesure du volume et du poids tumoral, mesure des taux de VEGF sériques, mesure de la densité microvasculaire intratumorale), Figure 10.

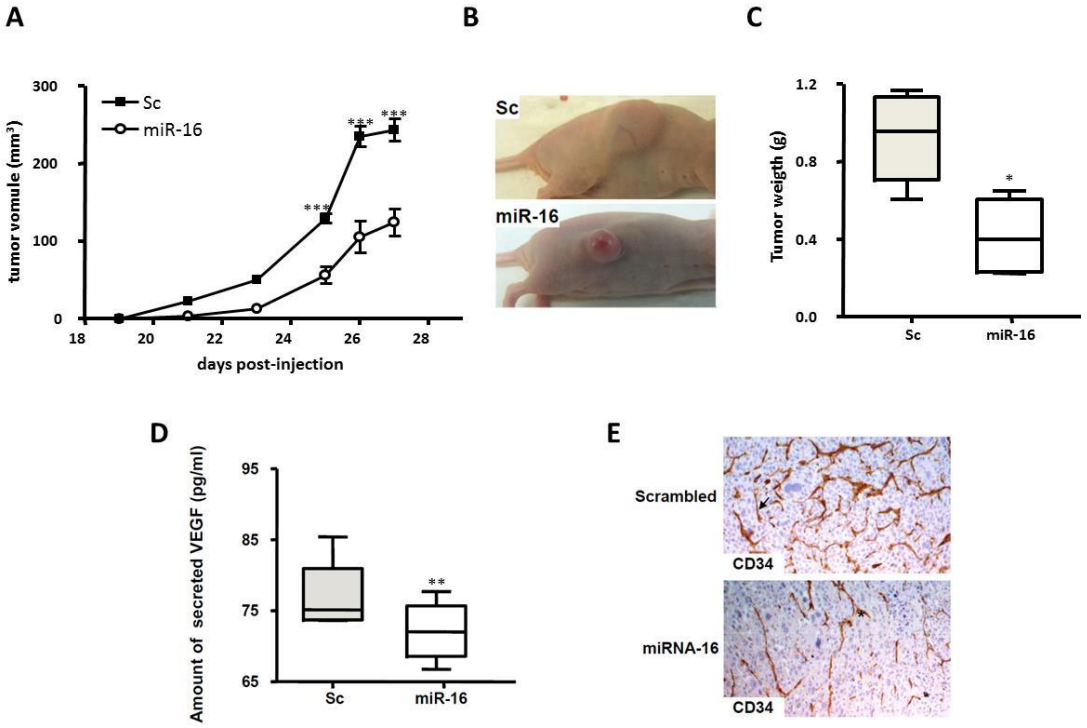

Figure 10: Défaut de croissance tumorale et d'angiogenèse par sur-expression de miR-16. Les cellules MEFs TPM3-ALK sur-exprimant miR-16 ou un miR control (Scramble, Sc) ont été injectées en sous-cutanée dans des souris *nude*. A) Le volume tumoral a été mesuré au pied à coulisse tous les deux jours. B) Photographies des tumeurs sous-cutanées 27 jours après l'inoculation. C) Poids des tumeurs sous-cutanées à la nécropsie. D) Le taux de VEGF secrété dans le sérum murin a été déterminé par test ELISA. E) La densité microvasculaire des tumeurs sous-cutanées prélevées au 27ème jour après inoculation a été déterminée par immunohistochime anti-CD34.

*une corrélation inverse entre les taux de VEGF et les taux de miR-16 dans des biopsies humaines de lymphomes ALK positifs (RT-qPCR, immunohistochime), Figure 11.

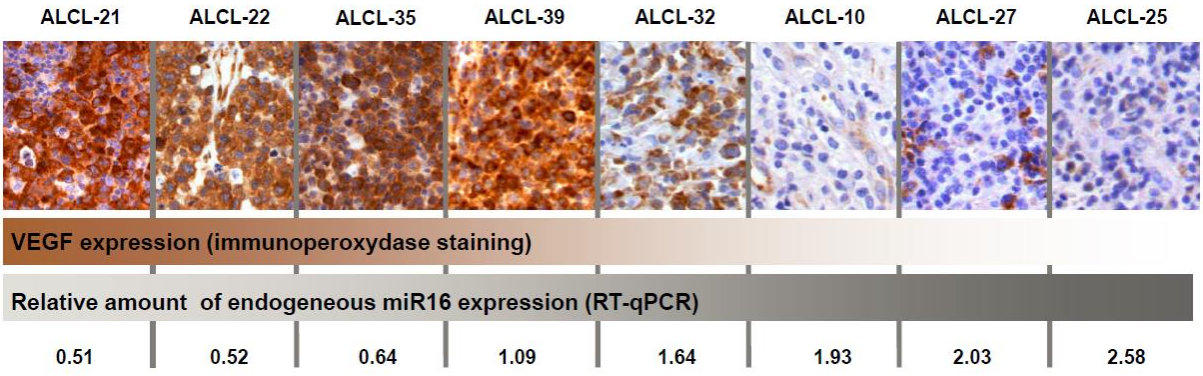

Figure 11: Corrélation inverse entre l'expression du VEGF et les taux de miR-16 endogène dans les LAGC ALK positif. L'expression du VEGF dans huit biopsies de patients atteints de LAGC ALK positif a été réalisée par immunohistochimie. Les taux de miR-16 endogène, sur ces mêmes échantillons tumoraux, ont été déterminés par RT-qPCR.

C-3/ Conclusion

Notre étude a été l'une des premières à mettre au jour le rôle de l'angiogenèse dans le développement des tumeurs ALK-positives. Elle démontre une sécrétion accrue de VEGF, sous la dépendance de l'oncogène ALK, selon l'axe « ALK / régulation négative de miR16 / traduction augmentée de l'ARNm codant pour le VEGF ». Ce lien entre ALK et angiogenèse, publié en 2011 dans le journal Leukemia,[57] a été conforté la même année, par deux études complémentaires. Les travaux de Marzec et al., d'une part, ont montré dans une lignée de LAGC ALK positif (SU-DHL-1) que l'expression de HIF1α, induite sous le contrôle de NPM-ALK, permettait de freiner la prolifération cellulaire en condition d'hypoxie et d'augmenter, en partie, la biosynthèse de VEGF.[90] D'autre part, les travaux de Di Paolo et al. ont décrit, dans les neuroblastomes, un rôle pour la protéine ALK pleine taille activée dans la croissance tumorale, la sécrétion de VEGF et la formation de néo-vaisseaux.[91] Enfin, plus récemment, en 2014, l'équipe du Dr Roberto Chiarle a clairement démontré le rôle prévalent du facteur de transcription HIF2α (par rapport à HIF1)α pour le développement et le maintien tumoral dans des modèles de xénogreffes de LAGC ALK positif (lignées SU-DHL-1 et TS) dans des souris NOD/ SCID. De plus, le traitement de ces animaux par l'anticorps anti-VEGF bevacizumab diminue fortement le développement tumoral et la formation des vaisseaux sanguins intra-tumoraux. [92]

Ainsi nos travaux, comme ceux d'autres groupes et collègues internationaux, concordent à démontrer la régulation positive de l'expression du VEGF par l'oncogène ALK. Il apparaît également que l'angiogenèse participe activement au développement tumoral puisque son inhibition, par des stratégies d'interférence ARN (notamment siHIF2α) ou par sur-expression de miR-16, entraîne un fort ralentissement de la croissance sous-cutanée de xénogreffes de LAGC ALK positif. Ces travaux concourent donc à démontrer que des thérapies anti-angiogéniques pourraient être bénéfiques pour certains patients atteints de LAGC ALK positif.

D/ Rôle de l'autophagie dans la réponse des LAGC ALK positif au traitement Crizotinib (2011-2016 ; Inserm U1037, Equipe 7 ; Dir : Pr P. Brousset)

Le Crizotinib est l'inhibiteur de l'activité tyrosine kinase de ALK le plus avancé sur le plan clinique. Lorsqu'administré in vitro sur des lignées de LAGC ALK positif, il induit l'arrêt du cycle cellullaire et l'apoptose. In vivo, nous avons démontré qu'il permet, rapidement, la régression des lymphomes murins ALK positif (chapitre B). En clinique, lorsqu'administré en seconde ligne thérapeutique, sans discontinuation, à des patients adultes ou enfants atteints de LAGC ALK positif, il permet leur rémission (chapitre A). Cependant, comme déjà décrit pour les cancers du poumon EML4-ALK positif traités par le Crizotinib, des résistances sont apparues chez des patients atteints de LAGC ALK positif. Dans ce contexte de résistance

thérapeutique, il a été proposé que l'autophagie (processus intracellulaire d'autodigestion) participe à la cytoprotection des cellules cancéreuses, favorisant ainsi leur échappement aux traitements anti-cancéreux. De façon intéressante, l'autophagie, poussée à l'extrême, a également été associée à la mort des cellules tumorales. Ainsi, il m'est apparu très intéressant, pour les thérapies anti-ALK, d'exploiter cette dualité fonctionnelle de survie ou de mort cellulaires associées à l'autophagie, ce que j'ai entrepris en 2012 grâce aux soutiens financiers d'une ANR Jeune Chercheur et des Ligues Régionales et Nationales contre le cancer.

D-1/ Introduction

Le rôle de l'autophagie en physiopathologie humaine est un domaine de recherche en émergence. Le terme « autophagie » a été proposé pour la première fois par le Pr Christian de Duve (prix Nobel en 1974), qui, en visualisant des vésicules d'autophagosomes en microscopie électronique, a compris que les cellules étaient capables de digérer une partie de leur contenu. Un effort considérable a été porté ces dernières années sur la compréhension de la biogenèse de ce processus, sur sa régulation et sur son implication dans diverses pathologies. L'autophagie est donc un mécanisme intracellulaire d'auto-digestion. Ce processus permet la dégradation des protéines à durée de vie longue, des agrégats toxiques et des organelles défectueuses, par leur séquestration dans des vésicules à doubles membranes (appelées autophagosomes). Les autophagosomes fusionnent ensuite avec les lysosomes, entraînant la dégradation de leur contenu (Figure 12).[93] Un niveau basal d'autophagie est présent dans la plupart des cellules, assurant ainsi un « contrôle qualité » du cytoplasme. Lors d'un stress cellulaire, la stimulation de ce processus permet l'adaptation de la cellule ainsi que sa survie en assurant l'élimination et le recyclage des protéines et organelles altérées. Poussé à l'extrême, ce processus atteint un point de non-retour et la mort cellulaire, associée à l'autophagie, est observée.[94] Ainsi, selon les conditions, l'autophagie peut être un mécanisme associé à la survie ou à la mort cellulaire. Cette dualité fonctionnelle culmine en situation pathologique, et notamment dans les cancers où la cellule maligne détourne l'autophagie à son profit, notamment pour assurer sa survie lors d'un stress métabolique (lors du développement tumoral) ou thérapeutique (suite à l'administration d'une chimio-, radio-thérapie ou thérapie ciblée).[95] Elle apparaît donc comme un mécanisme régulateur clé de la tumorigenèse, en assurant un apport énergétique lors du développement tumoral, mais aussi en permettant la résistance des cellules cancéreuses au traitement thérapeutique.

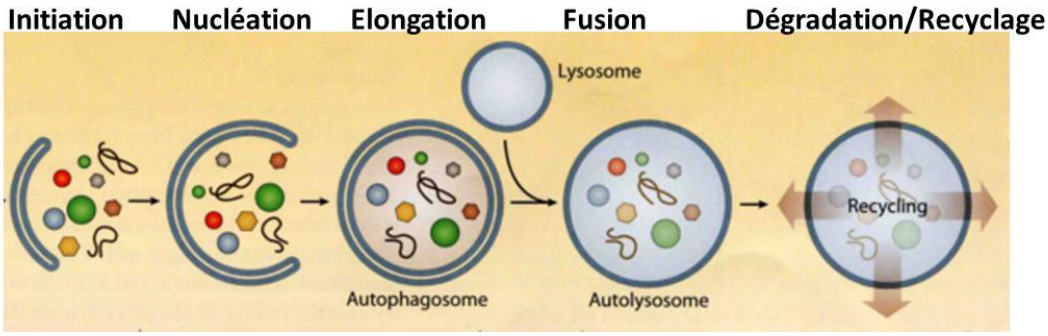

Figure 12: Les étapes clés de l'autophagie. Ce processus catabolique lysosomal est initié par l'isolement de matériel cytoplasmique défectueux ou toxique (aussi appelé « cargo ») au sein d'une vésicule pré-autophagosomale (aussi appelée phagophore). Celle-ci séquestre le cargo, s'allonge et se ferme sur elle-même pour former un autophagosome, caractérisé par sa double membrane lipidique. La fusion de l'autophagosome au lysosome résulte en la formation d'un autophagolysosome (ou autolysosome) où s'effectue la dégradation du cargo, en vue du recyclage de ses composantes premières (acides aminés, acides gras…) dans le cytoplasme.

Rien n'étant connu sur l'autophagie dans les lymphomes anaplasiques à grandes cellules (LAGC) exprimant l'oncogène ALK, je me suis attachée, avec mes deux étudiantes, le Dr Géraldine Mitou (post-doctorante, financée par l'ANR Jeune Chercheur « ALK-phagie ») et Melle Julie Frentzel (doctorante, financée par la Ligue Nationale Contre le Cancer), à démontrer la mise en place d'un flux autophagique cytoprotecteur lors du stress thérapeutique induit par inactivation de l'oncogène ALK dans deux lignées de LAGC.

D-2/ Résultats

Nous avons utilisé deux lignées de lymphome anaplasique à grandes cellules : Karpas-299 et SU-DHL-1, exprimant l'oncogène NPM-ALK, pour démontrer selon différentes techniques complémentaires (recommandées par les « Guidelines for the use and interpretation of assays for monitoring autophagy »[96]), l'activation de l'autophagie suite au stress thérapeutique induit par administration du Crizotinib (inhibiteur de l'activité tyrosine kinase de ALK) ou par l'utilisation de petits ARN interférents, ciblant spécifiquement l'oncogène NPM-ALK (siRNA ALK). Seuls quelques résultats majeurs seront exposés ci-dessous. Ainsi, nous avons observé que l'inactivation pharmacologique (Crizo) ou moléculaire de l'oncogène ALK (siALK) induit:

*Un nombre accru d'autophagosomes dans le cytoplasme des cellules. Ces structures vésiculaires à double membrane sont caractéristiques de l'autophagie. Nous les avons visualisées et quantifiées par microscopie électronique (Figure 13A et B).

*Une activation du flux autophagique par visualisation (en western-blot) de l'accumulation des protéines LC3-II après inhibition de la fusion autophagosome/lysosome (par la chloroquine[97]). En effet, LC3 est une protéine clef de la machinerie autophagique impliquée dans la formation de l'autophagosome. Elle est clivée puis associée à la phosphatidylethanolamine (PE). Les deux formes LC3-I (non lipidée, cytoplasmique) et LC3-II

(forme lipidée, autophagosomale) peuvent être séparées, visualisées et quantifiées par western-blot (Figure 13C).

*Une expression accrue des gènes codant pour des acteurs et régulateurs clefs de l'autophagie. Nous avons utilisé pour cela un « autophagy array », développé par la société Qiagen (Figure 13D).

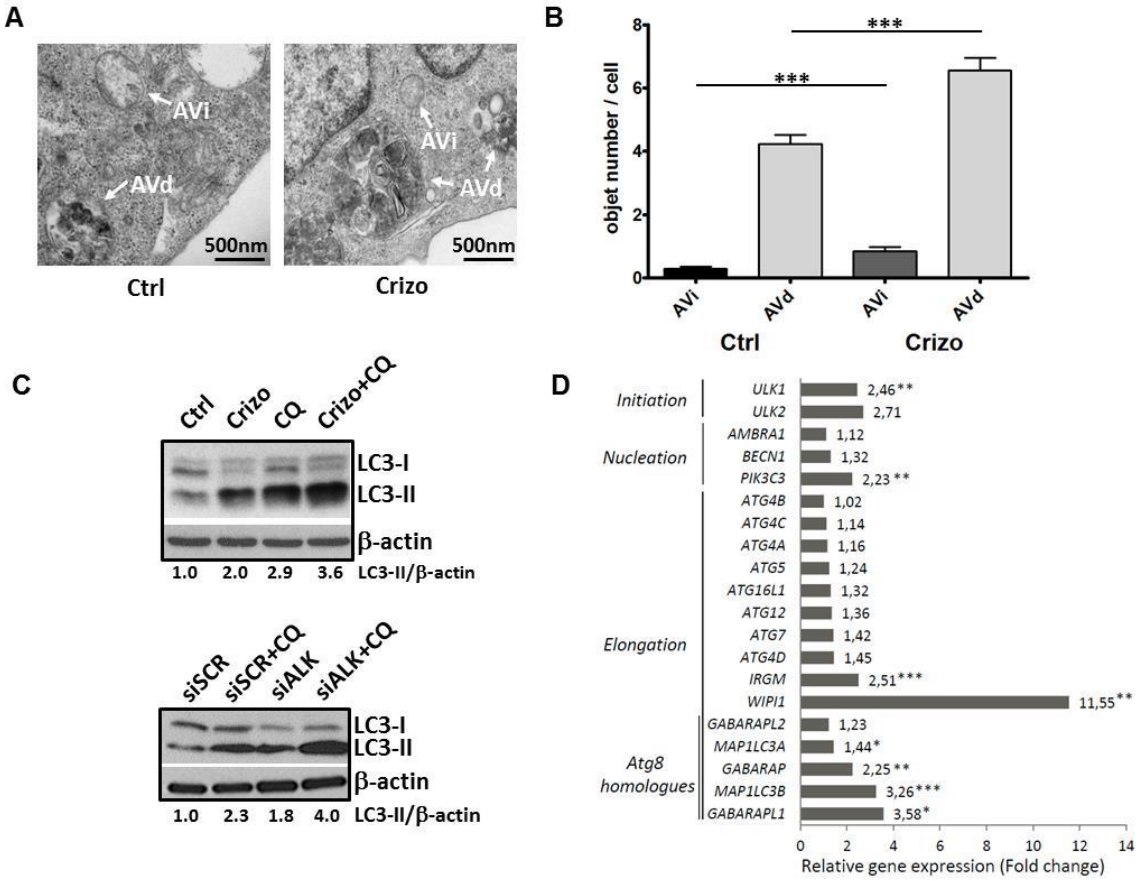

Figure 13: Activation de l'autophagie par inactivation de l'oncogène NPM-ALK. A et B) Visualisation (grossissement x10000) et quantification des vésicules autophagiques observées en microscopie électronique sur des préparations de cellules de LAGC ALK positif (Karpas-299), traitées ou pas par le Crizotinib (500nM, 24h). Les autophagosomes ont été dénombrés en tant que AVi (initial autophagic vacuoles); les autophagolysosomes (après fusion avec le lysosome) ont été dénombrés en tant que AVd (degradative autophagic vacuoles). C) L'activation du flux autophagique par inhibition pharmacologique (Crizotinib, panel supérieur) ou moléculaire (siALK, panel inférieur) de NPM-ALK est visualisée et quantifiée par analyse en western-blot de la conversion LC3-I en LC3-II et de l'accumulation de LC3-II en présence de chloroquine (CQ, 30μM, 24h). D) Analyse du profil d'expression d'une sélection de gènes d'un « autophagy array » (SABiosciences) indiquant le facteur d'augmentation entre des cellules Karpas-299 traitées par du Crizotinib (500nM, 24h) et non traitées (valeur normalisée à1).

Dans un second temps, nous nous sommes attachés à démontrer le rôle cytoprotecteur de cette autophagie par des mesures de viabilité cellulaire et des tests de clonogénicité, effectués en combinant ou pas l'inactivation de l'oncogène NPM-ALK (Crizotinib ou siRNA ALK) avec l'inhibition de l'autophagie. Trois approches ont été utilisées pour inhiber

l'autophagie : -deux traitements pharmacologiques, soit par de la 3-methyladenine (3MA), soit par de la chloroquine (CQ), qui sont des inhibiteurs des phases précoces et tardives de l'autophagie, respectivement; -l'utilisation de petits ARN interférents, ciblant spécifiquement un acteur clef de l'autophagie (siRNA ATG7). Nos résultats indiquent, de façon très reproductible:

*une synergie entre l'inactivation de l'oncogène ALK et l'inhibition de l'autophagie, quelle que soit la méthode utilisée (3MA, CQ ou siRNA ATG7), en terme de réduction de viabilité cellulaire, d'incapacité à former des colonies et d'induction d'apoptose (Figure 14).

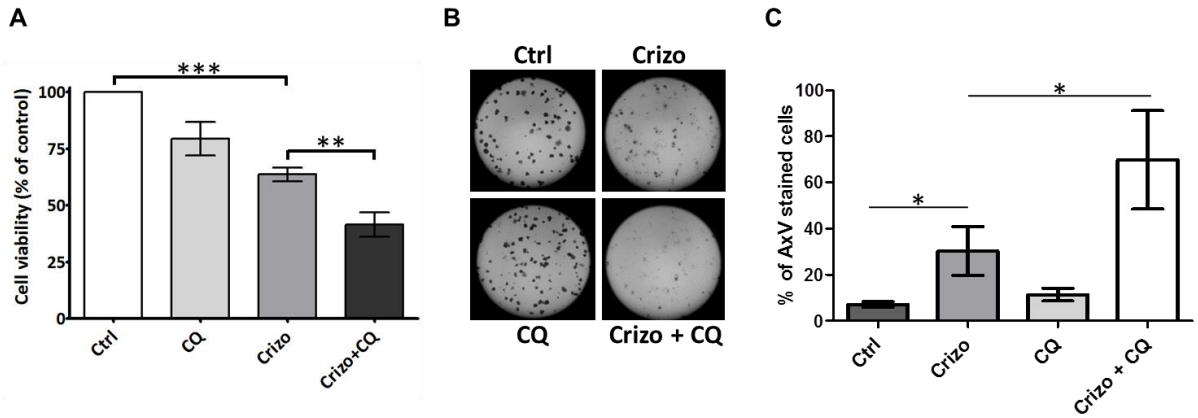

Figure 14: Rôle cytoprotecteur de l'autophagie induite par inactivation de l'oncogène ALK. A) La viabilité de cellules Karpas-299, traitées ou non par le Crizotinib (Crizo, 500nM) et/ou la Chloroquine (CQ, 30μM) a été déterminée après 48h par test MTS. B) Photographies représentatives de l'effet du Crizotinib (500nM), de la Chloroquine (30mM) et d'un traitement combinant ces deux drogues sur la capacité des cellules Karpas-299 à former des colonies en agar mou. Les cellules ont été traitées 16h comme indiqué avant leur ensemencement en plaque d'agar. Six jours plus tard, les colonies sont visualisées par addition du réactif MTT. C) Le traitement combinant le Crizotinib et la Chloroquine (Crizo + CQ) induit plus d'apoptose par rapport à chacun des mono-traitements. L'apoptose cellulaire a été mesurée par marquage Annexin V-PE / 7-AAD et analyse au cytomètre.

*un défaut de croissance tumorale *in vivo* par la combinaison thérapeutique : « inhibition de l'oncogène ALK (Crizotinib) + inhibition de l'autophagie (Chloroquine)» (Figure 15).

D-3/ Conclusion

Nos résultats ont été publiés récemment dans le journal « Oncotarget ».[58] Ils démontrent pour la première fois dans les LAGC ALK positif l'activation de l'autophagie lors de l'inactivation de l'oncogène ALK ainsi que son rôle cytoprotecteur. La capacité des cellules tumorales ALK-positives à activer un processus autophagique de résistance au stress thérapeutique pourrait donc participer à l'émergence de rechutes tumorales. Nos résultats suggèrent fortement que le traitement combiné des tumeurs ALK-positives par un inhibiteur de l'oncogène ALK et un inhibiteur de l'autophagie serait bénéfique pour les patients atteints de LAGC ALK positif.

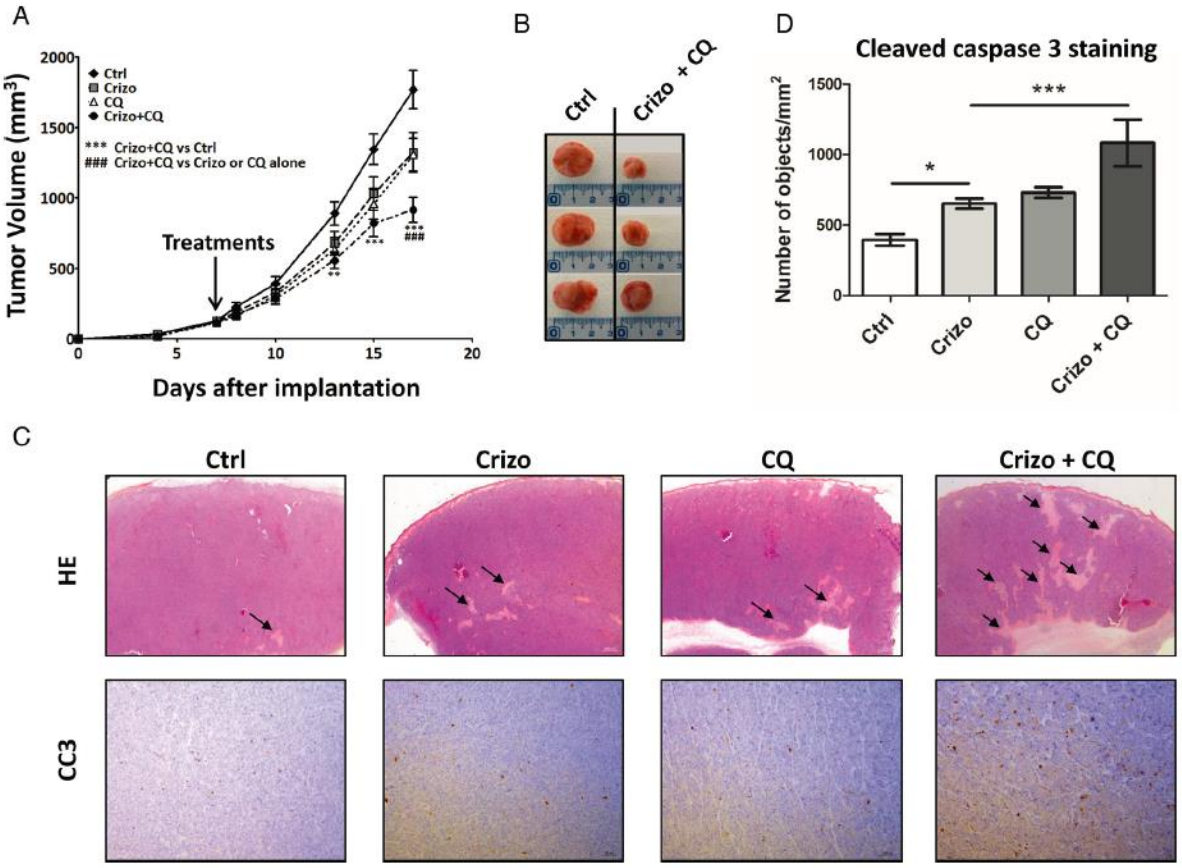

Figure 15: Bénéfice thérapeutique, *in vivo*, des inhibitions combinées de l'oncogène ALK et de l'autophagie. A) Des souris NOD/SCID transplantées en sous-cutanée par des cellules Karpas-299 ont été traitées ou pas par une dose sous-optimale de Crizotinib (Crizo, 10 mg/kg), de la Chloroquine (CQ, 60 mg/kg) ou une combinaison des deux drogues (Crizo+CQ). La croissance tumorale a été suivie deux fois par semaine par mesure au pied à coulisse. B) Photographies représentatives des tumeurs sous-cutanées à la nécropsie. C) Photographies des colorations à l'hematoxyline/eosine (HE) et des immunomarquages anti-caspase 3 clivée (CC3), réalisés sur des coupes de tissus tumoraux isolés à partir des différents groupes de souris cités en A. Les zones tumorales nécrosées sont indiquées par des flèches sur les colorations HE. D) La quantification de l'immunomarquage anti-caspase 3 clivée (CC3) a été réalisée sur lames scannées à l'aide des logiciels Pannoramic Viewer et HistoQuant.

PROJETS DE RECHERCHE

A/ Projet 1 : Régulation post-transcriptionnelle de l'autophagie via les microARNs.

A-1/ Introduction

L'autophagie est un mécanisme régulateur clé de la tumorigenèse. [95,98] Son maintien à un niveau basal et son activation reposent sur des régulations fines, tant au niveau protéique qu'aux niveaux transcriptionnel et post-transcriptionnel. Notre laboratoire s'étant réorienté ces dernières années vers l'étude de la biologie des ARNs dans les hémopathies malignes, nous nous sommes particulièrement intéressés à la régulation post-transcriptionnelle de l'autophagie médiée par une famille de petits ARNs non-codants : les microARNs, ce qui est un domaine de recherche en émergence. [99] Ce projet s'inscrit dans la continuité du travail de thèse de mon étudiante en doctorat : Melle Julie Frentzel (soutenance prévue en Octobre 2016).

A-2/ Résultats préliminaires

Afin d'identifier les mécanismes de régulation de l'autophagie qui dépendent des microARNs dans notre modèle d'étude : le lymphome anaplasique à grandes cellules ALK positif, la stratégie utilisée a été, chronologiquement:

-de développer un outil de mesure rapide et quantitative du flux autophagique par FACS [100], en utilisant des cellules Karpas-299 (LAGC ALK positif) exprimant de façon stable la construction RFP-GFP-LC3 (obtenue par le laboratoire du Dr P. Codogno). Ce nouvel outil permet en effet de suivre le devenir des autophagosomes (marquées par la protéine fluorescente RFP-GFP-LC3) et notamment de « voir » leur fusion avec le lysosome du fait de la perte de fluorescence GFP en milieu acide. C'est donc l'augmentation du ratio « signal RFP/signal GFP » qui reflète l'activation du flux autophagique, Figure 16.

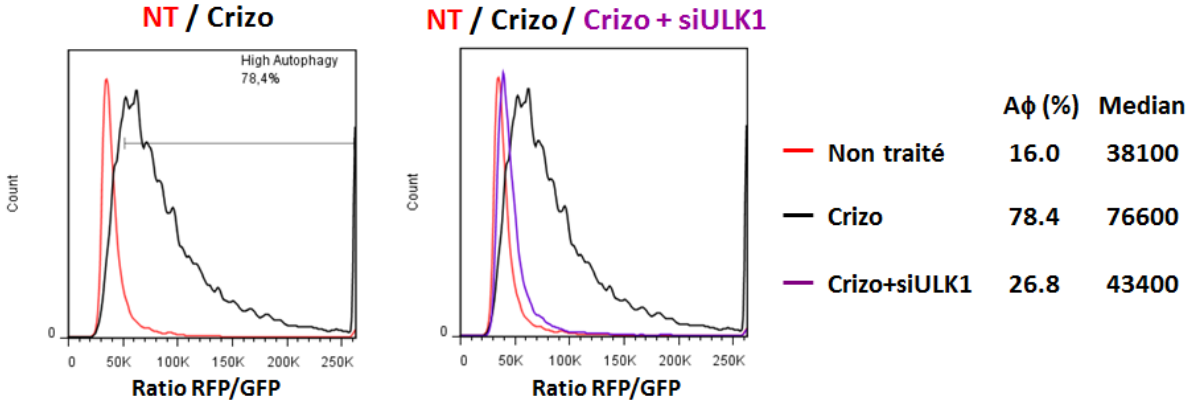

Figure 16 : Quantification du flux autophagique par cytométrie de flux. Les cellules Karpas-299 exprimant de façon stable la protéine de fusion RFP-GFP-LC3 ont été transfectées ou pas par un siRNA ciblant ULK1 (siULK1) et traitées ou pas (NT) par le Crizotinib (Crizo, 500nM, 24h). L'augmentation du ratio RFP/GFP indique l'activation du flux autophagique sous Crizotinib. Ce flux est inhibé en présence d'un siRNA ciblant ULK1 (protéine essentielle dans l'étape d'initiation de l'autophagie).

- d'établir les profils d'expression 1) des gènes de l'autophagie (« autophagy array » – Qiagen) et 2) des microARNs (cancer miRNA array - Qiagen) dans les cellules Karpas-299 traitées ou non par le Crizotinib, à la dose connue (de par nos travaux précédents [58]), pour induire une autophagie cytoprotectrice.

- de sélectionner le (ou les microARNs) dont l'expression est le plus significativement down-régulée. C'est ainsi que nous nous sommes focalisés sur miR-7-5p, Figure 17A.

- de valider par RT-qPCR la régulation négative de ce miARN d'intérêt (miR-7-5p) lors du traitement des cellules Karpas-299 par le Crizotinib ou par un siALK, Figure 17B et C. Ces résultats ont été reproduits dans la lignée SU-DHL-1.

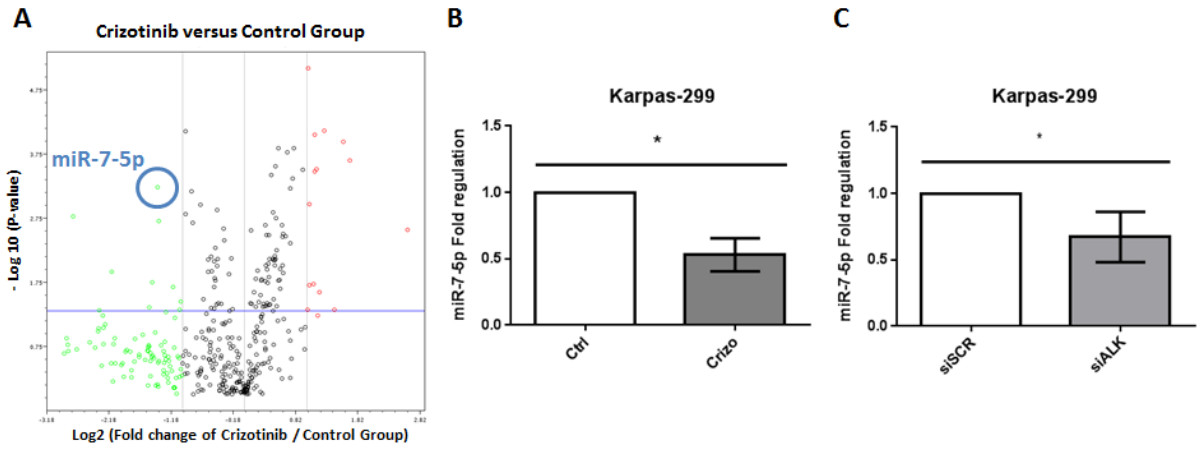

Figure 17 : Régulation négative de miR-7-5p dans les LAGC ALK positif lors de l'inactivation de l'oncogène ALK. A) Les cellules Karpas-299 ont été traitées ou pas avec du Crizotinib (500nM, 24h). Les culots cellulaires (en triplicat) ont été envoyés à la société Qiagen pour réaliser un « cancer miRNA PCR array ». Les résultats sont représentés en « Volcano plot ». En vert, les miRNAs sous-exprimés ; en rouge, les miRNAs sur-exprimés ; en noir, les miRNAs dont l'expression est peu modulée par le traitement Crizotinib. B-C) Validation par RT-qPCR de la down-régulation de miR-7-5p par traitement Crizotinib (500nM, 24h) (B) ou par transfection d'un siRNA ciblant ALK (analyse post 72h de transfection) (C).

- de sur-exprimer miR-7-5p dans les cellules Karpas-299 RFP-GFP-LC3, traitées ou non par le Crizotinib, afin d'évaluer son impact sur la viabilité cellulaire (MTS) et le flux autophagique (analyse par FACS). Nos résultats indiquent que la sur-expression de miR-7-5p induit une potentialisation du flux autophagique et des effets cytotoxiques du Crizotinib, Figure 18.

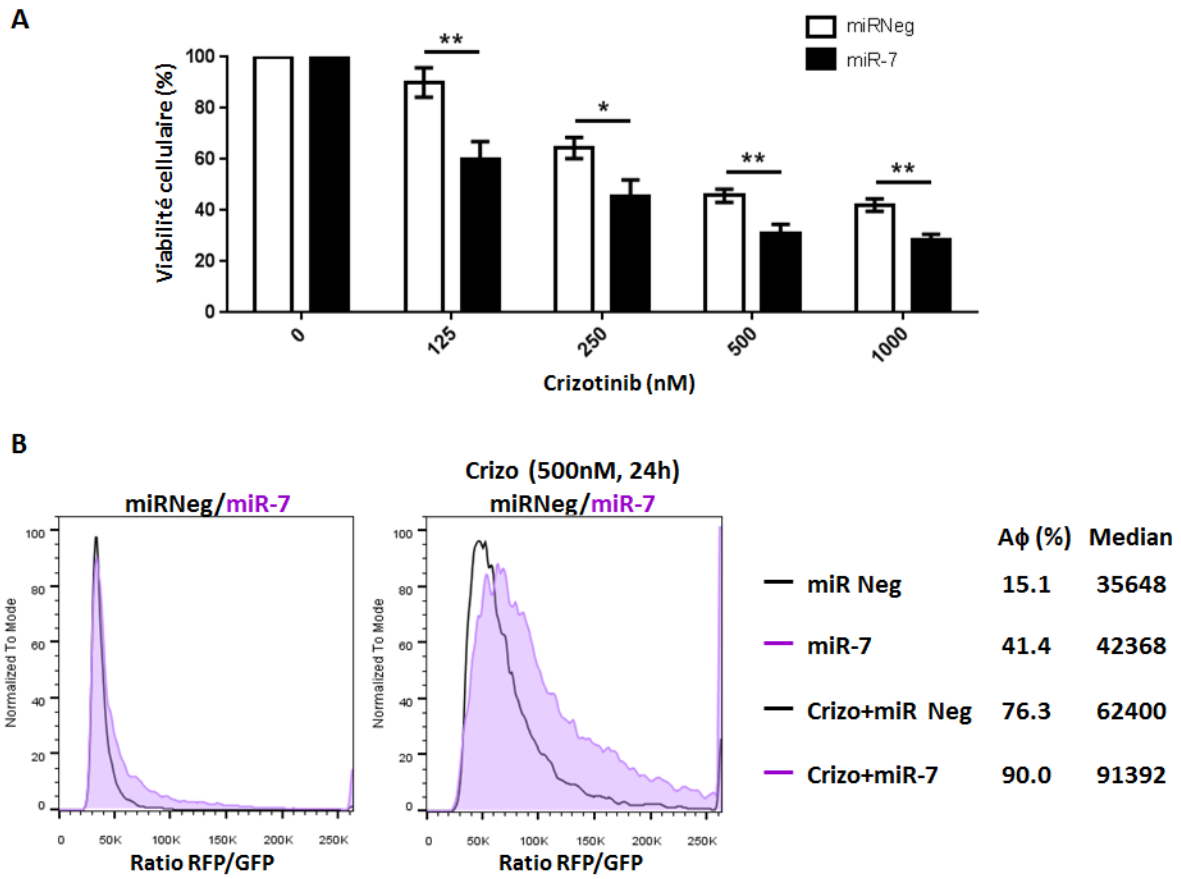

Figure 18 : La sur-expression de miR-7-5p potentialise l'effet anti-tumoral et le flux autophagique induit par le Crizotinib. A) Les cellules Karpas-299, transfectées par miR-7-5p ou un miR scramble (miR Neg), ont été traitées par du Crizotinib aux concentrations indiquées. La mesure de la viabilité cellulaire (test MTS) a été réalisée 72h après transfection des miRs, incluant 48h de traitement Crizotinib. B) Les cellules Karpas-299 RFP-GFP-LC3 ont été traitées comme indiqué au point A et analysées par FACS pour l'activation du flux autophagique.

A-3/ Perspectives

Nos résultats préliminaires indiquent que miRNA-7-5p est le microARN le plus significativement down-régulé dans les cellules de LAGC ALK positif, soumises au Crizotinib ; et que la sur-expression de miR-7-5p induit la potentialisation du flux autophagique ainsi que la potentialisation des effets cytotoxiques du Crizotinib.

Une analyse de la littérature indique que l'autophagie revêt plusieurs « visages ». Elle peut être non protectrice, cytoprotectrice, cytostatique ou cytotoxique.[101] Il apparaît aussi que selon son intensité et/ou sa durée, ses propriétés peuvent basculer (on parle de *switch* autophagique) d'un effet cytoprotecteur à un effet cytotoxique.[102] Les mécanismes moléculaires de régulation de cette balance sont encore peu connus.

Nous proposons l'hypothèse selon laquelle miR-7-5p serait un fin régulateur de la balance entre cytoprotection et cytotoxicité, lors du traitement des LAGC ALK positif par le Crizotinib. Nous nous attachons actuellement, par analyse de la littérature et par analyse bio-informatique (utilisation des bases de données miRWalk et MEDIANTE), à identifier le ou les les ARN messagers cibles de miR-7-5p, qui pourraient participer au contrôle de ce switch autophagique.

B/ Projet 2: Autophagie : carrefour thérapeutique des approches vaccinales et ciblées contre l'oncogène ALK. (Boston Children's Hospital, Collaboration Dr R. Chiarle, Septembre 2016 - Août 2017):

Les grandes lignes de ce projet ont émergé il y a quelques mois, à l'issue de trois conférences scientifiques auxquelles j'ai assisté. Le congrès de l'association américaine contre le cancer (AACR), en avril 2015, le congrès EMBO « Autophagy signalling and progression in health and disease» en septembre 2015 et le premier meeting « ALKATRAS » du réseau européen ERIA (European Research initiatives on ALK-related malignancies), focalisé sur les recherches fondamentales et cliniques des tumeurs exprimant l'oncogène ALK. J'ai été très sensible (i) à la révolution actuelle dans le domaine de l'immunothérapie des cancers (AACR), (ii) au rôle important que peut jouer l'autophagie dans l'immunité (EMBO meeting), (iii) et aux résultats présentés par le Dr Roberto Chiarle sur la vaccination anti-ALK (ERIA).

J'ai alors proposé au Dr Roberto Chiarle une collaboration, dans le cadre d'une mise à disposition demandée à l'INSERM, afin de tenter d'apporter ma connaissance de l'autophagie dans ses travaux sur la vaccination anti-ALK. Toutes les démarches administratives sont en cours. Voici donc ci-dessous quelques questions posées dans ce projet.

B-1/ Autophagie et immunité: quelques données de la littérature

Un nombre croissant de publications montre que l'autophagie joue un rôle certain à la fois dans l'immunité innée et adaptative.[103] Il a été décrit notamment que les autophagosomes, en fusionnant avec le compartiment de charge des molécules du Complexe majeur d'Histocompatibilité (CMH), participait à la stimulation de l'immunité adaptative, en participant au processus de présentation d'antigènes aux lymphocytes T CD4+ (via le chargement du CMHII) ainsi qu'aux lymphocytes T CD8+ (via le chargement du CMHI), Figure 19. Classiquement, le CMHI se charge de peptides issus de la dégradation par le protéasome et le CMHII se charge de peptides issus de la dégradation lysosomale. Les travaux pionniers de l'équipe du Dr C. Münz démontrent en 2007 que les autophagosomes peuvent délivrer des antigènes cytosoliques au compartiment CMHII.[104] Lorsque la dégradation via le protéasome est déficiente, les autophagosomes sont également capables de délivrer des peptides au CMHII.[105] Enfin, une littérature émergente décrit la sécrétion ou exocytose d'autophagosome (sous forme de Dribbles, Figure 20) permettant, de façon

efficace, le transfert d'antigène d'une cellule donneuse à une cellule présentatrice d'antigènes, pour une cross-présentation impliquant le CMHI.[106,107] Ce résultat a conduit au développement de « Tumor-derived autophagosome vaccines », qui ont été décrits comme ayant une efficacité supérieure que des lysats tumoraux pour stimuler les cellules dendritiques et la réponse immune anti-tumorale.[107–109]

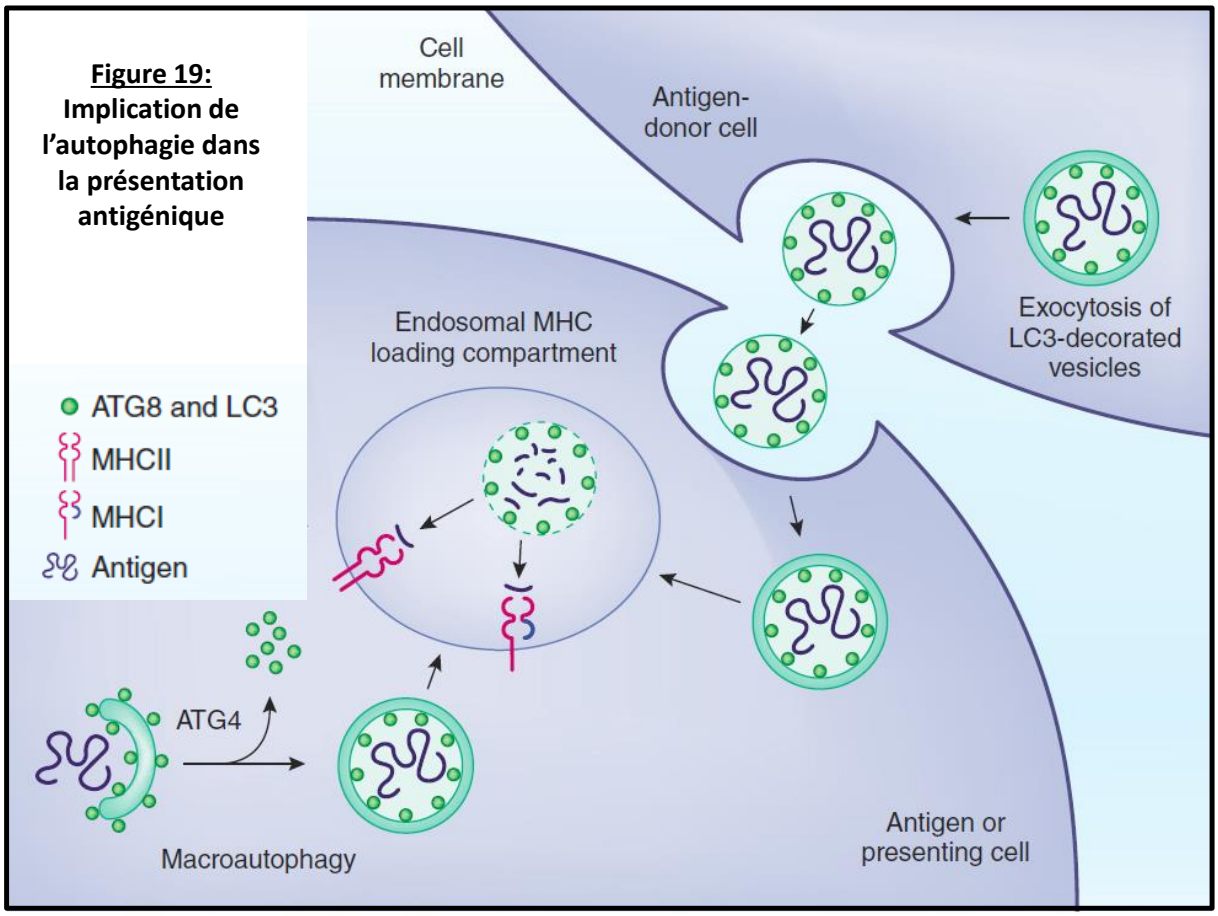

Figure 19 : Implication de l'autophagie dans la présentation antigénique. L'autophagie peut contribuer à l'immunité adaptative par au moins deux mécanismes : 1) Chargement sur le CMHI : les autophagosomes d'une cellule donneuse d'antigènes peuvent fusionner avec la membrane plasmique, permettant ainsi l'exocytose du cargo entouré de la membrane interne de l'autophagosome (voir figure 20 ci-dessous). Cette vésicule peut alors être re-capturée par des cellules présentatrices de l'antigène pour une cross-présentation via le CMHI. 2) Chargement sur le CMHII : les autophagosomes peuvent fusionner avec le compartiment de charge du CMH et délivrer ainsi des constituants cytoplasmiques sur le CMHII. *Adapté de Shibutani et al., Nat Immunol, 2015.*[103]

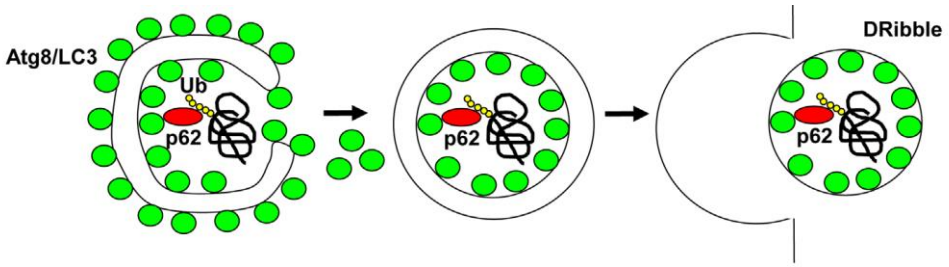

Figure 20: Exocytose des « autophagosomes ». Les protéines ubiquitinilées, incluant des DRiPs (Defective Ribosomal Products), sont séquestrées dans un autophagosome en formation. Lorsque la fusion avec le lysosome est inhibée, l'autophagosome peut fusionner avec la membrane plasmique pour permettre l'exocytose de son contenu. Ainsi, la membrane interne de l'autophagosome (contenant le cargo) est relâchée dans le mileu extra-cellulaire en tant que Dribbles (Defective ribosomal products-containing autophagosome-rich blebs). *Adapté de Christian Münz, Frontiers in Immunology, 2015.* [110]

B-2/ Vaccination anti-ALK : une thérapie d'avenir

Les thérapies anti-cancéreuses à base de vaccins sont étudiées depuis de nombreuses années. Les vaccins à base d'ADN, à base de peptides ou à base de cellules dendritiques activées sont les trois approches thérapeutiques qui ont mobilisé l'attention de nombreux groupes de recherche.[111–113] L'équipe du Dr Roberto Chiarle s'est investie dans le développement d'une thérapie vaccinale contre les cancers dépendants de l'oncogène ALK.[114,115] En effet, l'accumulation de plusieurs arguments sont en faveur du succès d'une telle thérapie : (i) Des études *in vitro* et *in vivo* montrent que les cellules de lymphome ALK positif présentent une addiction pour cet oncogène.[81,116] (ii) L'expression de la protéine ALK native est restreinte à quelques cellules neuronales, minimisant ainsi le risque de réactions autoimmunes suite à la vaccination. (iii) L'oncogène ALK est immunogène. En effet, les patients atteints de LAGC ALK positif sont capables de développer une réponse immunitaire, à la fois humorale et cytotoxique, contre l'oncogène ALK.[117,118] Des anticorps anti-ALK ont été détectés dans le sérum des patients et un titre élevé a été corrélé à un bon pronostic.[119] Ces réponses pourraient être amplifiées par la vaccination. (iv) Des études précliniques, à la fois dans un modèle murin de lymphome NPM-ALK positif et de cancer du poumon non à petites cellules EML4-ALK positif, ont démontré l'efficacité de vaccins anti-ALK à base d'ADN [120,121] ainsi qu'à base de peptide (Dr Chiarle, communication personnelle) pour limiter le développement tumoral, et ce en stimulant une réponse cytotoxique T CD8 positif.

B-3/ Développement d'un vaccin anti-ALK à base d'autophagosomes

Mon projet, en collaboration étroite avec le Dr Chiarle, est de développer un vaccin anti-ALK à base de cellules dendritiques (DCs) activées et de tester son efficacité dans les modèles murins de tumeur ALK positives qu'il a développés (lymphome et cancer du poumon).[65,80] Notre étude comprendra :

-la préparation d'une « suspension enrichie en autophagosomes » (chargés en antigène ALK) à partir de lignées cellulaires (établies à partir de lymphome et cancer du poumon ALK positif murins, lignées disponibles dans le laboratoire du Dr Chiarle). Pour cela, ces lignées seront incubées en présence d'un cocktail de trois drogues : la rapamycine, pour induire l'autophagie ; le bortezomib, pour bloquer le protéasome ; et la chloroquine, pour bloquer la fusion des autophagosomes au lysosome. Par des centrifugations différentielles successives, les autophagosomes (ou Dribbles, Figure 20) secrétés seront récupérés.[106–108]

-l'incubation de cette préparation d'autophagosomes avec des DCs, fraîchement isolés à partir de la moelle osseuse de souris saine, en présence d'un cocktail de cytokines activatrices. L'incorporation des Dribbles dans ces DCs devrait permettre la charge des antigènes tumoraux ALK sur le CMHI (Figure 19). Les DCs ainsi « primées » constituent donc le « Tumor-derived autophagosome vaccine », que j'appellerai ci-dessous le « vaccin autophagosomal ».

B-4/ Evaluation *in vivo* de l'efficacité du vaccin autophagosomal seul et de la combinaison thérapeutique « Crizotinib + inhibition de l'autophagie + vaccin autophagosomal » pour le traitement des tumeurs ALK positive.

Le vaccin autophagosomal sera administré à des souris saines (Figure 21A) ou à des souris développant des tumeurs ALK positive (lymphome ou cancer du poumon) (Figure 21B et C), pour évaluer l'efficacité du vaccin utilisé respectivement en prévention ou en thérapie.

Nous envisageons également d'évaluer les associations thérapeutiques : 1) « Vaccin autophagosomal + Crizotinib » (Figure 21B) ; 2) « Vaccin autophagosomal + Crizotinib + Inhibiteur de l'autophagie cytoprotectrice (induite par le Crizotinib) » (Figure 21C).

Les efficacités de ces traitements seront étudiées et comparées. Les paramètres suivis seront : la survie des animaux ; le développement et la taille des tumeurs (imagerie par résonance magnétique) [121]; le niveau d'autophagie dans les tumeurs (immunohistochimie [122], microscopie électronique); la réponse T cytotoxique *in vivo* [120,123]; l'immunoscore (par immunohistochimie [124]) ; la régression tumorale (apoptose).

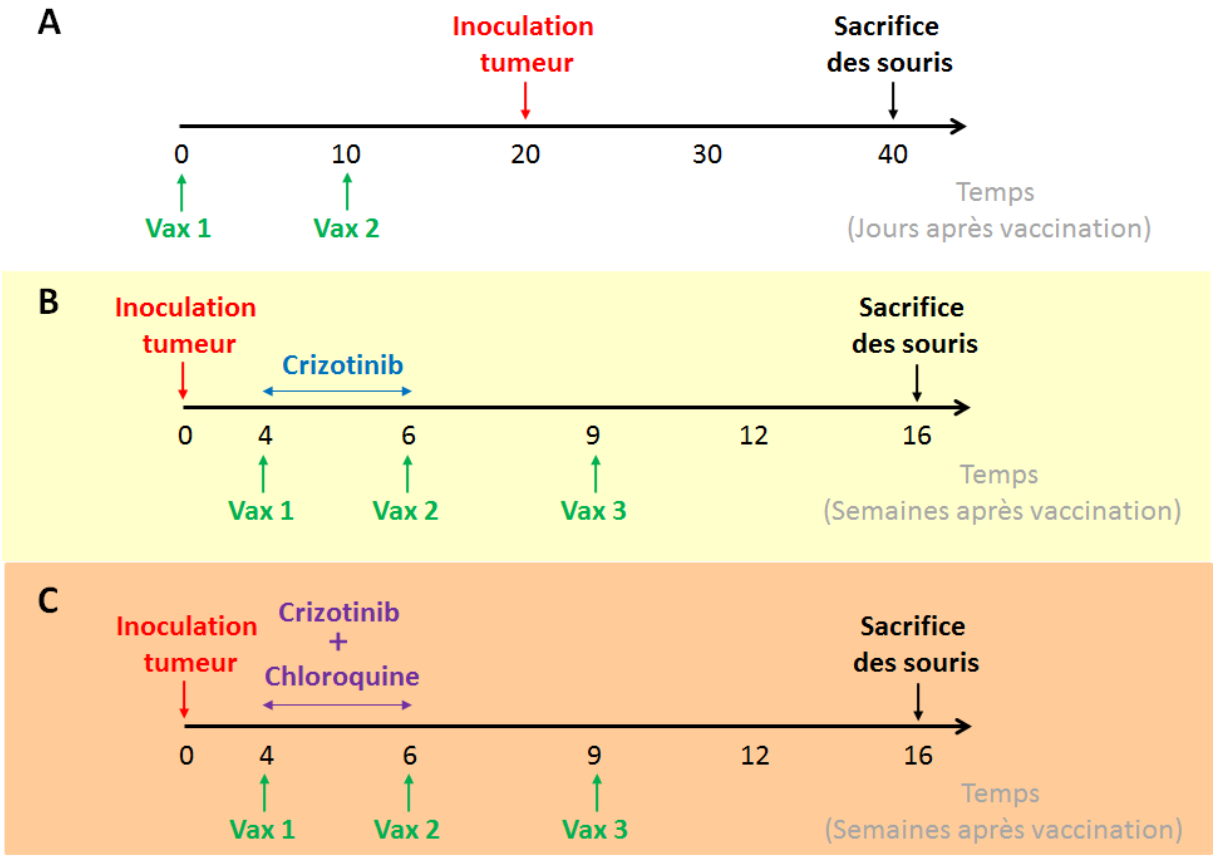

Figure 21 : Représentation schématique des protocoles de vaccination envisagés. A) Utilisation du vaccin en prophylaxie. B et C) Utilisation du vaccin en thérapie. Vax, Vaccination. Les échelles de temps sont données à titre indicatif et nécessiteront des mises au point.

Ce projet complèterait ainsi mes travaux sur l'optimisation des thérapies anti-ALK, après mes études sur l'angiogenèse et l'autophagie cytoprotectrice comme cibles thérapeutiques potentielles. Il me permettrait de tisser une collaboration étroite avec le Dr Chiarle, membre du réseau ERIA. Enfin, il me permettrait de poursuivre, pour un an et dans un cadre scientifique exceptionnel, mes deux thématiques d'intérêt que sont l'étude des tumeurs ALK positive et l'autophagie.

BIBLIOGRAPHIE

1. Sandlund JT. Non-Hodgkin Lymphoma in Children. Curr. Hematol. Malig. Rep. 2015;10:237–43.

2. Wright D, McKeever P, Carter R. Childhood non-Hodgkin lymphomas in the United Kingdom: findings from the UK Children's Cancer Study Group. J. Clin. Pathol. 1997;50:128–34.

3. Tilly H, Gaulard P, Lepage E, Dumontet C, Diebold J, Plantier I, Berger F, Symann M, Petrella T, Lederlin P, Brière J. Primary Anaplastic Large-Cell Lymphoma in Adults: Clinical Presentation, Immunophenotype, and Outcome. Blood 1997;90:3727–34.

4. Sibon D, Fournier M, Brière J, Lamant L, Haioun C, Coiffier B, Bologna S, Morel P, Gabarre J, Hermine O, Sonet A, Gisselbrecht C, Delsol G, et al. Long-term outcome of adults with systemic anaplastic large-cell lymphoma treated within the Groupe d'Étude des Lymphomes de l'Adulte Trials. J. Clin. Oncol. 2012;30:3939–46.

5. Williams D, Mori T, Reiter A, Woessman W, Rosolen A, Wrobel G, Zsiros J, Uyttebroeck A, Marky I, Le Deley MC, Brugières L. Central nervous system involvement in anaplastic large cell lymphoma in childhood: Results from a multicentre European and Japanese study. Pediatr. Blood Cancer 2013;60.

6. Stein H, Mason DY, Gerdes J, O'Connor N, Wainscoat J, Pallesen G, Gatter K, Falini B, Delsol G, Lemke H. The expression of the Hodgkin disease associated antigen Ki-1 in reactive and neoplastic lymphoid tissue: evidence that Reed-Sternberg cells and histiocytic malignancies are derived from activated lymphoid cells. Blood 1985;66:848–58.

7. Morris SW, Kirstein MN, Valentine MB, Dittmer KG, Shapiro DN, Saltman DL, Look AT. Fusion of a kinase gene, ALK, to a nucleolar protein gene, NPM, in non- Hodgkin's lymphoma. Science (80-.). 1994;263:1281–4.

8. Roskoski R. Anaplastic lymphoma kinase (ALK): Structure, oncogenic activation, and pharmacological inhibition. Pharmacol. Res. 2013;68:68–94.

9. Lamant L, Dastugue N, Pulford K, Delsol G, Mariame B. A new fusion gene TPM3-ALK in anaplastic large cell lymphoma created by a (1;2)(q25;p23) translocation. Blood 1999;93:3088–95.

10. Delsol G. The 2008 WHO lymphoma classification. Ann Pathol 2008;28 Spec No:S20–4.

11. Tabbo F, Barreca A, Piva R, Inghirami G. ALK Signaling and Target Therapy in Anaplastic Large Cell Lymphoma. Front Oncol 2012;2:41.

12. Hsi ED, Said J, Macon WR, Rodig SJ, Ondrejka SL, Gascoyne RD, Morgan EA, Dorfman DM, Maurer MJ, Dogan A. Diagnostic accuracy of a defined immunophenotypic and molecular genetic approach for peripheral T/NK-cell lymphomas. A North American PTCL study group project. Am. J. Surg. Pathol. 2014;38:768–75.

13. Bonzheim I, Steinhilber J, Fend F, Lamant L, Quintanilla-Martinez L. ALK-positive anaplastic large cell lymphoma: an evolving story. Front. Biosci. (Schol. Ed). 2015;7:248–59.

14. Bonzheim I, Geissinger E, Roth S, Zettl A, Marx A, Rosenwald A, Müller-Hermelink HK, Rüdiger T. Anaplastic large cell lymphomas lack the expression of T-cell receptor molecules or molecules of proximal T-cell receptor signaling. Blood 2004;104:3358–60.

15. Ambrogio C, Martinengo C, Voena C, Tondat F, Riera L, di Celle PF, Inghirami G, Chiarle R. NPM-ALK oncogenic tyrosine kinase controls T-cell identity by transcriptional regulation and epigenetic silencing in lymphoma cells. Cancer Res 2009;69:8611–9.

16. Turner SD, Lamant L, Kenner L, Brugières L. Anaplastic large cell lymphoma in paediatric and young adult patients. Br. J. Haematol. 2016.

17. Malcolm TIM, Villarese P, Fairbairn CJ, Lamant L, Trinquand A, Hook CE, Burke GAA, Brugieres L, Hughes K, Payet D, Merkel O, Schiefer A-I, Ashankyty I, et al. Anaplastic large cell lymphoma arises in thymocytes and requires transient TCR expression for thymic egress. Nat Commun 2016 12;7.

18. Cools J, Wlodarska I, Somers R, Mentens N, Pedeutour F, Maes B, De Wolf-Peeters C, Pauwels P, Hagemeijer A, Marynen P. Identification of novel fusion partners of ALK, the anaplastic lymphoma kinase, in anaplastic large-cell lymphoma and inflammatory myofibroblastic tumor. Genes Chromosom. Cancer 2002;34:354–62.

19. Hernandez L, Pinyol M, Hernandez S, Bea S, Pulford K, Rosenwald A, Lamant L, Falini B, Ott G, Mason DY, Delsol G, Campo E. TRK-fused gene (TFG) is a new partner of ALK in anaplastic large cell lymphoma producing two structurally different TFG-ALK translocations. Blood 1999;94:3265–8.

20. Tort F, Pinyol M, Pulford K, Roncador G, Hernandez L, Nayach I, Kluin-Nelemans HC, Kluin P, Touriol C, Delsol G, Mason D, Campo E. Molecular characterization of a new ALK translocation involving moesin (MSN-ALK) in anaplastic large cell lymphoma. Lab Invest 2001;81:419–26.

21. Meech SJ, McGavran L, Odom LF, Liang X, Meltesen L, Gump J, Wei Q, Carlsen S, Hunger SP. Unusual childhood extramedullary hematologic malignancy with natural killer cell properties that contains tropomyosin 4--anaplastic lymphoma kinase gene fusion. Blood 2001;98:1209–16.

22. Colleoni GW, Bridge JA, Garicochea B, Liu J, Filippa DA, Ladanyi M. ATIC-ALK: A novel variant ALK gene fusion in anaplastic large cell lymphoma resulting from the recurrent cryptic chromosomal inversion, inv(2)(p23q35). Am J Pathol 2000;156:781–9.

23. Lamant L, Gascoyne RD, Duplantier MM, Armstrong F, Raghab A, Chhanabhai M, Rajcan-Separovic E, Raghab J, Delsol G, Espinos E. Non-muscle myosin heavy chain (MYH9): a new partner fused to ALK in anaplastic large cell lymphoma. Genes Chromosom. Cancer 2003;37:427–32.

24. Touriol C, Greenland C, Lamant L, Pulford K, Bernard F, Rousset T, Mason DY, Delsol G. Further demonstration of the diversity of chromosomal changes involving 2p23 in ALK-positive lymphoma: 2 cases expressing ALK kinase fused to CLTCL (clathrin chain polypeptide-like). Blood 2000;95:3204–7.

25. Feldman AL, Vasmatzis G, Asmann YW, Davila J, Middha S, Eckloff BW, Johnson SH, Porcher JC, Ansell SM, Caride A. Novel TRAF1-ALK fusion identified by deep RNA sequencing of anaplastic large cell lymphoma. Genes Chromosom. Cancer 2013;52:1097–102.

26. Swerdlow SH, Campo E, Harris NL, Jaffe ES, Pileri SA, Stein H, Thiele J, Vardiman JW. WHO Classification of Tumours of Haematopoietic and Lymphoid Tissues. 2008.

27. Marzec M, Halasa K, Liu X, Wang HY, Cheng M, Baldwin D, Tobias JW, Schuster SJ, Woetmann A, Zhang Q, Turner SD, Odum N, Wasik MA. Malignant transformation of CD4+ T lymphocytes mediated by oncogenic kinase NPM/ALK recapitulates IL-2-induced cell signaling and gene expression reprogramming. J Immunol 2013;191:6200–7.

28. Newrzela S, Al-Ghaili N, Heinrich T, Petkova M, Hartmann S, Rengstl B, Kumar A, Jack HM, Gerdes S, Roeder I, Hansmann ML, von Laer D. T-cell receptor diversity prevents T-cell lymphoma development. Leukemia 2012;26:2499–507.

29. Moti N, Malcolm T, Hamoudi R, Mian S, Garland G, Hook CE, Burke G a a, Wasik M a, Merkel O, Kenner L, Laurenti E, Dick JE, Turner SD. Anaplastic large cell lymphoma-propagating cells are detectable by side population analysis and possess an expression profile reflective of a primitive origin. Oncogene 2014;1–10.

30. Laurent C, Lopez C, Desjobert C, Berrebi A, Damm-Welk C, Delsol G, Brousset P, Lamant L. Circulating t(2;5)-positive cells can be detected in cord blood of healthy newborns. Leukemia 2012;26:188–90.

31. Lamant L, Pileri S, Sabattini E, Brugières L, Jaffe ES, Delsol G. Cutaneous presentation of ALK-positive anaplastic large cell lymphoma following insect bites: Evidence for an association in five cases. Haematologica 2010;95:449–55.

32. Duyster J, Bai RY, Morris SW. Translocations involving anaplastic lymphoma kinase (ALK). Oncogene 2001;20:5623–37.

33. Zamo A, Chiarle R, Piva R, Howes J, Fan Y, Chilosi M, Levy DE, Inghirami G. Anaplastic lymphoma kinase (ALK) activates Stat3 and protects hematopoietic cells from cell death. Oncogene 2002;21:1038–47.

34. Chiarle R, Simmons WJ, Cai H, Dhall G, Zamo A, Raz R, Karras JG, Levy DE, Inghirami G. Stat3 is required for ALK-mediated lymphomagenesis and provides a possible therapeutic target. Nat Med 2005;11:623–9.

35. Bai RY, Ouyang T, Miething C, Morris SW, Peschel C, Duyster J. Nucleophosmin-anaplastic lymphoma kinase associated with anaplastic large-cell lymphoma activates the phosphatidylinositol 3-kinase/Akt antiapoptotic signaling pathway. Blood 2000;96:4319–27.

36. Marzec M, Kasprzycka M, Liu X, El-Salem M, Halasa K, Raghunath PN, Bucki R, Wlodarski P, Wasik MA. Oncogenic tyrosine kinase NPM/ALK induces activation of the rapamycin-sensitive mTOR signaling pathway. Oncogene 2007;26:5606–14.

37. Marzec M, Kasprzycka M, Liu X, Raghunath PN, Wlodarski P, Wasik MA. Oncogenic tyrosine kinase NPM/ALK induces activation of the MEK/ERK signaling pathway independently of c-Raf. Oncogene 2007;26:813–21.

38. Turner SD, Yeung D, Hadfield K, Cook SJ, Alexander DR. The NPM-ALK tyrosine kinase mimics TCR signalling pathways, inducing NFAT and AP-1 by RAS-dependent mechanisms. Cell. Signal. 2007;19:740–7.

39. Bai RY, Dieter P, Peschel C, Morris SW, Duyster J. Nucleophosmin-anaplastic lymphoma kinase of large-cell anaplastic lymphoma is a constitutively active tyrosine kinase that utilizes phospholipase C-gamma to mediate its mitogenicity. Mol Cell Biol 1998;18:6951–61.

40. Cussac D, Greenland C, Roche S, Bai RY, Duyster J, Morris SW, Delsol G, Allouche M, Payrastre B. Nucleophosmin-anaplastic lymphoma kinase of anaplastic large-cell lymphoma recruits, activates and uses pp60c-src to mediate its mitogenicity. Blood 2003;16:16.

41. Chiarle R, Voena C, Ambrogio C, Piva R, Inghirami G. The anaplastic lymphoma kinase in the pathogenesis of cancer. Nat Rev Cancer 2008;8:11–23.

42. Lai R, Ingham RJ. The pathobiology of the oncogenic tyrosine kinase NPM-ALK: a brief update. Ther Adv Hematol 2013;4:119–31.

43. Pearson JD, Lee JK, Bacani JT, Lai R, Ingham RJ. NPM-ALK: The Prototypic Member of a Family of Oncogenic Fusion Tyrosine Kinases. J Signal Transduct 2012;2012:123253.

44. Lowe EJ, Lim MS. Potential therapies for anaplastic lymphoma kinase-driven tumors in children: progress to date. Paediatr. Drugs 2013;15:163–9.

45. Brugieres L, Deley MC Le, Rosolen A, Williams D, Horibe K, Wröbel G, Uyttebroeck A, Beishuizen A, Mann G, Mellgren K, Reiter A. ANAPLASTIC LARGE CELL LYMPHOMA (ALCL) IN CHILDREN: RESULTS OF THE ALCL99-R1 RANDOMISED TRIAL. Pediatr. Blood Cancer 2007;49:420.

46. Le Deley MC, Rosolen A, Williams DM, Horibe K, Wrobel G, Attarbaschi A, Zsiros J, Uyttebroeck A, Marky IM, Lamant L, Woessmann W, Pillon M, Hobson R, et al. Vinblastine in children and adolescents with high-risk anaplastic large-cell lymphoma: Results of the randomized ALCL99-vinblastine trial. J. Clin. Oncol. 2010;28:3987–93.

47. Woessmann W, Zimmermann M, Lenhard M, Burkhardt B, Rossig C, Kremens B, Lang P, Attarbaschi A, Mann G, Oschlies I, Klapper W, Reiter A. Relapsed or refractory anaplastic large-cell lymphoma in children and adolescents after Berlin-Frankfurt-Muenster (BFM)-type first-line therapy: A BFM-Group study. J. Clin. Oncol. 2011;29:3065–71.

48. Ruf S, Brugieres L, Pillon M, Zimmermann M, Attarbaschi A, Mellgren K, Williams D, Uyttebroeck A, Wrobel G, Reiter A, Woessmann W. Risk-adapted therapy for patients with relapsed or refractory ALCL – final report of the prospective ALCL-relapse trial of the EICNHL. Br. J. Haematol. 2015;171:78.

49. Cui JJ, Tran-Dubé M, Shen H, Nambu M, Kung PP, Pairish M, Jia L, Meng J, Funk L, Botrous I, McTigue M, Grodsky N, Ryan K, et al. Structure based drug design of crizotinib (PF-02341066), a potent and selective dual inhibitor of mesenchymal-epithelial transition factor (c-MET) kinase and anaplastic lymphoma kinase (ALK). J. Med. Chem. 2011;54:6342–63.

50. Christensen JG, Zou HY, Arango ME, Li Q, Lee JH, McDonnell SR, Yamazaki S, Alton GR, Mroczkowski B, Los G. Cytoreductive antitumor activity of PF-2341066, a novel inhibitor of anaplastic lymphoma kinase and c-Met, in experimental models of anaplastic large-cell lymphoma. Mol Cancer Ther 2007;6:3314–22.

51. Gambacorti-Passerini C, Messa C, Pogliani EM. Crizotinib in anaplastic large-cell lymphoma. N Engl J Med 2010;364:775–6.

52. Gambacorti Passerini C, Farina F, Stasia A, Redaelli S, Ceccon M, Mologni L, Messa C, Guerra L, Giudici G, Sala E, Mussolin L, Deeren D, King MH, et al. Crizotinib in advanced, chemoresistant anaplastic lymphoma kinase-positive lymphoma patients. J Natl Cancer Inst 2014;106:djt378.

53. Mosse YP, Lim MS, Voss SD, Wilner K, Ruffner K, Laliberte J, Rolland D, Balis FM, Maris JM, Weigel BJ, Ingle AM, Ahern C, Adamson PC, et al. Safety and activity of crizotinib for paediatric patients with refractory solid tumours or anaplastic large-cell lymphoma: a Children's Oncology Group phase 1 consortium study. Lancet Oncol 2013;14:472–80.

54. Ceccon M, Mologni L, Bisson W, Scapozza L, Gambacorti-Passerini C. Crizotinib-resistant NPM-ALK mutants confer differential sensitivity to unrelated Alk inhibitors. Mol Cancer Res 2013;11:122–32.

55. Crescenzo R, Inghirami G. Anaplastic lymphoma kinase inhibitors. Curr. Opin. Pharmacol. 2015;23:39–44.

56. Mologni L. Current and future treatment of anaplastic lymphoma kinase-rearranged cancer. World J. Clin. Oncol. 2015;6:104–8.

57. Dejean E, Renalier MH, Foisseau M, Agirre X, Joseph N, de Paiva GR, Al Saati T, Soulier J, Desjobert C, Lamant L, Prosper F, Felsher DW, Cavaille J, et al. Hypoxia-microRNA-16 downregulation induces VEGF expression in anaplastic lymphoma kinase (ALK)-positive anaplastic large-cell lymphomas. Leukemia 2011;25:1882–90.

58. Mitou G, Frentzel J, Desquesnes A, Le Gonidec S, AlSaati T, Beau I, Lamant L, Meggetto F, Espinos E, Codogno P, Brousset P, Giuriato S. Targeting autophagy enhances the anti-tumoral action of crizotinib in ALK-positive anaplastic large cell lymphoma. Oncotarget 2015 6;6:30149–64.

59. Giuriato S, Felsher DW. How cancers escape their oncogene habit. Cell Cycle 2003;2:329–32.

60. Giuriato S, Rabin K, Fan AC, Shachaf CM, Felsher DW. Conditional animal models: A strategy to define when oncogenes will be effective targets to treat cancer. Semin. Cancer Biol. 2004;14:3–11.

61. Giuriato S, Ryeom S, Fan AC, Bachireddy P, Lynch RC, Rioth MJ, van Riggelen J, Kopelman AM, Passegué E, Tang F, Folkman J, Felsher DW. Sustained regression of tumors upon MYC inactivation requires p53 or thrombospondin-1 to reverse the angiogenic switch. Proc. Natl. Acad. Sci. U. S. A. 2006;103:16266–71.

62. Tran PT, Fan AC, Bendapudi PK, Koh S, Komatsubara K, Chen J, Horng G, Bellovin DI, Giuriato S, Wang CS, Whitsett JA, Felsher DW. Combined inactivation of MYC and K-ras oncogenes reverses tumorigenesis in lung adenocarcinomas and lymphomas. PLoS One 2008;3.

63. Turner SD, Tooze R, Maclennan K, Alexander DR. Vav-promoter regulated oncogenic fusion protein NPM-ALK in transgenic mice causes B-cell lymphomas with hyperactive Jun kinase. Oncogene 2003;22:7750–61.

64. Turner SD, Alexander DR. What have we learnt from mouse models of NPM-ALK-induced lymphomagenesis? Leukemia 2005;19:1128–34.

65. Chiarle R, Gong JZ, Guasparri I, Pesci A, Cai J, Liu J, Simmons WJ, Dhall G, Howes J, Piva R, Inghirami G. NPM-ALK transgenic mice spontaneously develop T-cell lymphomas and plasma cell tumors. Blood 2003;101:1919–27.

66. Gossen M, Bujard H. Tight control of gene expression in mammalian cells by tetracycline-responsive promoters. Proc Natl Acad Sci U S A 1992;89:5547–51.

67. Kistner A, Gossen M, Zimmermann F, Jerecic J, Ullmer C, Lubbert H, Bujard H. Doxycycline-mediated quantitative and tissue-specific control of gene expression in transgenic mice. Proc Natl Acad Sci U S A 1996;93:10933–8.

68. Turturro F, Arnold MD, Frist AY, Pulford K. Model of inhibition of the NPM-ALK kinase activity by herbimycin A. Clin Cancer Res 2002;8:240–5.

69. Giuriato S, Faumont N, Bousquet E, Foisseau M, Bibonne A, Moreau M, Al Saati T, Felsher DW, Delsol G, Meggetto F. Development of a conditional bioluminescent transplant model for TPM3-ALK-induced tumorigenesis as a tool to validate ALK-dependent cancer targeted therapy. Cancer Biol. Ther. 2007;6:1318–23.

70. Felsher DW, Bishop JM. Reversible tumorigenesis by MYC in hematopoietic lineages. Mol Cell 1999;4:199–207.

71. Harris AW, Langdon WY, Alexander WS, Hariharan IK, Rosenbaum H, Vaux D, Webb E, Bernard O, Crawford M, Abud H, et al. Transgenic mouse models for hematopoietic tumorigenesis. Curr Top Microbiol Immunol 1988;141:82–93.

72. van Lohuizen M, Verbeek S, Krimpenfort P, Domen J, Saris C, Radaszkiewicz T, Berns A. Predisposition to lymphomagenesis in pim-1 transgenic mice: cooperation with c-myc and N-myc in murine leukemia virus-induced tumors. Cell 1989;56:673–82.

73. Moroy T, Fisher P, Guidos C, Ma A, Zimmerman K, Tesfaye A, DePinho R, Weissman I, Alt FW. IgH enhancer deregulated expression of L-myc: abnormal T lymphocyte development and T cell lymphomagenesis. Embo J 1990;9:3659–66.

74. Carron C, Cormier F, Janin A, Lacronique V, Giovannini M, Daniel MT, Bernard O, Ghysdael J. TEL-JAK2 transgenic mice develop T-cell leukemia. Blood 2000;95:3891–9.

75. Kwon H, Ogle L, Benitez B, Bohuslav J, Montano M, Felsher DW, Greene WC. Lethal cutaneous disease in transgenic mice conditionally expressing type I human T cell leukemia virus Tax. J Biol Chem 2005;280:35713–22.

76. Giuriato S, Turner SD. Twenty years of modelling NPM-ALK-induced lymphomagenesis. Front Biosci (Schol Ed) 2015;7:236–47.

77. Kuefer MU, Look AT, Pulford K, Behm FG, Pattengale PK, Mason DY, Morris SW. Retrovirus-mediated gene transfer of NPM-ALK causes lymphoid malignancy in mice. Blood 1997;90:2901–10.

78. Miething C, Grundler R, Fend F, Hoepfl J, Mugler C, von Schilling C, Morris SW, Peschel C, Duyster J. The oncogenic fusion protein nucleophosmin-anaplastic lymphoma kinase (NPM-ALK) induces two distinct malignant phenotypes in a murine retroviral transplantation model. Oncogene 2003;22:4642–7.

79. Piganeau M, Ghezraoui H, De Cian A, Guittat L, Tomishima M, Perrouault L, Rene O, Katibah GE, Zhang L, Holmes MC, Doyon Y, Concordet JP, Giovannangeli C, et al. Cancer translocations in human cells induced by zinc finger and TALE nucleases. Genome Res 2013;23:1182–93.

80. Blasco RB, Karaca E, Ambrogio C, Cheong T-C, Karayol E, Minero VG, Voena C, Chiarle R. Simple and rapid in vivo generation of chromosomal rearrangements using CRISPR/Cas9 technology. Cell Rep. 2014 20;9:1219–27.

81. Giuriato S, Foisseau M, Dejean E, Felsher DW, Al Saati T, Demur C, Ragab A, Kruczynski A, Schiff C, Delsol G, Meggetto F. Conditional TPM3-ALK and NPM-ALK transgenic mice develop reversible ALK-positive early B-cell lymphoma/leukemia. Blood 2010;115:4061–70.

82. Folkman J. Tumor angiogenesis: therapeutic implications. N Engl J Med 1971;285:1182–6.

83. Moehler TM, Ho AD, Goldschmidt H, Barlogie B. Angiogenesis in hematologic malignancies. Crit. Rev. Oncol. Hematol. 2003;45:227–44.

84. Koster A, Raemaekers JM. Angiogenesis in malignant lymphoma. Curr Opin Oncol 2005;17:611–6.

85. Ruan J, Hajjar K, Rafii S, Leonard JP. Angiogenesis and antiangiogenic therapy in non-Hodgkin's lymphoma. Ann. Oncol. 2009;20:413–24.

86. Bastide A, Karaa Z, Bornes S, Hieblot C, Lacazette E, Prats H, Touriol C. An upstream open reading frame within an IRES controls expression of a specific VEGF-A isoform. Nucleic Acids Res. 2008;36:2434–45.

87. Touriol C, Bornes S, Bonnal S, Audigier S, Prats H, Prats AC, Vagner S. Generation of protein isoform diversity by alternative initiation of translation at non-AUG codons. Biol. Cell 2003;95:169–78.

88. Hua Z, Lv Q, Ye W, Wong CKA, Cai G, Gu D, Ji Y, Zhao C, Wang J, Yang BB, Zhang Y. Mirna-directed regulation of VEGF and other angiogenic under hypoxia. PLoS One 2006;1.

89. Krol J, Loedige I, Filipowicz W. The widespread regulation of microRNA biogenesis, function and decay. Nat. Rev. Genet. 2010;11:597–610.

90. Marzec M, Liu X, Wong W, Yang Y, Pasha T, Kantekure K, Zhang P, Woetmann A, Cheng M, Odum N, Wasik MA. Oncogenic kinase NPM/ALK induces expression of HIF1alpha mRNA. Oncogene 2011;30:1372–8.

91. Di Paolo D, Ambrogio C, Pastorino F, Brignole C, Martinengo C, Carosio R, Loi M, Pagnan G, Emionite L, Cilli M, Ribatti D, Allen TM, Chiarle R, et al. Selective therapeutic targeting of the anaplastic lymphoma kinase with liposomal siRNA induces apoptosis and inhibits angiogenesis in neuroblastoma. Mol. Ther. 2011;19:2201–12.

92. Martinengo C, Poggio T, Menotti M, Scalzo MS, Mastini C, Ambrogio C, Pellegrino E, Riera L, Piva R, Ribatti D, Pastorino F, Perri P, Ponzoni M, et al. ALK-dependent control of hypoxia-inducible factors mediates tumor growth and metastasis. Cancer Res. 2014 1;74:6094–106.

93. Levine B, Klionsky DJ. Development by self-digestion: molecular mechanisms and biological functions of autophagy. Dev Cell 2004;6:463–77.

94. Fulda S, Kögel D. Cell death by autophagy: emerging molecular mechanisms and implications for cancer therapy. Oncogene 2015 1;34:5105–13.

95. Rosenfeldt MT, Ryan KM. The role of autophagy in tumour development and cancer therapy. Expert Rev Mol Med 2009;11:e36.

96. Klionsky DJ, Abdalla FC, Abeliovich H, Abraham RT, Acevedo-Arozena A, Adeli K, Agholme L, Agnello M, Agostinis P, Aguirre-Ghiso JA, Ahn HJ, Ait-Mohamed O, Ait-Si-Ali S, et al. Guidelines for the use and interpretation of assays for monitoring autophagy. Autophagy 2012;8:445–544.

97. Mizushima N, Yoshimori T, Levine B. Methods in mammalian autophagy research. Cell 2010;140:313–26.

98. Galluzzi L, Pietrocola F, Pedro JMB, Amaravadi RK, Baehrecke EH, Cecconi F, Codogno P, Debnath J, Gewirtz DA, Karantza V, Kimmelman A, Kumar S, Levine B, et al. Autophagy in malignant transformation and cancer progression. EMBO J. 2015;34:e201490784.

99. Zhai H, Fesler A, Ju J. MicroRNA: a third dimension in autophagy. Cell Cycle 2013;12:246–50.

100. Gump JM, Thorburn A. Sorting cells for basal and induced autophagic flux by quantitative ratiometric flow cytometry. Autophagy 2014;10:1327–34.

101. Gewirtz DA. The four faces of autophagy: implications for cancer therapy. Cancer Res 2014;74:647–51.

102. Wilson EN, Bristol ML, Di X, Maltese WA, Koterba K, Beckman MJ, Gewirtz DA. A switch between cytoprotective and cytotoxic autophagy in the radiosensitization of breast tumor cells by chloroquine and vitamin D. Horm Cancer 2011;2:272–85.

103. Shibutani ST, Saitoh T, Nowag H, Münz C, Yoshimori T. Autophagy and autophagy-related proteins in the immune system. Nat. Immunol. 2015;16:1014–24.

104. Schmid D, Pypaert M, Münz C. Antigen-loading compartments for major histocompatibility complex class II molecules continuously receive input from autophagosomes. Immunity 2007;26:79–92.

105. Tey SK, Khanna R. Autophagy mediates transporter associated with antigen processing-independent presentation of viral epitopes through MHC class I pathway. Blood 2012;120:994–1004.

106. Li Y, Wang L-X, Yang G, Hao F, Urba WJ, Hu H-M. Efficient cross-presentation depends on autophagy in tumor cells. Cancer Res. 2008 1;68:6889–95.

107. Su H, Luo Q, Xie H, Huang X, Ni Y, Mou Y, Hu Q. Therapeutic antitumor efficacy of tumor-derived autophagosome (DRibble) vaccine on head and neck cancer. Int. J. Nanomedicine 2015;10:1921–30.

108. Li Y, Wang L-X, Pang P, Cui Z, Aung S, Haley D, Fox BA, Urba WJ, Hu H-M. Tumor-derived autophagosome vaccine: mechanism of cross-presentation and therapeutic efficacy. Clin. Cancer Res. 2011 15;17:7047–57.

109. Su S, Zhou H, Xue M, Liu JY, Ding L, Cao M, Zhou ZX, Hu HM, Wang LX. Anti-tumor efficacy of a hepatocellular carcinoma vaccine based on dendritic cells combined with tumor-derived autophagosomes in murine models. Asian Pacific J. Cancer Prev. 2013;14:3109–16.

110. Münz C. Of LAP, CUPS, and DRibbles - Unconventional Use of Autophagy Proteins for MHC Restricted Antigen Presentation. Front. Immunol. 2015;6:200.

111. Pol J, Bloy N, Obrist F, Eggermont A, Galon J, Hervé Fridman W, Cremer I, Zitvogel L, Kroemer G, Galluzzi L. Trial Watch: DNA vaccines for cancer therapy. Oncoimmunology 2014 1;3:e28185.

112. Pol J, Bloy N, Buqué A, Eggermont A, Cremer I, Sautès-Fridman C, Galon J, Tartour E, Zitvogel L, Kroemer G, Galluzzi L. Trial Watch: Peptide-based anticancer vaccines. Oncoimmunology 2015;4:e974411.

113. Bloy N, Pol J, Aranda F, Eggermont A, Cremer I, Fridman WH, Fučíková J, Galon J, Tartour E, Spisek R, Dhodapkar M V, Zitvogel L, Kroemer G, et al. Trial watch: Dendritic cell-based anticancer therapy. Oncoimmunology 2014;3:e963424.

114. Mastini C, Martinengo C, Inghirami G, Chiarle R. Anaplastic lymphoma kinase: an oncogene for tumor vaccination. J. Mol. Med. (Berl). 2009;87:669–77.

115. Voena C, Peola S, Chiarle R. The anaplastic lymphoma kinase as an oncogene in solid tumors. Front. Biosci. (Schol. Ed). 2015;7:269–82.

116. Piva R, Chiarle R, Manazza AD, Taulli R, Simmons W, Ambrogio C, D'Escamard V, Pellegrino E, Ponzetto C, Palestro G, Inghirami G. Ablation of oncogenic ALK is a viable therapeutic approach for anaplastic large-cell lymphomas. Blood 2006;107:689–97.

117. Ait-Tahar K, Cerundolo V, Banham AH, Hatton C, Blanchard T, Kusec R, Becker M, Smith GL, Pulford K. B and CTL responses to the ALK protein in patients with ALK-positive ALCL. Int. J. Cancer 2006 1;118:688–95.

118. Passoni L, Gallo B, Biganzoli E, Stefanoni R, Massimino M, Di Nicola M, Gianni AM, Gambacorti-Passerini C. In vivo T-cell immune response against anaplastic lymphoma kinase in patients with anaplastic large cell lymphomas. Haematologica 2006;91:48–55.

119. Ait-Tahar K, Damm-Welk C, Burkhardt B, Zimmermann M, Klapper W, Reiter A, Pulford K, Woessmann W. Correlation of the autoantibody response to the ALK oncoantigen in pediatric anaplastic lymphoma kinase-positive anaplastic large cell lymphoma with tumor dissemination and relapse risk. Blood 2010 22;115:3314–9.

120. Chiarle R, Martinengo C, Mastini C, Ambrogio C, D'Escamard V, Forni G, Inghirami G. The anaplastic lymphoma kinase is an effective oncoantigen for lymphoma vaccination. Nat. Med. 2008;14:676–80.

121. Voena C, Menotti M, Mastini C, Di Giacomo F, Longo DL, Castella B, Merlo MEB, Ambrogio C, Wang Q, Minero VG, Poggio T, Martinengo C, D'Amico L, et al. Efficacy of a Cancer Vaccine against ALK-Rearranged Lung Tumors. Cancer Immunol. Res. 2015 29;3:1333–43.

122. Schläfli AM, Berezowska S, Adams O, Langer R, Tschan MP. Reliable LC3 and p62 autophagy marker detection in formalin fixed paraffin embedded human tissue by immunohistochemistry. Eur. J. Histochem. 2015;59:2481.

123. Ingulli E. Tracing tolerance and immunity in vivo by CFSE-labeling of administered cells. Methods Mol. Biol. 2007;380:365–76.

124. Galon J, Mlecnik B, Bindea G, Angell HK, Berger A, Lagorce C, Lugli A, Zlobec I, Hartmann A, Bifulco C, Nagtegaal ID, Palmqvist R, Masucci G V, et al. Towards the introduction of the "Immunoscore" in the classification of malignant tumours. J. Pathol. 2014;232:199–209.

PRINCIPALES PUBLICATIONS

Article 1

Sustained regression of tumors upon MYC inactivation requires p53 or thrombospondin-1 to reverse the angiogenic switch

Sylvie Giuriato, Sandra Ryeom, Alice C. Fan, Pavan Bachireddy, Ryan C. Lynch, Matthew J. Rioth, Jan van Riggelen, Andrew M. Kopelman, Emmanuelle Passegué, Flora Tang, Judah Folkman and Dean W. Felsher

PNAS

Vol. 103, No. 44, Issue of October 31, pp. 16266–16271, 2006

Sustained regression of tumors upon MYC inactivation requires p53 or thrombospondin-1 to reverse the angiogenic switch

Sylvie Giuriato*†, Sandra Ryeom‡, Alice C. Fan*, Pavan Bachireddy*, Ryan C. Lynch‡, Matthew J. Rioth‡, Jan van Riggelen*, Andrew M. Kopelman*, Emmanuelle Passegué§¶, Flora Tang*, Judah Folkman‡, and Dean W. Felsher*‖

*Departments of Medicine and Pathology, Division of Oncology, Stanford University School of Medicine, CCSR Building, Room 1120, 269 Campus Drive, Stanford, CA 94305-5151; ‡Department of Surgery, Vascular Biology Program, Children's Hospital Boston and Harvard Medical School, Karp 12.129, 300 Longwood Avenue, Boston, MA 02115; and §Department of Pathology, Stanford University School of Medicine, B259 Beckman Center, 279 Campus Drive, Stanford, CA 94305

Contributed by Judah Folkman, September 13, 2006

The targeted inactivation of oncogenes offers a rational therapeutic approach for the treatment of cancer. However, the therapeutic inactivation of a single oncogene has been associated with tumor recurrence. Therefore, it is necessary to develop strategies to override mechanisms of tumor escape from oncogene dependence. We report here that the targeted inactivation of MYC is sufficient to induce sustained regression of hematopoietic tumors in transgenic mice, except in tumors that had lost p53 function. p53 negative tumors were unable to be completely eliminated, as demonstrated by the kinetics of tumor cell elimination revealed by bioluminescence imaging. Histological examination revealed that upon MYC inactivation, the loss of p53 led to a deficiency in thrombospondin-1 (TSP-1) expression, a potent antiangiogenic protein, and the subsequent inability to shut off angiogenesis. Restoration of p53 expression in these tumors re-established TSP-1 expression. This permitted the suppression of angiogenesis and subsequent sustained tumor regression upon MYC inactivation. Similarly, the restoration of TSP-1 alone in p53 negative tumors resulted in the shut down of angiogenesis and led to sustained tumor regression upon MYC inactivation. Hence, the complete regression of tumor mass driven by inactivation of the MYC oncogene requires the p53-dependent induction of TSP-1 and the shut down of angiogenesis. Notably, overexpression of TSP-1 alone did not influence tumor growth. Therefore, the combined inactivation of oncogenes and angiogenesis may be a more clinically effective treatment of cancer. We conclude that angiogenesis is an essential component of oncogene addiction.

tumorigenesis | angiogenesis inhibitors

Cancers harbor multiple genetic lesions contributing to tumorigenesis through the disruption of the normal function of proto-oncogenes and/or tumor suppressor genes (1, 2). The targeted repair of these mutant gene products may be a specific and effective therapy. For example, the use of Imatinib specifically inactivates the bcr-*abl* oncogene for the treatment of chronic myelogenous leukemia (3).

The notion that tumorigenesis can be reversed through the targeted inactivation of oncogenes has been broadly demonstrated through conditional transgenic models (4, 5). Previously, we have demonstrated that inactivation of MYC can induce sustained tumor regression even in highly genomically complex and unstable hematopoietic tumors (6); furthermore, the brief inactivation of MYC can induce sustained tumor regression in some tumors (7). MYC inactivation induces a state of tumor dormancy in yet other types of cancers, such as hepatocellular carcinoma (8). Thus, tumors appear to become "addicted" to oncogenes, but the consequences of oncogene inactivation depend on the cellular and genetic context (4, 9, 10).

Cancers escape oncogene dependence by acquiring other events (6, 11–15), thus becoming resistant to oncogene inactivation (14, 16). Understanding the molecular mechanisms of tumor escape from oncogene dependence may lead to the development of more effective targeted therapeutics for cancer treatment (15, 17, 18).

Here, we demonstrate that inactivation of MYC fails to induce the complete and sustained regression of hematopoietic tumors that have lost p53 expression. Moreover, we show that this defect in tumor regression is associated with the loss of the antiangiogenic regulator thrombospondin-1 (TSP-1) (19). Restoration of either p53 or TSP-1 in p53 negative tumors was sufficient to reverse the angiogenic switch (20) and restore sustained tumor regression upon MYC inactivation. Hence, MYC inactivation combined with antiangiogenic therapy may be a previously undescribed strategy for the treatment of cancer.

Results

MYC Inactivation Induces the Sustained Regression of Specific Hematopoietic Tumors. Previously, we have described a conditional mouse model for MYC-induced tumorigenesis in hematopoietic cells. To achieve inducible and reversible MYC transgene expression, we used the tetracycline regulatory system (Tet system). To drive MYC transgene expression to the hematopoietic lineage, we used the Ig heavy chain enhancer and the SRα promoter (EμSR) (21). Using this system, MYC overexpression in hematopoietic cells occurs in the absence of doxycycline and is repressed upon addition of doxycycline to the drinking water. MYC overexpression resulted in aggressive lymphoma development (mean survival: 10 weeks; Fig. 5*A*, which is published as supporting information on the PNAS web site) (21). Continuous doxycycline treatment led to sustained MYC inactivation and resulted in the regression of tumors in all mice (21). Notably, 40% of mice remained tumor free and alive at 50 weeks (Fig. 1*A*) (21). We then investigated whether even brief MYC inactivation could induce sustained regression of primary hematopoietic tumors. MYC transgene expression was suppressed for 10 days in cohorts of transgenic mouse moribund with primary hematopoietic tumors (Fig. 1*A*). Brief inactivation of MYC expres-

Author contributions: S.G., S.R., A.C.F., P.B., A.M.K., J.F., and D.W.F. designed research; S.G., S.R., A.C.F., P.B., R.C.L., M.J.R., J.v.R., A.M.K., E.P., and F.T. performed research; S.G. and D.W.F. contributed new reagents/analytic tools; S.G., S.R., A.C.F., P.B., R.C.L., M.J.R., J.F., and D.W.F. analyzed data; and S.G., S.R., A.C.F., J.F., and D.W.F. wrote the paper.

The authors declare no conflict of interest.

Abbreviation: TSP-1, thrombospondin-1.

†Present address: Département d'Oncogenèse et Signalisation dans les Cellules Hématopoiétiques, Institut National de la Santé et de la Recherche Médicale U563, Centre de Physiopathologie Toulouse Purpan, Centre Hospitalier Universitaire Purpan, 31024 Toulouse, France.

¶Present address: Comprehensive Cancer Center, Developmental and Stem Cell Biology, University of California, San Francisco, CA 94143-0525.

‖To whom correspondence should be addressed. E-mail: dfelsher@stanford.edu.

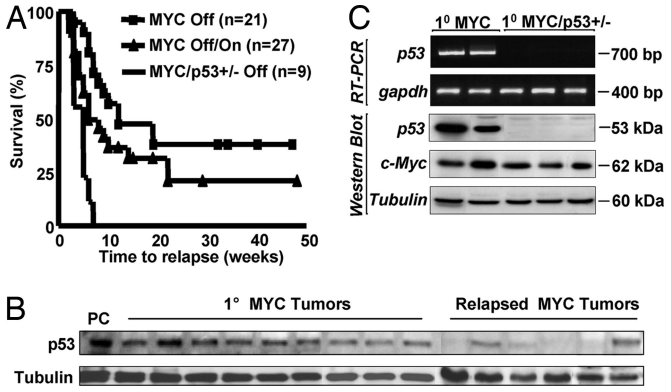

Fig. 1. Brief MYC inactivation can induce sustained tumor regression. (*A*) Kaplan–Meier plots for tumor-free survival after doxycycline treatment (100 μg/ml). The genotypes of the mice and the sustained (MYC Off) or brief (MYC Off/On) MYC inactivation are indicated. The number of mice in each group is denoted by the *n* values. Primary tumor regression and relapse were monitored for up to 50 weeks. Statistical comparison of Kaplan–Meier plots is based on the log-rank test. (*B*) p53 protein expression levels in MYC primary and relapsed tumors. Western blot analysis was performed on protein lysates prepared from MYC primary and relapsed tumors. Equal loading was confirmed by anti-α tubulin Western blot analysis. PC, positive control. (*C*) p53 protein and mRNA expression in primary (10) MYC versus primary MYC/p53$^{+/-}$ tumors. PCR was performed to measure p53 and gapdh mRNA. Western blot analysis of p53, MYC, and tubulin protein expression were performed.

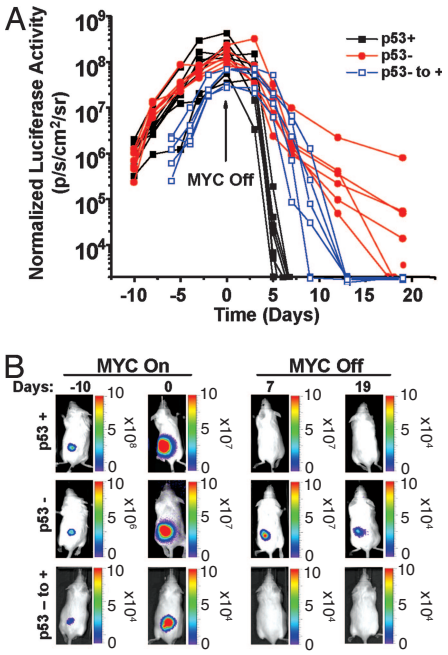

Fig. 2. p53 status and the rate of tumor cell elimination upon MYC inactivation. (*A*) Measurement of tumor cell elimination upon MYC inactivation. p53 wild-type (p53^{+}), p53 negative (p53^{-}), and p53 restored (p53^{-} to $^{+}$) tumor cells were retrovirally labeled with luciferase before s.c. injection into syngeneic mice. Mice were serially imaged by bioluminescence imaging at the indicated times, before and after MYC inactivation, to monitor transplanted tumor growth (MYC On) and tumor regression upon doxycycline treatment (100 μg/ml) (MYC Off). A summary of changes in luciferase activity is shown. Each cohort consisted of at least 5 mice. Representative data from one of three experiments is shown. (*B*) Representative images of bioluminescence imaging.

sion also was sufficient to induce sustained tumor regression and 20% of transgenic mice survived for as long as 50 weeks (Fig. 1*A*). No significant difference ($P = 0.1957$) was observed comparing survival upon sustained or brief MYC inactivation (Fig. 1*A*). When brief MYC inactivation was performed on secondary transplanted tumors into syngeneic hosts, we observed sustained tumor regression in three of four tumors (relapse rate versus injected mice: 2/4, 0/7, 0/5, or 0/7). Therefore, the ability of MYC inactivation to induce complete and sustained tumor regression appears to reflect an intrinsic tendency of each tumor.

Loss of p53 Function Facilitates Tumor Relapse. Loss of p53 function is common in tumors (22) and has been described to play a critical role in tumor recurrence (13). Therefore, we analyzed whether p53 loss would promote tumor relapse after MYC inactivation in our lymphoma model. Consistent with this possibility, primary lymphoid tumors that had relapsed after MYC inactivation often demonstrated loss of p53 expression (Fig. 1*B*). To directly investigate the effect of loss of p53 function, cohorts of mice that expressed a conditional MYC transgene in concert with the loss of one p53 allele were generated. Similar to previous reports (23–26), the loss of one p53 allele was sufficient to accelerate tumorigenesis with a reduction in the mean latency of tumor onset by 3 weeks (Fig. 5*A*, $P < 0.0001$). Primary tumors induced by the conditional MYC transgene expressed p53 mRNA and protein, whereas primary tumors arising from mice genetically heterozygous for p53, had lost p53 mRNA and protein expression, that could in some cases be explained by the loss of the second p53 allele (Figs. 1*C* and 5*B*).

The primary p53 negative tumors initially all regressed upon sustained MYC inactivation, and the mice clinically recovered, but these tumors always relapsed, in contrast to primary p53 wild-type tumors (Fig. 1*A*, $P = 0.0002$; Fig. 2). There are several possible explanations for our results. First, it was possible that loss of p53 function facilitated the ability of tumors to either bypass the Tet system and express the MYC transgene or activate expression of endogenous C-, N- or L-Myc. However, when relapsed tumors were examined for MYC protein expression, overexpression of the human MYC transgene or endogenous C-, N-, or L-Myc proteins was not observed (Fig. 6, which is published as supporting information on the PNAS web site). Thus, the relapsed tumors had become independent of MYC expression, similar to what we have described (6).

Another possibility was that tumors arising in the context of MYC overexpression and loss of p53 expression were different types of lymphomas that may account for their different response to MYC inactivation. Although this possibility cannot be excluded, the tumors induced by MYC overexpression versus MYC overexpression and loss of p53 exhibited similar histology and identical FACS phenotype: Thy-1, CD4, CD8, CD3, CD5, and T cell antigen receptor $\alpha\beta$ positive (data not shown). Another possibility is that loss of p53 induced genomic destabilization facilitating the ability of tumors to acquire genetic events that could compensate for loss of MYC overexpression. However, we have previously performed spectral karyotype analysis of tumors and failed to detect differences in genomic abnormalities in p53 positive versus negative tumors (6). A final possibility was that p53 loss allowed tumors to escape their dependence upon MYC overexpression by preventing the elimination of tumor cells.

p53 Loss Impairs the Eradication of Tumor Cells upon MYC Inactivation. To precisely evaluate how loss of p53 function influences tumor regression upon MYC inactivation, we used bioluminescence imaging (27) to compare the kinetics of transplanted p53 positive and negative tumor elimination upon MYC inactivation *in vivo*. We retrovirally introduced the luciferase enzyme into tumor-derived cell lines. The luciferase-labeled cells were detected with a minimal sensitivity of 1,000 cells per site and over a multiple log range in cell number (data not shown). Cohorts of mice were inoculated s.c. with luciferase-labeled p53-positive or -negative tumors and the intensity of the luminescent signal was monitored before and after MYC

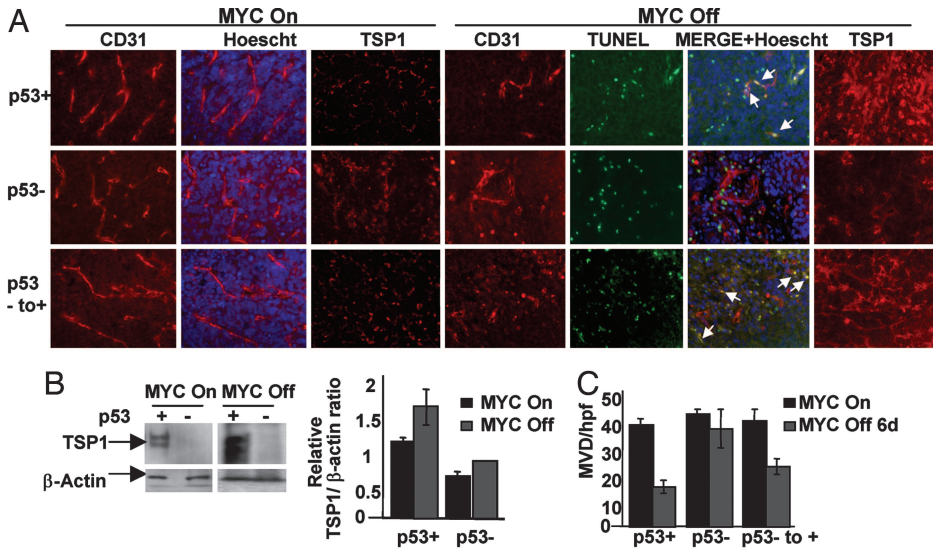

Fig. 3. p53 status modifies the angiogenic response of tumors upon MYC inactivation. (*A Left*) p53 status does not affect the angiogenic response of tumor onset upon MYC activation. p53 wild-type ($p53^+$), p53 negative ($p53^-$) and p53 restored ($p53^-$ to $^+$) transplanted tumors were examined by immunofluorescence for microvessel density (CD31) and TSP-1 expression (MYC on). (*A Right*) The loss of p53 decreases TSP-1 levels despite MYC inactivation. p53 wild-type ($p53^+$), p53 negative and p53 restored ($p53^-$ to $^+$) transplanted tumors were examined by immunofluorescence for microvessel density (CD31) and TSP-1 expression 6 days after MYC inactivation (MYC Off). Whereas there was no significant difference in the level of TUNEL reactivity, there were significantly more TUNEL-positive endothelial cells (white arrow) in p53 wild-type ($p53^+$) and p53 restored ($p53^-$ to $^+$) tumors as compared with p53 negative ($p53^-$) tumors. Specificity of staining was ensured by immunostaining of serial tumor sections with isotype matched control antibodies. (*B*) Western blot analysis of p53 wild-type ($p53^+$) and p53 negative ($p53^-$) transplanted tumors were performed for TSP-1 expression upon MYC activation and 6 days after MYC inactivation. Densitometric analysis demonstrated significantly higher TSP-1 expression in p53 wild-type ($p53^+$) tumor cells relative to β-actin as compared with p53 negative ($p53^-$) tumor cells. (*C*) Quantification of microvessel density (MVD) per high power field (hpf) demonstrated significantly increased MVD/hpf in p53 negative ($p53^-$) tumors 6 days after MYC inactivation as compared with p53 wild-type ($p53^+$) tumors. At least five fields were counted in representative tumor sections, and at least two different transplanted tumors were analyzed. Values are represented as means ± standard deviation.

inactivation to measure kinetics of tumor regression (Fig. 2*A*). The initial rate of tumor regression was similar in $p53^+$ and $p53^-$ tumors within the first 2 days of MYC inactivation and the first log in tumor reduction (Fig. 2). However, after 2 days, $p53^+$ tumors were rapidly eliminated, whereas $p53^-$ tumors continued to persist in the host after MYC inactivation. After 19 days of MYC inactivation, a bioluminescent signal was detected in mice injected with $p53^-$ tumor cells, whereas complete tumor elimination was observed in mice injected with $p53^+$ tumor cells (Fig. 2). Thus, the loss of p53 had no effect on the initial consequences of MYC inactivation but prevented the complete eradication of tumor cells.

p53 Loss Blocks a TSP-1-Mediated Antiangiogenic Response upon MYC Inactivation. Angiogenesis is critical for the expansion of tumor mass (28). The MYC oncogene has been shown to regulate angiogenesis and specifically inhibit the expression of the antiangiogenesis regulator TSP-1 (29–32). Conversely, p53 has been described to suppress tumor angiogenesis and also has been shown to regulate TSP-1 (33, 34). Hence, we speculated that the loss of p53 might impede complete tumor regression upon MYC inactivation by blocking the antiangiogenic response mediated via TSP-1. Transplanted p53 positive and negative tumors were examined by immunofluorescence for microvessel density (CD31) and TSP1 expression, at tumor onset and 6 days after MYC inactivation (Fig. 3 *A* and *B*). Whereas p53 status did not affect CD31 or TSP-1 expression during tumor onset (Fig. 3*A*, MYC On), striking differences in TSP-1 expression were observed upon MYC inactivation (Fig. 3*A*, MYC Off). Importantly, $p53^-$ tumors exhibited significantly lower levels of TSP-1 expression despite MYC inactivation. Reduced TSP-1 expression in $p53^-$ tumor cells was also confirmed by Western blot analysis (Fig. 3*B*). To further confirm that p53 loss influenced the angiogenic program upon MYC inactivation, tumor microvessel density was evaluated by performing endothelial cell specific CD31 staining. Even six days after MYC inactivation, we noticed the persistence of larger lumen vessels in p53 deficient tumors whereas $p53^+$ tumors exhibited reduced CD31 staining (Fig. 3*A*). Using TUNEL analysis, we observed endothelial cell apoptosis in $p53^+$, but not $p53^-$ tumors upon MYC inactivation. Furthermore, before MYC inactivation, microvessel density (MVD) was found to be similar in $p53^+$ and $p53^-$ tumors. However, after MYC inactivation, $p53^+$, but not $p53^-$ tumors, exhibited a significant reduction in MVD (Fig. 3*C*). Together these data suggest that $p53^-$ tumors failed to induce sufficient levels of TSP-1 to mediate the appropriate antiangiogenic response to MYC inactivation necessary for complete and sustained tumor regression.

Restoration of p53 Permits Sustained Tumor Regression upon MYC Inactivation. Loss of p53 resulted in a defect in tumor regression by preventing angiogenesis inhibition induced by MYC inactivation. We reasoned that by restoring p53, we would induce a more complete antiangiogenic response and subsequently sustain tumor regression upon MYC inactivation. To investigate the consequences of p53 restoration, three different $p53^-$ tumor derived cell lines (6814, 7031, and B-1601) were retrovirally transduced with p53. Importantly, the level of p53 protein expression was found to be comparable to several tumor-derived cell lines positive for p53, as measured by Western blot analysis (Fig. 7, which is published as supporting information on the PNAS web site).

We then investigated whether p53 restoration would rescue TSP-1 expression and decrease tumor neovascularization. TSP-1 and CD31 levels were examined in transplanted p53 restored ($p53^-$ to $^+$) tumor specimens isolated 6 days after MYC inactivation. Ectopic expression of p53 led to restoration of TSP-1 levels comparable to $p53^+$ tumors upon MYC inactivation (Fig. 3*A*). In addition, CD31 and TUNEL staining revealed both increased endothelial cell apoptosis and reduced microvessel density in p53 restored ($p53^-$ to $^+$) tumors (Fig. 3 *A* and *C*).

Finally, we examined the influence of p53 restoration on the

kinetics of tumor cell elimination *in vivo* upon MYC inactivation by bioluminescence imaging. We found that transplanted p53 restored tumors exhibited rapid and complete tumor cell elimination comparable to $p53^+$ tumors (Fig. 2). Thus, restoration of p53 now permitted complete tumor cell elimination upon MYC inactivation *in vivo*.

Restoration of Either TSP-1 or p53 Is Associated with Sustained Tumor Regression upon MYC Inactivation. Next we examined whether TSP-1 restoration alone could maintain tumor regression upon MYC inactivation even with the loss of p53. $p53^+$, $p53^-$, p53 restored, or $p53^-$/TSP-1^{HI} tumor cells were inoculated s.c. into syngeneic hosts and mice were treated with doxycycline. TSP-1^{HI} expression was achieved in $p53^-$ tumor cells through serial retroviral transduction. TSP-1 expression was confirmed by quantification of Western analysis and immunohistochemical staining and demonstrated similar expression levels as in $p53^+$ tumors (Fig. 8, which is published as supporting information on the PNAS web site). Whereas restoration of TSP-1 expression did not influence the kinetics of transplanted tumor growth, similar to restoration of p53, transplanted $p53^-$/TSP-1^{HI} tumor cells were eliminated rapidly and more completely as compared with transplanted $p53^-$ tumor cells (Fig. 4*A*, $P < 0.03$). Further, transplanted tumors with TSP-1^{HI} expression were associated with decreased CD31 staining and MVD (Fig. 8).

Finally, we examined whether p53 or TSP-1 restoration could prevent tumor relapse upon MYC inactivation. $p53^-$ or p53 restored tumor cells were inoculated i.p. into syngeneic hosts and mice were treated with doxycycline at tumor onset. As expected, after initial tumor regression, transplanted $p53^-$ tumors relapsed rapidly, with a mean relapse time of 5.5 weeks after MYC inactivation. However, transplanted p53 restored tumors exhibited a significant delay until tumor relapse ranging from 6 to 37 weeks (Fig. 4*B*, $P < 0.0001$) with 3 mice exhibiting sustained tumor regression even after 37 weeks. Similarly, transplanted TSP-1 restored tumors (TSP-1^{HI}) exhibited prolonged survival (Fig. 4*C*, $P = 0.0122$). Notably, the transplanted tumors that relapsed in the p53 restored cohort had lost p53 protein expression, as seen by Western blot analysis (Fig. 4*D*), with one exception (R4), which expressed higher levels of a most likely mutated p53 allele. Hence, the sustained restoration of p53 expression in tumors significantly enhanced the ability of MYC inactivation to induce sustained tumor regression. Thus, the restoration of either p53 or TSP-1 expression in $p53^-$ tumors is sufficient to permit tumor regression and to limit tumor relapse upon MYC inactivation.

Discussion

We found that the loss of p53 function prevents sustained tumor regression upon MYC inactivation corresponding with the loss of induction of the antiangiogenic regulator, TSP-1 and the suppression of tumor angiogenesis. Furthermore, the restoration of either p53 or TSP-1 in p53 negative tumor cells now permitted MYC inactivation to induce the shut off of the angiogenic switch and sustained tumor regression. Importantly, overexpression of TSP-1 alone did not influence tumor growth suggesting that only a combination of MYC inactivation and TSP-1 expression was sufficient to induce tumor regression. Hence, angiogenesis appears to be an essential component of oncogene addiction.

We have gained some critical insight into the mechanism of tumor regression upon MYC inactivation. Previously, we described that MYC inactivation induced cell autonomous proliferative arrest and apoptosis of hematopoietic tumor cells. Here we have demonstrated that MYC inactivation in hematopoietic tumors also appears to require a blockade in tumor angiogenesis. Furthermore, we demonstrate that p53 is required for a TSP-1 mediated antiangiogenic response upon MYC inactivation. Therefore, MYC inactivation appears to induce tumor regression at least in part through a p53-dependent induction of TSP-1 expression. Future studies should address whether in epithelial tumor models p53 similarly regulates TSP-1 expression.

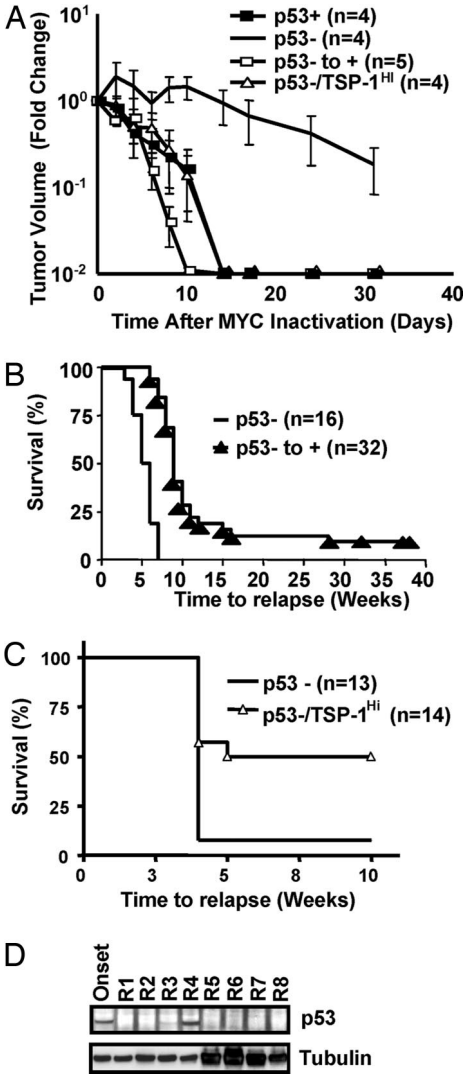

Fig. 4. Combined inactivation of MYC and restoration of p53 or TSP-1 expression is more effective in inducing tumor regression. (*A*) Restoration of p53 or TSP-1 and tumor regression upon MYC inactivation. In these experiments, p53 or TSP-1 was transduced into tumor cells and maintained under continuous selection *in vitro* to ensure expression. p53 positive ($p53^+$), p53 negative ($p53^-$), p53 restored ($p53^-$ to $^+$) and p53-/TSP-1^{HI} tumor cells were injected s.c. at a dose of 10^7 cells into cohorts of syngeneic FVB/N-recipient mice. When transplanted tumors reached 2 cm^2 in size, mice were treated with doxycycline (100 μg/ml) to inactivate MYC. Tumor volume is calculated from caliper measurement and is expressed as logarithmic fold changes in tumor volume before MYC inactivation. Data are presented as the mean for each cohort ± SEM with statistical analysis performed by the Mann–Whitney test. (*B* and *C*) MYC inactivation, combined with p53 or TSP-1 restoration, delays tumor relapse *in vivo*. p53 negative ($p53^-$), p53 restored ($p53^-$ to $^+$), or TSP-1 restored (p53-/TSP-1^{HI}) cells (10^7) were injected i.p. into syngeneic mice. When moribund with tumor burden, transplanted mice were treated with doxycycline (100 μg/ml) and monitored for tumor relapse. Kaplan–Meier survival curve are represented. Statistical comparison of Kaplan–Meier plots is based on the log-rank test. The number of mice in each group is denoted by *n* values. (*D*) Tumor relapse after MYC inactivation is frequently associated with reduced p53 protein expression. p53 expression levels in p53 restored tumor cells, at the time of tumor onset and relapse (R1–R8), was analyzed by Western blot on protein lysates (60 μg) prepared from transplanted relapsed tumor tissues. Protein loading was assayed by anti-α-tubulin Western blot.

Our results are consistent with previous studies that have suggested that MYC (29–32) or p53 (33–36) may be involved in the

regulation of tumor angiogenesis and that TSP-1 is a negative regulator of tumorigenesis (37, 38). This study illustrates that MYC inactivation requires either p53 or TSP-1 to inhibit angiogenesis and induce sustained tumor regression. Importantly, we demonstrate that tumor relapse due to the loss of p53 can be significantly delayed or even prevented, in some cases, by restoration of TSP-1 expression to maintain tumor regression after MYC inactivation.

Our results may be more generally relevant to the mechanisms by which targeted therapeutics induce tumor regression. The restoration of either p53 or TSP-1 may be similarly effective in permitting sustained tumor regression upon oncogene inactivation in other tumor models (11–13). In this context, it will be interesting to determine whether TSP-1 expression is systematically induced upon oncogene inactivation, regardless of the specific oncogene and cancer type (39). In addition, it will be important to determine whether tumor relapse after oncogene inactivation is associated with TSP-1 loss, especially in p53 wild-type tumors.

Human tumors are generally considered to be more complex than mouse tumors and targeting any single mutant gene product is unlikely to be sufficient to induce durable tumor regression. In this regard, it has been recently illustrated that the loss of p53 or p19ARF impairs the ability of Imatinib to regress BCR-ABL induced tumors through unknown mechanisms (40, 41). The restoration of p53 or p19ARF may enhance the clinical response of human tumors to Imatinib; and possibly this may occur through regulation of angiogenesis. Our results provide one illustration where the combined inactivation or repair of multiple gene products and/or pathways such as the inactivation of an oncogene, MYC, plus the restoration of a tumor suppressor, p53, or a regulator of angiogenesis, TSP-1, is more likely to be effective in the treatment of cancer. Generally, our results support the idea that the combined inactivation of an oncogene and the inhibition of angiogenesis will be an effective therapeutic strategy for cancer.

Materials and Methods

Transgenic Mice. The generation and characterization of Tet system transgenic lines for conditional expression of MYC, have been described (21). p53 knockout mice were kindly provided by Alan Bradley (Baylor University, Houston, TX) and were generously provided in the FVB/N background by Lisa Coussens (University of California, San Francisco). Genotyping was performed by PCR on genomic DNA from tails. Analysis of the p53 wild-type or mutated allele was performed as described (42). Animals were housed in the Stanford vivarium as per animal protocols approved by Stanford University.

Tumor Surveillance and Tumorigenicity Assays. Transgenic mice were observed biweekly for tumor development. When mice were moribund with tumor burden, they were either humanely euthanized or treated with doxycycline in their drinking water (100 μg/ml) to follow tumor regression and relapse. Percent survival of MYC overexpressing mice with or without p53 loss was measured as the mice life duration and used to assess lymphomagenesis. To monitor for tumor regression and relapse, percent survival was measured as the time between doxycycline treatment (if tumor regression occurred within 1 week) and relapse, which is defined as recurrence of signs of morbidity. Statistical comparison of Kaplan–Meier curves is based on the log-rank test. For transplantation experiments, primary tumors were first adapted to *in vitro* growth as described (21) and then 10^7 cells were washed once in PBS before i.p. or s.c. injection into FVB/N syngeneic mice. To assess for tumor regression, transplanted s.c. tumors were measured by using a caliper over a 30-day period of doxycycline treatment, and tumor volumes were calculated by using the formula length (mm) $\times$ width^2 (mm) $\times$ 0.52 (20, 43).

Cell Culture. Tumor-derived cell lines were generated by mechanical disruption of tumor tissue followed by Ficoll–Paque purification of the single cell suspension. Cells were then maintained *in vitro* as described (21). To inactivate human c-MYC transgene expression, tumor cells were treated with doxycycline at 20 ng/ml.

Retrovirus Constructs, Virus Production and Tumor Cell Infection. MSCV-IRES-GFP and MSCV-p53-IRES-GFP constructs were kindly provided by S. Lowe (Cold Spring Harbor Laboratory, Cold Spring Harbor, NY). MSCV-LUC-IRES-GFP construct was kindly provided by Luis Soares (Stanford University). MSCV-Puro-LUC construct, a modified version of the pDON plasmid vector (Takara Mirus Bio, Madison, WI), was kindly provided by Mobin Karimi and Robert Negrin (Stanford University). Retroviruses containing supernatants were prepared by transient transfection of 293T cells, and viral titers were measured as described (44). Tumor cells were incubated with retroviruses containing supernatants for 12 h at 32°C in media containing 4 μg/ml polybrene. Cells were then expanded at 37°C for an additional 48 h and GFP expressing cells were purified by flow cytometry on a FACS Vantage (Becton Dickinson, Franklin Lakes, NJ). Cells containing MSCV-Puro-LUC were selected with puromycin.

TSP-1 retrovirus was produced by transfecting GPG-293 cells with 8 μg of PWZL-TSP1 plasmid DNA or PWZL vector alone (Addgene, Cambridge, MA) and 24 μl of Mirus TransIT Express transfection reagent. High-titer viral supernatant was collected at days 5, 7, and 9 after transfection. Virus was concentrated by high-speed centrifugation, and used to infect 2×10^5 p53$^-$ cells by spin-infection at 2,000 $\times$ *g* for 2 h with vector alone or serially incubated with TSP-1 virus three times.

***In Vivo* Bioluminescence Imaging.** p53 wild-type (p53$^+$), p53 negative (p53$^-$) and p53 restored (p53$^-$ to $^+$) tumor cells, expressing the luciferase enzyme, were injected i.p. or s.c. into syngeneic mice. Tumors were allowed to develop until reaching a similar bioluminescent signal. Tumor regression was then induced by doxycycline treatment (100 μg/ml). Mice developing transplanted tumors were anesthetized with a combination of inhaled isoflorane/oxygen delivered by the Xenogen XGI-8 5-port Gas Anesthesia System. The substrate D-luciferin (150 mg/kg) was injected into the animal's peritoneal cavity 10 min. before imaging. Animals were then placed into a light-tight chamber and imaged with an IVIS-100 cooled CCD camera (Xenogen, Alameda, CA). First, a grayscale body surface reference image (digital photograph) was taken under weak illumination. Next, photons emitted from luciferase expressing cells within the animal and transmitted through the tissues were collected for a period of 5 sec to 1 min and quantified by the software program Living Image (Xenogen) as an overlay on the image analysis program "Igor" (Wavemetrics, Seattle, WA). For anatomical localization, a pseudocolor image representing light intensity (blue, least intense; red, most intense) was generated in Living Image and superimposed over the gray scale whole body reference image as described previously (45). Living Image was used to collect, archive, and analyze photon fluxes and transform them into pseudocolor images by using Living Image software (Xenogen). At least 5 mice per group were injected with tumors expressing luciferase.

Immunohistochemistry. Mice were euthanized at tumor onset and 6 days after MYC inactivation, and transplanted tumors were harvested and fixed in neutral buffered formalin for paraffin sections. Paraffin embedded tumor sections were deparaffinized by successive incubations in xylene, 95% ethanol, 90% ethanol, 70% ethanol followed by PBS. Epitopes were unmasked with 20 ug/ml proteinase K in PBS at room temperature for 30 min and rinsed twice in PBS plus 0.3% Triton X-100 (PBS-T). Sections were immunostained with rat anti-CD31 mAb (1:50; Pharmingen, San Diego, CA), mouse anti-TSP1 (clone A6.1, 1:50; Lab Vision, Fremont, CA), or an isotype matched control (Pharmingen) overnight at room temperature. This was followed by incubation for 2 h with

goat anti-rat Alexa 594 or goat anti-mouse Alexa 594 conjugated secondary antibody (1:500; Molecular Probes). Nuclei were labeled by brief washes in Hoechst dye (Sigma, St. Louis, MO; 1 ug/ml).

For TUNEL staining, after anti-CD31 immunostaining, sections were stained by using the DeadEnd Fluorometric TUNEL System (Promega). In brief, sections were incubated for 15 min in equilibration buffer followed by incubation with nucleotide mix (containing fluorescein-12-dUTP) and terminal deoxynucleotidyl transferase enzyme for 60 min at 37°C. Reactions were stopped by incubation in 2× SSC for 15 min followed by serial washes in PBS-T. Sections were mounted with glycerol, and images were obtained on a Zeiss microscope and analyzed by using AxioVision 4.0 software (Carl Zeiss Vision).

Western Blot Analysis. Tumor pieces or tumor-derived cell lines were lysed in Tris·HCl, pH 8/50 mM/NaCl 150 mM/1% Triton X-100/DTT 1 mM/1× inhibitor mixture mix (Calbiochem, San Diego, CA)/100 μg/ml PMSF. Western blots were performed on protein lysates (60 μg) by using conventional techniques. p53 protein expression was detected by using antibodies obtained from Novocastra Laboratories at a dilution of 1/400. As a positive control for p53 expression, a lysate prepared from MEF cells that overexpress p53 was used (46). MYC protein levels were assessed by using human c-MYC (9E10, Oncogene, San Diego, CA) (dilution 1/200), mouse c-Myc (c19; Santa Cruz Biotechnology, Santa Cruz, CA) (dilution 1/250), mouse N-Myc (OP13; Oncogene) (dilution 1/100), and mouse L-Myc (c20; Santa Cruz Biotechnology) (dilution 1/100) antibodies. As a positive control for N-Myc and L-Myc, protein lysates were prepared from BJAB cells (Santa Cruz Biotechnology) and NCI-H209 cells (American Type Culture Collection Biotechnology, Manassas, VA), respectively. The α-tubulin antibodies were purchased from Oncogene (Ab-1) and used at a dilution of 1/500. Horseradish peroxidase (HRP)-coupled secondary antibodies were obtained from Amersham Biosciences and used at a dilution of 1/2,000. Protein bands were visualized by using the ECL1$^+$ detection kit (Amersham Biosciences, Piscataway, NJ). Expression of TSP-1 was assessed by immunoblotting whole-cell lysates. Cells were treated for 10 h with doxycycline in RPMI media alone, washed three times with PBS, and then lysed with sample buffer. Cells (1×10^6) were loaded on a 6% Tris·HCl SDS/PAGE gel, subjected to gel electrophoresis, and transferred to a nitrocellulose membrane. The membrane was incubated with TSP-1 mAb (Neomarker Ab-11; 1/1,000) in TBST for 1 h at room temperature, then washed and incubated with goat anti-mouse HRP (Zymed; 1/1,000). Protein bands were visualized with the ECL detection kit (Amersham). Membranes were stripped and reprobed with anti-β-actin mAb (1/5,000) followed by goat anti-mouse HRP and visualized by ECL detection. Films were densitometrically analyzed, and TSP-1 levels were normalized to β-actin levels.

Microvessel Density. Transplanted tumors were harvested 6 days after MYC inactivation and paraffin embedded. Microvessel density was determined by immunofluorescence staining of deparaffinized tumor sections with an anti-CD31 mAb (PharMingen; 1/50) overnight at room temperature followed by a Goat anti-rat Alexa 594 (Molecular Probes; 1/500) for 2 h at room temperature. Sections were briefly rinsed with Hoechst dye to stain nuclei. By following the method as described (47), at low magnification (×40), regions of highest vessel density were captured and counted at ×200 magnification (0.738 mm^2 field). At least five fields were counted in a representative tumor section, and at least two different transplanted tumors were counted. Values are represented as means ± SD.

This work is dedicated in memory of Mr. Georges Guedj. We thank Drs. Michael Cleary, Laura Attardi, Steven Artandi, Mark Lee, and members of the D.W.F. laboratory for helpful discussions and a critical reading of the manuscript, Dr. Jack Lawler for helpful advice, and Randolph Watnick for helpful discussions. This work was supported by a postdoctoral fellowship from the Lymphoma Research Foundation (to S.G.); the Richard and Susan Smith Family Foundation (to S.R.); the Leukemia and Lymphoma Society Career Development Special Fellow in Clinical Research Award (to A.F.); the Stanford Medical Scholars Program (to P.B.); the Howard Hughes Medical Institute Medical Student Research Fellowship (to A.K.); a postdoctoral fellowship from the Jose Carreras Leukemia Foundation (to E.P.); the Breast Cancer Research Foundation (to J.F.); and National Cancer Institute (NCI) Grants R01-CA85610, R01-CA105102, 3R01CA089305-03S1; National Institutes of Health (NIH)/NCI *In Vivo* Cellular and Molecular Imaging Center Grant P50; NIH/NCI Grant 1P20 CA112973; the Leukemia and Lymphoma Society; the Burroughs Wellcome Fund; and the Damon Runyon Lilly Clinical Investigator Award (to D.W.F.).

1. Bishop JM (1991) *Cell* 64:235–248.
2. Hahn WC, Weinberg RA (2002) *N Engl J Med* 347:1593–1603.
3. Sawyers CL (2002) *Cancer Cell* 1:13–15.
4. Felsher DW (2003) *Nat Rev Cancer* 3:375–379.
5. Giuriato S, Rabin K, Fan AC, Shachaf CM, Felsher DW (2004) *Semin Cancer Biol* 14:3–11.
6. Karlsson A, Giuriato S, Tang F, Fung-Weier J, Levan G, Felsher DW (2003) *Blood* 101:2797–2803.
7. Jain M, Arvanitis C, Chu K, Dewey W, Leonhardt E, Trinh M, Sundberg CD, Bishop JM, Felsher DW (2002) *Science* 297:102–104.
8. Shachaf CM, Kopelman AM, Arvanitis C, Karlsson A, Beer S, Mandl S, Bachmann MH, Borowsky AD, Ruebner B, Cardiff RD, *et al.* (2004) *Nature* 431:1112–1117.
9. Weinstein IB (2002) *Science* 297:63–64.
10. Jonkers J, Berns A (2004) *Cancer Cell* 6:535–538.
11. D'Cruz CM, Gunther EJ, Boxer RB, Hartman JL, Sintasath L, Moody SE, Cox JD, Ha SI, Belka GK, Golant A, *et al.* (2001) *Nat Med* 7:235–239.
12. Giuriato S, Felsher DW (2003) *Cell Cycle* 2:329–332.
13. Gunther EJ, Moody SE, Belka GK, Hahn KT, Innocent N, Dugan KD, Cardiff RD, Chodosh LA (2003) *Genes Dev* 17:488–501.
14. Shah NP, Nicoll JM, Nagar B, Gorre ME, Paquette RL, Kuriyan J, Sawyers CL (2002) *Cancer Cell* 2:117–125.
15. Shah NP, Tran C, Lee FY, Chen P, Norris D, Sawyers CL (2004) *Science* 305:399–401.
16. Gorre ME, Mohammed M, Ellwood K, Hsu N, Paquette R, Rao PN, Sawyers CL (2001) *Science* 293:876–880.
17. Tipping AJ, Baluch S, Barnes DJ, Veach DR, Clarkson BM, Bornmann WG, Mahon FX, Goldman JM, Melo JV (2004) *Leukemia* 18:1352–1356.
18. Wendel HG, De Stanchina E, Fridman JS, Malina A, Ray S, Kogan S, Cordon-Cardo C, Pelletier J, Lowe SW (2004) *Nature* 428:332–337.
19. Rodriguez-Manzaneque JC, Lane TF, Ortega MA, Hynes RO, Lawler J, Iruela-Arispe ML (2001) *Proc Natl Acad Sci USA* 98:12485–12490.
20. Hanahan D, Folkman J (1996) *Cell* 86:353–364.
21. Felsher DW, Bishop JM (1999) *Mol Cell* 4:199–207.
22. Soussi T, Beroud C (2001) *Nat Rev Cancer* 1:233–240.
23. Blyth K, Terry A, O'Hara M, Baxter EW, Campbell M, Stewart M, Donehower LA, Onions DE, Neil JC, Cameron ER (1995) *Oncogene* 10:1717–1723.
24. Elson A, Deng C, Campos-Torres J, Donehower LA, Leder P (1995) *Oncogene* 11:181–190.
25. Eischen CM, Weber JD, Roussel MF, Sherr CJ, Cleveland JL (1999) *Genes Dev* 13:2658–2669.
26. Yu D, Thomas-Tikhonenko A (2002) *Oncogene* 21:1922–1927.
27. Edinger M, Cao YA, Hornig YS, Jenkins DE, Verneris MR, Bachmann MH, Negrin RS, Contag CH (2002) *Eur J Cancer* 38:2128–2136.
28. Folkman J (2002) *Semin Oncol* 29:15–18.
29. Baudino TA, McKay C, Pendeville-Samain H, Nilsson JA, Maclean KH, White EL, Davis AC, Ihle JN, Cleveland JL (2002) *Genes Dev* 16:2530–2543.
30. Brandvold KA, Neiman P, Ruddell A (2000) *Oncogene* 19:2780–2785.
31. Janz A, Sevignani C, Kenyon K, Ngo CV, Thomas-Tikhonenko A (2000) *Nucleic Acids Res* 28:2268–2275.
32. Watnick RS, Cheng YN, Rangarajan A, Ince TA, Weinberg RA (2003) *Cancer Cell* 3:219–231.
33. Browder T, Folkman J, Hahnfeldt P, Heymach J, Hlatky L, Kieran M, Rogers MS (2002) *Science* 297:471, discussion 471.
34. Dameron KM, Volpert OV, Tainsky MA, Bouck N (1994) *Cold Spring Harb Symp Quant Biol* 59:483–489.
35. Hammond EM, Giaccia AJ (2002) *Science* 297:471, discussion 471.
36. Yu JL, Rak JW, Coomber BL, Hicklin DJ, Kerbel RS (2002) *Science* 295:1526–1528.
37. Lawler J (2002) *J Cell Mol Med* 6:1–12.
38. Sund M, Hamano Y, Sugimoto H, Sudhakar A, Soubasakos M, Yerramalla U, Benjamin LE, Lawler J, Kieran M, Shah A, Kalluri R (2005) *Proc Natl Acad Sci USA* 102:2934–2939.
39. Folkman J, Ryeom S (2005) *Cold Spring Harbor Symp Quant Biol* 70:389–397.
40. Wendel HG, de Stanchina E, Cepero E, Ray S, Emig M, Fridman JS, Veach DR, Bornmann WG, Clarkson B, McCombie WR, *et al.* (2006) *Proc Natl Acad Sci USA* 103:7444–7449.
41. Williams RT, Roussel MF, Sherr CJ (2006) *Proc Natl Acad Sci USA* 103:6688–6693.
42. Donehower LA, Harvey M, Slagle BL, McArthur MJ, Montgomery CA, Jr., Butel JS, Bradley A (1992) *Nature* 356:215–221.
43. Kuo CJ, Farnebo F, Yu EY, Christofferson R, Swearingen RA, Carter R, von Recum HA, Yuan J, Kamihara J, Flynn E, *et al.* (2001) *Proc Natl Acad Sci USA* 98:4605–4610.
44. Pear WS, Nolan GP, Scott ML, Baltimore D (1993) *Proc Natl Acad Sci USA* 90:8392–8396.
45. Contag CH, Spilman SD, Contag PR, Oshiro M, Eames B, Dennery P, Stevenson DK, Benaron DA (1997) *Photochem Photobiol* 66:523–531.
46. Jimenez GS, Nister M, Stommel JM, Beeche M, Barcarse EA, Zhang XQ, O'Gorman S, Wahl GM (2000) *Nat Genet* 26:37–43.
47. Weidner N, Semple JP, Welch WR, Folkman J (1991) *N Engl J Med* 324:1–8.

Article 2

Conditional TPM3-ALK and NPM-ALK transgenic mice develop reversible ALK-positive early B-cell lymphoma/leukemia

Sylvie Giuriato, Marianne Foisseau, Emilie Dejean, Dean W. Felsher, Talal Al Saati, Cécile Demur, Ashraf Ragab, Anna Kruczynski, Claudine Schiff, Georges Delsol and Fabienne Meggetto

BLOOD

Vol. 115, No. 20, Issue of May 115, pp. 4061-4070, 2010

Conditional TPM3-ALK and NPM-ALK transgenic mice develop reversible ALK-positive early B-cell lymphoma/leukemia

Sylvie Giuriato,[1,2] Marianne Foisseau,[1,2] Emilie Dejean,[1,2] Dean W. Felsher,[3] Talal Al Saati,[4] Cécile Demur,[1,2,5] Ashraf Ragab,[1,2] Anna Kruczynski,[6] Claudine Schiff,[7-9] Georges Delsol,[1,2] and Fabienne Meggetto[1,2]

[1]Inserm, U563, Centre de Physiopathologie de Toulouse Purpan, Toulouse, France; [2]Université Toulouse III Paul Sabatier, IFR150-IFR BMT, Toulouse, France; [3]Stanford University, Center for Clinical and Science Research, Oncology Division, CA; [4]Plateau technique d'histopathologie expérimentale de l'IFR150-IFR BMT/Génopôle Toulouse-Midi Pyrénées, CHU Purpan, Toulouse, France; [5]CHU Toulouse, Hôpital Purpan, Laboratoire d'Hématologie, Toulouse, France; [6]Institut de Recherche Pierre Fabre, Centre de recherche en oncologie expérimentale, Toulouse, France; [7]Centre d'Immunologie de Marseille-Luminy (CIML), Université de la Méditerranée, Marseille, France; [8]Inserm, U631, Marseille, France; and [9]CNRS-UMR6102, Case 906, Marseille, France

NPM-ALK (nucleophosmin-anaplastic lymphoma kinase) and TPM3-ALK (nonmuscular tropomyosin 3-anaplastic lymphoma kinase) are oncogenic tyrosine kinases implicated in the pathogenesis of human ALK-positive lymphoma. We report here the development of novel conditional mouse models for ALK-induced lymphomagenesis, with the use of the tetracycline regulatory system under the control of the EμSRα enhancer/promoter. The expression of either oncogene resulted in the arrest of the differentiation of early B cells and lymphomagenesis. We also observed the development of skin keratoacanthoma lesions, probably because of aberrant ALK expression in keratinocytes. The inactivation of the ALK oncogene on doxycycline treatment was sufficient to induce sustained regression of both hematopoietic tumors and skin disease. Importantly, treatment with the specific ALK inhibitor (PF-2341066) also reversed the pathologic states, showing the value of these mouse models for the validation of ALK tyrosine kinase inhibitors. Thus, our results show (1) that NPM-ALK and TPM3-ALK oncogenes are sufficient for lymphoma/leukemia development and required for tumor maintenance, hence validating ALK as potentially effective therapeutic target; and (2) for the first time, in vivo, the equal tumorigenic potential of the NPM-ALK and TPM3-ALK oncogenic tyrosine kinases. Our models offer a new tool to investigate in vivo the molecular mechanisms associated with ALK-induced lymphoproliferative disorders. (*Blood.* 2010;115(20): 4061-4070)

Introduction

The anaplastic lymphoma kinase (ALK) is associated with a subset of non-Hodgkin lymphomas characterized by the translocation of *ALK* gene located on chromosome 2p23, which is fused to 1 of 13 partners.[1-6] The 2 most common fusion partners are the nucleophosmin 1 (*NPM1*) gene, on chromosome 5, and the nonmuscular tropomyosin 3 (*TPM3*) gene, on chromosome 1, that account for 75% and 15% of ALK-positive lymphomas, respectively. Two different ALK-positive lymphoproliferative disorders have been described and are now recognized as distinct entities: systemic anaplastic large cell lymphoma T/null (World Health Organization classification[7]) and a rare variety of diffuse large B-cell lymphoma often with plasmablastic features that we described in 1997.[8] More recently, we have shown that ALK-positive diffuse large B-cell lymphoma was namely associated with the t(2;17)(p23;q23) involving Clathrin-ALK rearrangement.[9] Occasional cases have been associated with the t(2;5)(p23;q35) translocations and found to express the NPM-ALK fusion protein.[10,11]

The oncogenic properties of NPM-ALK and TPM3-ALK fusion proteins have been shown in vitro, in fibroblastic and lymphoid cell lines,[12-15] in vivo with xenografts of ALK-expressing cells,[16,17] retroviral transduction,[18,19] or transgenic mouse models.[20,21] In particular, it has been established that to induce ALK in transgenic models, it is critical both to use the correct lineage-specific promoter and to induce significant levels of protein expression.[22,23] Hence, the ideal mouse model should use conditional and lineage-specific promoter to closely mimic the human malignancy and to allow reversible expression of the transgene, as has been suggested.[23,24] To achieve these objectives, we used the tetracycline regulatory system to generate conditional transgenic mice overexpressing NPM-ALK or TPM3-ALK oncogenes. To drive expression of the tetracycline-regulated transactivator (tTA) in the lymphoid lineage, we chose the EμSRα enhancer/promoter, as has been previously described.[25,26] Here, we will show that double-transgenic mice develop an ALK-positive B-cell lymphoproliferative disorder, corresponding to an early B lymphoma/leukemia, after a short period of latency. Suppression of ALK fusion protein expression by administration of doxycycline (Dox), or a specific ALK inhibitor (PF-2341066), to mice exhibiting florid disease led to a complete regression of ALK-associated lesions. Our results suggest that NPM-ALK and TPM3-ALK oncogenes are sufficient for tumor development and are required for tumor maintenance, therefore placing ALK as an optimal therapeutic target and further support the notion that, in mouse, ALK preferentially malignantly transforms B cells.[22,23]

Methods

Generation of transgenic constructs and transgenic founder mice

The human NPM-ALK cDNA, from pBluescript2 SK+ plasmid, a generous gift of Dr S. W. Morris (St Jude Children's Research Hospital),[1] was subcloned into

Submitted June 18, 2008; accepted February 13, 2010. Prepublished online as *Blood* First Edition paper, March 11, 2010; DOI 10.1182/blood-2008-06-163386.

The online version of this article contains a data supplement.

The publication costs of this article were defrayed in part by page charge payment. Therefore, and solely to indicate this fact, this article is hereby marked "advertisement" in accordance with 18 USC section 1734.

*Hin*dIII- and *Not*I-restricted pBIL vector (Clontech). The human TPM3-ALK cDNA, cloned in our laboratory,[2] from the pcDNA3 plasmid,[12] was subcloned into the *Hin*dIII-restricted pBIL vector. DNA fragments (7267 base pair [bp] for NPM-ALK construct and 7517 bp for TPM3-ALK construct) were isolated (Kit QIAGEN), diluted at 5 μg/mL in Brinster buffer [Tris (tris(hydroxymethyl)aminomethane) 10mM, pH 7.5; EDTA (ethylenediaminetetraacetic acid) 0.1mM], microinjected into the pronuclei of FVB/N zygotes (R. Janvier Breeding Center), and implanted into pseudopregnant foster mothers (Transgenesis facility, IFR30). Screening of transgenic founder mice were performed by polymerase chain reaction (PCR) genotyping with the following primers: NA forward, 5′-AGAGGCAATGAATTACGAAGGCAGT-3′,and NA reverse, 5′-AGCAGTAGTTGGGGT TGTAGTCGGT-3′, for NPM-ALK (287 bp) and TPM3 forward, 5′-CTGGCAGAGTCCCGTTGCCGAG-3′, and ALK reverse, 5′-GGCTCTGCAGCTCCAT-CTGCATGG-3′, for TPM3-ALK (270 bp). Endogenous myogenin gene (*Myo*) was used as an internal control: *Myo* forward, 5′-CCAAGTTGGTGTCAAAAGCC-3′, and *Myo* reverse, 5′-CTCTCTGCTTTAAGGAGTCAG-3′ (170 bp).

Assessment of tetracycline-regulated NPM-ALK, TPM3-ALK, and luciferase expression in vitro

After collagenase type I isolation (1 mg/mL in phosphate-buffered saline; Sigma-Aldrich), ear fibroblasts isolated from founder mice were transfected with the tTA-coding plasmid (Clontech). Transfections were performed with or without Dox (Sigma-Aldrich) in the culture media (20 ng/mL), and NPM-ALK or TPM3-ALK expression was analyzed by Western blotting and luciferase expression, as previously described.[17] Positive founder lines were maintained by crossing with wild-type FVB/N mice.

Generation of double-transgenic mice

The NPM-ALK and TPM3-ALK heterozygous founder transgenic mice were bred with EμSRα-tTA homozygous transgenic mice, provided by Dr D. W. Felsher (Stanford University).[26] PCR genotyping was performed with the NPM-ALK or TPM3-ALK primers described in "Generation of transgenic constructs and transgenic founder mice," and the following tTA gene primers: tTA forward, 5′-AGGCCTGTACGGAAGTGT-3′; tTA reverse, 5′-CTCTGCACCTTGGTGATC-3′. All transgenic mice were housed under pathogen-free conditions at Toulouse, IFR150-IFR BMT (ex IFR30) animal facility, as per animal protocols approved by Inserm.

Doxycycline administration

Dox was added in the drinking water (100 μg/mL) of pregnant females or moribund double-transgenic animals. In addition, moribund animals were also injected once intraperitoneally with 100 μL of Dox solution (100 μg/mL).

ALK inhibitor treatment Racemic

PF-2341066 (3-[1-(2,6-dichloro-3-fluoro-phenyl)-ethoxy]-5-(1-piperidin-4-yl-1*H*-pyrazol-4-yl)-pyridin-2-ylamine) was synthesized according to the method described in the patent international application WO 2006/021881. Moribund double-transgenic mice were administered PF-2341066 in sterile water by oral gavage daily for 10 days at 100 mg/kg/day.

Double-transgenic mouse monitoring

Mice were observed biweekly for early detection of disease symptoms. When mice were moribund with palpable tumor burden, they were humanely killed.

Bone marrow transplantation

Bone marrow cells were harvested from the femurs and tibias of double-transgenic mice (maintained with Dox for 4 weeks after birth) and littermate mice. Unfractionated bone marrow cells were treated with 0.15M NH_4Cl, 1mM $KHCO_3$, and 0.1mM Na_2EDTA to eliminate erythrocytes before injection into the retro-orbital plexus of lethally γ-irradiated FVB/N mice (8.5 Gy) or sublethally γ-irradiated nonobese diabetic/severe combined immunodeficient (NOD/SCID) mice (1 Gy; ^{137}Cs source). Recipient mice irradiated 1 day before injections (5×10^6 bone marrow cells in 200 μL of phosphate-buffered saline) were not treated with Dox and were given antibiotic-containing water for 4 weeks after irradiation. All irradiated mice were monitored closely over their life spans, and, at the first sign of illness, they were killed. Peripheral blood, bone marrow, lymph nodes, spleen, skin, lung, kidney, and liver were collected for cytopathologic and histopathologic analyses, as described in "Histology and immunohistochemistry."

Western blotting

Western blotting was performed with the use of conventional techniques[17] with monoclonal antibodies (mAbs) against ALK (ALKc; a gift from Dr B. Falini, Institute of Hematology, University of Perugia; 1/200[27]), phosphotyrosine (clone 4G10; 1/1000; Upstate Biotechnology), and β-actin (clone AC-15; ascites fluid; 1/20 000; Sigma-Aldrich). NPM-ALK–positive Karpas cell line was used as positive control.

Histology and immunohistochemistry

Sections from formalin-fixed and paraffin-embedded tissues were stained with hematoxylin and eosin. Immunohistochemical analysis was performed with several mAbs or polyclonal antibodies directed against B220/CD45R (rat mAb; clone RA3-6B2; 1 /400), CD3 (rat mAb; clone CD3-12; 1/100), and F4/80 (rat mAb; clone CI:A3-1; 1/100) purchased from AbD Serotec; anti–CD138/Syndecan-1 (rat mAb; clone 281-2; 1/100; BD PharMingen), anti–Pax-5 (goat polyclonal antibody; sc-1974; 1/50; Santa Cruz Biotechnologies), and rabbit anti-ALK mAb (clone SP8; 1/100; Lab Vision Corporation). Antibody binding was detected with the streptavidin-biotin-peroxidase complex method (Vector Laboratories). The heat antigen retrieval procedure was used when necessary.

Confocal immunofluorescence microscopy

Sections were immunostained with a mouse monoclonal anti–human ALK protein (Clone ALK1, 1/100; Dako) and processed as previously described.[28] Nuclei were stained with TO-PRO-3 iodide (1/1000; Molecular Probe). Antibody binding was detected using a Leica DMR microscope equipped with the DFC300FX camera and a 40×/0.85 NA objective lens. Image processing was performed using IM50 software from Leica.

Flow cytometry

Cells isolated from tumor tissues were incubated with 5 mg/mL Fc receptors blocking antibody (anti–mouse CD16/32; clone 93; eBioscience) and 3% of heat-inactivated mouse serum diluted in staining buffer. Cells (1×10^6/well) were immunostained for 30 minutes at 4°C with mixtures of cell-surface markers, including directly labeled fluorescein isothiocyanate (FITC) anti-CD3 (clone 145-2C11; eBioscience), allophycocyanin–cyanin 5.5 (APL-Cy5.5) anti-CD19 (clone 6D5; eBioscience), phycoerythrin (PE)-–Cy7 anti-CD23 (clone B3B4; eBioscience), PE-Cy7 anti-CD25 (clone PC61.5; eBioscience), FITC anti-CD43 (clone eBioR2/60; eBioscience), biotin-conjugated anti–pre-B cell receptor (clone SL156; BD PharMingen), and biotin-conjugated anti–immunoglobulin M (clone II,41; eBioscience) for surface cytofluorimetric analysis. Biotin-conjugated antibodies were shown by allophycocyanin streptavidin (BD PharMingen; 554067). Cells were fixed and permeabilized with the use of the BD Cytofix/Cytoperm kit (554714) and stained with PE anti-ALK or isotype control (BD PharMingen; 559257) or FITC anti–μ heavy chain (1021-02; Southern Biotech) or FITC anti–κ light chain (BD PharMingen; 550003). Cell phenotype was determined with the use of an LSRII flow cytometer, followed by BD FACSDiva or WinMDI software analyses.

Apoptosis detection

Apoptosis was assessed by immunohistochemical analysis for caspase 3 (R&D Systems; AF835) and by fluorescence-activated cell sorting (FACS) for annexin V–PE (BD Biosciences) and 7-amino-actinomycin D (7-AAD; BD Biosciences) stainings, according to the manufacturer's instructions, and analyzed by LSRII flow cytometer and by BD FACSDiva software.

Statistical analysis

Statistical significance of differences was determined with the Mann-Whitney test. The minimal level of significance was a P value less than .05. Overall survival was assessed with Kaplan-Meier curves. Statistical comparison of Kaplan-Meier curves is based on the log-rank test. All statistical analyses were performed with GraphPad Prism software (GraphPad Software Inc).

Results

Generation of a conditional transgenic system for expression of the NPM-ALK or TPM3-ALK oncogenes

To generate transgenic mice conditionally expressing the ALK oncogenes (NPM-ALK or TPM3-ALK), we used the tetracycline regulatory system (Tet system) in which the tTA protein mediates the transcription of a transgene placed under the control of the tetracycline-responsive promoter (Tet-O).[29] In the Tet off version of this system, the addition of tetracycline or Dox, an analog of tetracycline, inhibits tTA action, promoting silencing of transgene expression.

Our conditional transgenic mice were generated in 2 steps. First, the human NPM-ALK and TPM3-ALK cDNAs were inserted downstream of a Tet-regulated cytomegalovirus minimal promoter into the pBIL vector,[30] allowing the concomitant expressions of ALK and firefly luciferase.[17] This construct (supplemental Figure 1A, available on the *Blood* Web site; see the Supplemental Materials link at the top of the online article) was introduced into the pronucleus of freshly fertilized FVB/N mouse oocytes. The resulting NPM-ALK or TPM3-ALK transgenic mouse lines were designated pBIL-NA and pBIL-TA, respectively. Three transgenic founder mice were obtained for pBIL-NA (pBIL-NA-1; pBIL-NA-2, and pBIL-NA-3) and 2 for pBIL-TA (pBIL-TA-1 and pBIL-TA-2) (supplemental Figure 1B). All transgenic lines developed into phenotypically normal and fertile mice. To assess ALK oncogene and luciferase expression, fibroblast primary cultures were generated from ear biopsies from each founder line. Then, these cells were transfected with a Tet-Off plasmid allowing tTA protein expression, and, after 2 days in culture with or without Dox (20 ng/mL), we observed that ALK oncogene and luciferase expression were induced in pBIL-NA-1–, pBIL-NA-2–, and pBIL-TA-2–derived cells (supplemental Figure 1C-D). NPM-ALK and TPM3-ALK were not detected in tTA-untransfected fibroblasts (S.G. and F.M., unpublished data, June 2006), showing a highly regulated expression in our system. Next, the conditional and lymphoid lineage-restricted activation of ALK transgene expression was achieved by breeding pBIL-NA-1, pBIL-NA-2, and pBIL-TA-2 founder mice with "driver" mice expressing tTA protein under the control of the EμSRα promotor/enhancer cassette to restrict the expression of the ALK transgenes to B or T lymphocytes[26,31,32] (Figure 1A).

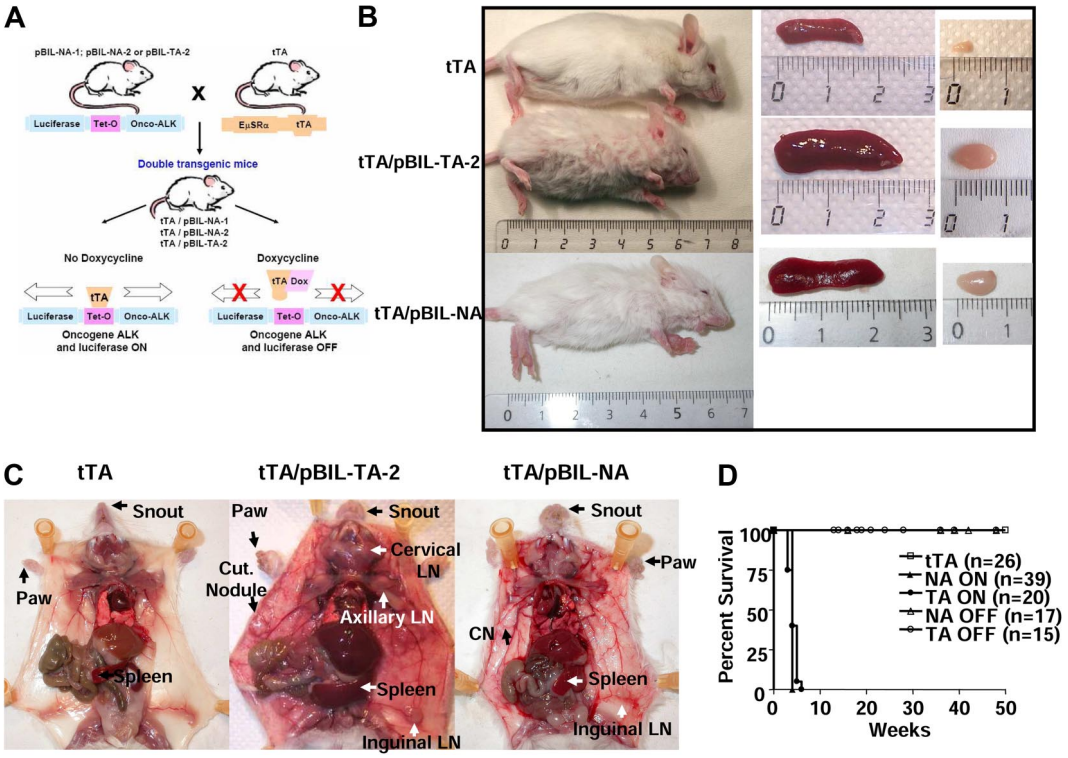

Figure 1. Macroscopic analysis of ALK-expressing double-transgenic mice. (A) Schematic representation of the generation of double-transgenic mice conditional for the expression of the ALK oncogene in the lymphoid lineage. Three heterozygous transgenic founder mice (pBIL-NA-1, pBIL-NA-2, and pBIL-TA-2) were crossed with homozygous EμSRα tTA mice. Double-transgenic mice were designated as tTA/pBIL-NA-1, tTA/pBIL-NA-2, and tTA/pBIL-TA-2. According to the absence (ON) or presence (OFF) of Dox, the tTA transactivator allows or not the expression of both ALK oncogene and luciferase genes. (B) The size of representative 4-week-old tTA/pBIL-TA-2 (TPM3-ALK) and tTA/pBIL-NA (NPM-ALK) double-transgenic mice are shown in comparison with a control age- and sex-matched tTA littermate animal. Spleen and lymph node enlargements in tTA/pBIL-TA-2 and tTA/pBIL-NA double-transgenic versus control tTA littermate mice are also shown. (C) Necropsy findings in tTA/pBIL-TA-2 and tTA/pBIL-NA double-transgenic mice show (arrows) disseminated lymphadenopathies (LN indicates lymph node) and spleen enlargement associated with multiple skin lesions and hypertrophy of the snout and paws (Cut Nodule indicates cutaneous nodules) in comparison with a control age- and sex-matched tTA littermate animal. (D) Survival curves showing the reduced life time of tTA/pBIL-TA-2 (TA ON) and tTA/pBIL-NA (NA ON) double-transgenic mice compared with control tTA littermate mice and Dox-treated tTA/pBIL-TA-2 (TA OFF) and tTA/pBIL-NA (NA OFF) double-transgenic mice.

Embryonic expression of the ALK oncogene is lethal

When conditional transgenic mice gestations occurred in the absence of Dox (No Dox), progeny number was consistently reduced (4 ± 1 newborns for the tTA/pBIL-NA-1 line, 6 ± 1 newborns for the tTA/pBIL-NA-2 line, and 4.3 ± 2.5 newborns for the tTA/pBIL-TA-2 line in comparison with 10 ± 2 newborns for normal wild-type FVB/N; supplemental Table 1; S.G. and F.M., unpublished data, August 2006). In addition, we failed to identify progeny that expressed both transgenes (supplemental Table 1). Among animals born alive, no NPM-ALK– or TPM3-ALK–positive animals were detected with the use of PCR genotyping (supplemental Table 1). These results strongly suggested that embryonic expression of the ALK oncogene is lethal. Preliminary results suggest that ALK fusion protein is expressed very early during embryogenesis (data not shown). To circumvent embryonic lethality, pregnant females were given Dox in their drinking water to block tTA protein and transgenes expression during gestation. Under these conditions, normal progeny number was observed, and 50% of double-transgenic mice (tTA/pBIL-NA or tTA/pBIL-TA) expressing ALK protein were obtained (supplemental Table 1). Such a frequency was expected because the tTA parents were homozygous and pBIL-NA and pBIL-TA were heterozygous.

Expression of NPM-ALK or TPM3-ALK in newborn mice resulted in aggressive lymphoma/leukemia

Expression of the ALK oncogene was induced in newborn mice by removing Dox from their drinking water. We observed that double-transgenic animals were easily identified because they developed an unexpected skin disease affecting the snout and paws, first detectable at 3 weeks of age (Figure 1B-C). These mice also exhibited general growth retardation (Figure 1B; supplemental Figure 2A-B) and died within a mean latency of 4 weeks (Figure 1D; $P < .001$). Note, we did not observe a significant difference in overall survival of NPM-ALK or TPM3-ALK double-transgenic mice (Figure 1D; $P = .113$).

At necropsy, we observed that mice exhibited multiple findings consistent with lymphoid malignancy, including marked splenomegaly (supplemental Figure 2C-D) and generalized lymphadenopathy (Figure 1B-C). Histopathologic studies showed that the architecture of lymph nodes (Figure 2A-B; supplemental Figure 3A-B) and spleen (Figure 2C-D; supplemental Figure 3C-D) was obliterated by malignant lymphoid cells. The lymphoid neoplasia consisted of medium to large-sized cells showing slightly irregular nuclei, with fine chromatin and small nucleoli, and scanty cytoplasms (Figure 2B-D; supplemental Figure 3B-D). Cytologic examination of blood smear showed an increase in circulating lymphocytes (supplemental Table 2), including large cells displaying a clumped nuclear chromatin (Figure 2E; supplemental Figure 3E), suggesting a leukemic dissemination of the disease. Large cells also invaded the skin (Figure 2F; supplemental Figure 3F), kidney (Figure 2G; supplemental Figure 3G), lung (Figure 2H; supplemental Figure 3H), and liver (Figure 2I; supplemental Figure 3I). We conclude that TPM3-ALK (Figure 2) and NPM-ALK (supplemental Figure 3) induce the same aggressive lymphoma/leukemia. Of note, no significant involvement was found in the thymus.

All transgenic mice also presented with skin nodules consisting of a hyperplasia of the epidermis, suggesting a keratoacanthoma-like lesion (Figure 2F; supplemental Figure 3F). A lymphomatous infiltration was sometimes observed in the dermis below the keratoacanthoma-like lesion (Figure 2F; supplemental Figure 3F). Histopathologic examination showed that snout and paw abnormalities were also because of keratoacanthoma-like lesions. Because all founder lines of double-transgenic mice (tTA/pBIL-NA-1, tTA/pBIL-NA-2, and tTA/pBIL-TA-2) developed the same hematopoietic and cutaneous diseases, we decided to focus our investigations only on one transgenic line for each oncogene. Those lines are now referred to as tTA/pBIL-NA and tTA/pBIL-TA.

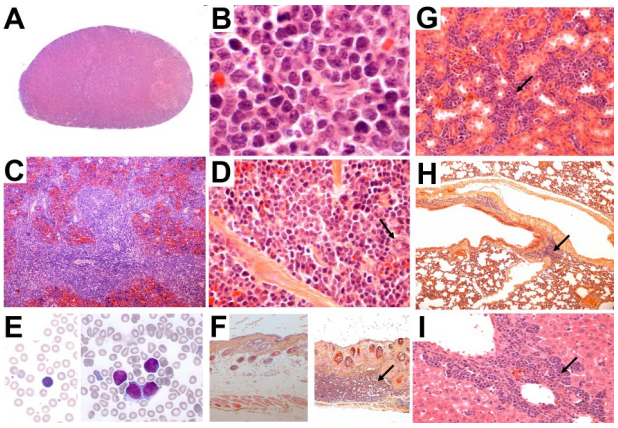

Figure 2. Histologic and cytologic analysis of TPM3-ALK–positive lymphoma and leukemic cells in blood from tTA/pBIL-TA double-transgenic mice. Hematoxylin and eosin staining on tissue sections from lymph node, spleen, kidney, lung, liver, and skin. The lymph node architecture is obliterated by abnormal lymphoid cells showing slightly irregular nuclei and scanty cytoplasms (A, original magnification ×50; B, original magnification ×1000). In the spleen, lymphoma cells are predominantly localized in the white pulp and show comparable morphologic features as seen in the lymph nodes. Note scattered megakaryocytes (arrow) (C, original magnification ×50; D, original magnification ×640). Wright-Giemsa–stained smear of peripheral blood showing presence of circulating abnormal lymphoid cells (E right, original magnification ×1000) compared with normal circulating lymphoid cells from control age-matched tTA littermate mice (E left, original magnification ×1000). All animals presented with skin nodules consisting of a hyperplasia of the epidermis, suggesting a keratoacanthoma-like lesion (F right, original magnification ×50) in comparison with normal skin from control age-matched tTA littermate mice (F left, original magnification ×50). (F right) As shown, a lymphomatous infiltration (arrow) was sometimes observed in the dermis below the keratoacanthoma-like lesion. Infiltration of various intensity was also found in kidney (G, original magnification ×400; arrow), lung (H, original magnification ×100; arrow), and liver (I, original magnification ×400; arrow).

NPM-ALK and TPM3-ALK are expressed in tumors

Immunohistochemistry with anti-ALK antibody performed on spleen (Figure 3B-C) and lymph node (Figure 3E-F) tissue sections from 10 diseased double-transgenic mice showed a heterogeneous staining of lymphoma cells. Some cells from tTA/pBIL-NA transgenic mice exhibited a strong cytoplasmic, nuclear, and nucleolar staining. A significant proportion of the remaining cells displayed a weak positivity (Figure 3C,F,I). Confocal microscopy highlighted weakly positive cells, and the subcellular distribution of NPM-ALK protein (Figure 3L,O). As observed in TPM3-ALK–positive human tumors, lymphoma cells from tTA/pBIL-TA showed a restricted cytoplasmic staining (Figure 3B,K). In lymph nodes, scattered lymphoma cells were also observed in lymphatic sinuses (Figure 3E-F). As expected, abnormal lymphoid cells in peripheral blood were positive for ALK (Figure 3H,I). The heterogeneity of lymphoma cells regarding the level of ALK expression was further confirmed by FACS analysis. Indeed, an overlay representation of ALK and isotype control intracellular staining showed that lymphoma cells isolated from lymph nodes expressed the ALK oncogene (right shift), in a continuum from weak to strong expression (Figure 3N), a feature also seen on confocal microscopy (Figure 3O). Immunoblotting of protein extracts from pathologic lymph nodes and spleen confirmed the expression of the 75-kDa NPM-ALK and 103-kDa TPM3-ALK fusion proteins as well as their tyrosine phosphorylation (Figure 3M). As expected, ALK oncogene was not expressed in age-matched littermate controls (tTA) and pBIL-NA and pBIL-TA single-transgenic mice (Figure

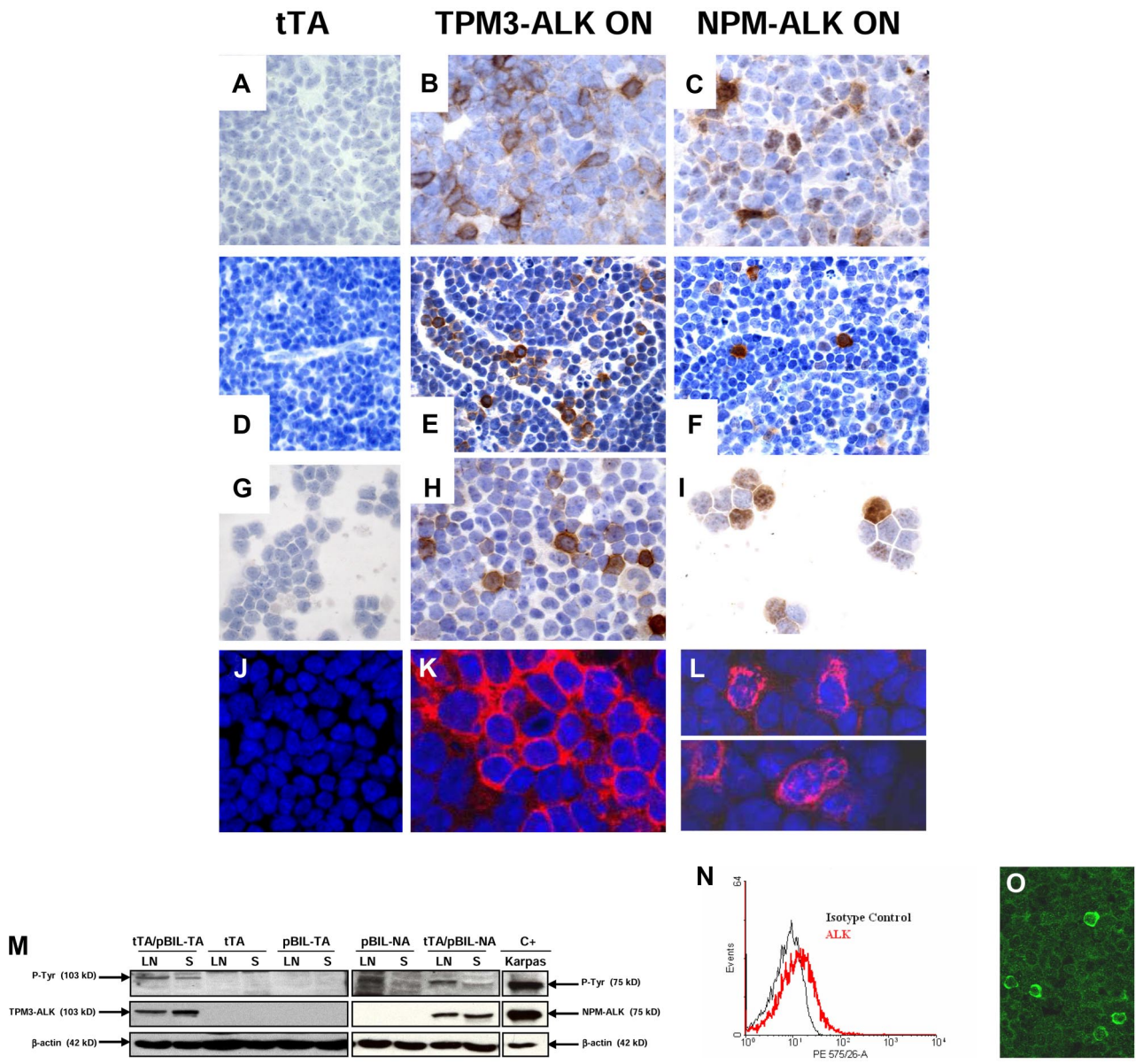

Figure 3. ALK oncogene expression in spleen, lymph node, and blood of TPM3-ALK and NPM-ALK double-transgenic mice. Immunohistochemical analysis of spleen (A-C, original magnification ×1000), lymph node (D, original magnification ×640; E-F, original magnification ×1000), blood lymphoid cells (G-I, original magnification ×1000) from control age-matched tTA (A,D,G), TPM3-ALK ON (tTA/pBIL-TA) (B,E,H), and NPM-ALK ON (tTA/pBIL-NA) (C,F,I) double-transgenic mice. Sections were stained with the rabbit anti-ALK antibody, and nuclei were counterstained with hematoxylin. NPM-ALK–positive tumor cells show a cytoplasmic and nuclear and nucleolar staining (C,F,I) in comparison with TPM3-ALK–positive tumor cells, which harbored a cytoplasmic and membrane staining (B,E,H). The staining intensity varies from cell to cell. Scattered ALK-positive lymphoma cells are observed in lymphatic sinuses (E-F). Confocal microscopy analysis shows the restricted cytoplasmic staining in TPM3-ALK (K) and the cytoplasmic and nucleolar staining in NPM-ALK (L) double-transgenic mice. Sections were stained with the mouse anti-ALK antibody, and nuclei were counterstained with TO-PRO-3 iodide. (M) Western blotting analysis of TPM3-ALK and NPM-ALK expressions. Protein lysates (100 μg) extracted from lymph nodes (LN) and spleens (S) of tTA/pBIL-TA and tTA/pBIL-NA double-transgenic mice; tTA, pBIL-TA, and pBIL-NA control transgenic mice; and positive control Karpas cell line overexpressing NPM-ALK (lane C+) were subjected to Western blotting analysis with anti-ALKc, antiphosphotyrosine, and anti–β-actin antibodies. (N) Flow cytometric analysis of ALK expression in lymph node cells from NPM-ALK double-transgenic mice. The histograms show ALK expression (red line) and isotype control (black line). Confocal microscopy (O) of lymphoma cells shows the heterogeneity of ALK expression as seen with flow cytometric analysis.

3M). Of note, the keratoacanthoma-like lesions of the skin were also strongly positive for ALK. In the thymus, only epithelial cells of the Hassall corpuscles were found to be positive for ALK protein. We conclude that conditional NPM-ALK and TPM3-ALK transgenic mice developed hematopoietic and cutaneous diseases exhibiting robust transgene expression.

NPM-ALK– and TPM3-ALK–induced lymphoma/leukemia are derived from B cells

We further characterized the phenotype of the lymphoma/leukemia. We found that the lymphomas induced by TMP3-ALK or NPM-ALK showed a massive expansion of CD45R/B220 and Pax5-positive large cells (B-cell markers) associated with residual normal $CD3^+$ T cells (Figure 4D-I). Lymphoma cells were negative for the plasma cell–associated marker CD138 and the macrophage marker F4/80 (S.G. and F.M., unpublished data, June 2007). Flow cytometric analysis with either CD19 or CD3 antibodies showed that the lymphoid population of pathologic lymph nodes consisted of 60% B cells and 28% T cells, whereas tTA normal lymph nodes displayed 75% T cells and 12% B cells (Figure 5A). To evaluate if the tumors were derived from B cells, tumor cells were stained for CD19, CD3, and ALK.[33] We found a population of

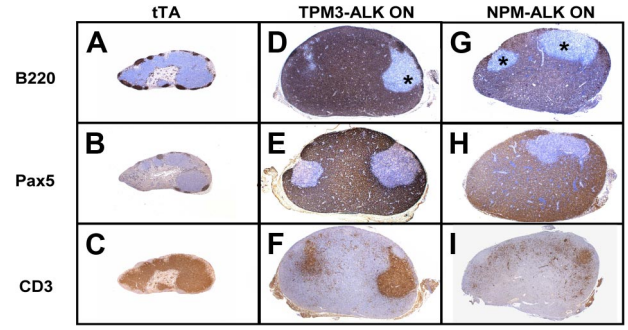

Figure 4. ALK oncogene double-transgenic mice develop B-cell lymphoma. Comparison of immunohistochemical stainings of lymph nodes from tTA control littermate (A-C), TPM3-ALK (ON; D-F), and NPM-ALK (ON; G-I) double transgenic mice. Serial sections show a massive involvement by lymphoma cells of B phenotype positive for B220 (D,G) and Pax5 (E,H). Negative areas (*) correspond to residual T cells positive for CD3 (F,I; original magnification ×40).

$CD19^+$ lymphoma cells positive for ALK (16% for TPM3-ALK and 15% for NPM-ALK cells, respectively; red plotted; Figure 5B-C), in agreement with results of ALK immunohistochemical staining (Figure 3). Taken together, these data showed that the NPM-ALK and TPM3-ALK double-transgenic mice developed the same ALK-positive B-cell lymphomas.

NPM-ALK– and TPM3-ALK–positive B-cell lymphoma development is independent of skin disease and can be induced by adoptive transfer into normal mice

Because conditional NPM-ALK and TPM3-ALK transgenic mice developed hematopoietic and cutaneous diseases exhibiting robust transgene expression, we investigated whether lymphoma development was autonomous to the hematopoietic system and not dependent on the skin disease. Bone marrow transplantation was performed with cells from (1) wild-type donor mice (n = 3) and (2) double-transgenic donor mice, maintained with Dox for 4 weeks after birth, into irradiated pure-bred recipient FVB/N (n = 10) or NOD/SCID (n = 3) mice. By 17 to 20 weeks after transplantation, 100% of the recipient FVB/N and NOD/SCID mice exhibited ALK-positive large cells in spleen and lymph nodes without skin lesions (supplemental Figures 5-6). Lymphoma cells positive for ALK were also observed in blood (data not shown) and bone marrow smears (supplemental Figure 6G-H). In addition, macroscopic examination of one NOD/SCID mouse showed a large mesenteric tumor mass (supplemental Figure 6D-F). Histopathologic examination of this mass showed that the architecture of lymph nodes was obliterated by sheets of ALK-positive B cells, confirming that the ALK-positive lymphoma cells were transplantable and able to grow independently of skin lesions.

NPM-ALK– and TPM3-ALK–induced B-cell lymphoma/leukemia are blocked at an early B-cell stage

Several markers were used to precisely identify the B-cell differentiation stage of the ALK/CD19-positive lymphoma cells. According to the Melchers-Rolinks classification,[34] $ALK/CD19^+$ cells (Figure 5C plotted in red) corresponded to pro-B/pre-B-1 cells because they were positive for CD19 and CD43 (92.17% ± 2.92%; Figure 5D) and a small proportion (20.70% ± 5.60%) also were positive for cytoplasmic μ heavy chain (Figure 5E). These cells were negative for serum immunoglobulin M, κ light chain, pre-B cell receptor, CD23, and CD25 (Figure 5F-H). Altogether, these results suggested that the ALK oncogene began to be expressed in pro-B cells but block the differentiation at the early pre-B cell stage. Similar results were obtained with $ALK/CD19^+$ lymphoma cells from tTA/pBIL-NA transgenic mice: CD43 (93.57% ± 2.29%) and μ heavy chain (17.33% ± 5.27%; data not shown).

ALK oncogene inactivation is sufficient to induce tumor regression

To determine whether the suppression of *ALK* transgene expression is sufficient to cause regression of lymphadenopathies, splenomegaly, and skin lesions, transgenic mice that were moribund with tumors were treated with Dox for 12 days to suppress ALK expression. Within a few days of treatment, the mice became more physically active, gained weight, and exhibited a major clearing of skin lesions and the regrowth of hair within 3 weeks (Figure 6A-B; supplemental Figure 4A-B). In addition, Dox administration resulted in the reduction in abdominal girth, and lymph nodes and spleen returned to their normal sizes (Figure 6G,H; supplemental Figure 4G,H). Twelve days after the initiation of Dox treatment, 10 mice were killed (10 regressed tTA/pBIL-NA and tTA/

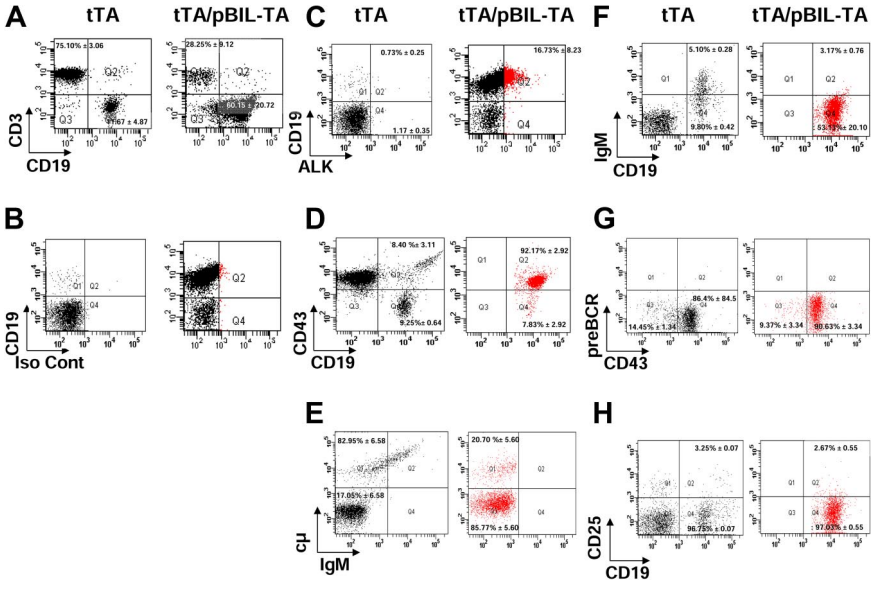

Figure 5. Flow cytometric analysis of the B-cell differentiation stage in TPM3-ALK double-transgenic mice. Representative dot plots of flow cytometric analysis of lymph node cells prepared from 4-week-old control tTA littermate and TPM3-ALK (tTA/pBIL-TA) double-transgenic mice. CD19 versus CD3 profiles of live gated lymphocytes are shown (A). ALK or isotype control (Iso Cont) versus membrane CD19 FACS profiles are shown (B-C). Lymph node cells were labeled with anti-CD19 and with anti-ALK antibodies and with anti-CD43 (D), anti-μ heavy chain (E), anti-immunoglobulin M (IgM; F), anti–pre-B cell receptor (BCR; G), and CD25 (H) antibodies. ALK-positive cells are plotted in red (C-H). Vertical and horizontal cursors were set so that > 99% of events in control unstained samples were in the bottom left quadrants. The numbers indicate the median percentage of cells with SD in a quadrant, relative to the plots of tTA and tTA/pBIL-TA transgenic mice.

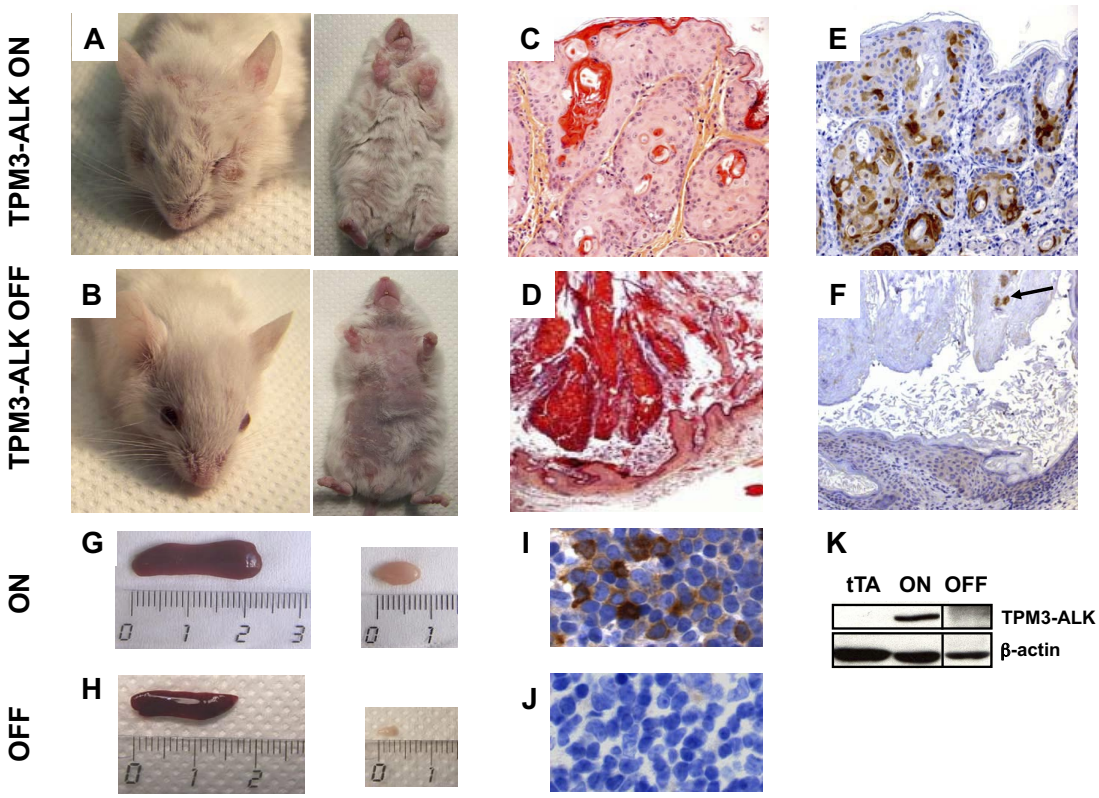

Figure 6. Lymphoma and cutaneous disease regression on ALK oncogene inactivation in TPM3-ALK mice. Clinical examination and autopsy findings show that all animals with fully developed disease (TPM3-ALK ON; n=10) presented with disseminated lymphoma with lymph node and spleen enlargement and skin nodules mostly related to keratoacanthoma-like lesions involving the skin, snout, and paws (TPM3-ALK ON: A,C,E,G,I). Ten additional moribund mice were treated with Dox in drinking water (100 μg/mL) and 1 intraperitoneal injection of 100 μL of Dox solution (100 μg/mL; TPM3-ALK OFF; B,D,F,H,J). Compared with the ON mice, the OFF mice exhibited, after 12 days of Dox treatment, a major clearing of the skin lesions (A,C vs B,D) associated with the regrowth of hair within 3 weeks, a regression of spleen and lymph node enlargement (G vs H), and an ALK oncogene expression down-regulation as assessed by anti-ALK immunostaining (E,I vs F,J) and Western blotting analysis (K lane ON vs OFF). Note, in panel K, a vertical line has been inserted to indicate a repositioned gel lane. In panel F, apoptotic ALK-positive cells admixed with exfoliated material (arrow). Original magnifications ×50 (C-F) and ×640 (I-J).

pBIL-TA; ie ALK-OFF), and tumor regression and disappearance of lymphoma cells were confirmed by histopathologic and immunophenotypic analyses of the tumor tissues (mesenteric and axillary lymph nodes, spleen, liver, kidney, lung, skin, and blood) after treatment. All these organs now were found to have normal architecture, and no ALK-positive cells were detected (Figures 6C-F,I,J and 7; supplemental Figures 4C-F,I,J and 7). In the skin, we observed a regression of keratoacanthoma-like lesions associated with an exfoliation (Figure 6C-D; supplemental Figure 4C-D) of apoptotic ALK-positive cells (Figure 6F). We then checked that tumor regression occurred as a result of Dox-induced ALK oncogene mRNA (data not shown) and protein expression (Figure 6K; supplemental Figure 4K) down-regulation. Thus, ALK inactivation for 12 days appeared sufficient to lead to tumor cell eradication from lymph node, spleen, blood, skin, and other organs. We conclude that in conditional NPM-ALK and TPM3-ALK transgenic mice the inactivation of ALK is sufficient to reverse tumorigenesis.

To determine whether ALK suppression exerted any effect on the viability of lymphoma cells, TPM3-ALK (supplemental Figure 8) and NPM-ALK (data not shown) double-transgenic mice were treated for 3 and 15 hours with Dox. After this time, B- and T-cell populations from lymph nodes were analyzed by immunohistochemistry with caspase 3 and FACS annexin V/7-AAD staining (supplemental Figure 8). We found an increase in the percentage of dead $CD19^+$ B cells (ie, lymphoma cells) during Dox treatment (from 14% in the first 3 hours to 22% at 15 hours; supplemental Figure 8). We also found a correlation between the percentage of caspase 3 and annexin V/7-AAD–positive cells, indicating that apoptosis was involved in dying cells. Beyond 15 hours of Dox treatment, the percentage of apoptotic cells decreased close to the value observed in untreated animals.

To further confirm that the tumor regression was related to the loss of ALK oncogene functional activity, we examined the affects of the treatment of NPM-ALK transgenic mice with a novel ALK phosphorylation inhibitor PF-2341066.[35] Seven moribund transgenic mice were treated for 10 days with this compound. We observed a progressive clearing of skin lesions together with an improvement of the general health status of treated mice compared with untreated controls. Necropsy findings showed tumor regression, confirmed by histopathologic examination, as after Dox treatment (supplemental Figures 7,9). Of note, the lymphoma regression after PF-2341066 treatment was not due to the inhibition of c-met phosphorylation (another target of this inhibitor)[35] because lymphoma cells in our model are negative for this receptor (date not shown). Hence, we conclude that this inhibitor of ALK is sufficient to induce reversal of tumorigenesis in our ALK conditional transgenic tumor model.

Discussion

Our results suggest that ALK-induced tumorigenesis can be reversed through the inactivation of ALK. They have important

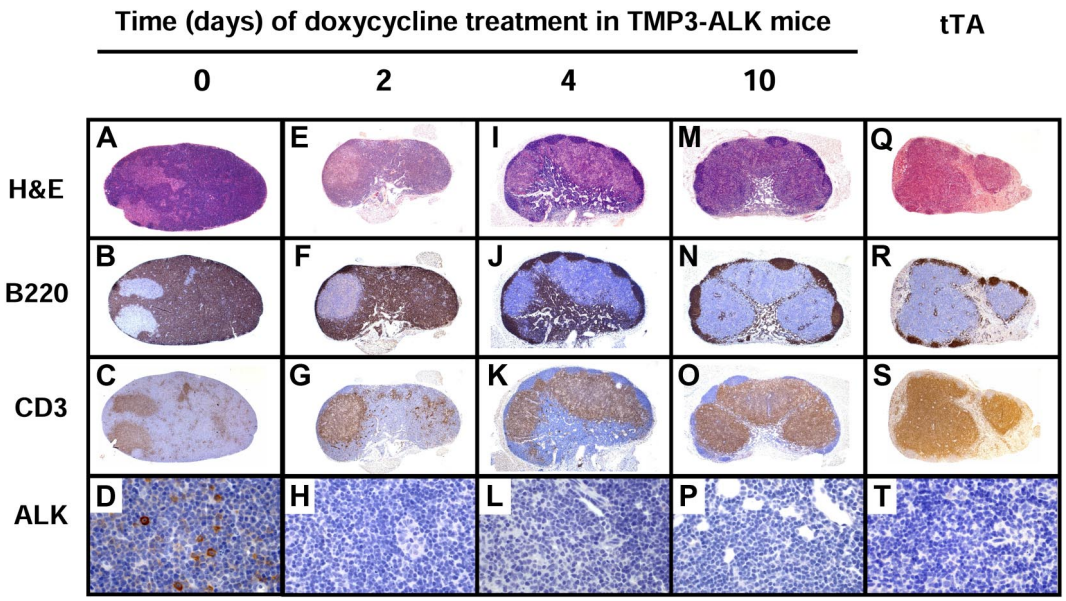

Figure 7. Histopathologic changes of lymph nodes after ALK inactivation by Dox treatment in lymph nodes of TMP3-ALK mice. The architecture of lymph node from mice with fully developed disease (day 0; A-D) is obliterated by lymphoma cells strongly positive for B220 (B). Negative area corresponds to residual T cells as seen in panel C. Lymphoma cells are positive for ALK (D). After Dox treatment (days 2-10: E-P), the lymph node progressively recovers its normal immunoarchitecture together with the decrease of ALK-positive lymphoma cells (H,L,P) and increase in normal B and T cells (M-O). Lymph node from tTA transgenic mice was used as a normal control (Q-T). Original magnification ×50 (A-C), ×40 (E-G,I-K,M-O,Q-S), and ×640 (D,H,L,P,T).

implications for the understanding of the role of ALK in the initiation and maintenance of tumorigenesis. We have developed a mouse model that will be useful for dissecting the contribution of pathologic activation of ALK to the pathogenesis of lymphoma/leukemia. Pathologic activation of ALK is well known to be associated with 2 major types of non-Hodgkin lymphomas, namely systemic anaplastic large cell lymphoma, T/Null and rare cases of diffuse large B-cell lymphomas with immunoblastic/plasmablastic features.[1,5,6] Most systemic T/Null anaplastic large cell lymphomas expressed NPM-ALK or TPM3-ALK, whereas ALK-positive diffuse large B-cell lymphomas are mostly associated with Clathrin-ALK and more rarely with NPM-ALK fusion protein.[8,9,11] However ALK tyrosine kinase is also involved in some nonhematopoietic neoplasia such as inflammatory myofibroblastic tumors (TPM3-ALK) as well as in some (< 5%) non–small cell lung tumors in which ALK protein is fused to EML4, the echinoderm microtubule-associated protein-like 4.[6,36,37] Our conditional transgenic model appears to recapitulate only some of the features of human ALK-positive lymphoma because lymphoma cells are of pro-B/pre-B phenotype (negative for CD138) and not of terminal B-cell stage of differentiation as seen in human ALK-positive B-cell lymphomas that are positive for CD138 antigen.[8,9,11]

Our results are consistent with previous reports that ALK activation can result in tumorigenesis in transgenic mouse models. The first description of a murine model to investigate the oncogenic events mediated by NPM-ALK was reported by Kuefer et al,[18] who used a retrovirus-mediated gene transfer strategy. After this report, several transgenic lines were generated in which the full-length NPM-ALK cDNA was placed under the control of various promoters such as CD4,[20] vav,[38] Lck,[21] or CD2.[39] Whatever the promoter used, transgenic mice developed mostly B-cell tumors, some with plasma cell differentiation,[19,20,38] and only a few T-cell lymphomas (mostly lymphoblastic lymphoma) have been reported.[20,21] As suggested by Chiarle et al,[20] the high incidence of B-cell tumors in NPM-ALK transgenic mice could be due to the forced expression of ALK oncogene. Our results are in agreement with those previously reported because NPM-ALK and TPM3-ALK transgenic mice developed lymphoma/leukemia of B-cell phenotype, further stressing the fact that in mouse, the ALK oncogene preferentially transforms the B-cell lineage. However, our results suggest that ALK oncogene overexpression could block B-cell differentiation at early B stage, even if the Eμ enhancer was previously described to be active throughout the entire B-lymphoid compartment, as reported in Eμ-*myc* and Eμ-*BrD2* transgenic mice.[40-42]

An important unique feature of our model system is that we have generated a transgenic mouse model in which ALK is conditionally expressed with the Tet-off system. We demonstrated that transgenic mice conditionally expressing the NPM-ALK or TPM3-ALK oncoprotein with tyrosine kinase activity developed a lethal lymphoproliferative disorder of early B-cell origin associated with skin lesions resembling keratoacanthoma. Of note, comparable skin lesions were previously described by a group using the same EμSRα enhancer/promoter to drive Tax transactivator protein overexpression. This is probably due to the high level of tTA expression in skin as reported in tTA/tax mice.[43] The results obtained in bone marrow transplantation experiments in FVB/N and NOD/SCID mice clearly showed that the lymphoma development was autonomous to the hematopoietic system and not dependent on the skin disease. The development of a lymphoid proliferation could be anticipated because, using our strategy, the hematopoietic lineage expression is controlled by the EμSRα enhancer/promoter sequence,[25,26,40,42] that drives the expression of the tTA protein. By crossing EμSRα-tTA homozygous transgenic mice with Tet-O-NPM-ALK or Tet-O-TPM3-ALK transgenic mice, we consistently obtained double-transgenic mice developing the same early B-cell tumor phenotype. Our results show for the first time, in an animal model, that activation of either NPM-ALK or TPM3-ALK oncogenic tyrosine kinases exhibit equal tumorigenic potential. In addition, our findings are consistent with previous reports showing that ALK fusion proteins can form homodimers (or oligomers) with dimerization sites at the N-terminus of ALK fusion protein, a mechanism which mimics ligand binding and is responsible for the activation of the catalytic domain

through the autophosphorylation of the tyrosine kinase domain of ALK.[6,13] Our observation of the very short tumor latency suggests that ALK activation alone is sufficient to result in the transformation of early B cells. Moreover, our observation that the inactivation of a conditional ALK transgene by Dox administration leads to the rapid, complete, and stable tumor regression suggests that ALK alone is required for tumor maintenance.

Our results are the first demonstration that ALK-induced tumorigenesis is reversible, even at a very advanced stage of the disease. The sustained regression on ALK oncogene inactivation suggests that malignant ALK-positive cells depend on the continued activation of ALK oncogene, a finding in agreement with the concept of "oncogene addiction" that was proposed.[44-46] Indeed, it is unlikely that the ALK oncogene promotes the emergence of additional genetic lesions that could compensate for ALK inactivation in the maintenance of the tumor phenotype. Our findings are in agreement to what has been reported in human anaplastic large cell lymphoma because, except for rare studies,[47,48] neither NPM-ALK nor other ALK fusion oncogenes have been described to induce genomic instability both in human cancers and in animal models. The striking loss of lymph node and spleen enlargement under Dox treatment raises the question of the underlying mechanism(s) responsible for the disappearance of ALK-positive lymphoma cells.

The relatively low percentage of apoptotic lymphoma cells in lymph nodes of animals treated for 15 hours together with the rapid recovery of the normal lymph node immunoarchitecture lead us to speculate that after the switch-off of ALK oncogene, a significant proportion of lymphoma cells can take a normal B-cell differentiation process again. Such a hypothesis is in agreement with what has been previously described by Felsher and Bishop[26] in mice overexpressing the *myc* oncogene. Similarly, the associated resolution of the ALK-induced keratoacanthoma-like lesions on ALK inactivation appears to be secondary to the exfoliation of apoptotic ALK-positive cells and regrowth of hair. Interestingly, preliminary results that we observed with the specific ALK inhibitor (PF-2341066)[35] are comparable with those obtained with Dox treatment. Thus, our results generally support the notion that oncogene inactivation can result in sustained tumor regression.[24] They also strongly suggest that NPM-ALK or TPM3-ALK tyrosine kinases are therapeutic targets comparable with Bcr-Abl in chronic myeloid leukemia and that ALK-specific inhibitors[16,35,49] would give therapeutic effects comparable with imatinib mesylate (STI571) that targets the Bcr-Abl oncogene in chronic myeloid leukemia.[50] It is now important to determine whether the targeted inactivation of the ALK tyrosine kinase oncogene would be sufficient to induce tumor regression in human neoplasia.

In conclusion, we have developed a conditional transgenic mouse model that mimics some of the features of human ALK-positive non-Hodgkin lymphomas. Our model offers a new tool to investigate in vivo the molecular mechanisms involved in the initiation and maintenance of ALK-associated lymphoproliferative disorders. Moreover, we have shown that our model can be used to preclinically test protein tyrosine kinase inhibitors, potentially useful for patients with ALK-associated tumors.

Acknowledgments

We thank members of the Pr G. Delsol laboratory, Dr S. Mancini, Dr B. Payrastre, and Dr K. Rabin for helpful discussions and critical reading. We thank Dr M. Rousseau (Centre de Distribution, Typage et Archivage animal, CNRS, Orléans) and Dr F. Cormier (Institut Curie, Paris) for their help to transfer the EμSRα-tTA mice from Paris to Toulouse. We thank, for their excellent technical assistance, S. Pillipenko, A. Huchenq, M. Calise, A. Tridon, and M. A. Daussion (Services de transgenèse et de zootechnie, IFR150-IFR BMT [ex IFR30], CHU Purpan, Toulouse); F. Capilla and D. Lestrade (Plateau technique d'histopathologie expérimentale, IFR150-IFR BMT, CHU Purpan, Toulouse); F. Ezzahra L'Faqihi-Olive and V. Duplan-Eche (Plateau technique de cytométrie, IFR150-IFR BMT, CHU Purpan, Toulouse); D. Roda and D. Lhuillier (Laboratoire d'Anatomie et Cytologie pathologiques, CHU Purpan, Toulouse); and J. Boyes (Inserm U563, CHU Purpan, Toulouse).

This work was supported by grants from Inserm, the "Cancéropôle Grand Sud-Ouest," the "Institut National du Cancer" (INCa), the Région Midi-Pyrénées, and the "Pôle de Compétitivité Cancer-Bio Santé/Fonds uniques interministériels des pôles de compétitivité" (G.D.), "la Fondation de France" (F.M.) and Comités 31 et 09 de la Ligue contre le cancer (F.M.); by postdoctoral fellowships from the "Association pour la Recherche sur le Cancer," "La Fondation de France," and "Pôle de Compétitivité Cancer-Bio Santé/Fonds uniques interministériels des pôles de compétitivité" (S.G.); by "Pôle de Compétitivité Cancer-Bio Santé/Fonds uniques interministériels des pôles de compétitivité" and "La Fondation de France" (M.F.); and by a PhD fellowship from the "Association pour la Recherche sur le Cancer" (E.D.).

This work is dedicated to the memory of Mr David Mason.

Authorship

Contribution: S.G., G.D., and F.M. designed research; S.G., M.F., E.D., T.A.S., C.D., A.R., and F.M. performed research; A.K., C.S. and D.W.F. helped with discussions and critical reading; S.G., T.A.S., C.D., C.S., G.D., and F.M. analyzed data; and S.G., D.W.F., G.D., and F.M. wrote the paper.

Conflict-of-interest disclosure: The authors declare no competing financial interests.

Correspondence: Georges Delsol, Inserm, U563, Centre de Physiopathologie de Toulouse Purpan, Toulouse, F-31300 France; e-mail: georges.delsol@inserm.fr.

References

1. Morris SW, Kirstein MN, Valentine MB, et al. Fusion of a kinase gene, ALK, to a nucleolar protein gene, NPM, in non-Hodgkin's lymphoma. *Science.* 1994;263(5151):1281-1284.
2. Lamant L, Dastugue N, Pulford K, Delsol G, Mariame B. A new fusion gene TPM3-ALK in anaplastic large cell lymphoma created by a (1;2)(q25;p23) translocation. *Blood.* 1999;93(9):3088-3095.
3. Touriol C, Greenland C, Lamant L, et al. Further demonstration of the diversity of chromosomal changes involving 2p23 in ALK-positive lymphoma: 2 cases expressing ALK kinase fused to CLTCL (clathrin chain polypeptide-like). *Blood.* 2000;95(10):3204-3207.
4. Lamant L, Gascoyne RD, Duplantier MM, et al. Non-muscle myosin heavy chain (MYH9): a new partner fused to ALK in anaplastic large cell lymphoma. *Genes Chromosomes Cancer.* 2003;37(4):427-432.
5. Pulford K, Lamant L, Espinos E, et al. The emerging normal and disease-related roles of anaplastic lymphoma kinase. *Cell Mol Life Sci.* 2004;61(23):2939-2953.
6. Chiarle R, Voena C, Ambrogio C, Piva R, Inghirami G. The anaplastic lymphoma kinase in the pathogenesis of cancer. *Nat Rev Cancer.* 2008;8(1):11-23.
7. Swerdlow SH, Campo E, Harris NL, et al. *WHO Classification of Tumours of Haematopoietic and*

Lymphoid Tissues. 4th ed. Lyon, France, IARC Press; 2008.

8. Delsol G, Lamant L, Mariame B, et al. A new subtype of large B-cell lymphoma expressing the ALK kinase and lacking the 2; 5 translocation. *Blood.* 1997;89(5):1483-1490.
9. Gascoyne RD, Lamant L, Martin-Subero JI, et al. ALK-positive diffuse large B-cell lymphoma is associated with Clathrin-ALK rearrangements: report of 6 cases. *Blood.* 2003;102(7):2568-2573.
10. Adam P, Katzenberger T, Seeberger H, et al. A case of a diffuse large B-cell lymphoma of plasmablastic type associated with the t(2;5)(p23; q35) chromosome translocation. *Am J Surg Pathol.* 2003;27(11):1473-1476.
11. Onciu M, Behm FG, Downing JR, et al. ALK-positive plasmablastic B-cell lymphoma with expression of the NPM-ALK fusion transcript: report of 2 cases. *Blood.* 2003;102(7):2642-2644.
12. Armstrong F, Duplantier MM, Trempat P, et al. Differential effects of ×-ALK fusion proteins on proliferation, transformation, and invasion properties of NIH3T3 cells. *Oncogene.* 2004;23(36): 6071-6082.
13. Bischof D, Pulford K, Mason DY, Morris SW. Role of the nucleophosmin (NPM) portion of the non-Hodgkin's lymphoma-associated NPM-anaplastic lymphoma kinase fusion protein in oncogenesis. *Mol Cell Biol.* 1997;17(4):2312-2325.
14. Fujimoto J, Shiota M, Iwahara T, et al. Characterization of the transforming activity of p80, a hyperphosphorylated protein in a Ki-1 lymphoma cell line with chromosomal translocation t(2;5). *Proc Natl Acad Sci U S A.* 1996;93(9):4181-4186.
15. Wellmann A, Doseeva V, Butscher W, et al. The activated anaplastic lymphoma kinase increases cellular proliferation and oncogene up-regulation in rat 1a fibroblasts. *FASEB J.* 1997;11(12):965-972.
16. Galkin AV, Melnick JS, Kim S, et al. Identification of NVP-TAE684, a potent, selective, and efficacious inhibitor of NPM-ALK. *Proc Natl Acad Sci U S A.* 2007;104(1):270-275.
17. Giuriato S, Faumont N, Bousquet E, et al. Development of a conditional bioluminescent transplant model for TPM3-ALK-induced tumorigenesis as a tool to validate ALK-dependent cancer targeted therapy. *Cancer Biol Ther.* 2007;6(8):1318-1323.
18. Kuefer MU, Look AT, Pulford K, et al. Retrovirus-mediated gene transfer of NPM-ALK causes lymphoid malignancy in mice. *Blood.* 1997;90(8): 2901-2910.
19. Miething C, Grundler R, Fend F, et al. The oncogenic fusion protein nucleophosmin-anaplastic lymphoma kinase (NPM-ALK) induces two distinct malignant phenotypes in a murine retroviral transplantation model. *Oncogene.* 2003;22(30): 4642-4647.
20. Chiarle R, Gong JZ, Guasparri I, et al. NPM-ALK transgenic mice spontaneously develop T-cell lymphomas and plasma cell tumors. *Blood.* 2003; 101(5):1919-1927.
21. Jager R, Hahne J, Jacob A, et al. Mice transgenic for NPM-ALK develop non-Hodgkin lymphomas. *Anticancer Res.* 2005;25(5):3191-3196.
22. Miething C, Peschel C, Duyster J. Targeting the oncogenic tyrosine kinase NPM-ALK in lymphoma: the role of murine models in defining pathogenesis and treatment options. *Curr Drug Targets.* 2006;7(10):1329-1334.
23. Turner SD, Alexander DR. What have we learnt from mouse models of NPM-ALK-induced lymphomagenesis? *Leukemia.* 2005;19(7):1128-1134.
24. Giuriato S, Rabin K, Fan AC, Shachaf CM, Felsher DW. Conditional animal models: a strategy to define when oncogenes will be effective targets to treat cancer. *Semin Cancer Biol.* 2004; 14(1):3-11.
25. Adams JM, Cory S. Transgenic models for haemopoietic malignancies. *Biochim Biophys Acta.* 1991;1072(1):9-31.
26. Felsher DW, Bishop JM. Reversible tumorigenesis by MYC in hematopoietic lineages. *Mol Cell.* 1999;4(2):199-207.
27. Falini B, Bigerna B, Fizzotti M, et al. ALK expression defines a distinct group of T/null lymphomas ("ALK lymphomas") with a wide morphological spectrum. *Am J Pathol.* 1998;153(3):875-886.
28. Honorat JF, Ragab A, Lamant L, Delsol G, Ragab-Thomas J. SHP1 tyrosine phosphatase negatively regulates NPM-ALK tyrosine kinase signaling. *Blood.* 2006;107(10):4130-4138.
29. Gossen M, Bujard H. Tight control of gene expression in mammalian cells by tetracycline-responsive promoters. *Proc Natl Acad Sci U S A.* 1992;89(12):5547-5551.
30. Baron U, Freundlieb S, Gossen M, Bujard H. Co-regulation of two gene activities by tetracycline via a bidirectional promoter. *Nucleic Acids Res.* 1995;23(17):3605-3606.
31. Alexander WS, Schrader JW, Adams JM. Expression of the c-myc oncogene under control of an immunoglobulin enhancer in E mu-myc transgenic mice. *Mol Cell Biol.* 1987;7(4):1436-1444.
32. Harris AW, Langdon WY, Alexander WS, et al. Transgenic mouse models for hematopoietic tumorigenesis. *Curr Top Microbiol Immunol.* 1988; 141:82-93.
33. Damm-Welk C, Schieferstein J, Schwalm S, Reiter A, Woessmann W. Flow cytometric detection of circulating tumour cells in nucleophosmin/anaplastic lymphoma kinase-positive anaplastic large cell lymphoma: comparison with quantitative polymerase chain reaction. *Br J Haematol.* 2007;138(4):459-466.
34. Osmond DG, Rolink A, Melchers F. Murine B lymphopoiesis: towards a unified model. *Immunol Today.* 1998;19(2):65-68.
35. Christensen JG, Zou HY, Arango ME, et al. Cytoreductive antitumor activity of PF-2341066, a novel inhibitor of anaplastic lymphoma kinase and c-Met, in experimental models of anaplastic large-cell lymphoma. *Mol Cancer Ther.* 2007; 6(12):3314-3322.
36. Rikova K, Guo A, Zeng Q, et al. Global survey of phosphotyrosine signaling identifies oncogenic kinases in lung cancer. *Cell.* 2007;131(6):1190-1203.
37. Soda M, Choi YL, Enomoto M, et al. Identification of the transforming EML4-ALK fusion gene in non-small-cell lung cancer. *Nature.* 2007;448 (7153):561-566.
38. Turner SD, Tooze R, Maclennan K, Alexander DR. Vav-promoter regulated oncogenic fusion protein NPM-ALK in transgenic mice causes B-cell lymphomas with hyperactive Jun kinase. *Oncogene.* 2003;22(49):7750-7761.
39. Turner SD, Merz H, Yeung D, Alexander DR. CD2 promoter regulated nucleophosmin-anaplastic lymphoma kinase in transgenic mice causes B lymphoid malignancy. *Anticancer Res.* 2006; 26(5A):3275-3279.
40. Adams JM, Harris AW, Pinkert CA, et al. The c-myc oncogene driven by immunoglobulin enhancers induces lymphoid malignancy in transgenic mice. *Nature.* 1985;318(6046):533-538.
41. Greenwald RJ, Tumang JR, Sinha A, et al. E mu-BRD2 transgenic mice develop B-cell lymphoma and leukemia. *Blood.* 2004;103(4):1475-1484.
42. Langdon WY, Harris AW, Cory S, Adams JM. The c-myc oncogene perturbs B lymphocyte development in E-mu-myc transgenic mice. *Cell.* 1986; 47(1):11-18.
43. Kwon H, Ogle L, Benitez B, et al. Lethal cutaneous disease in transgenic mice conditionally expressing type I human T cell leukemia virus Tax. *J Biol Chem.* 2005;280(42):35713-35722.
44. Felsher DW. Opinion: cancer revoked: oncogenes as therapeutic targets. *Nat Rev Cancer.* 2003;3(5):375-379.
45. Sharma SV, Settleman J. Oncogenic shock: turning an activated kinase against the tumor cell. *Cell Cycle.* 2006;5(24):2878-2880.
46. Weinstein IB. Cancer. Addiction to oncogenes–the Achilles heal of cancer. *Science.* 2002; 297(5578):63-64.
47. Ventura RA, Martin-Subero JI, Knippschild U, et al. Centrosome abnormalities in ALK-positive anaplastic large-cell lymphoma. *Leukemia.* 2004; 18(11):1910-1911.
48. Salaverria I, Bea S, Lopez-Guillermo A, et al. Genomic profiling reveals different genetic aberrations in systemic ALK-positive and ALK-negative anaplastic large cell lymphomas. *Br J Haematol.* 2008;140(5):516-526.
49. Li R, Morris SW. Development of anaplastic lymphoma kinase (ALK) small-molecule inhibitors for cancer therapy. *Med Res Rev.* 2008;28(3):372-412.
50. Druker BJ, Talpaz M, Resta DJ, et al. Efficacy and safety of a specific inhibitor of the BCR-ABL tyrosine kinase in chronic myeloid leukemia. *N Engl J Med.* 2001;344(14):1031-1037.

Article 3

Hypoxia-microRNA-16 downregulation induces VEGF expression in anaplastic lymphoma kinase (ALK)-positive anaplastic large-cell lymphomas

E Dejean, MH Renalier, M Foisseau, X Agirre, N Joseph, GR de Paiva, T Al Saati, J Soulier, C Desjobert, L Lamant, F Prosper, DW Felsher, J Cavaillé, H Prats, G Delsol, S Giuriato * and F Meggetto*

**co-senior auteurs*

LEUKEMIA

Vol.25, pp. 1882–1890, 2011

Leukemia (2011) 25, 1882–1890

www.nature.com/leu

ORIGINAL ARTICLE

Hypoxia-microRNA-16 downregulation induces VEGF expression in anaplastic lymphoma kinase (ALK)-positive anaplastic large-cell lymphomas

E Dejean[1], MH Renalier[2], M Foisseau[1], X Agirre[3], N Joseph[2], GR de Paiva[4], T Al Saati[5], J Soulier[6,7], C Desjobert[1], L Lamant[1,8], F Prósper[3], DW Felsher[9], J Cavaillé[2], H Prats[1], G Delsol[1,8], S Giuriato[1,8,10] and F Meggetto[1,8,10]

[1]*Centre de Recherches en Cancérologie de Toulouse, INSERM-UMR 1037-Université Toulouse III Paul Sabatier, Toulouse, France;* [2]*CNRS UMR 5099, Laboratoire de Biologie Moléculaire Eucaryote and Université de Toulouse III Paul Sabatier, Toulouse, France;* [3]*Foundation for Applied Medical Research, Division of Oncology, Universidad de Navarra, Navarra, Spain;* [4]*Laboratoire d'Anatomie Pathologique, CHU Rangueil, Toulouse, France;* [5]*Plateau technique d'histopathologie expérimentale de l'IFR150-IFR BMT/Génopôle Toulouse-Midi Pyrénées, CHU Purpan, Toulouse, France;* [6]*INSERM U944 and Laboratoire d'hématologie APHP, Hôpital Saint-Louis, PARIS, France;* [7]*Institut Universitaire d'hématologie, Université Paris Diderot, PARIS, France;* [8]*European Research Initiative on ALCL (ERIA), (http://www.erialcl.net) and* [9]*Oncology Division, Center for Clinical and Science Research, Stanford University, Stanford, CA, USA*

The anaplastic lymphoma kinase (ALK), tyrosine kinase oncogene we used conditional onco-ALK (NPM-ALK and TPM3-ALK) mouse MEF cell lines (ALK+ fibroblasts) and transgenic models (ALK+ B-lymphoma) to investigate the involvement and regulation of angiogenesis in ALK tumor development. First, we observed that ALK expression leads to downregulation of miR-16 and increased Vascular Endothelial Growth Factor (VEGF) levels. Second, we found that modification of miR-16 levels in TPM3-ALK MEF cells greatly affected VEGF levels. Third, we demonstrated that miR-16 directly interacts with VEGF mRNA at the 3′-untranslated region and that the regulation of VEGF by miR-16 occurs at the translational level. Fourth, we showed that expression of both the ALK oncogene and hypoxia-induced factor 1α (HIF1α) is a prerequisite for miR-16 downregulation. Fifth, *in vivo*, miR-16 gain resulted in reduced angiogenesis and tumor growth. Finally, we highlighted an inverse correlation between the levels of miR-16 and VEGF in human NPM-ALK+ Anaplastic Large Cell Lymphomas (ALCL). Altogether, our results demonstrate, for the first time, the involvement of angiogenesis in ALK+ ALCL and strongly suggest an important role for hypoxia-miR-16 in regulating VEGF translation.
Leukemia (2011) **25,** 1882–1890; doi:10.1038/leu.2011.168; published online 22 July 2011
Keywords: onco-ALK; lymphomas; microRNA; VEGF

Introduction

The role of Vascular Endothelial Growth Factor (VEGF) in solid tumor pathologies has been extensively investigated and evidence has recently emerged that it may also have a role in hematological malignancies.[1,2] VEGF expression by neoplastic cells has been demonstrated in non-Hodgkin lymphomas and has been correlated with tumor progression and poor survival rates.[3] VEGF promotes the formation of new blood vessels by stimulating endothelial cell division and migration; this neo-vascular network allows tumor growth and metastasis.[4] Regulation of VEGF occurs at multiple levels, including transcription, mRNA stabilization and splicing, and translation.[5,6]

MicroRNAs (miRNAs) are 20–25-nucleotide-long non-coding RNAs that act as negative regulators of gene expression. They bind to a specific sequence of mRNA, usually located in the 3′-UTR (untranslated region). This interaction can lead either to targeted mRNA cleavage or to repression of mRNA translation, in both cases resulting in reduced levels of the encoded protein.[7] miRNAs are important in the regulation of cellular differentiation, proliferation and apoptosis.[8] Some miRNAs are considered to be oncogenes or tumor suppressors and are aberrantly expressed in tumors including hematological malignancies.[9,10] Aberrant expression of miRNAs can arise via a number of different mechanisms, such as genomic abnormalities or epigenetic modifications.[9–11] Recently, several miRNAs have been found to regulate angiogenic processes.[12] Notably, miR-15a and miR-16-1 have an important role via regulation of VEGF expression.[13] miR-16, is downregulated by hypoxia,[14] supporting the notion that a hypoxia-induced reduction of miR-16 levels contributes to an increase in VEGF expression.

Anaplastic lymphoma kinase (ALK) fusion proteins (onco-ALK) have been detected in several human malignancies, including Anaplastic Large Cell Lymphomas (ALCL),[15] diffuse large B-cell lymphomas[16,17] and a wide variety of solid cancers, such as inflammatory myofibroblastic tumors[18] and non-small cell lung cancers.[19] The mechanisms of malignant cell transformation mediated by oncogenic ALK tyrosine kinase expression are not clearly understood. Recently, Marzec *et al.* reported that ALK-positive (ALK+) ALCL strongly express hypoxia-induced factor 1α (HIF1α) mRNA, even under normoxic conditions. They found that inhibition of HIF1α expression markedly suppressed cell growth and proliferation and decreased VEGF synthesis in ALCL cell line.[20] As lymphoma tissues are predominantly under hypoxic conditions, it is possible that HIF1α has an important role in the pathogenesis of ALK+ ALCL.

Compared with ALK-negative (ALK−) ALCL, ALK+ ALCL have a better prognosis when undergoing CHOP-based chemotherapy,[21,22] however, ALK+ ALCL relapses after chemotherapy are very invasive and have a worse prognosis.[23,24] We recently developed conditional mouse models for NPM- and TPM3-ALK-induced lymphomagenesis using the tetracycline system.[25] In these models, ALK oncogenes induce B lymphoma formation associated with a robust angiogenesis. Although these models do not truly reproduce the human disease, they represent a powerful

Correspondence: Dr F Meggetto, Department of Hematology and Immunology, CRCT, INSERM-UMR 1037, Bâtiment B—Pavillon Lefevre, CHU Purpan, BP-3028, 31024 Toulouse Cedex-3, France.
E-mail: fabienne.meggetto@inserm.fr
[10]These authors are senior co-authors.
Received 1 February 2011; revised 18 April 2011; accepted 30 May 2011; published online 22 July 2011

tool to investigate the molecular mechanisms involved in ALK-associated disorders.

Until now, the role of VEGF in ALCL development and post-treatment relapse has not been studied. Here, we used onco-ALK (NPM-ALK and TPM3-ALK) mouse conditional MEF cell line (ALK+ fibroblasts),[25] as well as transgenic models (ALK+ B-lymphoma),[26] to both determine whether ALK oncogenes regulate VEGF levels and tumor angiogenesis and investigate the mechanisms involved.

Materials and methods

Conditional murine models

Generation of conditional transgenic mice and MEF Tet-OFF cells (Clontech, Saint Quentin Yvelines, France) for expression of NPM-ALK or TPM3-ALK oncogenes was described by Giuriato *et al*.[25,26] The tetracycline regulatory system was used to control the transgene transcription. The addition of doxycycline (an analog of tetracycline) allowed silencing of onco-ALK expression (OFF condition, ALK–), whereas doxycycline removal permitted onco-ALK expression (ON condition, ALK+). Lymph nodes from ALK+, ALK− and healthy mice, that is, normal littermate transgenic mice were used for RNA and DNA extractions.

Tumor and normal samples

The study was carried out in accordance with the institutional review board-approved protocols and the procedures followed were in accordance with the Helsinki Declaration of 1975, as revised in 2000. The diagnosis of ALCL was based on morphologic and immunophenotypic criteria as described in the last WHO classification.[27,28] The percentage of malignant cells was assessed by ALK1 or CD30 staining and was greater than 80% for all selected cases. Frozen tumor samples from 20 ALK+ ALCL, 6 ALK− ALCL, and 5 reactive lymph nodes were retrieved from the tumor bank from Toulouse CHU and used for RNA and DNA extractions. A total of 100cases with available paraffin blocks, of which 86 cases were positive for the ALK protein, were used to prepare tissue microarrays. Sera from ALCL patients (ALK+: $n=17$ and ALK−: $n=16$) and five healthy donors were used to perform VEGF ELISA.

RNA preparation

Total RNA was prepared using the TRIzol reagent (Invitrogen, Carlsbad, CA, USA) according to the manufacturer's protocol. The concentration of RNA was quantified using a NanoDrop Spectrophotometer (Nanodrop Technologies, Wilmington, DE, USA). RNA integrity was evaluated using an Agilent 2100 BioAnalyzer (Agilent Technologies, Palo Alto, CA, USA). RNAs with an RNA integrity number >7.5 were used for miRNA and mRNA quantifications.

Real-time RT-PCR assays

All qPCR were performed using an ABI 7300 Real-Time instrument (Applied Biosystems, Foster, CA, USA). TaqMan miRNA assays (Applied Biosystems, CA, USA) were used to measure miR-15a and miR-16 expression following manufacturer's instructions. RNU24 for human and SnoRNA202 for mice served as internal controls.

Expression of *S14*, *HIF1α* and *VEGF* genes were estimated by qPCR using a primer pair designed as follows: for human or mouse VEGF, the forward primer was 5′-CGAGATAGAGTA CATCTTCAAGC-3′ and the reverse primer was 5′-TTGATCCG CATGATCTGCATGG-3′. For human HIF1α, the forward primer was 5′-CATAAAGTCTGCAACATGGAAGGT-3′ and the reverse primer was 5′-ATTTGATGGGTGAGGAATGGGTT-3′. Human or mouse S14 was used as reference or housekeeping gene; the forward primer 5′-ATCAAACTCCGGGCCACAGGA-3′ and the reverse primer was 5′-CTGCTGTCAGAGGGGATGGGG-3′ for human and the forward primer was 5′-GGTGGCTGAGG GAGAGAATG-3′ and the reverse primer was 5′-CTCGGCA GATGGGTTTCCTTG-3′ for mouse. cDNA was synthesized from total RNA using M-MLV reverse transcriptase (Promega, Madison, WI, USA). qPCR was performed using SYBR green real-time PCR master mix (Eurogentec, Angers, France). The PCR mixture (25 μl) consisted of 12.5 μl master mixture, 0.75 μl for each PCR primer at 10 μM, 5 μl diluted cDNA and 6 μl DNase and RNase free water. qPCR was done using 40 cycles of 15 s at 90 °C and 1 min at 60 °C.

Relative fold changes of miRNA and target transcript expression were calculated by the ΔΔCT method and the values were expressed as $2(-\Delta\Delta CT)$. Detected target transcripts were normalized to the endogenous housekeeping gene *S14*.

miRNA northern blotting

Northern blots were performed using 10 μg of total RNA on denaturing PAGE. After blotting on Amersham Hybond-N+, miR oligonucleotides complementary to miR-15a and miR-16 5′-end-labeled using T4 polynucleotide kinase and γ-^{32}P ATP, were used as a probe.

miRNA transient transfections and target validations

MEF-TPM3-ALK cells[25] were transfected with 50 nM of pre-miR-15a (miR-15a) *or* pre-miR-16 (miR-16) (Ambion, Applied Biosystems, Austin, TX, USA), negative control miRNA (pre-miR control no. 1 or scramble; Ambion, Applied Biosystems), locked nucleic acid (LNA) (5′-CGCCAATATTTACGTGCTGCTA-3′) (LNA-16) (Sigma-Aldrich Chimie, Saint-Quentin Fallavier, France) or anti-miR-16 (Ambion, Applied Biosystems), using MEF transfection reagent (Altogen, Las Vegas, NV, USA) following the manufacturer's protocol. The expression of miR-16 was detected by RT-qPCR 48 h after transfection.

MEF-TPM3-ALK cells were transfected with 20 ng of pRLCMV-VEGF 3′-UTR wild-type (pRL-VEGF 3′-UTR)[29] and 250 ng of pCMV-β-Gal control vector serving as transfection control in a 12-well plate. For the co-transfection of miR-16, LNA-16, anti-miR-16 or scrambled miRNA was added with the reporter vectors, 50 nM of each miRNA or 50 nM of each inhibitor or control was transfected using Lipofectamine 2000 (Invitrogen, Cergy Pontoise, France). Cell lysate was collected and assayed 48 h after transfection. *Renilla* luciferase (LucR) activities were measured with a luminometer (Centro LB960, Berthold, Berthold Technologies, Thoiry, France) using the Luciferase Reporter Assay (Promega) and galactosidase activity was measured using the β-galactosidase enzyme assay system (Promega) according to the manufacturer's instructions. The results are expressed as relative luciferase activity/galactosidase activity.

All transfections and measurements were performed in triplicate and repeated at least three times.

VEGF ELISA

In all 96-well plates coated with anti-mouse or -human VEGF monoclonal antibody (Calbiochem, Merck KGaA, Darmstadt, Germany) were used to measure VEGF secretion following the manufacturer's guidelines. Absorbance was measured at 450 nm

with a wavelength correction at 570 nm. Each experiment was performed in triplicate and repeated three times.

VEGF and HIF1α immunohistochemistry

Sections (5 μM) were cut from each tissue microarray, deparaffinized, subjected to heat antigen retrieval and stained with rabbit polyclonal anti-VEGF antibody (A20, 1/40 dilution, Santa Cruz Biotechnology, Santa Cruz, CA, USA) or anti-HIF-1α antibody (clone H1α67, 1/100, Novus Biologicals, Cambridge, UK). *Antibody binding was detected with Dako REAL Detection System* (Code K5001, Dako France, Trappes, France). The percentage of positive cells was evaluated using a Leica DMR microscope (Leica Geosystems France, Le Pecq, France) equiped with a DFC300FX camera and a ×200/0.85 NA objective lens. Cases were considered positive when more than 10% of neoplastic cells were stained. Image processing was performed using the IM50 software from Leica Geosystems France.

DNA methylation analysis

We searched the human and mouse genome database (http://genome.ucsc.edu/) (University of California Santa Cruz, Genome Bioinformatics) for the existence of miRNAs embedded in a CpG island. Genomic DNA samples were modified by sodium bisulfite using the CpGenome DNA modification kit (Chemicon, Temecula, CA, USA) following the manufacturer's instructions. The DNA methylation status was analyzed by methylation-specific PCR after sodium bisulfite modification of DNA. Human male and mouse genomic DNA universally methylated for all genes (Intergen Company, Purchase, NY, USA) was used as a positive control for methylated alleles. Water blanks were included with each assay. The *deleted in leukemia* and *structural maintenance of chromosomes-4* genes are the host genes for miR-16-1 and miR-16-2, respectively. Primer sequences of methylation-specific PCR of miR-16 are described in Supplementary Table S2. Following amplification, PCR products were subjected to gel electrophoresis through a 2.5% agarose gel and were visualized by ethidium bromide staining and UV transillumination.

Tumorigenicity assays

MEF-TPM3-ALK cells[25] were transfected, as described above, with pre-miR-16 or scrambled control miRNA (pre-miR control no. 1), resuspended in PBS (2×10^6 cells/site) and then injected subcutaneouslyinto female Balb/c nu/nu mice, 4–6 weeks old (Iffa Credo, L'Arbresle, France). Five mice were used for each tested condition. Tumor volume was calculated as $v =$ length (mm) × width (mm) × thickness (mm) × 0.52 and measured every 2 days.

Statistical analysis

Values were expressed as mean ± s.d. Non-parametrical Mann–Whitney test and/or unpaired *t*-test or two-way ANOVA were applied to analyze the differences between groups. Analyses were performed using GraphPad Prism version 4.00 for Windows (San Diego, CA, USA). $P<0.05$ was considered to be significant.

Results

VEGF overexpression and miR-16 downregulation in murine onco-ALK models

We have previously developed conditional transgenic mice that express onco-ALK (NPM-ALK and TPM3-ALK) and exhibit robust angiogenesis (Supplementary Figure S1a). These mice were used to investigate whether ALK oncogene expression induces an increase in VEGF mRNA levels using RT-qPCR. We observed that the level of VEGF mRNA was significantly upregulated in lymph nodes isolated from mice with ALK+ tumors (Supplementary Figure S1b) when compared with lymph nodes isolated from normal littermate transgenic mice (normalized to 1) and from onco-ALK OFF healthy mice (Supplementary Figure S1b). We next checked whether the ALK oncogene-mediated increase in VEGF mRNA was followed by an increase in VEGF protein levels. The amount of secreted VEGF was measured by performing ELISA assays on mice sera. We observed that VEGF secretion was significantly upregulated in sera prepared from mice with ALK+ tumors in comparison with sera prepared from onco-ALK OFF healthy mice (*P*: 0.0173 for NPM-ALK; *P*: 0.0303 for TPM-ALK) and from control littermate animals (Supplementary Figure S1c).

Since miR-15 and miR-16 contribute to an increase in VEGF,[14] we used northern-blotting to compare miR-15a and miR-16 expression levels in tumor lymph nodes isolated from onco-ALK transgenic mice (ALK+) with lymph nodes isolated from doxycycline-treated animals (ALK−) (Supplementary Data). *To test for significant differences in expression of miR-15 and miR-16, two statistical tests* (the two-sample *t*-test and the Mann–Whitney test) *were performed* (Supplementary Table S1). In onco-ALK mice (ALK+), we found that miR-15a and miR-16 were significantly downregulated in lymphoma cells when compared with lymph node cells isolated from onco-ALK OFF healthy mice (ALK−) (0.471 ± 0.086 vs 0.761 ± 0.058 mean expression for miR-15a; 0.493 ± 0.025 vs 0.863 ± 0.044 mean expression for miR-16) (Supplementary Table S1).

To further confirm the upregulation of VEGF levels and the downregulation of miR-15a and miR-16 in onco-ALK-expressing cells *in vitro*, we used another murine onco-ALK model: MEF cells conditionally expressing the TPM3-ALK oncogene (MEF-TPM3-ALK cells).[25] Using ELISA assays, we observed a substantial increase in secreted VEGF (mean: 617 ± 126.33 pg/ml; p: 0.0318) in the supernatants of MEF TPM3-ALK-positive cells (ALK+) when compared with MEF TPM3-ALK-negative cells (ALK−) (Figure 1a). These data are consistent with the results obtained in transgenic mice harboring onco-ALK lymphomas (Supplementary Figures S1b and c and Supplementary Table S1). No significant variation in VEGF mRNA levels was observed between ALK+ and ALK− conditions (Figure 1b). We therefore used RT-qPCR, to analyse the expression levels of miRNA and observed that ALK+ cells express reduced levels of miR-15a and miR-16 when compared with ALK− cells (Figure 1c), however only miR-16 downregulation was significant ($P<0.05$) (Figure 1c). Altogether, these results suggest that miR-16 downregulation contributes to a decrease in VEGF levels in ALK+ cells.

VEGF mRNA is an miR-16 target in MEF TPM3-ALK cells

To understand the role of miR-16 in controlling VEGF levels, we looked at the consequences of either over-expressing or silencing miR-16 in ALK+ cells. The amount of miR-16 in transfected ALK+ cells was more than 700 fold higher than in control cells (Supplementary Figure S2). Transfection with miR-16, but not with the negative controls, resulted in a significant decrease in secreted VEGF protein levels 48 h after transfection (Figure 2a). Conversely, when endogeneous miR-16 was downregulated using an antisense locked nucleic acid to miR-16 (LNA-16), we observed an increase in VEGF secretion

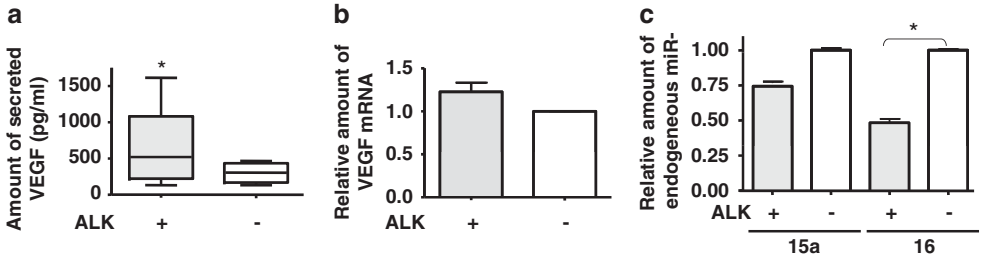

Figure 1 miR-16 down- and VEGF upregulation in conditional TPM3-ALK MEF cells. (**a**) ELISA and (**b**) RT-qPCR assays were performed to determine VEGF expression at the protein and mRNA level. (**c**) Endogeneous miR-15a and miR-16 levels were evaluated by RT-qPCR. miR-16 and miR-15a were normalized to Sno202 and VEGF mRNA to S14 rRNA. Bars represent standard deviation and asterisks depict statistically significant differences (*$P<0.05$; Student's *t*-test). Doxycycline was added or not to repress (ALK−) or induce (ALK+) TPM3-ALK expression. Each experiment was performed in triplicate and repeated three times.

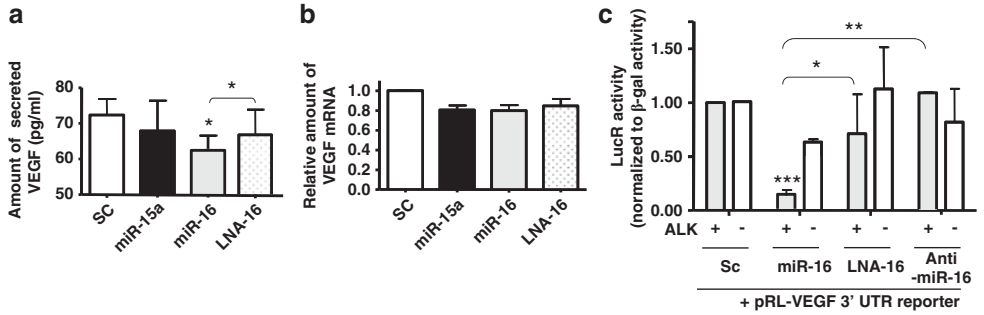

Figure 2 VEGF mRNA is an miR-16 target in TPM3-ALK MEF cells. (**a**, **b**) The effect of miR-16 overexpression on VEGF protein and mRNA levels was analysed in MEF TPM3-ALK cells transfected with pre-miR-16 (miR-16). The following negative controls were used: pre-*miR-15a* (miR-15a), a scrambled miRNA control (Sc) and an antisense LNA (LNA-16). (**c**) pRL-VEGF 3′-UTR construct was co-transfected with miR-16, antisense LNA-16 or miR-16 inhibitor (anti-miR-16) in TPM3-ALK MEF cells. Doxycycline was added or not to repress (ALK−) or induce (ALK+) TPM3-ALK expression. LucR activities were normalized to the cotransfected β-galactosidase activities. ELISA (**a**) and RT-qPCR (**b**, **c**) were performed to detect changes in VEGF expression levels 48 h after transfection. First, miR-16 was normalized to SnoRNA202 and VEGF mRNA to S14 rRNA then both were normalized to Sc experiments (**b**, **c**). Bars represent SD and asterisks depict statistically significant differences compared with scramble (*$P<0.05$, **$P<0.01$, ***$P<0.001$; Student's *t*-test). Each experiment was performed in triplicate and repeated three times.

(Figure 2a). Importantly, RT-qPCR did not show any differences in VEGF mRNA levels under all transfection conditions (Figure 2b). Thus, miR-16 levels inversely correlate with VEGF protein levels with mRNA levels unaffected. We therefore postulated that, in ALK+ cells, VEGF is controlled by miR-16 at a translational level.

To investigate further, we used a LucR reporter construct to examine whether miR-16 regulated VEGF translation through binding to its target site in the VEGF mRNA 3′-UTR. LucR activity was 6.5-fold lower in ALK+ cells transfected with miR-16 when compared with a scrambled miRNA control normalized to 1 ($P<0.001$, two-way ANOVA) (Figure 2c). Transfection with LNA-16 ($P<0.05$, two-way ANOVA) or a chemically modified inhibitor against miR-16 (anti-miR-16) ($P<0.01$, two-way ANOVA) led to a significant increase in the normalized LucR activity in ALK+ cells when compared with miR-16 transfection (Figure 2c). In ALK-inactivated cells (ALK−), reporter activity was not significantly changed under all conditions (Figure 2c). We conclude that, in ALK+ cells, VEGF mRNA is a target for miR-16 binding and that VEGF expression is controlled, at least in part, by the amount of miR-16.

miR-16 downregulation is not dependent on DNA loss and epigenetic modifications in murine TPM3-ALK models

In an attempt to identify the mechanisms involved in miR-16 downregulation in murine onco-ALK models, we first searched for DNA loss by high-resolution array-based comparative genomic hybridization array analysis (see Supplementary Data), on tumoral lymph nodes from TPM3-ALK transgenic mice. DNA karyotype changes did not seem to be involved in miR-16 downregulation (data not shown).

Mus musculus miR-16 is expressed from two loci, *deleted in leukemia 2* located on chromosome 3 and *structural maintenance of chromosomes-4* located on chromosome 14; these code for miR-16-1 and miR-16-2, respectively. We sought to determine whether aberrant methylation of the putative promoter regions of *deleted in leukemia 2* and *structural maintenance of chromosomes-4* was responsible for miR-16 downregulation through analysis of their methylation profile by methylation-specific PCR on DNA isolated from MEF TPM3-ALK-positive cells before (ALK+) and after (ALK−) ALK inactivation by doxycycline. As shown in Figure 3a, the miR-16-1 putative promoter was found non-methylated in both ALK+ and ALK− cells. Our data show that miR-16 downregulation is not mediated by an epigenetic mechanism.

ALK oncogene tyrosine kinase activity and hypoxia marker HIF1α may be involved in miR-16 downregulation in MEF TPM3-ALK cells

We next analysed whether regulation of miR-16 and VEGF was dependent upon functional ALK activity. First, we confirmed that TPM3-ALK kinase activity was inhibited following treatment with the ALK tyrosine kinase inhibitor, crizotinib,[30] by using

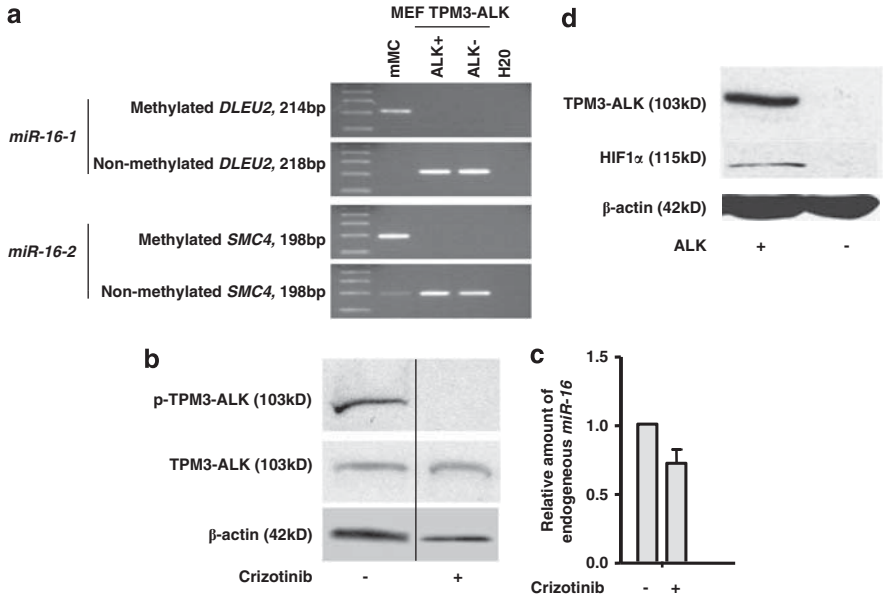

Figure 3 Mechanisms involved in miR-16 downregulation in TPM3-ALK-positive MEF cells. (**a**) Methylation-specific PCR (MSP) analysis of the mouse miR-16-1 (mmu-miR-16-1/*deleted in leukemia 2 (DLEU2) host gene*) and miR-16-2 (mmu-miR-16-2/*structural maintenance of chromosomes-4* (*SMC4*) *host gene*) CpG island regions were performed on DNA prepared from TPM3-ALK MEF cells, treated or not with doxycycline to repress (ALK−) or induce (ALK+) TPM3-ALK expression, and from mouse positive methylated control (mMC). H_20 indicates water blanks. (**b**, **c**) TPM3-ALK MEF cells were treated (+) or not (−) with 1 μM of Crizotinib. (**b**) Protein lysates (60 μg) were subjected to western-blotting analysis using anti-ALKc, anti-tyrosine and anti-β-actin antibodies. (**c**) RT-qPCR assays were performed to evaluate endogeneous miR-16 expression levels. MiR-16 was normalized to SnoRNA202. Bars represent SD. Each experiment was performed in triplicate and repeated three times. (**d**) Protein lysates (60 μg) isolated from TPM3-ALK MEF cells treated (ALK−) or not (ALK+) with doxycycline, were subjected to western-blotting analysis using anti-ALKc, anti-HIF1α and anti-β-actin antibodies.

western-blotting to confirm loss of TPM3-ALK autophosphorylation (Figure 3b and Supplementary Data). Using RT-qPCR we also observed that, in cells treated with crizotinib, miR-16 levels were decreased, although not significantly, following ALK tyrosine kinase inhibition (Figure 3c). This result suggests that ALK tyrosine kinase activity may partially contribute to under-expression of miR-16.

As hypoxia and HIF1α are known regulators of miR-16 expression, we analysed the expression profile of HIF1α in ALK+ and ALK− MEF cells. ALK inactivation via crizotinib resulted in significantly lower HIF1α expression (Figure 3d) when compared with ALK-expressing cells (ALK+). Together, these results suggest that the expression of ALK and HIF1α is a prerequisite for miR-16 downregulation in ALK-positive cells.

In vivo *repression of onco-ALK tumor growth and angiogenesis by miR-16 over-expression*

To provide *in vivo* evidence for a negative impact of miR-16 on tumor growth and angiogenesis, we subcutaneously transplanted MEF TPM3-ALK cells transfected with either miR-16 or a scrambled miRNA control into athymic nude mice. In miR-16-transfected cells tumor growth was reduced, as assessed by both tumor volume (Figures 4a and b) (*P* at 26 days: <0.001, two-way ANOVA test) and weight measurements (Figure 4c) (*P* at 26 days: 0.0255) VEGF serum levels were also reduced in tumors from ALK+ MEF cells transfected with miR-16 when compared with tumors from ALK+ MEF cells transfected with a scrambled miRNA control (Figure 4d). We performed CD34 immunostaining to examine vascular morphology in both cases. In control tumors, a high density of CD34 immunostaining and collapsed vessels were apparent (Figure 4e, upper panel, arrow). In contrast, decreased microvessel density and open lumen vessels (Figure 4e, lower panel, asterisk), were observed in subcutaneous tumors induced by ALK+ MEF cells transfected with miR-16. Altogether, these results demonstrate that miR-16 over-expression is able to reduce tumor growth and angiogenesis. Thus, our results strongly suggest that miR-16 down-regulation is a key event in ALK tumoral angiogenesis.

Association between miR-16 expression and VEGF levels in human ALK-positive lymphomas

To investigate a possible association between miR-16 expression and VEGF levels in human ALK+ cells, we looked at whether miR-16 was downregulated in ALCL tumor samples using RT-qPCR. We observed miR-16 levels to be significantly lower in ALK-positive ALCL lymph node biopsies ($n=20$) when compared with ALK-negative ALCL biopsies ($n=6$) (*P*: 0.0068) (Figure 5a). We then sought to identify the mechanisms involved in the reduction of miR-16 mRNA in ALK-expressing cells by searching for DNA structural or epigenetic modifications. As observed in the mouse models, the miR-16 downregulation in ALCL patients was not related to DNA promoter epigenetic methylation (Supplementary Figure S3) or DNA deletion; in the 32 ALK+ ALCL cases tested, comparative genomic hybridization array analysis (Supplementary Data) shows and only one case with a deletion of the 13q14.2 region coding for miR-16-1 and no deletion of the miR-16-2 region coding, 3q25.33 (data not shown).

Next, we wanted to investigate VEGF mRNA and protein expression in ALK+ human cells. VEGF mRNA amounts were evaluated by RT-qPCR on lymph node biopsies from ALCL patients. Our results show that levels of VEGF mRNA were increased in ALK+ ALCL lymph node biopsies ($n=20$), when compared with ALK− ALCL biopsies ($n=6$) or reactive lymph

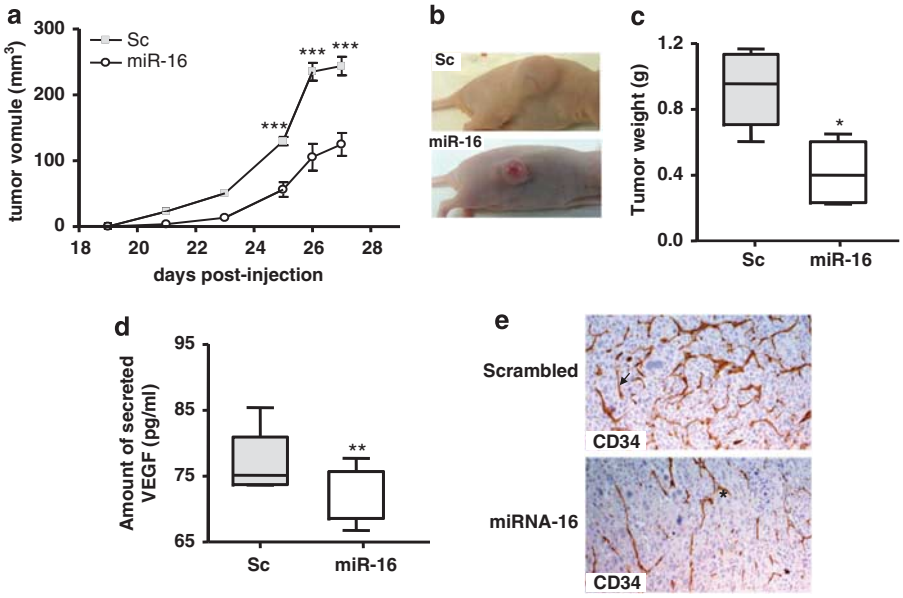

Figure 4 *In vivo* repression of tumor growth and angiogenesis by miR-16 gain of function. TPM3-ALK MEF cells, transfected with pre-miR-16 (miR-16) or scrambled pre-miRNA control (Sc), were injected subcutaneously into five female Balb/c nude mice for each tested condition. (**a**) Tumor volume was measured every 2 days using callipers. (**b**) Macroscopic observation of tumor-bearing mice 27 days post subcutaneous injection. (**c**) Tumor weight at necropsy. (**d**) ELISA assays were performed on mice sera to measure VEGF levels. (**c, d**) Bars represent SD and asterisks depict statistically significant differences compared with scrambled control (*$P<0.05$, **$P<0.01$ and ***$P<0.001$; Student's *t*-test). (**e**) Microvessel density was evaluated by CD34 immunoperoxidase staining 27 days post subcutaneous injection. (→) collapsed vessel, (*) open lumen vessel. Original magnification 400 × 0.85.

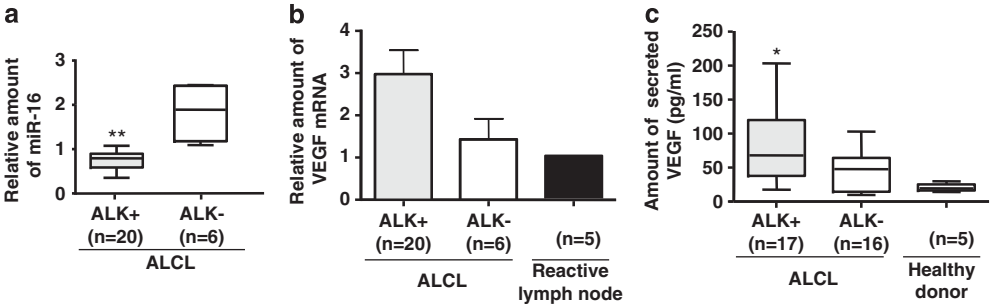

Figure 5 Endogeneous miR-16 down- and VEGF upregulation in human ALK-positive ALCL. (**a**, **b**) Endogeneous miR-16 mRNA was evaluated by RT-qPCR on biopsies. (**c**) VEGF expression was measured using an ELISA assay on sera (**c**) from ALK+ and ALK− ALCL. VEGF mRNA amounts were normalized to reactive lymph nodes. Bars represent SD and asterisks depict statistically significant differences (*$P<0.05$ and **$P<0.01$; Student's *t*-test). Each experiment was performed in triplicate. The number of biopsies in each group is denoted by the *n* value.

nodes ($n=5$) (Figure 5b). VEGF protein expression was tested using ELISA assays on ALCL sera and immunohistochemistry staining on tissue microarrays from lymph node biopsies of ALCL patients. We observed that VEGF protein expression was significantly enhanced in sera from ALK+ ALCL patients ($n=17$, p: 0.0242) when compared with sera from healthy donors ($n=5$) (Figure 5c). Immunohistochemistry staining was performed on 86 ALK+ ALCL samples and 14 ALK− ALCL samples. Endothelial cells, myofibroblasts and rare reactive lymphocytes admixed with lymphoma cells were used as an internal positive control and, as expected, were positive for VEGF (data not shown). In the tumor cells, we found no significant variation in VEGF expression between ALK+ and ALK-samples. Indeed, VEGF staining was detected in 68% (59 of 86) of ALK+ patients and in 57% of ALK− patients (8 of 14). However, a low VEGF staining intensity was predominantly seen in ALK− ALCL, while variations in the intensity of the staining was observed in ALK+ ALCL samples; some ALK+ ALCL showed strong VEGF staining, whereas other showed a moderate to weak staining, as illustrated for 8 cases in Figure 6a. Importantly, we also observed HIF1α protein expression in ALK+ ALCL lymph nodes biopsies (Supplementary Figure S4). Together, these results suggest that the ALK oncogene is able to induce VEGF expression, probably through both transcriptional and translational regulation, and involving both transcription factor HIF1-α and miR-16.

Finally, we used RT-qPCR to search for a correlation between VEGF protein levels, as assessed by immunohistochemistry, and the amount of endogeneous miR-16 in ALK+ ALCL cells. The percentage of tumoral cells expressing VEGF was graded as follows: 0: negative (0%); 1: <50%; 2: 50–75% and 3: >75%. We noted a strong inverse correlation between the amount of miR-16 and the VEGF grade of ALK+ tumoral cells (Pearson's correlation test, $R^2=0.9768$, Figure 6b). In the majority of the cases, low and intermediate miR-16 expression (relative amount <2) was associated with more than 50% of tumoral cells

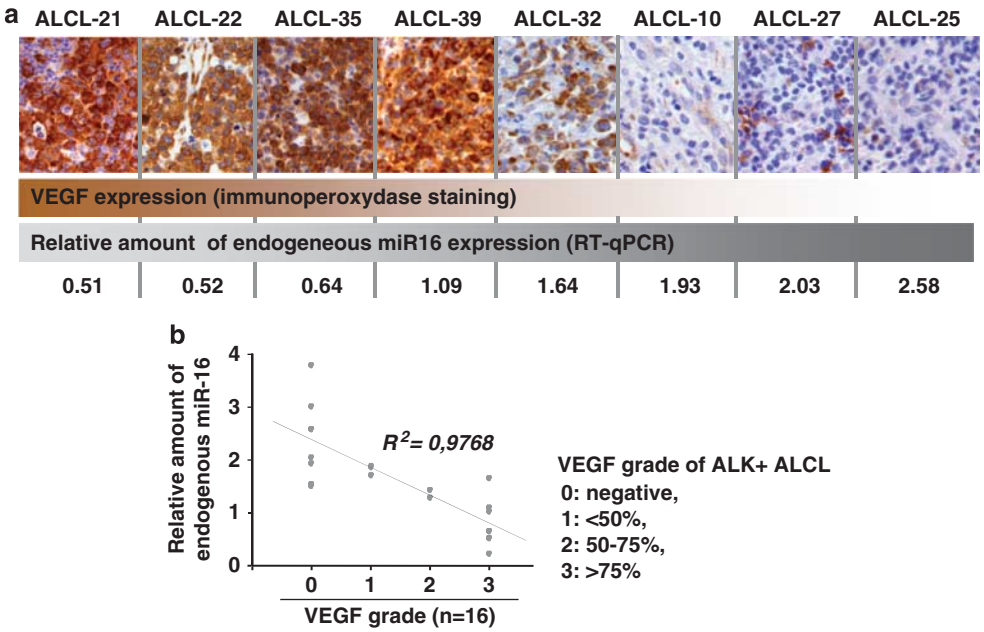

Figure 6 Inverse correlation between VEGF expression and relative amount of endogenous miR-16 in ALK-positive ALCL. (**a**) Immunohistochemistry (immunoperoxidase staining, original magnification, 400 × 0.85) and RT-qPCR were performed to determine VEGF and miR-16 expression in 8 human ALK+ lymphomas (ALCL-10, -21, -22, -25, -27, -32, -35 and -39). (**b**) Pearson's correlation test in 16 ALK+ ALCL. The percentage of tumoral cells expressing VEGF was graded as negative (0); 1: <50%, 2: 50–75% and 3: >75%.

expressing VEGF (Figure 6b). In contrast, enhanced miR-16 expression was associated with a low percentage or no ALK+ tumoral cells expressing VEGF (Figure 6b). Collectively, these results suggest that a decrease in miR-16 may be associated with an increase in VEGF protein levels in a substantial proportion of human ALK+ ALCL.

Discussion

Various hematological disorders and epithelial malignancies such as non-small cell lung cancer are associated with translocation of the *ALK* gene, located on chromosome 2p23. Around 17 chimera proteins have been characterized so far.[15,16,18,19,31] The majority of ALK translocations lead to diffuse large B-cell lymphomas and ALCL, a peripheral T-cell-derived malignancy. NPM-ALK and TPM3-ALK are the main translocations recorded in ALCL.[32]

A direct role for NPM-ALK in cellular transformation has been shown both *in vitro and in vivo*, and such studies have shed light on the mechanisms of malignant transformation by this onco-protein.[33,34] These mechanisms include activation of several downstream signal-transduction pathways, which regulate cell survival, proliferation, migration and, more recently, hypoxia.[20,24] Although hypoxia has been reported to upregulate HIF-1α and VEGF in ALK-positive (ALK+) ALCL,[20] so far no studies have implicated it in angiogenesis in ALK tumor development.

In this study, we have used onco-ALK (NPM-ALK and TPM3-ALK) cellular and mouse models conditional for ALK expression[25,26] to report for the first time, an increase in VEGF secretion both *in vitro* and *in vivo*. The increase in VEGF secretion in these models was not seen in normal cells, that is, following doxycycline-induced onco-ALK inactivation. Importantly, high VEGF serum levels were also detected in ALK+ ALCL patients when compared with healthy donors. These results led us to search for the underlying mechanism for this VEGF upregulation following ALK expression.

Extensive literature has shown that VEGF levels are tightly regulated at transcriptional, post-transcriptional and translational levels.[5,6] Recently, miR-16 was shown to regulate VEGF mRNA stability and protein expression levels.[14,29] In this study we have demonstrated that miR-16 is downregulated upon ALK expression both *in vitro* and *in vivo* using our onco-ALK conditional cellular and mouse models for ALK tumorigenesis.[25,26] Importantly, a weaker expression of miR-16 was also observed in ALK+ ALCL patients when compared with ALK− ALCL patients.

The mechanisms for regulation of miRNA levels are not yet understood, despite the wealth of publications about the biological effects of miRNAs. A few reports have shown that downregulation of some miRNAs in haematopoietic cancer occurs through epigenetic factors or by genomic abnormalities. This has been observed for the miR-16 sequence at chromosomal locus 13q14, which is deleted in more than 50% of chronic lymphocytic leukemia or multiple myeloma patients.[9,10] ALK+ ALCL harbor genomic alterations including 13q losses but the locus 13q14 is rarely lost.[35,36] In accordance with these data, we did not observe any abnormalities on chromosome 13 in ALK lymphomas from onco-ALK conditional transgenic mouse models and in only one of the human ALK+ ALCL samples. We also found that miR-16 downregulation was not related to DNA promoter epigenetic methylation changes in both the onco-ALK mouse models and in the human ALK+ ALCL samples. As we found an over-expression of HIF1α in ALK+ tumoral cells, we cannot rule out a possible hypoxia-mediated mechanism for miR-16 downregulation, as previously described by Hua *et al*.[14] However, a mechanism for this hypoxia-miR-16 regulation is not yet known.

To confirm the close relationship between miR-16 and VEGF levels in ALK tumors, we performed miR-16 gain expression in TPM3-ALK-positive MEF cells and studied the subsequent levels of VEGF secreted *in vitro* as well as the cells' ability to induce subcutaneous tumor growth in nude mice. Our results indicate that VEGF mRNA is a target of miR-16 and that forced

expression of miR-16 leads to a reduction in tumor growth, microvessel density and serum VEGF levels in MEF TPM3-ALK cells engrafted into nude mice. In human ALK+ tumors, we were able to demonstrate for the first time a strong inverse correlation between miR-16 and VEGF expression levels. Nevertheless, as the increase in VEGF mRNA was detected in ALK+ lymphoma cells, that is, in conditional transgenic models as well as ALCL patients, we suggest that VEGF is regulated at both transcriptional, as reported by Marzec *et al.*,[20] and post-transcriptional levels in ALK+ ALCL.

Several trials have been opened for ALK+ tumors (http://www.ClinicalTrials.gov). Only one agent, PF-02341066/crizotinib, an inhibitor of the tyrosine kinase activity of both ALK and the MET oncogene,[30] has recently reached the clinical arena in the treatment of ALK+ non-small cell lung cancer.[37] Relapsed advanced ALK+ ALCL are also sensitive to ALK inhibition by crizotinib.[38] However, recently two secondary mutations were reported following ALK inhibitor treatment.[39] They were within the kinase domain of the EML4-ALK oncogene involved in non-small cell lung cancer, and conferred marked resistance to crizotinib.[39]

As ALK signaling activates multiple downstream pathways, it is reasonable to speculate that small molecules, targeting key effectors within these pathways, will represent valuable targets to kill ALK+ cancer cells. Therefore, the development of combined therapies should help prevent the occurrence of resistance.[40] To this end, we recently demonstrated the efficiency of an antibody against CD160 in TPM3-ALK-induced fibroblast tumors in athymic nude mice.[41] This unusual anti-angiogenic therapeutic is a glycophosphatidylinositol-anchored protein which is expressed by growing but not quiescent endothelial cells.[42] We found that the antibody not only inhibited tumor vascular density but also slowed down the growth of ALK tumors.[41]

Anti-angiogenic strategies have become an important therapy for solid tumors[43] as well as hemato-lymphoid malignancies.[44] Importantly, an improvement in response, progression-free survival and/or overall survival has been demonstrated when conventional therapy was supplemented by VEGF inhibitors. As miRNAs can act both as oncogenes and tumor-suppressor genes, a very appealing therapeutic option is the combination of miRNAs with chemotherapy.[45] Indeed, several studies *in vitro* and *in vivo* using anti-miRNA molecules (antagomirs), LNA-anti-miRNA oligonucleotides or anti-miRNA oligonucleotides, have validated the efficiency of such agents in both solid tumors[46] and haematopoietic malignancies.[47] Importantly, the first clinical trial applying anti-miRNA agents as drugs has already been launched.[48,49]

In conclusion, our results report a new fundamental process for ALK-mediated tumorigenesis involving angiogenesis and VEGF upregulation through, at least in part, miR-16 down-regulation. These new data should encourage further work to optimize multi-target therapies and increase the chances of eradicating ALK+ tumors.

Conflict of interest

The authors declare no conflict of interest.

Acknowledgements

The authors thank, Dr L Vandel for providing the pCMV-β-Gal vector and, for their excellent technical assistance: F Capilla and D Lestrade (Plateau technique d'histopathologie expérimentale, CPTP-UMR1043, Toulouse); M March (Laboratoire d'Anatomie et Cytologie pathologiques, CHU Purpan, Toulouse), C Lopez (CRCT-UMR1037, Toulouse) and S Quentin (Plateforme Génomique IUH, Hôpital Saint-Louis, Paris). We thank Dr N Jabrane-Ferrat for critical reading. English proofreading was performed by Scientific Scripts (http://scientificscripts.com). This work was supported by grants from the INSERM, 'Association pour la Recherche sur le Cancer', no. A09/1/5073 (FM), Cancéropôle Grand-Sud-Ouest (FM), CITTIL (Coopération Transpyrénéenne de recherche de traitements innovants contre la leucémie) and INCa (projet PAIR Lymphomes). ED was supported by a doctoral fellowship from the 'Association pour la Recherche sur le Cancer' and MF was under a contract supported initially by the 'La Fondation de France' then 'La Fondation pour la Recherche Médicale'. This work is dedicated to my 'Dou'.

References

1 Moehler TM, Neben K, Ho AD, Goldschmidt H. Angiogenesis in hematologic malignancies. *Ann Hematol* 2001; **80**: 695–705.
2 Salven P. Angiogenesis in lymphoproliferative disorders. *Acta Haematol* 2001; **106**: 184–189.
3 Ruan J, Hajjar K, Rafii S, Leonard JP. Angiogenesis and antiangiogenic therapy in non-Hodgkin's lymphoma. *Ann Oncol* 2009; **20**: 413–424.
4 Roskoski Jr R. Vascular endothelial growth factor (VEGF) signaling in tumor progression. *Crit Rev Oncol Hematol* 2007; **62**: 179–213.
5 Bastide A, Karaa Z, Bornes S, Hieblot C, Lacazette E, Prats H *et al.* An upstream open reading frame within an IRES controls expression of a specific VEGF-A isoform. *Nucleic Acids Res* 2008; **36**: 2434–2445.
6 Touriol C, Bornes S, Bonnal S, Audigier S, Prats H, Prats AC *et al.* Generation of protein isoform diversity by alternative initiation of translation at non-AUG codons. *Biol Cell* 2003; **95**: 169–178.
7 Krol J, Loedige I, Filipowicz W. The widespread regulation of microRNA biogenesis, function and decay. *Nat Rev Genet* 2010; **11**: 597–610.
8 Croce CM, Calin GA. miRNAs, cancer, and stem cell division. *Cell* 2005; **122**: 6–7.
9 Garzon R, Calin GA, Croce CM. MicroRNAs in cancer. *Annu Rev Med* 2009; **60**: 167–179.
10 Lee YS, Dutta A. MicroRNAs in cancer. *Annu Rev Pathol* 2009; **4**: 199–227.
11 Saito Y, Jones PA. Epigenetic activation of tumor suppressor microRNAs in human cancer cells. *Cell Cycle* 2006; **5**: 2220–2222.
12 Wang S, Aurora AB, Johnson BA, Qi X, McAnally J, Hill JA *et al.* The endothelial-specific microRNA miR-126 governs vascular integrity and angiogenesis. *Dev Cell* 2008; **15**: 261–271.
13 Roccaro AM, Sacco A, Thompson B, Leleu X, Azab AK, Azab F *et al.* MicroRNAs 15a and 16 regulate tumor proliferation in multiple myeloma. *Blood* 2009; **113**: 6669–6680.
14 Hua Z, Lv Q, Ye W, Wong CK, Cai G, Gu D *et al.* MiRNA-directed regulation of VEGF and other angiogenic factors under hypoxia. *PLoS One* 2006; **1**: e116.
15 Morris SW, Kirstein MN, Valentine MB, Dittmer KG, Shapiro DN, Saltman DL *et al.* Fusion of a kinase gene, ALK, to a nucleolar protein gene, NPM, in non- Hodgkin's lymphoma. *Science* 1994; **263**: 1281–1284.
16 Arber DA, Sun LH, Weiss LM. Detection of the t(2;5)(p23;q35) chromosomal translocation in large B-cell lymphomas other than anaplastic large cell lymphoma. *Hum Pathol* 1996; **27**: 590–594.
17 Delsol G, Lamant L, Mariame B, Pulford K, Dastugue N, Brousset P *et al.* A new subtype of large B-cell lymphoma expressing the ALK kinase and lacking the 2; 5 translocation. *Blood* 1997; **89**: 1483–1490.
18 Griffin CA, Hawkins AL, Dvorak C, Henkle C, Ellingham T, Perlman EJ. Recurrent involvement of 2p23 in inflammatory myofibroblastic tumors. *Cancer Res* 1999; **59**: 2776–2780.

19 Rikova K, Guo A, Zeng Q, Possemato A, Yu J, Haack H *et al.* Global survey of phosphotyrosine signaling identifies oncogenic kinases in lung cancer. *Cell* 2007; **131**: 1190–1203.
20 Marzec M, Liu X, Wong W, Yang Y, Pasha T, Kantekure K *et al.* Oncogenic kinase NPM/ALK induces expression of HIF1alpha mRNA. *Oncogene* 2010; **30**: 1372–1378.
21 Brugieres L, Quartier P, Le Deley MC, Pacquement H, Perel Y, Bergeron C *et al.* Relapses of childhood anaplastic large-cell lymphoma: treatment results in a series of 41 children–a report from the French Society of Pediatric Oncology. *Ann Oncol* 2000; **11**: 53–58.
22 Williams DM, Hobson R, Imeson J, Gerrard M, McCarthy K, Pinkerton CR. Anaplastic large cell lymphoma in childhood: analysis of 72 patients treated on The United Kingdom Children's Cancer Study Group chemotherapy regimens. *Br J Haematol* 2002; **117**: 812–820.
23 Armstrong F, Lamant L, Hieblot C, Delsol G, Touriol C. TPM3-ALK expression induces changes in cytoskeleton organisation and confers higher metastatic capacities than other ALK fusion proteins. *Eur J Cancer* 2007; **43**: 640–646.
24 Palmer RH, Vernersson E, Grabbe C, Hallberg B. Anaplastic lymphoma kinase: signalling in development and disease. *Biochem J* 2009; **420**: 345–361.
25 Giuriato S, Faumont N, Bousquet E, Foisseau M, Bibonne A, Moreau M *et al.* Development of a conditional bioluminescent transplant model for TPM3-ALK-induced tumorigenesis as a tool to validate ALK-dependent cancer targeted therapy. *Cancer Biol Ther* 2007; **6**: 1318–1323.
26 Giuriato S, Foisseau M, Dejean E, Felsher DW, Al Saati T, Demur C *et al.* Conditional TPM3-ALK and NPM-ALK transgenic mice develop reversible ALK-positive early B-cell lymphoma/leukemia. *Blood* 2010; **115**: 4061–4070.
27 Delsol GFB, Mûller-hermelink HK, Campo E, Jaffe ES, Gascoyne RD, Stein H *et al. Anaplastic Large Cell Lymphoma, ALK-Positive*. IARC Press: Lyon, 2008, pp 312–316.
28 Mason DYHN, Delsol G, Stein H, Campo E, Kinney MC, Jaffe ES *et al. Anaplastic Large Cell Lymphoma, ALK-Negative*. IARC Press: Lyon, 2008, pp 317–319.
29 Karaa ZS, Iacovoni JS, Bastide A, Lacazette E, Touriol C, Prats H. The VEGF IRESes are differentially susceptible to translation inhibition by miR-16. *Rna* 2009; **15**: 249–254.
30 Christensen JG, Zou HY, Arango ME, Li Q, Lee JH, McDonnell SR *et al.* Cytoreductive antitumor activity of PF-2341066, a novel inhibitor of anaplastic lymphoma kinase and c-Met, in experimental models of anaplastic large-cell lymphoma. *Mol Cancer Ther* 2007; **6** (12 Pt 1): 3314–3322.
31 Perez-Pinera P, Chang Y, Astudillo A, Mortimer J, Deuel TF. Anaplastic lymphoma kinase is expressed in different subtypes of human breast cancer. *Biochem Biophys Res Commun* 2007; **358**: 399–403.
32 Piccaluga PP, Gazzola A, Mannu C, Agostinelli C, Bacci F, Sabattini E *et al.* Pathobiology of anaplastic large cell lymphoma. *Adv Hematol* 2010; **2010**: 345053.
33 Chiarle R, Voena C, Ambrogio C, Piva R, Inghirami G. The anaplastic lymphoma kinase in the pathogenesis of cancer. *Nat Rev Cancer* 2008; **8**: 11–23.
34 Turner SD, Alexander DR. What have we learnt from mouse models of NPM-ALK-induced lymphomagenesis? *Leukemia* 2005; **19**: 1128–1134.
35 Salaverria I, Bea S, Lopez-Guillermo A, Lespinet V, Pinyol M, Burkhardt B *et al.* Genomic profiling reveals different genetic aberrations in systemic ALK-positive and ALK-negative anaplastic large cell lymphomas. *Br J Haematol* 2008; **140**: 516–526.
36 Youssif C, Goldenbogen J, Hamoudi R, Carreras J, Viskaduraki M, Cui YX *et al.* Genomic profiling of pediatric ALK-positive anaplastic large cell lymphoma: a Children's Cancer and Leukaemia Group Study. *Genes Chromosomes Cancer* 2009; **48**: 1018–1026.
37 Kwak EL, Bang YJ, Camidge DR, Shaw AT, Solomon B, Maki RG *et al.* Anaplastic lymphoma kinase inhibition in non-small-cell lung cancer. *N Engl J Med* 2010; **363**: 1693–1703.
38 Gambacorti-Passerini C, Messa C, Pogliani EM. Crizotinib in anaplastic large-cell lymphoma. *N Engl J Med* 2010; **364**: 775–776.
39 Choi YL, Soda M, Yamashita Y, Ueno T, Takashima J, Nakajima T *et al.* EML4-ALK mutations in lung cancer that confer resistance to ALK inhibitors. *N Engl J Med* 2010; **363**: 1734–1739.
40 Wodarz D, Komarova NL. Emergence and prevention of resistance against small molecule inhibitors. *Semin Cancer Biol* 2005; **15**: 506–514.
41 Chabot S, Jabrane-Ferra N, Bigot K, Provost A, Golzio M, Tabiasco J *et al.* A novel antiangiogenic and vascular normalization therapy targeted against human CD160 receptor. *J Exp Med* 2011; **208**: 973–986.
42 Fons P, Chabot S, Cartwright JE, Lenfant F, L'Faqihi F, Giustiniani J *et al.* Soluble HLA-G1 inhibits angiogenesis through an apoptotic pathway and by direct binding to CD160 receptor expressed by endothelial cells. *Blood* 2006; **108**: 2608–2615.
43 Palazzo A, Iacovelli R, Cortesi E. Past, present and future of targeted therapy in solid tumors. *Curr Cancer Drug Targets* 2010; **10**: 433–461.
44 Medinger M, Mross K. Clinical trials with anti-angiogenic agents in hematological malignancies. *J Angiogenes Res* 2010; **2**: 10.
45 Iliopoulos D, Lindahl-Allen M, Polytarchou C, Hirsch HA, Tsichlis PN, Struhl K. Loss of miR-200 inhibition of Suz12 leads to polycomb-mediated repression required for the formation and maintenance of cancer stem cells. *Mol Cell* 2010; **39**: 761–772.
46 Hebert C, Norris K, Scheper MA, Nikitakis N, Sauk JJ. High mobility group A2 is a target for miRNA-98 in head and neck squamous cell carcinoma. *Mol Cancer* 2007; **6**: 5.
47 Agirre X, Vilas-Zornoza A, Jimenez-Velasco A, Martin-Subero JI, Cordeu L, Garate L *et al.* Epigenetic silencing of the tumor suppressor microRNA Hsa-miR-124a regulates CDK6 expression and confers a poor prognosis in acute lymphoblastic leukemia. *Cancer Res* 2009; **69**: 4443–4453.
48 Henke JI, Goergen D, Zheng J, Song Y, Schuttler CG, Fehr C *et al.* microRNA-122 stimulates translation of hepatitis C virus RNA. *Embo J* 2008; **27**: 3300–3310.
49 Jopling CL. Regulation of hepatitis C virus by microRNA-122. *Biochem Soc Trans* 2008; **36** (Pt 6): 1220–1223.

Supplementary Information accompanies the paper on the Leukemia website (http://www.nature.com/leu)

Article 4

Twenty years of modelling NPM-ALK-induced lymphomagenesis

Sylvie Giuriato and Suzanne D. Turner

FRONTIERS IN BIOSCIENCE
Vol. 7, Issue of June 1, pp. 236-47, 2015

[Frontiers in Bioscience, Scholar, 7, 236-247, June 1, 2015]

Twenty years of modelling NPM-ALK-induced lymphomagenesis

Sylvie Giuriato[1,2,3,5], Suzanne D. Turner[4,5]

[1]Inserm, UMR1037 CRCT, F-31000 Toulouse, France, [2]Université Toulouse III-Paul Sabatier, UMR1037 CRCT, F-31000 Toulouse, France, [3]CNRS, ERL5294 CRCT, F-31000 Toulouse, France, [4]Division of Molecular Histopathology, Department of Pathology, Lab Block Level 3, Box 231, Addenbrooke's Hospital, Cambridge CB20QQ, [5]European Research Initiative on ALK-related malignancies (ERIA)

TABLE OF CONTENTS

1. ABSTRACT

Our current understanding of oncogenic Anaplastic Lymphoma Kinase (ALK)-induced lymphomagenesis has relied for over 20 years on multiple and complementary studies performed on various experimental models, encompassing ALK oncogene expressing cells, their grafts into immune-compromised mice, the generation of genetically engineered mouse models (GEMMs) and, when available, the use of patient samples from Anaplastic Large Cell Lymphoma (ALCL) tumour banks. Of note, and to our knowledge, no ALK-positive ALCL 3D culture system has been described so far. In this review, we will first outline how these different cell and mouse models were designed, and what key findings they revealed (or confirmed) towards oncogenic ALK-induced lymphomagenesis. Secondly, we will discuss how recent and revolutionary advances in genetic engineering technology are likely to complete our understanding of ALK-related diseases in an effort to improve current therapeutic approaches.

2. INTRODUCTION

The discovery of the t(2;5)(p23;q35) encoding Nucleophosmin-Anaplastic Lymphoma Kinase (NPM-ALK) some 20 years ago signalled the start of considerable research efforts to determine the mechanism(s) by which this aberrantly expressed protein might induce lymphoma development (1). In the intervening period, oncogenic forms of ALK have been implicated in many further forms of cancer and activated by a variety of mechanisms, some still to be elucidated (2). Indeed, the common presence of activated ALK/ALK fusion proteins in many malignancies begs the question as to whether there are common underlying mechanisms and/or tissue-specific effects. In this regard the development of model systems has been instrumental to our research efforts as it has been to cancer research in general although, as with most model systems there remain many caveats particularly when considering the tumour as a mini-organ with its own blood supply, stroma and inflammatory milieu to name but a few assets. In this review we will discuss our current understanding on the biology of ALCL as gleaned from model systems generated to mimic some aspects of ALCL.

3. CONFIRMATION OF THE ONCOGENIC POTENTIAL OF NPM-ALK

3.1. *In vitro* studies

The first port of call for many studies into mechanisms of oncogenesis commence with cell line model systems, either those created from patient-derived tumours or exogenously expressed oncogenes in established cell lines. An extensive literature on *in vitro* ALK-oncogene signalling has been carried out using cell line models that were and still are useful for the biochemical analysis of the classical and newly proposed cancer hallmarks (2, 3). Initial studies sought to confirm the oncogenic potential of the newly identified NPM-ALK protein by expressing it in rat1a fibroblasts and IL3-dependent BaF3 B-cells. In both cases features of transformation were observed including anchorage-independent growth, foci formation and in the latter case independence from IL3-mediated signalling (4, 5). However, ALCL is a T-cell malignancy and therefore whilst it had been shown that NPM-ALK was able to induce some of the hallmarks of cancer *in vitro*, its relevance to T-cell biology was lacking. In this regard, effects of exogenous expression in the Jurkat T-cell leukaemia line was investigated but given that this cell line is already transformed, data were less informative and more restricted to understanding the signalling pathways that could be activated by NPM-ALK in a T-cell context (6). More recently, NPM-ALK expressing cell lines have been established from lentivirally transduced primary human mature $CD4^+$ T-cells (7). These have been reported to faithfully mimic key ALCL characteristics (increased cell volume and biomarker expression (CD30, Ki-67) as well as expression of immunosuppressive molecules (IL-10, PD-L1, STAT3/mTORC1 signalling activation)) (7). ALK oncogene mediated transformation of these cells relies, at least in part, on the use of the pre-existing IL-2 dependent signalling pathway (8). Importantly, this study demonstrates that the ALK oncogene is able to transform the cell type that is considered its cell of origin, i.e. normal T lymphocytes, thus providing the first cell system allowing *in vitro* studies both on ALK oncogene-mediated early mechanisms of lymphoma development and on the effects of early (new and/or combined) therapeutic interventions (9). However, all these cellular models more or less have limitations: as just described, they do not exactly recapitulate the T cell lineage characteristics of ALK-positive ALCL (except in the latter case) which also compromises their use for studying early stages of lymphomagenesis and disease progression mechanisms. In addition, all models remain *in vitro* experimental tools which obviously do not recapitulate the impacts of environmental factors known to influence tumour development and response to therapy (tumour and stromal cell interactions, immune system contribution, angiogenesis etc.). Thus, over the years and as in many others cancer studies (10), the mouse has emerged as the model organism of choice to study ALK-induced tumorigenesis including transgenic mouse models as well as murine chimeras and xenotransplantation models (human cell lines or patient material transplanted in most cases sub-cutaneously into immune deficient mice).

3.2. *In vivo* studies

The generation of murine chimeras whereby bone marrow is transduced to express the oncogene of interest before transplantation into irradiated recipient mice is often the first step towards providing evidence of *in vivo* oncogenic potential. Indeed, the oncogenic potential of NPM-ALK *in vivo* was first shown in such a system whereby murine bone marrow cultures in the presence of stem cell factor and IL6, were retrovirally transduced to express NPM-ALK before implantation into irradiated recipient mice (11). Perhaps not surprisingly (due to the B-cell skew in culture conditions), these mice developed B-lymphoid malignancies but nonetheless provided the first *in vivo* evidence of the oncogenic potential of NPM-ALK. Many other murine models have since been generated confirming the *in vivo* oncogenic potential of NPM-ALK and these are discussed further below.

4. DISSECTING NPM-ALK SIGNALLING PATHWAYS

The large majority of studies have used a combination of cell lines including patient-derived established cell lines to examine the oncogenic effects of NPM-ALK, in particular with a view to the signalling pathways in which it is involved and/or activated (12) (these have been reviewed extensively elsewhere and will not be discussed here (2, 13)). The most highly cited ALCL cell lines in use include Karpas-299, SUDHL-1, SUP-M2, SR786 and DEL all available from tissue banks and largely retrospectively identified as being ALK^+ ALCL (see Table 1) (14). However, these are generally isolated from patients with advanced and/or aggressive disease and together with serial propagation *in vitro* over many years, the inherent (epi)genetics are less likely to mimic those observed in the original tumour (15). For example, the Karpas-299 cell line has a deletion of *PTEN* as well as mutation of *TP53* and it is not clear whether these additional genetic changes were present in the original tumour or gained through *in vitro* serial propagation (16). Moreover, their culture within different media and serum conditions, according to empirical use in any given laboratory, are likely to induce many cellular drifts that could potentially change their behaviour and response to any given insult. Therefore, whilst these cell lines have provided the workhouses for biochemical studies into NPM-ALK activity, these data must be interpreted with caution and backed-up in additional model systems. In this regard, a number of murine models have been utilised to assess the biochemical pathways driving tumour growth in tumours arising *de novo*. In particular, the roles of signalling proteins such as STAT3 and JNK have been confirmed in murine models (17-19).

Table 1. A non-exhaustive list of models used to investigate the biology of NPM-ALK induced lymphoma

Model system	Examples	Key findings	Refs
Cell lines engineered to express NPM-ALK	BaF3, Rat1a, MEFs, NIH3T3, 32D, Jurkat, 293TRex Tet ON, MEF Tet OFF	Growth factor independence, anchorage-independent growth, foci formation	(4-6, 37, 64-73)
Patient-derived cell lines	ALK^+: Karpas-299, SUDHL-1, DEL, SUP-M2, SR-786, COST, PIO, L82, KI-KJ, JB6, TS (variant of SUDHL-1 carrying a tet-inducible shRNA against ALK), ALK^- : FEPD, Mac-1, Mac-2a, Mac-2B, JK	Many NPM-ALK signalling pathways, NPM-ALK signalosome	(14, 69, 74-88)
Primary T-cells transformed by NPM-ALK	Human peripheral blood derived $CD4^+$ T-cells	First evidence of NPM-ALK induced transformation of mature human T-cells	(7, 8)
GEMMs	CD4/NPM-ALK, VAV/NPM-ALK, CD2/NPM-ALK, LCK/NPM-ALK, EμSRα-tTA/Tet-O-NPM-ALK	Proof of the oncogenic potential of NPM-ALK in the lymphoid compartment	(17, 18, 23, 24, 29)
Chimeras	Retroviral transduction of murine bone marrow from wild-type, Cre or other transgenic lines with NPM-ALK followed by implantation into irradiated recipients	Proof of the oncogenic potential of NPM-ALK in the lymphoid compartment	(11, 20, 21, 28)
Xenografts	ALCL cell lines implanted sub-cutaneously into immune deficient mice, patient derived primary tumours implanted sub-cutaneously or intra-peritoneally into immune deficient mice	Therapy and tumour heterogeneity studies	(33, 35, 36, 38-40, 43, 54, 89, 90)
NPM-ALK: Nucleophosmin-Anaplastic Lymphoma Kinase			

5. ELUCIDATING MECHANISMS OF TRANSFORMATION AND THE CELL OF ORIGIN

5.1. Role of murine chimeras

Since the initial study of Kuefer *et al* described above (11), refinements of the chimeric system have been made in an attempt to produce a murine mimic of ALCL. In particular, tweaking of the system has been partially successful in recapitulating ALCL *in vivo*; transduction of IL9 transgenic mouse (which are predisposed to thymic T-cell lymphomas) bone marrow before implantation into recipient mice resulted in mice developing some T-lymphoblastic lymphomas (T-LBL) but also plasmacytomas and plasmablastic diffuse large B-cell lymphomas (20); the multiplicity of infection (MOI) has also been shown to impact on disease phenotype with high levels (>5) resulting in the rapid development of polyclonal histiocytic disease and low MOI (<0.005) in later onset monoclonal B-lymphoid malignancies (21); use of bone marrow from cre reporter transgenic mice such as Lysozyme M-cre and Granzyme B-cre transduced with a Lox-STOP-Lox-NPM-ALK encoding vector implanted into recipient mice led to histiocytic malignancies and T-LBL/histiocytic disease respectively (22). This latter system has the potential to result in a murine mimic of ALCL dependent on promoter driven-Cre usage and it remains to be seen the effects of driving NPM-ALK expression specifically in T-cells as has been carried out with limited success for various transgenic mice (17, 18, 23, 24). Regardless, the major caveat of using such a model system is the requirement to generate new mice from scratch for each experiment and hence the propensity for inter-experiment variability although one might argue that this might more closely resemble the heterogeneity of the human patient population.

5.2. Role of transgenic mouse models

Whilst chimeric models have been informative in proving the oncogenic potential of NPM-ALK *in vivo* they have also divulged the promiscuity of NPM-ALK suggesting that in order to develop a malignancy in mice resembling human ALCL, that expression must be targeted to the T-cell compartment. This is exemplified by findings in one of the first described transgenic NPM-ALK expressing mouse models whereby expression was targeted to the haemopoietic compartment by driving expression from the pan-haemopoietic *vav* promoter (18, 25). Utility of this promoter essentially enabled lineage screening for that preferentially transformed by NPM-ALK and in keeping with the large majority of chimeric model systems, the predominant phenotype was that of a B-cell lymphoma, in particular plasmacytoma (18). However, even with use of a T-cell specific promoter, namely the minimal CD4 promoter, plasmacytomas also developed in transgenic mice suggesting either some promoter leakage or cell fate decisions guided by NPM-ALK expression (17). This was also apparent in NPM-ALK transgenic mice whereby expression was directed by the T-cell specific CD2 promoter yet mice developed B-lymphoid malignancies (24). Regardless, the CD4/NPM-ALK transgenic line remains to date the best transgenic model for use in future studies, in particular the N16 line (which develops thymic lymphomas in greater than 90% of mice) and emphasises the importance of promoter choice when generating GEMMs (17).

In all of these systems a true mimic of ALCL has remained elusive suggesting that either NPM-ALK must be expressed at a particular stage in T-cell ontogeny and/or that other events shape the final cell surface phenotype. In regard to the former, use of the T-cell specific lck proximal promoter also led to T-LBL development but with a disease so aggressive that a transgenic line could not be established again suggesting that expression at early stages in T-cell ontogeny is not conducive to the development of ALCL (23). Whereas in evidence of the latter scenario, ALCL has been associated with infectious agents varying from insect bites (ALK positive) to breast implants (ALK negative) suggestive of the aetiology of this disease and consistent with a mature T-cell origin (26, 27). Therefore, future efforts might need to concentrate on directing NPM-ALK expression to mature post-thymic T-cells and examining the effects of T-cell stimulation on lymphoma development. However, mice are not men and what can happen in mice does not necessarily correlate with what actually happens in humans although mature peripheral T-cell lymphomas in mice expressing NPM-ALK has been achieved following elimination of clonal competition: Newrzela *et al* recently reported that chimeric mice in which NPM-ALK is expressed in mature T-cells isolated from the spleens and lymph nodes of the T-cell receptor (TCR) transgenic mouse line OTI, before implantation into recipient mice, developed mature peripheral nodal T-cell lymphomas whereas mature T-cells from wild-type mice (also expressing NPM-ALK) or NPM-ALK expressing OTI T-cells co-transplanted with polyclonal wild-type T-cells could not. These data suggest that the polyclonal nature of wild-type T-cells is not permissive for lymphoma development whereas the OTI-derived T-cells expressing a clonal TCR (specifically recognising ovalbumin peptides) are (28). These data suggest that mature T-cells can be transformed by NPM-ALK to develop a disease more closely mimicking ALCL in keeping with the *in vitro* studies of Zhang *et al* (7).

Based on this literature, it clearly appears that essentially all chimeric/transgenic mouse models recapitulate only some features of human ALCL malignancies and that none of them precisely mimic the human disease. This statement could be explained first by the fact that the human ALCL stem cell has not yet been identified, thus making it difficult to identify the specific stage of T-cell ontogeny to genetically manipulate to reproduce ALCL; second the choice of promoter for expressing the ALK oncogene has been problematic for several research groups and has resulted in the diverse B-cell or immature T-cell lymphomas, as described above; third, ectopic expression of NPM-ALK does not use the endogenous promoter, is initiated from randomly integrated sites, and leaves intact both copies of each translocation participating gene (the one encoding ALK and the one encoding the dimerization partner). Thus, the tumour level of expression of the fusion protein and the heterozygosity of the translocation participating genes are not reproduced. Finally, chimeric models also suffer from intra-experimental variability and the requirement to generate a new set of mice with each experiment. We are now able to circumvent those caveats as explained below.

6. INVESTIGATING NOVEL THERAPEUTIC TARGETS AND FUTURE TREATMENT STRATEGIES

6.1. Genetically Engineered Mouse Models (GEMMs)

Tumours addicted to defined oncogenic events provide excellent model systems to investigate the effects of inhibiting said activity towards the therapy of the associated disease. Given the precedent set by Bcr-Abl and Imatinib, it was obvious that therapies targeting NPM-ALK might provide future therapeutic opportunities. A variety of *in vitro* studies, inhibiting NPM-ALK expression and activity through use of reagents as diverse as siRNA to small molecule inhibitors, have proven this potential and transgenic murine models have provided further evidence (reviewed extensively elsewhere). In particular, a transgenic model for ALK lymphomagenesis with inducible gene expression provided proof of principle (29). George Delsol's group used the tetracycline system (Tet OFF version) to conditionally express the ALK oncogene in the hematopoietic lineage, using the Eμ promoter previously reported in other systems to give rise to either B or T cell lymphoma (29-32). Not surprisingly, the preferential transformation of B-cells was observed in fitting with previous GEMMs as described above; tumours were blocked at the pro-B/pre-B-1 stage of differentiation, arising within a three-week latency but importantly were reversible upon doxycycline administration (and hence ALK silencing), thus confirming the role of the ALK oncogene in tumour maintenance and supportive of the use of ALK inhibitors as therapeutics (29).

Other studies have utilised GEMMs to illustrate therapeutic strategies in principle. Of note, a study by Chiarle *et al* showed that by back-crossing the CD4/NPM-ALK line to STAT3 knockout mice that the tumour incidence was severely reduced suggesting STAT3 as a therapeutic target although these findings remain to be translated to the clinic (19). Another noteworthy study that has successfully translated to clinical application from findings in murine models is the utility of PDGFR inhibitors, specifically Imatinib (33). In this study a human patient with ALCL refractory to existing available therapies was successfully treated with Imatinib and remains in complete clinical remission (personal communication Prof. L Kenner and (34)). Refined GEMMs more closely mimicking ALCL may provide useful in the future for assessing the efficacy of ALK inhibitors and other novel reagents. However, a number of xenograft systems have also proven useful in this regard, mostly cell line xenografts but increasingly PDX as well.

6.2. Cell line xenografts

Engraftment of the different cell models described above into immune-compromised mice were and still are widely performed for two main purposes: Demonstration of the oncogenic properties of the cell models as well as the ease and rapidity of generation of an *in vivo* model to test the efficiencies of ALK cancer therapeutics. However, these model systems are limited by the sub-cutaneous location of tumours as well as the lack of a *bona fide* tumour microenvironment devoid of any inflammatory component. Regardless, they have been used extensively to examine the therapeutic potential of small molecule inhibitors including not only ALK inhibitors but also those affecting pathways activated by NPM-ALK (35-40). Traditionally, a xenograft of just one cell line representing the entire disease spectrum is employed as proof of principle that the novel compound will have therapeutic efficacy. However, it is well known that many drugs fail early in clinical trials because of the heterogeneity of the patient population. Hence, there has been a gradual move towards PDX as a model system although in the case of ALCL this is slightly hampered by the relative rarity of this disease.

6.3. Patient-derived xenografts (PDX)

PDX are based on the "culturing", maintenance and propagation of tumours directly isolated from the patient in immune-compromised mice. PDX models present the notable advantage to both recapitulate expression and genetic profiles of primary tumours as well as to respond to known therapeutics in a similar fashion to the primary tumour (41). The first reports of PDX models of ALCL were reported in 1995 and 1999 by Marshall Kadin's group (42, 43). Their studies showed that ALCL PDX closely resemble the primary tumour in histopathology and could be used to test the efficacy of CD30 targeted immunotherapy (44). These initial studies have been repeated to assess the efficacy of other therapies for example ALK inhibitors and undoubtedly more will follow (43, 45). However, we must point out here that the latency period to develop tumours in PDX can vary between 2 and 12 months and that the most successful tumour engraftments originate classically from high grade tumours at late stages of tumour development, which is not ideal for studying early stages of tumorigenesis. Thus, PDX models are good tools for drug screening and preclinical studies, but less so for basic cancer research. In addition they do not fully recapitulate the patient tumour in that the mouse host is immune-deficient and the tumours are often sub-cutaneous rather than nodal as is the case for ALCL.

7. THE FUTURE OF ALCL MODEL SYSTEMS

7.1. Refinement of existing model systems

Whilst as a community we have made considerable progress in understanding the role of NPM-ALK and other ALK oncogenes towards the pathogenesis of cancer there still remain many unanswered questions. Of note, the natural progression of ALK-induced ALCL has not been elucidated and the question remains as to why in human patients we observe a peripheral T-cell lymphoma that has proven difficult to model *in vivo*. There are many possibilities, some more obvious than others but at its very heart we have not yet developed a mouse in which the exact genetic events are copied, in particular with the generation of the t(2;5)(p23;q35) is not only the gain of the *NPM-ALK* fusion gene but also a reduction of *ALK* and *NPM* gene dosage to 1 copy. Given that ALK appears to be a neural specific protein, this reduction in gene dosage is not likely to have an effect on lymphoid malignancies but given the ubiquitous expression and function of NPM this may be of significance (46-48). However, as a counter-argument, the presence of a large variety of ALK fusion proteins suggests that *NPM* heterozygosity is not of importance and this was backed up in an *in vitro* study whereby the importance of NPM was resigned to its ability to induce dimerization and hence autophosphorylation of NPM-ALK (48). In addition, a murine study in which *NPM-ALK* transgenic mice were back-crossed onto an *NPM* heterozygous background which did not result in any change in disease latency supports this theory although one might argue that the NPM-ALK GEMM of choice (CD2/NPM-ALK) did not sufficiently mimic human ALCL (49, 50). Hence, this remains to be explored further perhaps using model systems as detailed below.

Equally compelling is our lack of knowledge as to the true cell of origin for this malignancy and the events that shape the presenting disease phenotype, i.e. mature T-cells in some cases appearing of a cytotoxic phenotype and in others a helper CD4-expressing T-cell, Treg, Th17 or 'null' cell (9, 51, 52). However, many of these features that presume this array of T-cell subset phenotypes have been attributed to NPM-ALK activity perhaps independent of the cell of origin. For example, it has been shown that NPM-ALK can induce cellular production of cytotoxic proteins, IL17 and FoxP3 expression (51-53). Hence, it is possible that the cell of origin is a common precursor T-cell and in evidence a recent study has indicated that ALCL cancer stem cells (CSC) may well have origins in early thymic progenitors (54). If this is the case, then it is clear, at least in mouse models that other events must dictate the disease phenotype as expression of NPM-ALK in immature T-cells in mice leads predominantly to lymphoblastic lymphoma as discussed above, whereas expression in mature T-cells in the absence of polyclonal competition *in vivo* gives rise to peripheral T-cell lymphoma (28).

7.2. New technologies

Despite significant progress, a true murine mimic of ALCL, particularly a GEMM remains elusive but as technologies evolve as does our understanding of this disease, it is highly likely that model systems will improve to

become more informative. Zinc-Finger Nucleases (ZFNs), Transcription Activator-Like Effector Nucleases (TALENs) and Clustered Regulatory Interspaced Short Palindromic Repeats (CRISPR) / CRISPR-associated (Cas) systems are currently redefining the boundaries of genome engineering (55). ZFNs and TALENs are engineered nucleases composed of sequence-specific DNA-binding domains fused to a non-specific DNA cleavage module (56). The DNA binding domain can be customized at will, thus allowing the recognition and subsequent cleavage of any DNA sequence. CRISPR/Cas are programmable RNA-guided DNA endonucleases, that have multiplexed gene disruption capabilities (57). The precise DNA double strand breaks induced by either one of these three DNA nucleases, then stimulate classical DNA repair mechanisms (NHEJ or HDR) (58). Thus, programmable DNA breaks could create, *de novo*, at the exact endogenous loci, a translocation-associated oncogene. Most importantly, proof of principle of this powerful technology (notably TALENs) in genome editing has been reported for the *de novo* creation of the NPM-ALK translocation in two different cell settings: Jurkat T cells and RPE-1 cells (retinal pigment epithelial cells) (59). Thus, it is tempting to speculate that *de novo* creation of the NPM-ALK oncogene either in its natural target cell, in human induced-pluripotent stem cells (iPS), or in mouse blastocysts, hold the promise to lead to the generation of the most accurate model for ALK-positive ALCL. It is equally possible that other established technologies such as the 'translocator mouse' system developed in the lab of Terry Rabbitts might provide a source of GEMM mimics of ALCL (60). Alternatively, other model systems might provide better mimics of ALCL, for example zebrafish models are more commonly in use for the study of tumorigenesis, more recently models of T-LBL have been described (61).

8. CONCLUSIONS

We believe a new era for ALCL personalized medicine is coming, taking advantage of both the generation and use of PDX and GEMM models (closely mimicking ALCL pathology) and their potential enrolment in co-clinical trials (62) (as previously reported for EML4-ALK NSCLC (63)). Indeed, this real-time "GEMMs-to-human" transition allows the concurrent integration of murine and human data, thereby allowing better, personalized and timely clinical decisions to be made (41). In the particular field of ALCL, like in other types of cancers, this will considerably facilitate and improve both drug development and patient health care management. Thus, in the coming years, it is likely that the use of ALCL mouse models will evolve from the classical study of the oncogenic ALK lymphomagenesis process to more clinically oriented applications.

9. ACKNOWLEDGEMENTS

We apologise to all those authors whose work we have been unable to cite due to size constraints and would like to thank Dr Cyril Broccardo (CRCT, Inserm UMR1037), for helpful discussion. SG is supported by funding from the French National Research Agency-Young Researcher (ANR-JCJC). SDT is a Leukaemia and Lymphoma Research Senior Lecturer. The present review was concerted inside the European Research Initiative of ALK-related malignancies (ERIA) (http://www.erialcl.net).

10. REFERENCES

1. S. W. Morris, M. N. Kirstein, M. B. Valentine, K. G. Dittmer, D. N. Shapiro, D. L. Saltman and A. T. Look: Fusion of a kinase gene, ALK, to a nucleolar protein gene, NPM, in non-Hodgkin's lymphoma. *Science*, 263(5151), 1281-4 (1994)
DOI: 10.1126/science.8122112
2. B. Hallberg and R. H. Palmer: Mechanistic insight into ALK receptor tyrosine kinase in human cancer biology. *Nat Rev Cancer*, 13(10), 685-700 (2013)
DOI: 10.1038/nrc3580
3. D. Hanahan and R. A. Weinberg: Hallmarks of cancer: the next generation. *Cell*, 144(5), 646-74 (2011)
4. A. Wellmann, V. Doseeva, W. Butscher, M. Raffeld, P. Fukushima, M. Stetler-Stevenson and K. Gardner: The activated anaplastic lymphoma kinase increases cellular proliferation and oncogene up-regulation in rat 1a fibroblasts. *Faseb J*, 11(12), 965-72 (1997)
5. R. Y. Bai, P. Dieter, C. Peschel, S. W. Morris and J. Duyster: Nucleophosmin-anaplastic lymphoma kinase of large-cell anaplastic lymphoma is a constitutively active tyrosine kinase that utilizes phospholipase C-gamma to mediate its mitogenicity. *Mol Cell Biol*, 18(12), 6951-61 (1998)
6. C. Greenland, C. Touriol, G. Chevillard, S. W. Morris, R. Bai, J. Duyster, G. Delsol and M. Allouche: Expression of the oncogenic NPM-ALK chimeric protein in human lymphoid T-cells inhibits drug-induced, but not Fas-induced apoptosis. *Oncogene*, 20(50), 7386-97 (2001)
DOI: 10.1038/sj.onc.1204870
7. Q. Zhang, F. Wei, H. Y. Wang, X. Liu, D. Roy, Q. B. Xiong, S. Jiang, A. Medvec, G. Danet-Desnoyers, C. Watt, E. Tomczak, M. Kalos, J. L. Riley and M. A. Wasik: The potent oncogene

NPM-ALK mediates malignant transformation of normal human CD4(+) T lymphocytes. *Am J Pathol*, 183(6), 1971-80 (2013)
DOI: 10.1016/j.ajpath.2013.08.030

8. M. Marzec, K. Halasa, X. Liu, H. Y. Wang, M. Cheng, D. Baldwin, J. W. Tobias, S. J. Schuster, A. Woetmann, Q. Zhang, S. D. Turner, N. Odum and M. A. Wasik: Malignant transformation of CD4+ T lymphocytes mediated by oncogenic kinase NPM/ALK recapitulates IL-2-induced cell signaling and gene expression reprogramming. *J Immunol*, 191(12), 6200-7 (2013)
DOI: 10.4049/jimmunol.1300744
9. L. Krenacs, A. Wellmann, L. Sorbara, A. W. Himmelmann, E. Bagdi, E. S. Jaffe and M. Raffeld: Cytotoxic cell antigen expression in anaplastic large cell lymphomas of T- and null-cell type and Hodgkin's disease: evidence for distinct cellular origin. *Blood*, 89(3), 980-9 (1997)
10. W. T. Khaled and P. Liu: Cancer mouse models: past, present and future. *Semin Cell Dev Biol*, 27, 54-60 (2014)
DOI: 10.1016/j.semcdb.2014.04.003
11. M. U. Kuefer, A. T. Look, K. Pulford, F. G. Behm, P. K. Pattengale, D. Y. Mason and S. W. Morris: Retrovirus-mediated gene transfer of NPM-ALK causes lymphoid malignancy in mice. *Blood*, 90(8), 2901-10 (1997)
12. S. D. Turner and D. R. Alexander: Fusion tyrosine kinase mediated signalling pathways in the transformation of haematopoietic cells. *Leukemia*, 20(4), 572-82 (2006)
DOI:2404125 [pii]10.1038/sj.leu.2404125
13. R. Chiarle, C. Voena, C. Ambrogio, R. Piva and G. Inghirami: The anaplastic lymphoma kinase in the pathogenesis of cancer. *Nat Rev Cancer*, 8(1), 11-23 (2008)
DOI: nrc2291 [pii] 10.1038/nrc2291
14. W. G. Dirks, M. Zaborski, K. Jager, C. Challier, M. Shiota, H. Quentmeier and H. G. Drexler: The (2;5)(p23;q35) translocation in cell lines derived from malignant lymphomas: absence of t(2;5) in Hodgkin-analogous cell lines. *Leukemia*, 10(1), 142-9 (1996)
15. A. Ertel, A. Verghese, S. W. Byers, M. Ochs and A. Tozeren: Pathway-specific differences between tumor cell lines and normal and tumor tissue cells. *Mol Cancer*, 5(1), 55 (2006)
DOI: 10.1186/1476-4598-5-55
DOI: 10.1186/1476-4598-5-55
16. F. Turturro, A. Y. Frist, M. D. Arnold, P. Seth and K. Pulford: Biochemical differences between SUDHL-1 and KARPAS 299 cells derived from t(2;5)-positive anaplastic large cell lymphoma are responsible for the different sensitivity to the antiproliferative effect of p27(Kip1). *Oncogene*, 20(33), 4466-75 (2001)
DOI: 10.1038/sj.onc.1204582
17. R. Chiarle, J. Z. Gong, I. Guasparri, A. Pesci, J. Cai, J. Liu, W. J. Simmons, G. Dhall, J. Howes, R. Piva and G. Inghirami: NPM-ALK transgenic mice spontaneously develop T-cell lymphomas and plasma cell tumors. *Blood*, 101(5), 1919-27 (2003)
DOI: 10.1182/blood-2002-05-1343
18. S. D. Turner, R. Tooze, K. Maclennan and D. R. Alexander: Vav-promoter regulated oncogenic fusion protein NPM-ALK in transgenic mice causes B-cell lymphomas with hyperactive Jun kinase. *Oncogene*, 22(49), 7750-61 (2003)
DOI: 10.1038/sj.onc.1207048
19. R. Chiarle, W. J. Simmons, H. Cai, G. Dhall, A. Zamo, R. Raz, J. G. Karras, D. E. Levy and G. Inghirami: Stat3 is required for ALK-mediated lymphomagenesis and provides a possible therapeutic target. *Nat Med*, 11(6), 623-9 (2005)
DOI: nm1249 [pii] 10.1038/nm1249
20. K. Lange, W. Uckert, T. Blankenstein, R. Nadrowitz, C. Bittner, J. C. Renauld, J. van Snick, A. C. Feller and H. Merz: Overexpression of NPM-ALK induces different types of malignant lymphomas in IL-9 transgenic mice. *Oncogene*, 22(4), 517-27 (2003)
DOI: 10.1038/sj.onc.1206076
21. C. Miething, R. Grundler, F. Fend, J. Hoepfl, C. Mugler, C. von Schilling, S. W. Morris, C. Peschel and J. Duyster: The oncogenic fusion protein nucleophosmin-anaplastic lymphoma kinase (NPM-ALK) induces two distinct malignant phenotypes in a murine retroviral transplantation model. *Oncogene*, 22(30), 4642-7 (2003)
DOI: 10.1038/sj.onc.1206575
22. R. G. C. Miething, C. Mugler, C. Peschel and J. Duyster: A new method of retroviral lineage specific expression utilizing the Cre/Lox system induces T-lymphoid malignancy in a mouse model of ALCL. *Blood*, 104, 248 (2005)

23. R. Jager, J. Hahne, A. Jacob, A. Egert, J. Schenkel, N. Wernert, H. Schorle and A. Wellmann: Mice transgenic for NPM-ALK develop non-Hodgkin lymphomas. *Anticancer Res*, 25(5), 3191-6 (2005)

24. S. D. Turner, H. Merz, D. Yeung and D. R. Alexander: CD2 promoter regulated nucleophosmin-anaplastic lymphoma kinase in transgenic mice causes B lymphoid malignancy. *Anticancer Res*, 26(5A), 3275-9 (2006)

25. S. Ogilvy, D. Metcalf, L. Gibson, M. L. Bath, A. W. Harris and J. M. Adams: Promoter elements of vav drive transgene expression *in vivo* throughout the hematopoietic compartment. *Blood*, 94(6), 1855-63 (1999)

26. L. Lamant, S. Pileri, E. Sabattini, L. Brugieres, E. S. Jaffe and G. Delsol: Cutaneous presentation of ALK-positive anaplastic large cell lymphoma following insect bites: evidence for an association in five cases. *Haematologica*, 95(3), 449-55 (2010) DOI: 10.3324/haematol.2009.015024

27. D. de Jong, W. L. Vasmel, J. P. de Boer, G. Verhave, E. Barbe, M. K. Casparie and F. E. van Leeuwen: Anaplastic large-cell lymphoma in women with breast implants. *JAMA*, 300(17), 2030-5 (2008) DOI: 10.1001/jama.2008.585

28. S. Newrzela, N. Al-Ghaili, T. Heinrich, M. Petkova, S. Hartmann, B. Rengstl, A. Kumar, H. M. Jack, S. Gerdes, I. Roeder, M. L. Hansmann and D. von Laer: T-cell receptor diversity prevents T-cell lymphoma development. *Leukemia*, 26(12), 2499-507 (2012) DOI: 10.1038/leu.2012.142

29. S. Giuriato, M. Foisseau, E. Dejean, D. W. Felsher, T. Al Saati, C. Demur, A. Ragab, A. Kruczynski, C. Schiff, G. Delsol and F. Meggetto: Conditional TPM3-ALK and NPM-ALK transgenic mice develop reversible ALK-positive early B-cell lymphoma/leukemia. *Blood*, 115(20), 4061-70 (2010) DOI: blood-2008-06-163386 [pii]10.1182/blood-2008-06-163386

30. J. M. Adams and S. Cory: Transgenic models for haemopoietic malignancies. *Biochim Biophys Acta*, 1072(1), 9-31 (1991)

31. J. M. Adams, A. W. Harris, D. L. Vaux, W. S. Alexander, H. Rosenbaum, S. P. Klinken, A. Strasser, M. L. Bath, J. McNeall and S. Cory: The transgenic window on lymphoid malignancy. *Princess Takamatsu Symp*, 20, 297-309 (1989)

32. D. W. Felsher and J. M. Bishop: Reversible tumorigenesis by MYC in hematopoietic lineages. *Mol Cell*, 4(2), 199-207 (1999) DOI: 10.1016/S1097-2765(00)80367-6

33. D. Laimer, Dolznig, H., Kollmann, K., Vesely, P.W., Schlederer, M., Merkel, O., Schiefer, A., Hassler, M.R., Heider, S., Amenitsch, L., Thallinger, C., Staber, P.B., Simonitsch-Klupp, I., Artaker, M., Lagger, S., Turner, S.D., Pileri, S., Piccaluga, P.P., Valent, P., Messana, K., Landra, I., Weichhart, T., Knapp, S., Shehata, M., Todaro, M., Sexl, V., Höfler, G., Piva, R., Medico, E., Riggeri, B.A., Cheng, M., Eferl, R., Egger, G., Penninger, J.M., Jaeger, U., Moriggl, R., Inghirami, G. and Kenner, L. : Identification of PDGFR blockade as a rational and highly effective therapy for NPM-ALK driven lymphomas. *Nature Medicine* (2012) DOI: 10.1038/nm.2966

34. S. D. Turner: Inimitable Imatinib: the range of targeted tumours expands to include T-cell lymphoma. *Leukemia*, 27(4), 759 (2013) DOI: 10.1038/leu.2012.304

35. J. G. Christensen, H. Y. Zou, M. E. Arango, Q. Li, J. H. Lee, S. R. McDonnell, S. Yamazaki, G. R. Alton, B. Mroczkowski and G. Los: Cytoreductive antitumor activity of PF-2341066, a novel inhibitor of anaplastic lymphoma kinase and c-Met, in experimental models of anaplastic large-cell lymphoma. *Mol Cancer Ther*, 6(12 Pt 1), 3314-22 (2007) DOI: 6/12/3314[pii]10.1158/1535-7163.MCT-07-0365

36. S. K. George, D. Vishwamitra, R. Manshouri, P. Shi and H. M. Amin: The ALK inhibitor ASP3026 eradicates NPM-ALK(+) T-cell anaplastic large-cell lymphoma *in vitro* and in a systemic xenograft lymphoma model. *Oncotarget* (2014)

37. Q. Zhang, P. N. Raghunath, L. Xue, M. Majewski, D. F. Carpentieri, N. Odum, S. Morris, T. Skorski and M. A. Wasik: Multilevel dysregulation of STAT3 activation in anaplastic lymphoma kinase-positive T/null-cell lymphoma. *J Immunol*, 168(1), 466-74 (2002) DOI: 10.4049/jimmunol.168.1.466

38. M. Nieborowska-Skorska, A. Slupianek, L.

Xue, Q. Zhang, P. N. Raghunath, G. Hoser, M. A. Wasik, S. W. Morris and T. Skorski: Role of signal transducer and activator of transcription 5 in nucleophosmin/ anaplastic lymphoma kinase-mediated malignant transformation of lymphoid cells. *Cancer Res*, 61(17), 6517-23 (2001)

39. A. Slupianek, M. Nieborowska-Skorska, G. Hoser, A. Morrione, M. Majewski, L. Xue, S. W. Morris, M. A. Wasik and T. Skorski: Role of phosphatidylinositol 3-kinase-Akt pathway in nucleophosmin/anaplastic lymphoma kinase-mediated lymphomagenesis. *Cancer Res*, 61(5), 2194-9 (2001)
40. A. M. Coluccia, S. Perego, L. Cleris, R. H. Gunby, L. Passoni, E. Marchesi, F. Formelli and C. Gambacorti-Passerini: Bcl-XL down-regulation suppresses the tumorigenic potential of NPM/ALK *in vitro* and *in vivo*. *Blood*, 103(7), 2787-94 (2004) DOI: 10.1182/blood-2003-09-3144
41. P. Malaney, S. V. Nicosia and V. Dave: One mouse, one patient paradigm: New avatars of personalized cancer therapy. *Cancer Lett*, 344(1), 1-12 (2014) DOI: 10.1016/j.canlet.2013.10.010
42. L. Pasqualucci, M. Wasik, B. A. Teicher, L. Flenghi, A. Bolognesi, F. Stirpe, L. Polito, B. Falini and M. E. Kadin: Antitumor activity of anti-CD30 immunotoxin (Ber-H2/ saporin) *in vitro* and in severe combined immunodeficiency disease mice xenografted with human CD30+ anaplastic large-cell lymphoma. *Blood*, 85(8), 2139-46 (1995)
43. W. Pfeifer, E. Levi, T. Petrogiannis-Haliotis, L. Lehmann, Z. Wang and M. E. Kadin: A murine xenograft model for human CD30+ anaplastic large cell lymphoma. Successful growth inhibition with an anti-CD30 antibody (HeFi-1). *Am J Pathol*, 155(4), 1353-9 (1999) DOI: 10.1016/S0002-9440(10)65237-6
44. K. V. Foyil and N. L. Bartlett: Brentuximab vedotin and crizotinib in anaplastic large-cell lymphoma. *Cancer J*, 18(5), 450-6 (2012) DOI: 10.1097/PPO.0b013e31826aef4a
45. M. Cheng, M. R. Quail, D. E. Gingrich, G. R. Ott, L. Lu, W. Wan, M. S. Albom, T. S. Angeles, L. D. Aimone, F. Cristofani, R. Machiorlatti, C. Abele, M. A. Ator, B. D. Dorsey, G. Inghirami and B. A. Ruggeri: CEP-28122, a highly potent and selective orally active inhibitor of anaplastic lymphoma kinase with antitumor activity in experimental models of human cancers. *Mol Cancer Ther*, 11(3), 670-9 (2012) DOI: 10.1158/1535-7163.MCT-11-0776
46. K. Pulford, L. Lamant, E. Espinos, Q. Jiang, L. Xue, F. Turturro, G. Delsol and S. W. Morris: The emerging normal and disease-related roles of anaplastic lymphoma kinase. *Cell Mol Life Sci*, 61(23), 2939-53 (2004) DOI: 10.1007/s00018-004-4275-9
47. T. Iwahara, J. Fujimoto, D. Wen, R. Cupples, N. Bucay, T. Arakawa, S. Mori, B. Ratzkin and T. Yamamoto: Molecular characterization of ALK, a receptor tyrosine kinase expressed specifically in the nervous system. *Oncogene*, 14(4), 439-49 (1997) DOI: 10.1038/sj.onc.1200849
48. D. Bischof, K. Pulford, D. Y. Mason and S. W. Morris: Role of the nucleophosmin (NPM) portion of the non-Hodgkin's lymphoma-associated NPM-anaplastic lymphoma kinase fusion protein in oncogenesis. *Mol Cell Biol*, 17(4), 2312-25 (1997)
49. F. K. McDuff, C. E. Hook, R. M. Tooze, B. J. Huntly, P. P. Pandolfi and S. D. Turner: Determining the contribution of NPM1 heterozygosity to NPM-ALK-induced lymphomagenesis. *Lab Invest*, 91(9), 1298-303 (2011) DOI: 10.1038/labinvest.2011.96
50. J. Duyster, R. Y. Bai and S. W. Morris: Translocations involving anaplastic lymphoma kinase (ALK). *Oncogene*, 20(40), 5623-37 (2001) DOI: 10.1038/sj.onc.1204594
51. M. Kasprzycka, M. Marzec, X. Liu, Q. Zhang and M. A. Wasik: Nucleophosmin/anaplastic lymphoma kinase (NPM/ALK) oncoprotein induces the T regulatory cell phenotype by activating STAT3. *Proc Natl Acad Sci U S A*, 103(26), 9964-9 (2006)
52. H. Matsuyama, H. I. Suzuki, H. Nishimori, M. Noguchi, T. Yao, N. Komatsu, H. Mano, K. Sugimoto and K. Miyazono: miR-135b mediates NPM-ALK-driven oncogenicity and renders IL-17-producing immunophenotype to anaplastic large cell lymphoma. *Blood*, 118(26), 6881-92 (2011)
53. J. D. Pearson, J. Lee, J. T. Bacani, R. Lai and R. J. Ingham: NPM-ALK and the JunB

transcription factor regulate the expression of cytotoxic molecules in ALK-positive, anaplastic large cell lymphoma. *Int J Clin Exp Pathol*, 4(2), 124-33 (2011)

54. N. Moti, T. Malcolm, R. Hamoudi, S. Mian, G. Garland, C. E. Hook, G. A. Burke, M. A. Wasik, O. Merkel, L. Kenner, E. Laurenti, J. E. Dick and S. D. Turner: Anaplastic large cell lymphoma-propagating cells are detectable by side population analysis and possess an expression profile reflective of a primitive origin. *Oncogene* (2014)
55. T. Gaj, C. A. Gersbach and C. F. Barbas, 3rd: ZFN, TALEN, and CRISPR/Cas-based methods for genome engineering. *Trends Biotechnol*, 31(7), 397-405 (2013)
56. F. D. Urnov, E. J. Rebar, M. C. Holmes, H. S. Zhang and P. D. Gregory: Genome editing with engineered zinc finger nucleases. *Nat Rev Genet*, 11(9), 636-46 (2010)
57. L. Cong, F. A. Ran, D. Cox, S. Lin, R. Barretto, N. Habib, P. D. Hsu, X. Wu, W. Jiang, L. A. Marraffini and F. Zhang: Multiplex genome engineering using CRISPR/Cas systems. *Science*, 339(6121), 819-23 (2013
58. C. Wyman and R. Kanaar: DNA double-strand break repair: all's well that ends well. *Annu Rev Genet*, 40, 363-83 (2006)
59. M. Piganeau, H. Ghezraoui, A. De Cian, L. Guittat, M. Tomishima, L. Perrouault, O. Rene, G. E. Katibah, L. Zhang, M. C. Holmes, Y. Doyon, J. P. Concordet, C. Giovannangeli, M. Jasin and E. Brunet: Cancer translocations in human cells induced by zinc finger and TALE nucleases. *Genome Res*, 23(7), 1182-93 (2013)
60. T. H. Rabbitts, A. Appert, G. Chung, E. C. Collins, L. Drynan, A. Forster, M. N. Lobato, M. P. McCormack, R. Pannell, A. Spandidos, M. R. Stocks, T. Tanaka and E. Tse: Mouse models of human chromosomal translocations and approaches to cancer therapy. *Blood Cells Mol Dis*, 27(1), 249-59 (2001)
61. A. Gutierrez, R. Grebliunaite, H. Feng, E. Kozakewich, S. Zhu, F. Guo, E. Payne, M. Mansour, S. E. Dahlberg, D. S. Neuberg, J. den Hertog, E. V. Prochownik, J. R. Testa, M. Harris, J. P. Kanki and A. T. Look: Pten mediates Myc oncogene dependence in a conditional zebrafish model of T cell acute lymphoblastic leukemia. *J Exp Med*, 208(8), 1595-603 (2011)
62. C. Nardella, A. Lunardi, A. Patnaik, L. C. Cantley and P. P. Pandolfi: The APL paradigm and the "co-clinical trial" project. *Cancer Discov*, 1(2), 108-16 (2011)
63. S. A. Hayes, A. L. Hudson, S. J. Clarke, M. P. Molloy and V. M. Howell: From mice to men: GEMMs as trial patients for new NSCLC therapies. *Semin Cell Dev Biol*, 27, 118-27 (2014)
64. J. Fujimoto, M. Shiota, T. Iwahara, N. Seki, H. Satoh, S. Mori and T. Yamamoto: Characterization of the transforming activity of p80, a hyperphosphorylated protein in a Ki-1 lymphoma cell line with chromosomal translocation t(2;5). *Proc Natl Acad Sci U S A*, 93(9), 4181-6 (1996)
65. F. K. McDuff and S. D. Turner: Aberrant Anaplastic Lymphoma Kinase Activity Induces a p53 and Rb-Dependent Senescence-Like Arrest in the Absence of Detectable p53 Stabilization. *PLoS One*, 6(3), e17854 (2011)
66. R. Y. Bai, T. Ouyang, C. Miething, S. W. Morris, C. Peschel and J. Duyster: Nucleophosmin-anaplastic lymphoma kinase associated with anaplastic large-cell lymphoma activates the phosphatidylinositol 3-kinase/Akt antiapoptotic signaling pathway. *Blood*, 96(13), 4319-27 (2000)
67. D. Cussac, C. Greenland, S. Roche, R. Y. Bai, J. Duyster, S. W. Morris, G. Delsol, M. Allouche and B. Payrastre: Nucleophosmin-anaplastic lymphoma kinase of anaplastic large-cell lymphoma recruits, activates, and uses pp60c-src to mediate its mitogenicity. *Blood*, 103(4), 1464-71 (2004)
68. S. R. McDonnell, S. R. Hwang, V. Basrur, K. P. Conlon, D. Fermin, E. Wey, C. Murga-Zamalloa, Z. Zeng, Y. Zu, K. S. Elenitoba-Johnson and M. S. Lim: NPM-ALK signals through glycogen synthase kinase 3beta to promote oncogenesis. *Oncogene*, 31(32), 3733-40 (2012)
69. C. Ambrogio, C. Voena, A. D. Manazza, R. Piva, L. Riera, L. Barberis, C. Costa, G. Tarone, P. Defilippi, E. Hirsch, E. Boeri Erba, S. Mohammed, O. N. Jensen, G. Palestro, G. Inghirami and R. Chiarle: p130Cas mediates the transforming properties of the anaplastic lymphoma kinase. *Blood*, 106(12), 3907-16 (2005)

70. P. Martinelli, P. Bonetti, C. Sironi, G. Pruneri, C. Fumagalli, P. R. Raviele, S. Volorio, S. Pileri, R. Chiarle, F. K. McDuff, B. K. Tusi, S. D. Turner, G. Inghirami, P. G. Pelicci and E. Colombo: The lymphoma-associated NPM-ALK oncogene elicits a p16INK4a/pRb-dependent tumor-suppressive pathway. *Blood*, 117(24), 6617-26 (2011)

71. S. D. Turner, D. Yeung, K. Hadfield, S. J. Cook and D. R. Alexander: The NPM-ALK tyrosine kinase mimics TCR signalling pathways, inducing NFAT and AP-1 by RAS-dependent mechanisms. *Cell Signal*, 19(4), 740-7 (2007)

72. L. Quintanilla-Martinez, S. Pittaluga, C. Miething, M. Klier, M. Rudelius, T. Davies-Hill, N. Anastasov, A. Martinez, A. Vivero, J. Duyster, E. S. Jaffe, F. Fend and M. Raffeld: NPM-ALK-dependent expression of the transcription factor CCAAT/enhancer binding protein beta in ALK-positive anaplastic large cell lymphoma. *Blood*, 108(6), 2029-36 (2006)

73. S. Giuriato, N. Faumont, E. Bousquet, M. Foisseau, A. Bibonne, M. Moreau, T. Al Saati, D. W. Felsher, G. Delsol and F. Meggetto: Development of a conditional bioluminescent transplant model for TPM3-ALK-induced tumorigenesis as a tool to validate ALK-dependent cancer targeted therapy. *Cancer Biol Ther*, 6(8), 1318-23 (2007)

74. M. M. Duplantier, L. Lamant, F. Sabourdy, A. de Reynies, G. Delsol and E. Espinos: Serpin A1 is overexpressed in ALK+ anaplastic large cell lymphoma and its expression correlates with extranodal dissemination. *Leukemia*, 20(10), 1848-54 (2006) 75. S. Barbey, J. Gogusev, H. Mouly, O. Le Pelletier, W. Smith, S. Richard, J. Soulie and C. Nezelof: DEL cell line: a “malignant histiocytosis” CD30+ t(5;6)(q35;p21) cell line. *Int J Cancer*, 45(3), 546-53 (1990)

76. I. J. Su, S. P. Balk and M. E. Kadin: Molecular basis for the aberrant expression of T cell antigens in postthymic T cell malignancies. *Am J Pathol*, 132(2), 192-8 (1988)

77. R. Morgan, S. D. Smith, B. K. Hecht, V. Christy, J. D. Mellentin, R. Warnke and M. L. Cleary: Lack of involvement of the c-fms and N-myc genes by chromosomal translocation t(2;5)(p23;q35) common to malignancies with features of so-called malignant histiocytosis. *Blood*, 73(8), 2155-64 (1989)

78. A. L. Epstein and H. S. Kaplan: Biology of the human malignant lymphomas. I. Establishment in continuous cell culture and heterotransplantation of diffuse histiocytic lymphomas. *Cancer*, 34(6), 1851-72 (1974)

79. H. Merz, K. Lange, T. Gaiser, A. Muller, U. Kapp, C. Bittner, S. Harder, R. Siebert, M. Bentz, T. Binder, V. Diehl and A. C. Feller: Characterization of a novel human anaplastic large cell lymphoma cell line tumorigenic in SCID mice. *Leuk Lymphoma*, 43(1), 165-72 (2002)

80. M. Shimakage, T. Dezawa, S. Tamura, T. Tabata, N. Aoyagi, M. Koike, H. Inoue, M. Yutsudo, A. Hakura and N. Ikegami: A Ki-1-positive cell line expressing Epstein-Barr virus antigens, established from a child with Ki-1-positive lymphoma. *Intervirology*, 36(4), 215-24 (1993)

81. P. Fischer, E. Nacheva, D. Y. Mason, P. D. Sherrington, C. Hoyle, F. G. Hayhoe and A. Karpas: A Ki-1 (CD30)-positive human cell line (Karpas 299) established from a high-grade non-Hodgkin’s lymphoma, showing a 2;5 translocation and rearrangement of the T-cell receptor beta-chain gene. *Blood*, 72(1), 234-40 (1988)

82. A. del Mistro, A. Leszl, R. Bertorelle, M. L. Calabro, M. Panozzo, C. Menin, E. D’Andrea and L. Chieco-Bianchi: A CD30-positive T cell line established from an aggressive anaplastic large cell lymphoma, originally diagnosed as Hodgkin’s disease. *Leukemia*, 8(7), 1214-9 (1994)

83. L. Lamant, E. Espinos, M. Duplantier, N. Dastugue, A. Robert, M. Allouche, J. Ragab, P. Brousset, C. Villalva, R. D. Gascoyne, T. Al Saati and G. Delsol: Establishment of a novel anaplastic large-cell lymphoma-cell line (COST) from a ‘small-cell variant’ of ALCL. *Leukemia*, 18(10), 1693-8 (2004)

84. J. Willers, R. Dummer, W. Kempf, T. Kundig, G. Burg and M. E. Kadin: Proliferation of CD30+ T-helper 2 lymphoma cells can be inhibited by CD30 receptor cross-linking with recombinant CD30 ligand. *Clin Cancer Res*, 9(7), 2744-54 (2003)

85. T. H. Davis, C. C. Morton, R. Miller-Cassman, S. P. Balk and M. E. Kadin: Hodgkin’s disease, lymphomatoid papulosis, and cutaneous T-cell lymphoma derived from a common

T-cell clone. *N Engl J Med*, 326(17), 1115-22 (1992)

86. G. Ott, T. Katzenberger, R. Siebert, J. F. DeCoteau, J. A. Fletcher, J. H. Knoll, J. Kalla, A. Rosenwald, M. M. Ott, K. Weber-Matthiesen, M. E. Kadin and H. K. Muller-Hermelink: Chromosomal abnormalities in nodal and extranodal CD30+ anaplastic large cell lymphomas: infrequent detection of the t(2;5) in extranodal lymphomas. *Genes Chromosomes Cancer*, 22(2), 114-21 (1998)
87. W. P. Schiemann, W. M. Pfeifer, E. Levi, M. E. Kadin and H. F. Lodish: A deletion in the gene for transforming growth factor beta type I receptor abolishes growth regulation by transforming growth factor beta in a cutaneous T-cell lymphoma. *Blood*, 94(8), 2854-61 (1999)
88. D. K. Crockett, Z. Lin, K. S. Elenitoba-Johnson and M. S. Lim: Identification of NPM-ALK interacting proteins by tandem mass spectrometry. *Oncogene*, 23(15), 2617-29 (2004)
89. A. V. Galkin, J. S. Melnick, S. Kim, T. L. Hood, N. Li, L. Li, G. Xia, R. Steensma, G. Chopiuk, J. Jiang, Y. Wan, P. Ding, Y. Liu, F. Sun, P. G. Schultz, N. S. Gray and M. Warmuth: Identification of NVP-TAE684, a potent, selective, and efficacious inhibitor of NPM-ALK. *Proc Natl Acad Sci U S A*, 104(1), 270-5 (2007)
90. A. Colomba, S. Giuriato, E. Dejean, K. Thornber, G. Delsol, H. Tronchere, F. Meggetto, B. Payrastre and F. Gaits-Iacovoni: Inhibition of Rac controls NPM-ALK-dependent lymphoma development and dissemination. *Blood Cancer J*, 1(6), e21 (2011)

Abbreviations: ALCL, Anaplastic Large Cell Lymphoma; NPM, Nucleophosmin; ALK, Anaplastic Lymphoma Kinase; TCR, T-cell receptor; GEMMs, Genetically Engineered Mouse Models; PDX, Patient Derived Xenografts; CSC, Cancer Stem Cells; iPS, induced pluripotent stem cells; MOI, Multiplicity of Infection; T-LBL, T-Lymphoblastic Lymphoma; ZFN, Zinc Finger Nucleases; RPE-1, retinal pigment epithelial cells; TALEN, Transcription Factor Activator-Like Effector Nucleases; CRISPR, Clustered Interspaced Short Palindrome Repeats; cas, CRISPR-Associated Systems.

Key Words: ALCL, NPM-ALK, Mouse models, Cancer models, *In vitro* cancer models, Review

Send correspondence to: Suzanne Turner, Division of Molecular Histopathology, Department of Pathology, University of Cambridge, Lab Block Level 3, Box 231, Addenbrooke's Hospital, Cambridge CB20QQ, UK, Tel: 44-0-1223-762655, Fax: 44-0-1223-586670, E-mail: sdt36@cam.ac.uk

Article 5

Targeting autophagy enhances the anti-tumoral action of crizotinib in ALK-positive anaplastic large cell lymphoma

Géraldine Mitou, Julie Frentzel, Aurore Desquesnes, Sophie Le Gonidec, Talal AlSaati, Isabelle Beau, Laurence Lamant, Fabienne Meggetto, Estelle Espinos, Patrice Codogno, Pierre Brousset, Sylvie Giuriato

ONCOTARGET

Vol. 6, No. 30, Issue of October, pp. 30149-30164, 2015

Targeting autophagy enhances the anti-tumoral action of crizotinib in ALK-positive anaplastic large cell lymphoma

Géraldine Mitou[1,2,3,*], Julie Frentzel[1,2,3,*], Aurore Desquesnes[4], Sophie Le Gonidec[4,7], Talal AlSaati[5], Isabelle Beau[6], Laurence Lamant[1,2,3,7,8,10], Fabienne Meggetto[1,2,3,10], Estelle Espinos[1,2,3,7,10], Patrice Codogno[9], Pierre Brousset[1,2,3,7,8,10], Sylvie Giuriato[1,2,3,10]

[1]Inserm, UMR1037 CRCT, F-31000 Toulouse, France

[2]Université Toulouse III-Paul Sabatier, UMR1037 CRCT, F-31000 Toulouse, France

[3]CNRS, ERL5294 CRCT, F-31000 Toulouse, France

[4]Phenotyping Service, INSERM-US006 ANEXPLO/CREFRE, Toulouse, France

[5]INSERM/UPS - US006/CREFRE, Service d'Histopathologie, CHU Purpan, Toulouse, France

[6]INSERM UMRS 1185; Faculté de Médecine Paris Sud, Le Kremlin-Bicêtre, France

[7]Université Toulouse III - Paul Sabatier, Toulouse, France

[8]Department of Pathology, IUCT, Toulouse, France

[9]Institut Necker Enfants-Malades, INSERM U1151-CNRS UMR 8253, Paris, France

[10]European Research Initiative on ALK-related malignancies (ERIA)

[*]These authors have contributed equally to this work

Correspondence to:
Sylvie Giuriato, **e-mail:** sylvie.giuriato@inserm.fr

Keywords: *anaplastic large cell lymphoma, NPM-ALK, autophagy, crizotinib, cytoprotection*

Received: *March 02, 2015* ***Accepted:*** *August 07, 2015* ***Published:*** *August 17, 2015*

ABSTRACT

Anaplastic Lymphoma Kinase-positive Anaplastic Large Cell Lymphomas (ALK+ ALCL) occur predominantly in children and young adults. Their treatment, based on aggressive chemotherapy, is not optimal since ALCL patients can still expect a 30% 2-year relapse rate. Tumor relapses are very aggressive and their underlying mechanisms are unknown. Crizotinib is the most advanced ALK tyrosine kinase inhibitor and is already used in clinics to treat ALK-associated cancers. However, crizotinib escape mechanisms have emerged, thus preventing its use in frontline ALCL therapy. The process of autophagy has been proposed as the next target for elimination of the resistance to tyrosine kinase inhibitors. In this study, we investigated whether autophagy is activated in ALCL cells submitted to ALK inactivation (using crizotinib or ALK-targeting siRNA). Classical autophagy read-outs such as autophagosome visualization/quantification by electron microscopy and LC3-B marker turn-over assays were used to demonstrate autophagy induction and flux activation upon ALK inactivation. This was demonstrated to have a cytoprotective role on cell viability and clonogenic assays following combined ALK and autophagy inhibition. Altogether, our results suggest that co-treatment with crizotinib and chloroquine (two drugs already used in clinics) could be beneficial for ALK-positive ALCL patients.

INTRODUCTION

Anaplastic Large Cell Lymphoma (ALCL) is an aggressive form of malignant lymphoma of T/null lineage, which occurs mostly in children and young adults. Two systemic forms of ALCL have been defined according to the presence or absence of aberrant anaplastic lymphoma kinase (ALK) expression [1, 2]. The identification of ALK and its role in the pathogenesis of ALCL were originally described in 1994 by Morris et al. [3]. Since then, it has become increasingly clear that ALK is a prevalent oncogene that is aberrantly expressed in a variety of tumors, including some

B-cell lymphoma (DLBCL), inflammatory myofibroblastic tumors (IMT), some non-small-cell lung cancers (NSCLC), renal carcinoma (RCC), colorectal carcinoma (CRC) and neuroblastoma (NB) [4–6]. In the case of ALCL, ALK is mainly activated as a consequence of a chromosomal translocation whereby the oligomerization domain of the nucleophosmin (NPM) gene is juxtaposed to the kinase domain of ALK. The resultant NPM-ALK fusion protein is constitutively active, and has been described in different cell and mouse models for NPM-ALK tumorigenesis [4, 7–10]. In NSCLC, an inversion event fuses the echinoderm microtubule-associated protein-like 4 (EML4) gene to ALK. Other less represented chromosomal abnormalities involving the ALK gene have also been described both for ALCL and NSCLC [5]. In addition, ALK activation in cancer can also arise through overexpression and mutation of full-length ALK [6].

ALK-expressing tumors are sensitive to treatment with small molecule inhibitors [11–14]. Among these, crizotinib is a potent ATP-competitive inhibitor of ALK and c-Met [15]. It is already used in the clinic for the treatment of late stage and metastatic cases of ALK-positive NSCLC, and promising results have accumulated concerning its use in the treatment of IMT [16, 17] and recurring/refractory ALCL [17, 18]. However, as has been reported for other tyrosine kinase inhibitors, escape mechanisms to overcome the effects of crizotinib have been described in ALK-positive NSCLC and ALCL patients [6, 13, 18–23]. These mainly occur through ALK tyrosine kinase domain punctual mutations, ALK gene amplification and/or activation of compensatory signaling pathways and more than one mechanism can develop simultaneously within the same tumor [13, 24]. Thus, to circumvent resistance, second generation ALK inhibitors (AP26113, LDK 378, ASP3026, CH5424802) have been developed [5], and new combined therapies have also been proposed using a non-ALK-targeting drug alongside an ALK inhibitor [25, 26]. Despite this, our understanding of crizotinib resistance mechanisms at both the cellular and molecular levels needs improvement in order to develop better treatment options. For instance, tumor cell autophagy has been proposed as a new target for overcoming resistance to tyrosine kinase inhibitors [27–30], yet its role in crizotinib-treated ALCL has never been studied.

Autophagy is a highly-conserved catabolic pathway used by the cell to degrade and recycle its own constituents [31]. The autophagy process involves first the formation of an isolation membrane, which elongates and closes in on itself to isolate unwanted cytoplasmic components such as damaged or obsolete organelles and toxic protein aggregates within a double-membraned structure called an autophagosome. Autophagosomes then dock and fuse with lysosomes, where acidic hydrolases degrade the "cargo", therefore assuring a constant cytoplasmic quality control. All of the steps of this process are tightly regulated [32–34].

Malfunctioning autophagy is observed in many human diseases (including neurodegenerative diseases, infectious diseases, heart diseases and diabetes) [35]. In cancer development, autophagy plays a dual role [36–39]. During the initial stages of tumor development it exerts anti-tumoral effects, essentially by removing damaged mitochondria, preventing ROS accumulation, tissue damage, inflammation and genomic instability [40]. Conversely, once the tumor is formed it fuels tumorigenesis by delivering energy in a metabolically stressed environment [41].

Emerging evidence shows that these dual functions of autophagy, in promoting either death or survival mechanisms, are also observed in therapeutically-challenged tumor cells. Indeed, some tumor treatments have been associated with autophagy-mediated oncoprotein degradation [42, 43]. Other compounds have been shown to induce autophagy-mediated cell death [44–46] or autophagy-mediated immunogenic cell death [47]. Conversely, survival autophagy mechanisms have also been observed in different studies upon either chemo-, radio- or targeted therapies [27, 29, 48–50] and inhibiting autophagy in these contexts has been proven to enhance treatment efficiency [51, 52]. Thus, whether to use autophagy inducers or inhibitors to optimize a given cancer treatment is clearly a matter of context [50].

In this study we sought to investigate whether autophagy activation acts as a tumor survival mechanism to overcome ALK oncogene inactivation in ALCL cell lines and whether disabling autophagy may represent a clinical benefit for ALCL patients.

RESULTS

ALK inactivation induces autophagy in ALK-positive ALCL cell lines

To determine whether ALK inactivation induces autophagy, we used flow cytometry to assay the development of acidic vesicular organelles (AVOs), which are indicative of autophagy, using the lysosomo-tropic agent, acridine orange [53]. This compound accumulates in acidic compartments to form aggregates that fluoresce bright red. As a positive control, Karpas-299 cells were treated with rapamycin (100 nM, 24 h), a well-known inducer of autophagy (Figure 1A). We observed that when ALK-positive Karpas-299 (Figures 1A and 1B) or SU-DHL-1 cells (Supplemental Figures S1A and S1B) were submitted to pharmacological or molecular ALK inactivation, through crizotinib treatment or ALK-targeted siRNA transfection respectively, an increase in the red fluorescence (y-axis) was observed. This demonstrates the induction of AVOs following ALK inactivation, from 3.2 to 17.5% upon crizotinib treatment and from 5.4 to 16.7% following NPM-ALK downregulation. We confirmed the loss of NPM-ALK autophosphorylation (data not shown) and the decreased viability of the ALCL cell lines (Supplemental Figures S2A and S2B) following treatment with crizotinib at either 500 nM for Karpas-299

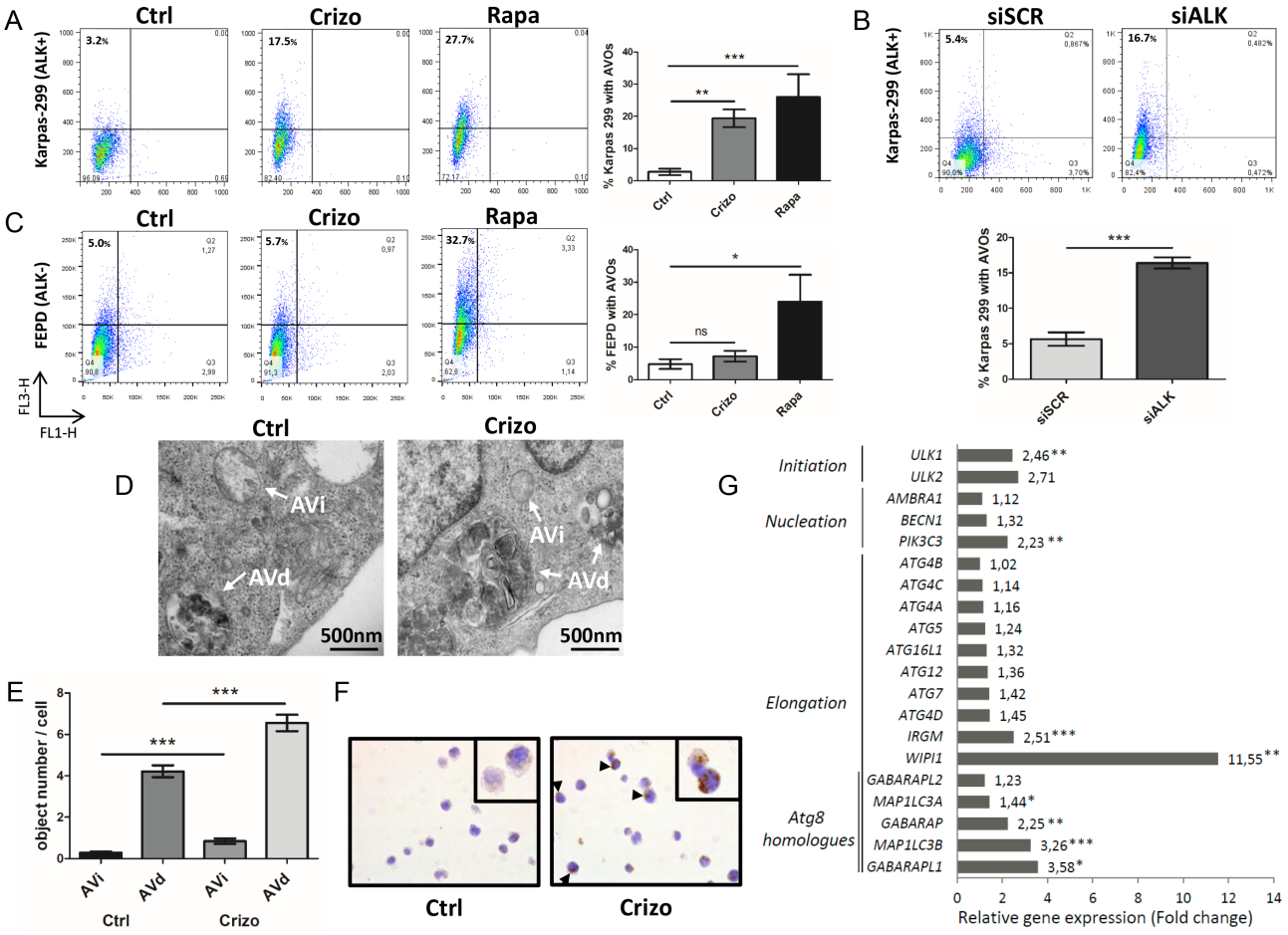

Figure 1: Induction of autophagy upon ALK inactivation in NPM-ALK-positive Karpas-299 ALCL cells. A. Acridine orange flow cytometry staining was performed to detect the formation of acidic vesicular organelles (AVOs) following crizotinib (Crizo) (500 nM, 24 h) or rapamycin (Rapa) (100 nM, 24 h) treatment, compared to control cells (Ctrl). FL1-H indicates green color intensity (cytoplasm and nucleus), while FL3-H shows red color intensity (AVOs). The percentage of AVOs is displayed in the left upper quadrants. Representative flow diagrams are shown. Data on graph represent mean AVOs quantification ± SD from three independent experiments. Statistical analysis was performed by unpaired *t*-tests; ***$p \leq 0.001$; **$p \leq 0.01$. **B.** AVOs development and quantification were determined, as indicated in (A), following transfection for 72 h with ALK-targeted siRNA (siALK) or scramble siRNA (siSCR). **C.** AVOs quantification was determined, as indicated in (A), for untreated, crizotinib-treated (500 nM, 24 h) and rapamycin-treated (100 nM, 24 h) ALK-negative FEPD ALCL cells. Mean AVOs percentages are represented ± SD, quantified from three independent experiments. Statistical analysis was performed by one-way ANOVA followed by the Newman–Keuls multiple comparison test; ***$p \leq 0.001$. **D.** Quantification of autophagic vacuoles was performed on around 100 cells from TEM sections prepared from untreated (Ctrl) and crizotinib-treated (Crizo) (500 nM, 24 h) conditions. Characteristic double membrane autophagosomes were counted as initial autophagic vacuoles (AVi) whereas autophagosomes that had fused with vesicles originated from the endo/lysosomal compartment were counted as degradative autophagic vacuoles (AVd). Representative images at x 10,000 magnification are shown. **E.** Data represent mean vesicle number per cell ± SEM. Statistical analysis was performed by an unpaired *t*-test; ***$p \leq 0.001$. **F.** LC3 immunohistochemical staining in control (Ctrl) and crizotinib-treated Karpas-299 cells (500 nM, 24 h) (Crizo). Sections were stained with anti-LC3 antibodies, and nuclei were counterstained with hematoxylin. Black arrows denote punctuate LC3 staining. Original images were produced with a leica DM4000B microscope (total magnification: x 400). **G.** Autophagy-related gene expression profile following crizotinib treatment. This selected data set was obtained using SABiosciences autophagy PCR arrays ($n = 3$). Results are expressed as fold change compared to levels measured in untreated Karpas-299 cells (set to 1). Statistical analysis was performed using unpaired *t*-tests; *$p \leq 0.05$; **$p \leq 0.01$; ***$p \leq 0.001$.

cells (a concentration which corresponds to the plasmatic dose measured in patients being treated for ALK tumors) or 400 nM for SU-DHL-1 cells, which are more sensitive to the drug [15]. The downregulation of NPM-ALK expression following ALK-targeted siRNA was also checked, and is shown in Supplemental Figure S3A.

To assess the specificity of AVOs induction following ALK inactivation, we used the ALK-negative ALCL cell line, FEPD, treated or not with crizotinib (500 nM, 24 h) or rapamycin (100 nM, 24 h). Rapamycin treatment induced AVOs formation, whereas crizotinib treatment did not (Figure 1C). This strongly argues for a

direct causal relationship between ALK inactivation and AVOs generation in ALK-positive ALCL cell lines.

This observed accumulation of AVOs prompted us to validate that autophagy was induced using other techniques. To this end, we first checked for the presence of autophagosomes by electron microscopy. As shown in Figures 1D and 1E, we observed an increased number of double-membrane autophagosomes (shown by arrows) upon crizotinib treatment in Karpas-299 cells compared to untreated cells. ALK-inhibition increased the number of autophagosomes at both their initial (AVi) and late maturation stages (AVd), as morphologically defined in the Eskelinen review [54]. We then used immunohistochemistry to demonstrate an increased percentage of cells harboring a punctate distribution of the autophagy marker microtubule-associated protein 1 light chain 3 (MAP1LC3) [55], hereafter referred to as LC3, upon crizotinib treatment compared to untreated cells (Figure 1F and Supplemental Table 1). Finally, we investigated whether crizotinib treatment in ALK-positive Karpas-299 cells could have an effect on the expression levels of genes involved in the autophagy initiation and elongation processes. The analysis of a focused autophagy RT-PCR array showed a global increase in the expression of autophagy-related genes upon crizotinib treatment, in comparison with untreated Karpas-299 cells (Figure 1G). Strikingly, the highest significant up-regulations were found for genes that orchestrate the three crucial steps for autophagosome formation: (i) ULK1: involved in initiation, 2.46 fold change, $p < 0.01$; (ii) PIK3C3: involved in nucleation, 2.23 fold change, $p < 0.01$; (iii) MAP1LC3B: involved in elongation/closure, 3.26 fold change, $p < 0.001$; and (iv) WIPI1: involved in elongation/closure, 11.55 fold change, $p < 0.01$. We validated the increased levels of these four mRNAs and some of their encoding proteins in Karpas-299 cells in which ALK inactivation had been achieved through the use of ALK-targeting siRNA (Supplemental Figure S4). Altogether, these observations demonstrate that a loss of ALK activity is able to elicit morphological and molecular signatures specific to the autophagic process.

To further confirm the induction of autophagy and address the question of the activation of autophagic flux in ALK-inactivated Karpas-299 cells, we first performed acridine orange FACS analysis to monitor AVOs generation upon disruption of the autophagy process at an early stage. Vps34 and Beclin1 are two key proteins belonging to the PI3-kinase/Beclin1 complex that is required early on in the activation of autophagy. We used the pharmacological drug 3-methyladenine (3MA) to specifically inhibit Vps34 (a class III PI3-kinase), and an siRNA approach to inactivate Beclin1 (Supplemental Figure S3B) [32, 56]. As shown in Figures 2A and 2B, in both experimental settings we observed a drop in crizotinib-induced AVOs generation, from 18.9 ± 2.6% to 10.2 ± 2.3% upon 3-methyladenine addition ($p \leq 0.001$) and from 13.6 ± 1.5% to 5.3 ± 2.1% upon Beclin1 downregulation ($p \leq 0.01$). Taken together, these results indicate that the crizotinib-induced increase in red fluorescence is attributable to the development of AVOs associated with autophagy. We then analyzed autophagic flux using the LC3 turnover assay [57, 58]. For this, we inhibited ALK in Karpas-299 cells using crizotinib or siALK transfection, combined or not with chloroquine (CQ), a drug known to block autophagy by impairing the lysosomal degradation of the autophagic cargo. We then monitored the conversion of the cytosolic LC3 form (LC3-I, 18kDa) to the pre-autophagosomal and autophagosomal membrane-bound form of LC3 (LC3-II, 16kDa). Levels of LC3-II were higher in cells submitted to chloroquine treatment alongside ALK inactivation (for both crizotinib treatment and ALK-targeted siRNA) than in cells submitted to either treatment alone (Figures 2C and 2D). Furthermore, when we analyzed the kinetics of crizotinib treatment (after 6 h, 24 h and 48 h) in the presence or absence of chloroquine, we observed an accumulation of the LC3-II form over time (Figure 2E). Similarly, a CQ-dependent accumulation of LC3-II was observed in ALK-positive SU-DHL-1 cells treated with crizotinib (400 nM, 24 h) (Supplemental Figure S1C). Overall, these results indicate that ALK inactivation, either through pharmacological (crizotinib) or molecular approaches (ALK-targeted siRNA), induces an increase in the number of autophagosomes and autophagic flux in at least two of the most commonly used ALK-positive ALCL cell lines: Karpas-299 and SU-DHL-1.

Synergistic loss of Karpas-299 cell viability upon pharmacological or molecular inhibition of both the ALK oncogene and the autophagic process

It is now well known that cancer cells that are able to mount an autophagic response under stress conditions are highly sensitive to chloroquine. We thus investigated, *in vitro*, how this drug would impact on ALCL cell viability following co-treatment with crizotinib. As shown in Figure 3A, we observed a decrease in ALK-positive Karpas-299 cell viability, from 63.6 ± 3.1% upon single crizotinib treatment to 41.5 ± 5.4% upon crizotinib and chloroquine co-treatment ($p \leq 0.01$). Similar results were obtained with SU-DHL-1 cells (Supplemental Figure S1D), and when another pharmacological drug targeting autophagy was used, *i.e.* 3-methyladenine (Figure 3B). Increasing concentrations of crizotinib (0–2000 nM), combined with increasing doses of either chloroquine (0–120 μM) or 3-methyladenine (0–10 mM) (Tables 1 and 2) allowed a Chou-Talalay analysis to be performed [59], which demonstrated the synergism (defined by a combination index (CI) < 1) of co-treatment. Indeed, the CI value for crizotinib+chloroquine was between 0.85 and 0.9, indicating a slight synergism between the two drugs, and the CI value of crizotinib+3-methyladenine was between 0.3 and 0.7, showing synergism, as described by Chou (Supplemental Figure S5A and S5B) [60].

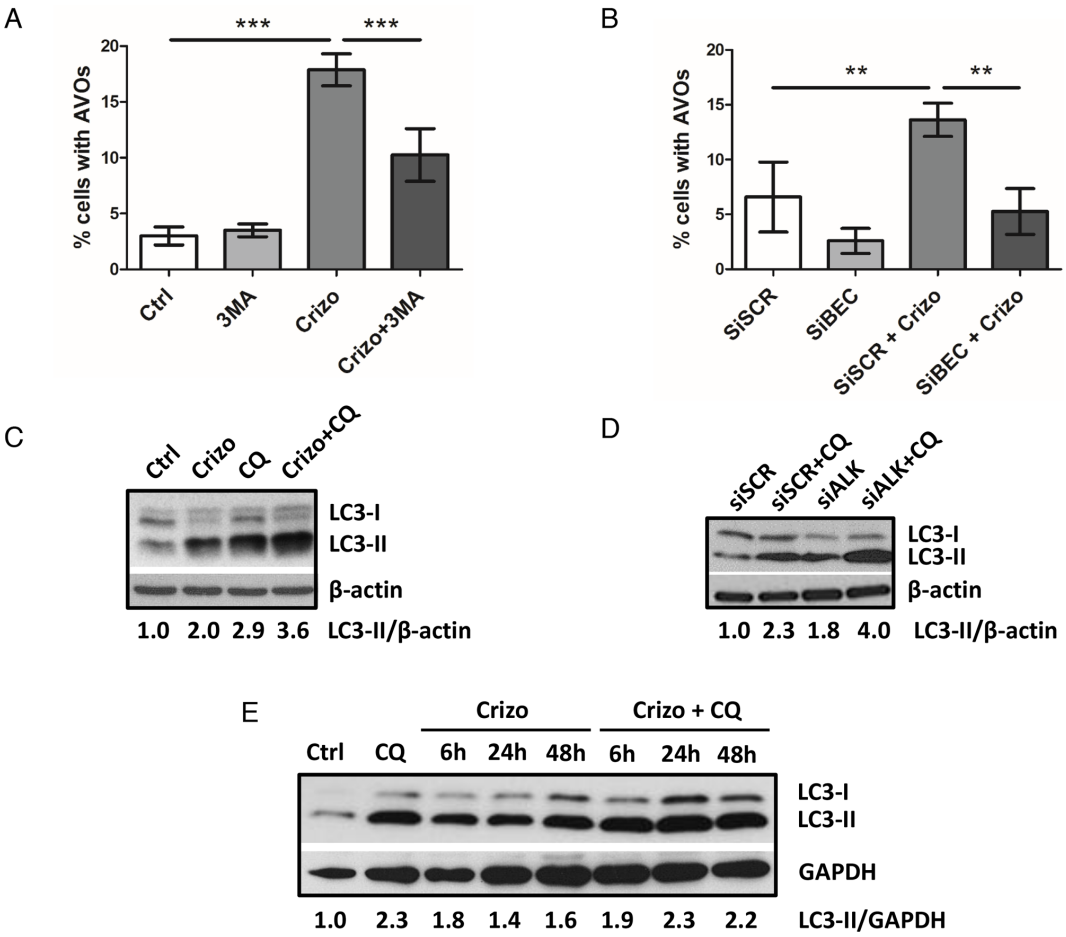

Figure 2: ALK inactivation increases autophagic flux in the Karpas-299 ALCL cell line. A-B. Effect of 3-methyladenine treatment or Beclin1 knockdown on the development of AVOs in crizotinib-treated cells. Karpas-299 cells were treated or not with crizotinib (500 nM, 24 h) (Crizo). 3-methyladenine (3MA) (10 mM) was added or not 4 h before AVOs quantification by acridine orange FACS staining (A). Karpas-299 cells, transfected with either scramble (siSCR) or Beclin-1-targeted siRNAs (siBECN1), were treated or not with crizotinib (500 nM, 24 h). AVOs quantification was performed by acridine orange FACS staining (B). Data are expressed as mean values ± SD quantified from at least three independent experiments. Statistical analysis was performed by one-way ANOVA followed by a Newman–Keuls multiple comparison test; $^{**}p \leq 0.01$; $^{***}p \leq 0.001$. **C-E.** Autophagic flux was determined in Karpas-299 cells following treatment with crizotinib (500 nM, 24 h) (Crizo) in the presence or absence of chloroquine (CQ) (30 μM, 24 h) (C). Karpas-299 cells were transfected with either scramble (siSCR) or ALK-targeted siRNAs (siALK) for 72 h and with additional treatment or not of 30 μM chloroquine (CQ) for the last 24 h (D). The kinetics of crizotinib treatment (500 nM, 6 h, 24 h and 48 h) (Crizo) was observed in Karpas-299 cells in the presence or absence of chloroquine (CQ) (30 μM, 24 h) (E). Total cell lysates were analyzed by western blotting using antibodies against LC3 and β-actin or GAPDH (as a loading control). Blots from three representative experiments are shown.

Similar results were also observed for ALK-positive SU-DHL-1 cells (Supplemental Figure S1E). Chloroquine and 3-methyladenine can also induce off-target or alternative target effects (besides autophagy inhibition) [61–63], which could have accounted for the reduced cell viability in our MTS assays. Thus, to rule out these potential effects we used siRNA targeting ATG7 to molecularly inhibit the autophagic machinery. ATG7 is a key protein involved in the maturation of the LC3 protein during the autophagosome elongation phase [32, 56]. We first checked the efficiency of ATG7 knockdown (Supplemental Figure S3C) and the effect of this on the conversion of LC3-I to LC3-II. As shown in Supplemental Figure S6, accumulation of the LC3-II form was reduced by 50% in siATG7-transfected Karpas-299 cells, both under basal and crizotinib-treated conditions, in comparison to cells transfected with scramble siRNA (siSCR). It is important to point out that under these conditions we found that ATG7 invalidation alone did not impair cell viability (Figure 3C) or cell growth on agar plates (Figure 4C). However, when combined with crizotinib treatment, it potently inhibited these two cell responses (Figures 3C and 4C). Similar results were observed with ALK-targeted siRNA combined with chloroquine (Figure 3D). Altogether, these results indicate that combined ALK and autophagy inhibition, even using diverse approaches, leads to a reduction in cell viability.

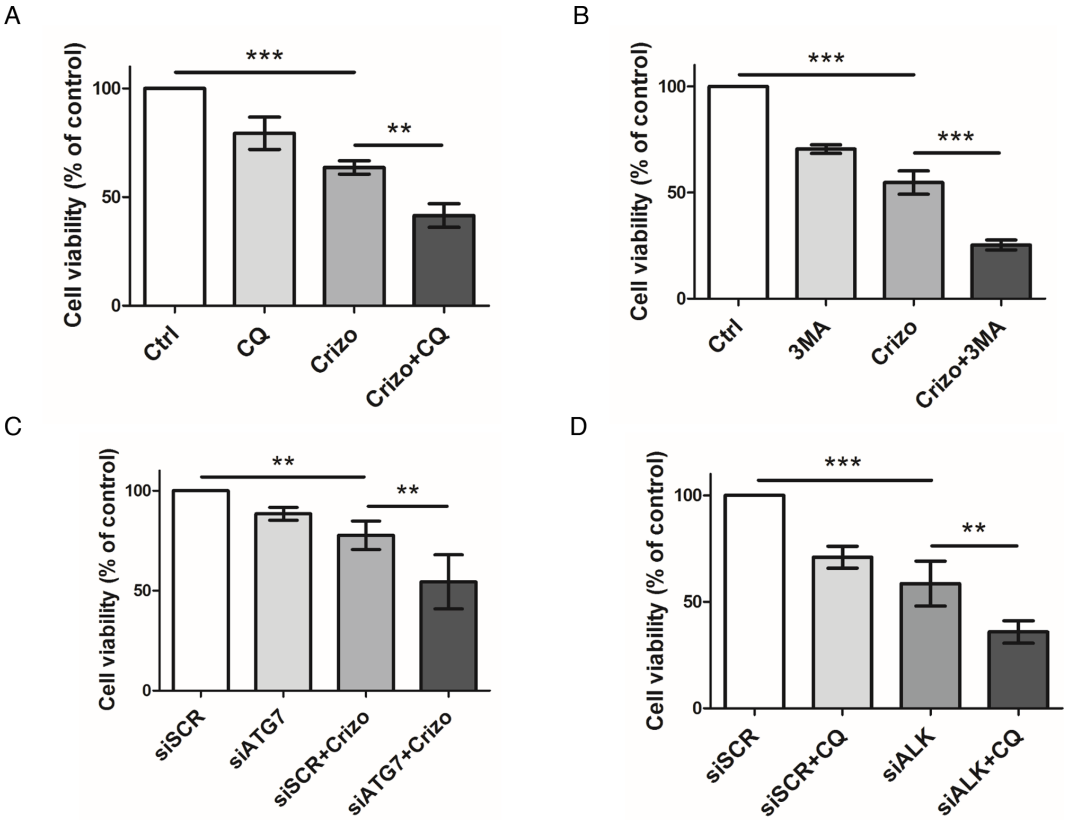

Figure 3: Effect of pharmacological or molecular inhibition of the ALK oncogene combined with inhibition of the autophagic process on Karpas-299 cell viability. A-B. Karpas-299 cells were treated with crizotinib (Crizo) (500 nM) with or without chloroquine (CQ) (30 μM) (A) or 3-methyladenine (3MA) (1.25 mM) (B) for 48 h, then cell viability was determined by MTS assay. **C-D.** Karpas-299 cells were transfected with either scramble (siSCR) or ATG7-targeted (siATG7) siRNAs (C) or with scramble (siSCR) or ALK-targeted (siALK) siRNAs (D) and treated or not with crizotinib (500 nM) (Crizo) (C) or chloroquine (30 μM) (CQ) (D). Cell viability was determined by MTS assay. The graph represents mean values ± SD from three to four independent experiments. Statistical analysis was performed by one-way ANOVA followed by the Newman–Keuls multiple comparison test; $^{**}p \leq 0.01$; $^{***}p \leq 0.001$.

Table 1: Viability (%) of Karpas-299 cells after a 48 h treatment with crizotinib and chloroquine alone or in combination

	Crizotinib (nM)					
	0	**125**	**250**	**500**	**1000**	**2000**
Chloroquine (μM)						
0	100	93,88 ± 5,66	80,27 ± 3,31	58,75 ± 9,64	46,07± 17,67	36,03 ± 21,11
7,5	100 ± 5,72	82,52 ± 7,05				
15	96,97 ± 3,83		69,01± 13,08			
30	79,35± 7,36			41,53 ± 5,36		
60	68,56 ± 3,37				20,90 ± 2,96	
120	15,13 ± 5,13					

Karpas-299 cells were treated for 48 h with the indicated concentrations of crizotinib (nM) and chloroquine (μM), either alone or in combination. A constant ratio design was used for combination experiments. Viability was measured by MTS assay. Experiments were done at least in triplicate and were normalized to cells incubated without drug (100%). Data represent the mean values ± SD.

Table 2: Viability (%) of Karpas-299 cells after a 48 h treatment with crizotinib and 3-methyladenine (3MA) alone or in combination

	Crizotinib (nM)					
	0	**125**	**250**	**500**	**1000**	**2000**
3MA (mM)						
0	100	83,65 ± 2,70	69,79 ± 3,38	52,48 ± 4,13	41,43 ± 3,87	37,5 ± 4,33
0,625	82,74 ± 3,17	62,42 ± 6,92				
1,25	71,23 ± 1,63		44,09 ± 3,89			
2,5	51,61 ± 0,38			15,81± 4,46		
5	31,24 ± 1,20				8,15 ± 4	
10	14,33± 3,82					

Karpas-299 cells were treated for 48 h with the indicated concentrations of crizotinib (nM) and 3-methyladenine (mM), either alone or in combination. A constant ratio design was used for combination experiments. Viability was measured by MTS assay. Experiments were done at least in triplicate and were normalized to cells incubated without drug (100%). Data represent the mean values ± SD.

Reduced clonogenic potential and increased apoptosis following combined ALK and autophagy inhibition

The synergistic effect of combined ALK and autophagy inhibition on reducing ALK-positive Karpas-299 and SU-DHL-1 cell viability raised the question of whether this was due to a decrease in cell growth and/or an increase in cell death. To address this point, we first analyzed the ability of Karpas-299 cells to grow in soft agar following treatment with either crizotinib or chloroquine or both drugs in combination (Figures 4A and 4B). To confirm these results, the same experiments were also performed using siRNAs targeting ATG7 to directly impair autophagy (Figures 4C and 4D). We found that the ability of tumor cells to form clones and grow in soft agar was significantly reduced by crizotinib alone but decreased further following combined treatment. To address the question of cell death, we performed annexinV/7-AAD flow cytometry analysis. We found a clear induction of apoptosis upon crizotinib and chloroquine co-treatment when compared to untreated or single treatments, in both ALK-positive Karpas-299 and SU-DHL-1 cells (Figures Supplemental S7A-C and S7B-D, respectively, red quadrants). Of note, necrotic SU-DHL-1 cells were also detected (Supplemental Figure S7B, dark quadrant). Altogether, these results indicate that the reduced viability, soft agar growth capacity, and survival of ALK-positive Karpas-299 cells submitted to a combined ALK and autophagy inhibition strongly relies on the inactivation of a cytoprotective autophagy.

Chloroquine treatment potentiates the growth inhibitory effect of crizotinib on Karpas-299 xenografted tumors

Having shown that autophagy inhibition enhances the anti-tumoral activity of crizotinib in ALCL cell lines *in vitro*, we next investigated the effect of the drug combination on the growth of Karpas-299 tumor grafts *in vivo*. As seen in Figure 5A, mice treated with a combination of crizotinib and chloroquine exhibited a significant decrease in tumor growth compared to untreated mice or mice treated with each drug alone. Overall these findings demonstrate that chloroquine treatment enhances the efficacy of crizotinib *in vivo*, and that the combined therapy, which was well-tolerated in mice, efficiently reduces ALCL tumor growth. We next examined the effects of these drugs on tumor cell necrosis/apoptosis using hematoxylin/eosin (HE) and anti-cleaved caspase 3 (CC3) staining in xenografted tumor tissues (Figures 5C and 5D). As shown in Figure 5C, HE staining reveals that tumor necrotic areas (arrows) were more extensive in tumors submitted to crizotinib and chloroquine co-treatment than in untreated (Ctrl) or individually-treated (Crizo or CQ) tumors, despite the fact that tumors submitted to a combined treatment were smaller than the untreated ones (Figures 5A and 5B). Similar findings were obtained for apoptosis using CC3 staining as an indicator of apoptosis (Figure 5C). Remarkably, a significant increase in CC3 staining was observed in the subcutaneous tumors harvested from animals that had been given the combined treatment compared to the individual treatments (Figure 5D). It should be noted that necrotic regions of the sections were excluded for the quantification of CC3. Altogether, these results suggest that the induction of necrosis/apoptosis could account for the anti-tumoral effects of the crizotinib and chloroquine co-treatment, which corroborates the *in vitro* findings shown in Supplemental Figure S7 and supports a cytoprotective role for autophagy upon crizotinib treatment (Figures 3 and 4). We conclude that crizotinib and chloroquine in combination is highly effective for impairing *in vivo* ALCL tumor growth.

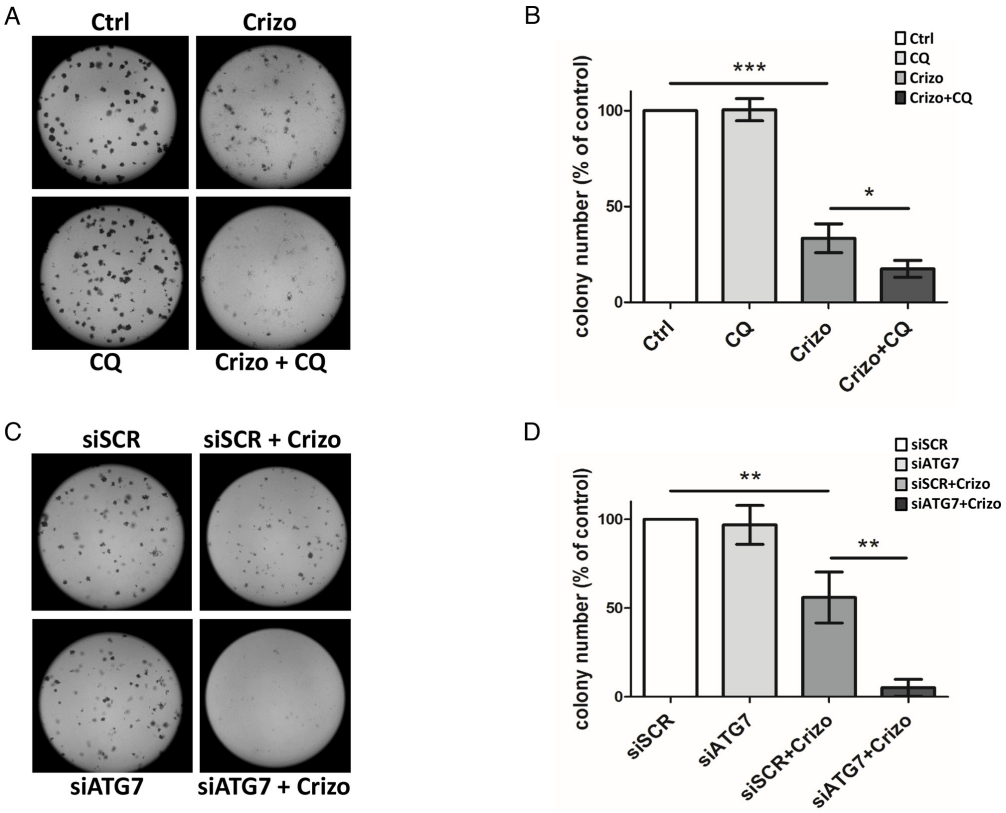

Figure 4: Effect of ALK oncogene inhibition combined with pharmacological or molecular inhibition of the autophagy machinery on Karpas-299 clonogenic survival. A-B. Karpas-299 cells were treated with crizotinib (Crizo) (500 nM) with or without chloroquine (CQ) (30 μM) for 16 h. Cells were then plated onto agar plates. Colonies were detected after 6 days upon addition of the MTT reagent and were scored by Image J quantification software. Representative pictures are shown (A). Results are expressed as the number of colony forming cells per field (B). The graph represents mean values ± SEM from four independent experiments. **C-D.** Karpas-299 cells were transfected with ATG7-targeted (siATG7) or scramble (siSCR) siRNAs then treated or not with crizotinib (Crizo) (500 nM) for 16 h. Cells were then plated onto agar plates. Colonies were detected after 6 days upon addition of the MTT reagent and were scored by Image J quantification software. Representative pictures are shown (C). Results are expressed as the number of colony forming cells per field (D). The graph represents mean values ± SEM from three independent experiments. Statistical analysis was performed by one-way ANOVA followed by the Newman–Keuls multiple comparison test; *$p \leq 0.05$; **$p \leq 0.01$; ***$p \leq 0.001$.

DISCUSSION

In this study, we demonstrate that crizotinib induces autophagy in ALK-positive ALCL cell lines, a result that has never been reported before in this particular subset of lymphoma. Since autophagy inhibition (either by pharmacological inhibition or by an siATG7-mediated approach) potentiates the anti-tumoral activity of ALK inactivation (either by crizotinib treatment or by an siALK-mediated approach), our results indicate that autophagy could act as a survival mechanism in therapeutically-challenged ALK-positive ALCL cells. ALK has previously been linked with autophagy, in glioblastoma and in crizotinib-resistant NSCLC cell lines [64, 65], however in both of these studies the ALK tyrosine kinases (the full length ALK receptor in glioblastoma, and the EML4-ALK fused oncoprotein in NSCLC) were not the direct target of the therapeutic treatment. In the glioblastoma cell lines autophagy was induced following cannabinoid therapy (acting on cannabinoid receptors), and in crizotinib-resistant NSCLC cells, high doses (1 to 8 μM) of crizotinib were used in cells harboring a loss of EML4-ALK. Therefore, another target point of crizotinib in those resistant NSCLC cell lines might be considered. We thus believe this ALCL study to be the very first one to reveal the induction of autophagy upon both pharmacological and molecular NPM-ALK inactivation. Indeed, our *in vitro* results demonstrate that an autophagy response is mounted and activated shortly after either crizotinib treatment (at a plasmatic concentration equivalent to that found in patients being treated for ALK tumors [66, 67]) or after siRNA-mediated specific ALK inhibition in ALCL cells. We observed five complementary results that support an autophagic response following ALK inhibition: 1) increased AVOs; 2) increased number of autophagosomes as identified by electron microscopy;

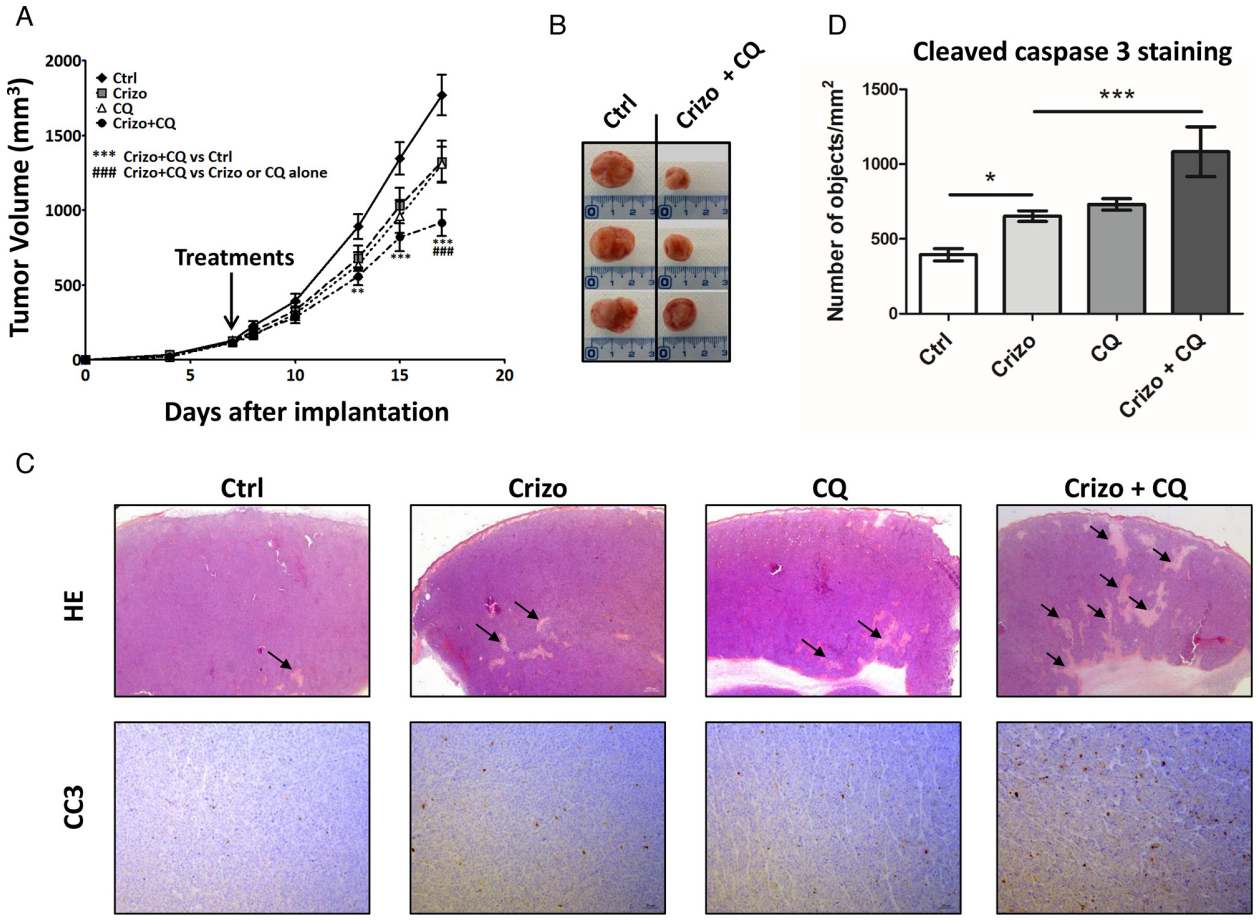

Figure 5: A combination of a low dose of crizotinib plus chloroquine inhibits Karpas-299 xenograft growth in NOD/SCID mice. A. Karpas-299 subcutaneous tumors (n = 8 for each condition) were allowed to grow and, when measurable (around 100 mm^3), mice were matched for tumor volumes and randomly assigned to receive crizotinib (Crizo, 10 mg/kg), chloroquine (CQ, 60 mg/kg) or a combination of both drugs (Crizo+CQ). Tumor volumes are reported as mean ± S.E.M.. Statistical analysis was performed by two-way ANOVA using the Bonferonni correction; $^{**}p < 0.01$; $^{***}p < 0.001$; $^{\#\#\#}p < 0.001$. **B.** Representative tumors resected from mice submitted to either vehicle (Ctrl) or 10 mg/kg crizotinib and 60 mg/kg chloroquine combined treatment (Crizo+CQ). **C.** Micrographs of hematoxylin/eosin (HE) staining (original magnification x 12.5) and anti-cleaved caspase 3 (CC3) immunohistochemistry staining (original magnification x 100). Photographs shown are representative of similar observations in three different control (Ctrl), crizotinib (Crizo), chloroquine (CQ) and crizotinib + chloroquine co-treated tumors (Crizo+CQ), harvested from NOD-SCID mice developing Karpas-299 subcutaneous tumor xenografts. **D.** Active caspase 3 in tumor sections as indicated in (C). Quantifications were performed on scanned immune-stained slides (Pannoramic 250 Flash digital microscope) using a Pannoramic Viewer and HistoQuant software. Segmentation of the detected objects and the calculation of their number per mm^2 were automatically performed. Statistical analyses were performed on individual raw data using one-way ANOVA followed by the Newman-Keuls multiple comparison test; $^{*}p < 0.05$; $^{***}p < 0.001$. Values are expressed as mean ± S.E.M.

3) increased LC3-II immunohistochemistry staining and relocation to autophagosomal membranes; 4) increased autophagy flux (with LC3-II accumulation observed via western blotting following ALK inactivation and chloroquine co-treatment); 5) increased expression of autophagy genes. To decipher whether this crizotinib-induced autophagy affected cell death or cell survival functions, we performed several assays, testing cell viability, clonogenic survival, apoptosis and the ability of ALCL cells to form xenografted tumors *in vivo*. Together these assays demonstrated the cytoprotective action of autophagy following ALK inactivation in ALCL. Indeed, we found that: 1) upon combined ALK and autophagy pharmacological inhibition (using crizotinib and chloroquine or 3-methyladenine), these drugs had a synergistic (and not just an additive) effect on the reduction of cell viability; 2) the molecular inactivation of autophagy using siRNA directed against ATG7 did not induce, *per se*, a loss in cell viability, as was recently highlighted by D.A. Gewirtz [68]. It is noteworthy that a potentiating effect of autophagy and ALK co-inhibition was still observed following ATG7 downregulation; 3) ALK inactivation combined with autophagy inhibition drove cells towards apoptotic/necrotic cell death;

4) combined crizotinib and chloroquine treatment strongly reduced ALK-positive Karpas-299 clonogenic survival, unequivocally proving that autophagy harbors cytoprotective functions [68], and impaired xenograft tumor growth.

Altogether, these results strongly suggest that a combination of ALK and autophagy inhibition could be beneficial for the treatment of ALK-dependent ALCL, a therapeutic combination that has never been considered before. ALK-positive ALCL patients are currently treated with aggressive chemotherapy (cyclophosphamide, hydroxydoxorubicin, oncovin and prednisone (CHOP)). The use of crizotinib for ALK-positive ALCL is currently under debate. A good response to crizotinib has been reported in a few adult patients with recurring ALK-positive ALCL, as well as in one phase I clinical trials [17, 69, 70]. Furthermore, a recent clinical study using crizotinib as a monotherapy was performed on eleven adult ALCL patients who were resistant/refractory to cytotoxic therapy [18]. Their results, showing that crizotinib exerted a potent antitumor activity with durable responses and a benign safety profile, encourage the future use of crizotinib as a front line therapy. However, ALK mutations conferring resistance to crizotinib have been identified in relapsed patients. Thus, in light of our new data we propose that crizotinib-induced autophagy, through its cytoprotective function, could allow some cells to escape the targeted therapy and survive in a dormant state, as proposed by White and DiPaola [36] and as demonstrated in models of ovarian carcinoma and gastrointestinal stromal tumors (GIST) [29, 71–73]. This dormant state may be used by tumor cells to develop and acquire resistance to crizotinib, allowing subsequent tumor recurrence. Thus, in line with previous studies on imatinib-treated CML or GIST, showing that autophagy inhibition may represent a new strategy to enhance sensitivity to tyrosine kinase inhibitors, our current work supports the concept that crizotinib resistance and subsequent ALCL tumor relapse might be prevented or diminished by blocking autophagy. Nevertheless, before considering autophagy inhibition in ALCL patient therapeutic protocols, further clinical and fundamental investigations are needed to demonstrate that cytoprotective autophagy does indeed occur in human tumors upon crizotinib treatment and to provide a better understanding of how crizotinib mechanistically triggers autophagy induction. A possible mechanism could be inhibition of the mTOR pathway, which is known to be a negative regulator of autophagy [74], and which is reported to be activated downstream of NPM-ALK [75, 76]. Further studies on hydroxychloroquine (or new improved autophagy inhibitors) are also essential to determine the dose, frequency and treatment duration that should be used in patients to achieve autophagy inhibition [52, 77, 78]. Finally, besides ALK-dependent ALCL, this study should motivate further investigation into the effects of modulating autophagy in other ALK-related malignancies that harbor either different ALK fusions or overexpressed/activated full length ALK oncogenes.

MATERIALS AND METHODS

Cell lines and cell culture conditions

Karpas-299 and SU-DHL-1 ALK-positive ALCL cell lines bearing the t(2;5)(p23;q35) translocation were obtained from DSMZ (German Collection of Microorganisms and Cell Culture, Braunschweig, Germany). The FEPD ALK-negative cell line was a gift from Dr. K. Pulford (Oxford University, Oxford, UK). Cells were cultured in Iscove's Modified Dulbecco's Medium (IMDM) supplemented with 20% Foetal Calf Serum (FCS), 2 mM L-glutamine, 1 mM sodium pyruvate, and 100 U/ml penicillin/streptomycin (all from Invitrogen (Carlsbad, CA, USA) at 37°C with 5% CO_2 and were maintained in exponential growth phase. This medium is hereafter referred to as "complete IMDM".

Chemicals

Crizotinib (Xalkori) was synthesized and purchased at @rtMolecule (Poitiers, France). Chloroquine (Aralen) (#C6628), 3-methyladenine (#M9281) and acridine orange (#318337) were purchased from Sigma-Aldrich (St. Louis, Missouri, USA). Stock solutions of crizotinib, chloroquine, acridine orange and 3-methyladenine were prepared in phosphate buffered saline (PBS).

Small interfering RNA (siRNA) transfections

SiRNA transfections were performed by electroporation using Gene Pulser Xcell Electroporation Systems (Biorad) (Hercules, CA, USA). Briefly 5.10^6 cells were electroporated at 950 µF to 250 V in 400 µl IMDM medium with 50 nM Beclin-1 siRNA, 100 nM ATG7 siRNA or 100 nM ALK siRNA from a 100 µmol/l stock solution or with the same quantity of a negative control siRNA (Eurogentec) (Seraing, Liège, Belgium). SiRNA sequences used were 5′-CAGUUUGGCACAAUCAAUATT-3′ for Beclin-1, 5′-GGAGUCACAGCUCUUCCUUTT-3′ for ATG7 and 5′-GGGCGAGCUACUAUAGAAATT–3′ for ALK. Following shock, cells were rapidly resuspended in 5 ml IMDM supplemented with 20% FCS. They were subsequently used for protein extraction, flow cytometry and viability/proliferation assays.

Detection of acidic vesicular organelles (AVOs) with acridine orange

AVOs were quantified by flow cytometry. ALK-positive (Karpas-299 and SU-DHL-1) and negative

(FEPD) cells (10^5 cells), were treated or not for 24 h with crizotinib (500 nM and 400 nM, respectively), in the presence or absence of 10 mM 3-methyladenine (3MA) (added 4 h prior to harvesting the cells), or were transfected with scramble siRNA or Beclin-1 siRNA. They were then stained for 17 min with acridine orange (AO), at a final concentration of 1 µg/ml. Cells were washed twice in PBS, then resuspended in 0.3 ml PBS and analyzed on a FACSCalibur from Beckton Dickinson, (NJ, USA) using FlowJo software.

Electron microscopy

Karpas-299 cells, treated or not for 24 h with 500 nM crizotinib, were collected, washed twice with PBS and fixed in 2% glutaraldehyde in 0.1 M Sorensen phosphate buffer (pH 7.4) for 4 h at 4°C. Cell pellets were then embedded in low melting point agarose to obtain solid blocks. These were washed overnight in 0.2 M phosphate buffer then post-fixed for 1 h at room temperature with 1% osmium tetroxide in 250 mM saccharose and 0.05 M phosphate buffer. Samples were then dehydrated in a series of graded ethanol solutions, followed by propylene oxide, and embedded in an Epon resin (Embed 812, Electron Microscopy Sciences (Hatfield, PA, USA)). Ultrathin sections (70 nm) were prepared (Ultracut Reichert Jung (Vienna, Austria)) and observed with a transmission Hitachi HT7700 electron microscope (TKY, Japan) at an accelerating voltage of 80 kV.

Immunohistochemistry

Sections from formalin-fixed and paraffin-embedded xenografted tumors were stained with hematoxylin and eosin. Immunohistochemical analysis was performed using antibodies directed against LC3b (Nanotools (Teningen, Allemagne) #0231–100; mouse mAb; clone 5F10; 1/100) and cleaved caspase 3 (R&D Systems (Minneapolis, MN, USA) #AF835; polyclonal rabbit Ab; 1/500). Karpas-299 cells, treated or not with 500 nM crizotinib for 24 h, were included in low melting agarose and then formalin-fixed and paraffin-embedded. Sections were immunostained with antibodies directed against LC3b (Nanotools) and nuclei were counterstained with hematoxylin. Antibody binding was detected with the streptavidin-biotin-peroxidase complex method (Vector Laboratories (Burlingame, CA, USA)). Pictures were taken using either a Leica DM4000B microscope (Wetzlar, Germany) or a Pannoramic 250 device (3DHISTECH) (Budapest, Hungary).

Autophagy RT-PCR array

Karpas-299 cells were treated or not for 24 h with 500 nM crizotinib, then washed once with PBS and harvested. Frozen cell pellets were sent to SABiosciences (Hilden, Germany), where both the RNA extraction and the Human Autophagy RT^2 Profiler PCR array were performed to study the expression profile of 84 key genes involved in autophagy. Amplification data (fold changes in C_t values of all the genes) were analyzed by the $\Delta\Delta C_t$ method. Data were normalized to controls (PBS-treated cells), assigned as 1.

qPCR

Briefly, 1 µg total RNA was reverse transcribed in 20 µl using the Superscript II reverse transcription kit (Invitrogen) and random hexamers (Roche), according to the manufacturer's protocol. Reverse Transcription (RT) reactions were diluted 10 fold prior to qPCR. Amplification was performed in a total volume of 10 µl containing 5 µl of a SYBR Premix Ex TaqTM (Tli RNaseH plus), Bulk master mix (Takara), 1 µl forward and reverse primers (final concentration of 300 nM each), and 2 µl diluted cDNA. The forward and reverse primers were, respectively: CCTCGCCAAGTCTCAGACGC/CCCCACCGTTGCAGTACTCC for ULK1, GAGCGCCTCTTCTCCAGCAG/CAGCCTTTGCCGGTTCAGCC for WIPI1, AAGCAGCGCCGCACCTTCGA/CGCTGACCATGCTGTGTCCG for MAP1LC3B, GGGAAGCCTTTGGCCTTGCC/CCACTTGGGCATTCCTGGGC for PIK3C3, and CAACGACCACTTTGTCAAGCT/CTCTCTTCCTCTTGTGCTCTTGC for GAPDH. Q-PCR cycling conditions were performed according to the manufacturer's protocol, using the StepOnePlus real-time PCR system (Applied Biosystems). Results were analysed with the StepOne software.

Western blotting

Cells were lyzed in radioimmunoprecipitation assay (RIPA) buffer (20 mM Tris HCl pH 7.4, 150 mM NaCl, 4 mM EDTA, 1% Triton X-100, and 0.2% SDS) supplemented with phosphatase inhibitors (1 mM Na_3VO_4, 1 mM NaF) and 1 mM phenylmethylsulfonylfluoride (PMSF), purchased from Sigma-Aldrich, and protease inhibitor cocktail (Roche Applied Science) (Penzberg, Upper Bavaria, Germany). Protein lysates were fractionated on SDS-PAGE (10 or 15%), and transferred to a nitrocellulose membrane (Whatman) (GE Healthcare, Little Chalfont, England). Western-blotting was performed using LC3-B (Sigma-Aldrich #L7543), ATG7 (Cell Signaling Technology #2631), Beclin-1 (Cell Signaling Technology #3738), ALK (D5F3 XP, Cell Signaling Technology #3633), ULK1 (Cell Signaling Technology #4773), GAPDH (Millipore MAB374) and β-actin (Santa Cruz #7210) antibodies. Proteins were visualized using the Chemiluminescent Peroxidase Substrate-3

Kit (Sigma-Aldrich) or the ECL™ Prime Western Blotting Detection Reagent (Amersham Biosciences) (Buckingshire, UK).

Cell viability assay and multiple drug effect analysis

Karpas-299 and SU-DHL-1 cells were counted and seeded in 96-well plates (10,000 cells/well, in 100 µl IMDM/20% FBS). Cells were incubated at 37°C in the presence of either increasing concentrations of crizotinib (0 to 2000 nM) or were transfected by siRNA targeting ALK; and either chloroquine (0 to 120 µM), 3-methyladenine (0.625 to 10 mM) or siRNA targeting ATG7, alone or in combination. Combination experiments were carried out at constant ratios. After 48 h, cell viability was assessed using the CellTiter 96 AQueous One Solution cell proliferation assay (Promega) (Fitchburg, Wisconsin USA). Drug combination analyses were performed following the median-effect method using the CompuSyn software (ComboSyn, Inc., Paramus, NJ, USA) [59]. Briefly, drug interactions were determined by calculating the Combination Index (CI). In this method, synergy is defined by a CI values < 1, an additive effect by CI = 1, and antagonism is defined by CI > 1. The results are shown on the Fa-CI plot where Fa represents the fraction affected by the drug tested.

Soft-agar colony formation assay

Karpas-299 cells were treated with 500 nM crizotinib and/or 30 µM chloroquine or were transfected with Atg7siRNA or scramble siRNA and allowed to recover for 8 h before treatment with 500 nM crizotinib. After 16 h, 20,000 Karpas-299 cells from each condition were resuspended in complete IMDM containing 0.33% agar onto the top of an agar underlay (complete IMDM containing 0.5% agar). Cells were fed twice a week with 400 µl complete IMDM containing the appropriate drug. After 7 days, viable cells were stained for 2 h with complete IMDM containing 3-(4,5-dimethylthiazol-2-yl)-2,5-diphenyltetrazolium bromide (MTT) (0.5 mg/ml). Four different fields were then scored from each plate and colony numbers were counted using Image J quantification software (U.S. National Institutes of Health, Bethesda, MD, USA). Experiments were carried out in triplicate.

Apoptosis measurement

Analysis of apoptosis was done using annexin V (AnnexinV-PE) and 7-amino-actinomycin (7-AAD) (BD Bioscience #559763) staining according to standard protocols, followed by flow cytometry using a FACSCalibur cytometer from Beckton Dickinson. Results were analyzed using FlowJo software.

Murine xenograft model

Mice were housed under specific pathogen-free conditions in an animal room at a constant temperature (20–22°C), with a 12 h/12 h light/dark cycle and free access to food and water. All animal procedures were performed following the principle guidelines of INSERM, and our protocol was approved by the Midi-Pyrénées Ethics Committee on Animal Experimentation. A total of 4.10^6 Karpas-299 cells were injected subcutaneously into both flanks of 6-week old female non-obese diabetic-severe combined immunodeficient (NOD-SCID) mice (Janvier Labs) (Laval, France). Mouse body weight and tumor volumes were measured three times a week (once a day at the end of the experiment) with calipers, using the formula "length × width^2 × π/6". Mice (4 per group) were treated 5 times per week (monday through friday) once the tumor volume reached 100 mm^3. Mice received crizotinib (10 mg/kg) or H_2O orally, and chloroquine (60 mg/kg) or PBS by intraperitoneal injection. At the end of the experiment, mice were humanely sacrificed. Subcutaneous tumors and adjacent inguinal lymph nodes were harvested and sections were fixed in 10% neutral buffered formalin for immunohistochemical analysis.

Active cleaved caspase 3-positive cell quantification

Immunohistochemical-stained slides were digitized using a Pannoramic 250 Flash digital microscope (P250 Flash, 3DHISTECH). Whole slides were scanned using brightfield scan mode with a 20X/NA0.80 Zeiss Plan-Apochromat dry objective (Zeiss) (Oberkochen, Germany), and images were acquired with a two megapixel 3CCD color camera (CIS Cam Ref #VCC-FC60FR19CL, CIS Americas Inc., Tokyo, Japan), achieving a 0.39 µm/pixel resolution. Pannoramic Viewer and HistoQuant software were used for viewing and analyzing the digital slides, respectively (RTM 1.15.3, 3DHISTECH). A minimum of 8 annotations per slide covering 50% of the entire tissue were analyzed using the same profile with the following characteristics: noise reduction (median filter strength = 0), object definition (HSV: 137 < Hue < 226, 26 < Saturation < 189, 17 < Value < 41), no filtering by size and no object separation. These settings allowed the automatic segmentation of the detected objects and the measurement of the number of detected objects per mm^2.

Statistical analyses

Results are presented as mean values ± standard deviations (SD) from at least 3 independent experiments unless otherwise indicated. Determination of statistical significance was performed using the Student's *t*-test

for side by side comparison of two conditions. Welsch's correction was applied when variances were significantly different. For the experiments comparing more than two conditions, determination of statistical significance was performed using one-way ANOVA followed by a Newman-Keuls multiple comparison test. Xenografted tumor growths were expressed as the mean ± S.E.M.. Statistical analyses were performed using the two-way analysis of variance (ANOVA) followed by the Bonferroni test using GraphPad Prism 5 software (GraphPad software) (La Jolla, CA, USA). For all tests, *p*-values less than 0.05 (*), 0.01 (**) or 0.001 (***) were considered statistically significant.

ACKNOWLEDGMENTS

We thank Dr Carine Joffre, Dr Stéphane Manenti, Dr Christian Touriol and Camille Daugrois at the UMR1037, CRCT, for critical reading and helpful discussions; Dr Etienne Chatelut at the IUCT Oncopole, for pharmacological advice; Fatima L'Faqihi and Valérie Dupan at the flow cytometry facility of INSERM UMR1043, Toulouse; Florence Capilla and Christine Salon at the histology facility of INSERM/UPS-US006/CREFRE; Manon Farcé at the flow cytometry facility at the UMR1037, CRCT; Isabelle Fourquaux and Bruno Payré at the "Centre de Microscopie Electronique Appliquée à la Biologie" (CMEAB), Université Paul Sabatier, Toulouse; and Jeannine Boyes at the UMR1037, CRCT, for their excellent technical assistance. S.G. dedicates this work to the memory of Mme Louise Attali-Guedj.

FUNDING

This work was supported by funding from the National Research Agency-Young Researcher (ANR-JCJC) (R12004BB), the French local league against cancer (R12020BB) and the Fondation ARC (R15002BB), awarded to S.G.; and fellowships from ANR to G.M. and from the French league against cancer (LNCC) to J.F.. This work was supported by the Institut Universitaire de France (IUF) and the LABEX TOUCAN.

CONFLICTS OF INTEREST

The authors declare that there is no conflict of interest.

Authorship contributions

G.M. and J.F. designed and performed experiments, analyzed data and contributed to writing the manuscript. S.L.G. helped design and performed experiments, analyzed data and contributed to writing the manuscript. A.D. and T.A. performed experiments and analyzed data. L.L., F.M., E.E. and P.B. participated in discussions. I.B. and P.C. helped design experiments and contributed to writing the manuscript. S.G. designed and performed experiments, analyzed data and wrote the manuscript.

REFERENCES

1. Campo E, Swerdlow SH, Harris NL, Pileri S, Stein H, Jaffe ES. The 2008 WHO classification of lymphoid neoplasms and beyond: evolving concepts and practical applications. Blood. 2011; 117:5019–32.
2. Delsol G. The WHO lymphoma classification. Ann Pathol. 2008; 28:S20–4.
3. Morris SW, Kirstein MN, Valentine MB, Dittmer KG, Shapiro DN, Saltman DL, Look AT. Fusion of a kinase gene, ALK, to a nucleolar protein gene, NPM, in non-Hodgkin's lymphoma. Science (80-.). 1994; 263:1281–4.
4. Chiarle R, Voena C, Ambrogio C, Piva R, Inghirami G. The anaplastic lymphoma kinase in the pathogenesis of cancer. Nat Rev Cancer. 2008; 8:11–23.
5. Gorczynski A, Prelowska M, Adam P, Czapiewski P, Biernat W. ALK-positive cancer: still a growing entity. Futur. Oncol. 2014; 10:305–21.
6. Hallberg B, Palmer RH. Mechanistic insight into ALK receptor tyrosine kinase in human cancer biology. Nat Rev Cancer. 2013; 13:685–700.
7. Giuriato S, Foisseau M, Dejean E, Felsher DW, Al Saati T, Demur C, Ragab A, Kruczynski A, Schiff C, Delsol G, Meggetto F. Conditional TPM3-ALK and NPM-ALK transgenic mice develop reversible ALK-positive early B-cell lymphoma/leukemia. Blood. 2010; 115:4061–70.
8. Turner SD, Alexander DR. What have we learnt from mouse models of NPM-ALK-induced lymphomagenesis? Leukemia. 2005; 19:1128–34.
9. Giuriato S, Turner SD. Twenty years of modelling NPM-ALK-induced lymphomagenesis. Front Biosci (Schol Ed). 2015; 7:236–47.
10. Tabbo F, Barreca A, Piva R, Inghirami G. ALK Signaling and Target Therapy in Anaplastic Large Cell Lymphoma. Front Oncol. 2012; 2:41.
11. Cheng M, Quail MR, Gingrich DE, Ott GR, Lu L, Wan W, Albom MS, Angeles TS, Aimone LD, Cristofani F, Machiorlatti R, Abele C, Ator MA, et al. CEP-28122, a highly potent and selective orally active inhibitor of anaplastic lymphoma kinase with antitumor activity in experimental models of human cancers. Mol Cancer Ther. 2012; 11:670–9.
12. George SK, Vishwamitra D, Manshouri R, Shi P, Amin HM. The ALK inhibitor ASP3026 eradicates NPM-ALK(+) T-cell anaplastic large-cell lymphoma *in vitro* and in a systemic xenograft lymphoma model. Oncotarget. 2014; 5:5750–63.

13. Kruczynski A, Delsol G, Laurent C, Brousset P, Lamant L. Anaplastic lymphoma kinase as a therapeutic target. Expert Opin Ther Targets. 2012; 16:1127–38.
14. Marzec M, Kasprzycka M, Ptasznik A, Wlodarski P, Zhang Q, Odum N, Wasik MA. Inhibition of ALK enzymatic activity in T-cell lymphoma cells induces apoptosis and suppresses proliferation and STAT3 phosphorylation independently of Jak3. Lab Invest. 2005; 85:1544–54.
15. Christensen JG, Zou HY, Arango ME, Li Q, Lee JH, McDonnell SR, Yamazaki S, Alton GR, Mroczkowski B, Los G. Cytoreductive antitumor activity of PF-2341066, a novel inhibitor of anaplastic lymphoma kinase and c-Met, in experimental models of anaplastic large-cell lymphoma. Mol Cancer Ther. 2007; 6:3314–22.
16. Butrynski JE, D'Adamo DR, Hornick JL, Dal Cin P, Antonescu CR, Jhanwar SC, Ladanyi M, Capelletti M, Rodig SJ, Ramaiya N, Kwak EL, Clark JW, Wilner KD, et al. Crizotinib in ALK-rearranged inflammatory myofibroblastic tumor. N Engl J Med. 2010; 363:1727–33.
17. Mosse YP, Lim MS, Voss SD, Wilner K, Ruffner K, Laliberte J, Rolland D, Balis FM, Maris JM, Weigel BJ, Ingle AM, Ahern C, Adamson PC, et al. Safety and activity of crizotinib for paediatric patients with refractory solid tumours or anaplastic large-cell lymphoma: a Children's Oncology Group phase 1 consortium study. Lancet Oncol. 2013; 14:472–80.
18. Gambacorti Passerini C, Farina F, Stasia A, Redaelli S, Ceccon M, Mologni L, Messa C, Guerra L, Giudici G, Sala E, Mussolin L, Deeren D, King MH, et al. Crizotinib in advanced, chemoresistant anaplastic lymphoma kinase-positive lymphoma patients. J Natl Cancer Inst. 2014; 106:djt378.
19. Choi YL, Soda M, Yamashita Y, Ueno T, Takashima J, Nakajima T, Yatabe Y, Takeuchi K, Hamada T, Haruta H, Ishikawa Y, Kimura H, Mitsudomi T, et al. EML4-ALK mutations in lung cancer that confer resistance to ALK inhibitors. N Engl J Med. 2010; 363:1734–9.
20. Doebele RC, Pilling AB, Aisner DL, Kutateladze TG, Le AT, Weickhardt AJ, Kondo KL, Linderman DJ, Heasley LE, Franklin WA, Varella-Garcia M, Camidge DR. Mechanisms of resistance to crizotinib in patients with ALK gene rearranged non-small cell lung cancer. Clin Cancer Res. 2012; 18:1472–82.
21. Katayama R, Shaw AT, Khan TM, Mino-Kenudson M, Solomon BJ, Halmos B, Jessop NA, Wain JC, Yeo AT, Benes C, Drew L, Saeh JC, Crosby K, et al. Mechanisms of acquired crizotinib resistance in ALK-rearranged lung Cancers. Sci Transl Med. 2012; 4:120ra17.
22. Sasaki T, Koivunen J, Ogino A, Yanagita M, Nikiforow S, Zheng W, Lathan C, Marcoux JP, Du J, Okuda K, Capelletti M, Shimamura T, Ercan D, et al. A novel ALK secondary mutation and EGFR signaling cause resistance to ALK kinase inhibitors. Cancer Res. 2011; 71:6051–60.
23. Laimer D, Dolznig H, Kollmann K, Vesely PW, Schlederer M, Merkel O, Schiefer AI, Hassler MR, Heider S, Amenitsch L, Thallinger C, Staber PB, Simonitsch-Klupp I, et al. PDGFR blockade is a rational and effective therapy for NPM-ALK-driven lymphomas. Nat Med. 2012; 18:1699–704.
24. Voena C, Chiarle R. The battle against ALK resistance: successes and setbacks. Expert Opin Investig Drugs. 2012; 21:1751–4.
25. Foyil K V, Kennedy DA, Grove LE, Bartlett NL, Cashen AF. Extended retreatment with brentuximab vedotin (SGN-35) maintains complete remission in patient with recurrent systemic anaplastic large-cell lymphoma. Leuk Lymphoma. 2012; 53:506–7.
26. Sequist L V, Gettinger S, Senzer NN, Martins RG, Janne PA, Lilenbaum R, Gray JE, Iafrate AJ, Katayama R, Hafeez N, Sweeney J, Walker JR, Fritz C, et al. Activity of IPI-504, a novel heat-shock protein 90 inhibitor, in patients with molecularly defined non-small-cell lung cancer. J Clin Oncol. 2010; 28:4953–60.
27. Bellodi C, Lidonnici MR, Hamilton A, Helgason G V, Soliera AR, Ronchetti M, Galavotti S, Young KW, Selmi T, Yacobi R, Van Etten RA, Donato N, Hunter A, et al. Targeting autophagy potentiates tyrosine kinase inhibitor-induced cell death in Philadelphia chromosome-positive cells, including primary CML stem cells. J Clin Invest. 2009; 119:1109–23.
28. Calabretta B, Salomoni P. Inhibition of autophagy: a new strategy to enhance sensitivity of chronic myeloid leukemia stem cells to tyrosine kinase inhibitors. Leuk Lymphoma. 2011; 52:54–9.
29. Gupta A, Roy S, Lazar AJ, Wang WL, McAuliffe JC, Reynoso D, McMahon J, Taguchi T, Floris G, Debiec-Rychter M, Schoffski P, Trent JA, Debnath J, et al. Autophagy inhibition and antimalarials promote cell death in gastrointestinal stromal tumor (GIST). Proc Natl Acad Sci U S A. 2010; 107:14333–8.
30. Mishima Y, Terui Y, Mishima Y, Taniyama A, Kuniyoshi R, Takizawa T, Kimura S, Ozawa K, Hatake K. Autophagy and autophagic cell death are next targets for elimination of the resistance to tyrosine kinase inhibitors. Cancer Sci. 2008; 99:2200–8.
31. Levine B, Klionsky DJ. Development by self-digestion: molecular mechanisms and biological functions of autophagy. Dev Cell. 2004; 6:463–77.
32. Mizushima N, Yoshimori T, Ohsumi Y. The role of Atg proteins in autophagosome formation. Annu Rev Cell Dev Biol. 2011; 27:107–32.
33. Rubinsztein DC, Shpilka T, Elazar Z. Mechanisms of autophagosome biogenesis. Curr Biol. 2012; 22:R29–34.
34. Lamb CA, Yoshimori T, Tooze SA. The autophagosome: origins unknown, biogenesis complex. Nat Rev Mol Cell Biol. 2013; 14:759–74.
35. Beau I, Mehrpour M, Codogno P. Autophagosomes and human diseases. Int J Biochem Cell Biol. 2011; 43:460–4.
36. White E, DiPaola RS. The double-edged sword of autophagy modulation in cancer. Clin Cancer Res. 2009; 15:5308–16.

37. Rosenfeldt MT, Ryan KM. The role of autophagy in tumour development and cancer therapy. Expert Rev Mol Med. 2009; 11:e36.
38. Lorin S, Hamai A, Mehrpour M, Codogno P. Autophagy regulation and its role in cancer. Semin Cancer Biol. 2013; 23:361–79.
39. Galluzzi L, Pietrocola F, Bravo-San Pedro JM, Amaravadi RK, Baehrecke EH, Cecconi F, Codogno P, Debnath J, Gewirtz DA, Karantza V, Kimmelman A, Kumar S, Levine B, et al. Autophagy in malignant transformation and cancer progression. EMBO, J. 2015; 23:34:856–80.
40. Mathew R, Kongara S, Beaudoin B, Karp CM, Bray K, Degenhardt K, Chen G, Jin S, White E. Autophagy suppresses tumor progression by limiting chromosomal instability. Genes Dev. 2007; 21:1367–81.
41. Jin S, White E. Role of autophagy in cancer: management of metabolic stress. Autophagy. 2007; 3:28–31.
42. Isakson P, Bjoras M, Boe SO, Simonsen A. Autophagy contributes to therapy-induced degradation of the PML/RARA oncoprotein. Blood. 2010; 116:2324–31.
43. Goussetis DJ, Gounaris E, Wu EJ, Vakana E, Sharma B, Bogyo M, Altman JK, Platanias LC. Autophagic degradation of the BCR-ABL oncoprotein and generation of antileukemic responses by arsenic trioxide. Blood. 2012; 120:3555–62.
44. Grander D, Kharaziha P, Laane E, Pokrovskaja K, Panaretakis T. Autophagy as the main means of cytotoxicity by glucocorticoids in hematological malignancies. Autophagy. 2009; 5:1198–200.
45. Puissant A, Robert G, Fenouille N, Luciano F, Cassuto JP, Raynaud S, Auberger P. Resveratrol promotes autophagic cell death in chronic myelogenous leukemia cells via JNK-mediated p62/SQSTM1 expression and AMPK activation. Cancer Res. 2010; 70:1042–52.
46. Salazar M, Carracedo A, Salanueva IJ, Hernandez-Tiedra S, Lorente M, Egia A, Vazquez P, Blazquez C, Torres S, Garcia S, Nowak J, Fimia GM, Piacentini M, et al. Cannabinoid action induces autophagy-mediated cell death through stimulation of ER stress in human glioma cells. J Clin Invest. 2009; 119:1359–72.
47. Michaud M, Martins I, Sukkurwala AQ, Adjemian S, Ma Y, Pellegatti P, Shen S, Kepp O, Scoazec M, Mignot G, Rello-Varona S, Tailler M, Menger L, et al. Autophagy-dependent anticancer immune responses induced by chemotherapeutic agents in mice. Science. 2011; 334:1573–7.
48. Lomonaco SL, Finniss S, Xiang C, Decarvalho A, Umansky F, Kalkanis SN, Mikkelsen T, Brodie C. The induction of autophagy by gamma-radiation contributes to the radioresistance of glioma stem cells. Int J Cancer. 2009; 125:717–22.
49. Torgersen ML, Engedal N, Boe SO, Hokland P, Simonsen A. Targeting autophagy potentiates the apoptotic effect of histone deacetylase inhibitors in t(8;21) AML cells. Blood. 2013; 122:2467–76.
50. White E. Deconvoluting the context-dependent role for autophagy in cancer. Nat Rev Cancer. 2012; 12:401–10.
51. Levy JM, Thorburn A. Targeting autophagy during cancer therapy to improve clinical outcomes. Pharmacol Ther. 2011; 131:130–41.
52. Mancias JD, Kimmelman AC. Targeting autophagy addiction in cancer. Oncotarget. 2011; 2:1302–6.
53. Paglin S, Hollister T, Delohery T, Hackett N, McMahill M, Sphicas E, Domingo D, Yahalom J. A novel response of cancer cells to radiation involves autophagy and formation of acidic vesicles. Cancer Res. 2001; 61:439–44.
54. Eskelinen EL. Maturation of autophagic vacuoles in Mammalian cells. Autophagy. 2005; 1:1–10.
55. Ladoire S, Chaba K, Martins I, Sukkurwala AQ, Adjemian S, Michaud M, Poirier-Colame V, Andreiuolo F, Galluzzi L, White E, Rosenfeldt M, Ryan KM, Zitvogel L, et al. Immunohistochemical detection of cytoplasmic LC3 puncta in human cancer specimens. Autophagy. 2012; 8:1175–84.
56. Yang Z, Klionsky DJ. An overview of the molecular mechanism of autophagy. Curr Top Microbiol Immunol. 2009; 335:1–32.
57. Tanida I, Minematsu-Ikeguchi N, Ueno T, Kominami E. Lysosomal turnover, but not a cellular level, of endogenous LC3 is a marker for autophagy. Autophagy. 2005; 1:84–91.
58. Mizushima N, Yoshimori T, Levine B. Methods in mammalian autophagy research. Cell. 2010; 140:313–26.
59. Chou TC, Talalay P. Quantitative analysis of dose-effect relationships: the combined effects of multiple drugs or enzyme inhibitors. Adv Enzym. Regul. 1984; 22:27–55.
60. Chou TC. Theoretical basis, experimental design, and computerized simulation of synergism and antagonism in drug combination studies. Pharmacol Rev. 2006; 58:621–81.
61. Wu YT, Tan HL, Shui G, Bauvy C, Huang Q, Wenk MR, Ong CN, Codogno P, Shen HM. Dual role of 3-methyladenine in modulation of autophagy via different temporal patterns of inhibition on class I and III phosphoinositide 3-kinase. J. Biol. Chem. 2010; 285:10850–61.
62. Maycotte P, Aryal S, Cummings CT, Thorburn J, Morgan MJ, Thorburn A. Chloroquine sensitizes breast cancer cells to chemotherapy independent of autophagy. Autophagy. 2012; 8:200–12.
63. Maes H, Kuchnio A, Peric A, Moens S, Nys K, De Bock K, Quaegebeur A, Schoors S, Georgiadou M, Wouters J, Vinckier S, Vankelecom H, Garmyn M, et al. Tumor vessel normalization by chloroquine independent of autophagy. Cancer Cell. 2014; 26:190–206.
64. Lorente M, Torres S, Salazar M, Carracedo A, Hernandez-Tiedra S, Rodriguez-Fornes F, Garcia-Taboada E, Melendez B, Mollejo M, Campos-Martin Y,

Lakatosh SA, Barcia J, Guzman M, et al. Stimulation of the midkine/ALK axis renders glioma cells resistant to cannabinoid antitumoral action. Cell Death Differ. 2011; 18:959–73.

65. Ji C, Zhang L, Cheng Y, Patel R, Wu H, Zhang Y, Wang M, Ji S, Belani CP, Yang JM, Ren X. Induction of autophagy contributes to crizotinib resistance in ALK-positive lung cancer. Cancer Biol Ther. 2014; 15.

66. Lovly CM, Heuckmann JM, de Stanchina E, Chen H, Thomas RK, Liang C, Pao W. Insights into ALK-driven cancers revealed through development of novel ALK tyrosine kinase inhibitors. Cancer Res. 2011; 71:4920–31.

67. Sang J, Acquaviva J, Friedland JC, Smith DL, Sequeira M, Zhang C, Jiang Q, Xue L, Lovly CM, Jimenez JP, Shaw AT, Doebele RC, He S, et al. Targeted inhibition of the molecular chaperone Hsp90 overcomes ALK inhibitor resistance in non-small cell lung cancer. Cancer Discov. 2013; 3:430–43.

68. Gewirtz DA. When cytoprotective autophagy isn't... and even when it is. Autophagy. 2014; 10.

69. Foyil K V, Bartlett NL. Brentuximab vedotin and crizotinib in anaplastic large-cell lymphoma. Cancer J. 2012; 18:450–6.

70. Gambacorti-Passerini C, Messa C, Pogliani EM. Crizotinib in anaplastic large-cell lymphoma. N Engl J Med. 2010; 364:775–6.

71. Lu Z, Luo RZ, Lu Y, Zhang X, Yu Q, Khare S, Kondo S, Kondo Y, Yu Y, Mills GB, Liao WS, Bast RC Jr. The tumor suppressor gene ARHI regulates autophagy and tumor dormancy in human ovarian cancer cells. J Clin Invest. 2008; 118:3917–29.

72. Rubin BP, Debnath J. Therapeutic implications of autophagy-mediated cell survival in gastrointestinal stromal tumor after treatment with imatinib mesylate. Autophagy. 2010; 6:1190–1.

73. Sosa MS, Bragado P, Debnath J, Aguirre-Ghiso JA. Regulation of tumor cell dormancy by tissue microenvironments and autophagy. Adv Exp Med Biol. 2013; 734:73–89.

74. Jung CH, Ro SH, Cao J, Otto NM, Kim DH. mTOR regulation of autophagy. FEBS Lett. 2010; 584:1287–95.

75. Vega F, Medeiros LJ, Leventaki V, Atwell C, Cho-Vega JH, Tian L, Claret FX, Rassidakis GZ. Activation of mammalian target of rapamycin signaling pathway contributes to tumor cell survival in anaplastic lymphoma kinase-positive anaplastic large cell lymphoma. Cancer Res. 2006; 66:6589–97.

76. Marzec M, Kasprzycka M, Liu X, El-Salem M, Halasa K, Raghunath PN, Bucki R, Wlodarski P, Wasik MA. Oncogenic tyrosine kinase NPM/ALK induces activation of the rapamycin-sensitive mTOR signaling pathway. Oncogene. 2007; 26:5606–14.

77. Poklepovic A, Gewirtz DA. Outcome of early clinical trials of the combination of hydroxychloroquine with chemotherapy in cancer. Autophagy. 2014; 10.

78. Garber K. Inducing indigestion: companies embrace autophagy inhibitors. J Natl Cancer Inst. 2011; 103:708–10.

RÉSUMÉ

Au cours de mon doctorat (Toulouse, 1996-1999, INSERM U326, Dir : Dr B. Payrastre) et de mon premier stage post-doctoral (Bruxelles, 1999-2001, IRIBHM, Dir : Dr C. Erneux), j'ai acquis une expertise dans le domaine de la signalisation cellulaire, en particulier dans la régulation du métabolisme des phosphoinositides, dans deux modèles cellulaires hématopoïétiques (plaquette sanguine humaine et lignée de leucémie myéloïde chronique). Mes travaux dans ces deux laboratoires ont porté sur le rôle des enzymes SHIP1 et SHIP2, deux inositol 5-phosphatases, impliquées dans la dégradation du second messager lipidique PI(3,4,5)P_3 en PI(3,4)P_2. Mes travaux de thèse ont montré que SHIP1 et SHIP2 participaient activement à la signalisation plaquettaire induite par la thrombine en permettant une nouvelle voie de biosynthèse du PI(3,4)P_2. Puis mes travaux de post-doctorat ont démontré les propriétés anti-tumorales de la protéine SHIP2 lors de sa surexpression dans la lignée cellulaire K562, du fait de sa capacité, commune avec le suppresseur de tumeur PTEN, à hydrolyser le PI(3,4,5)P_3.

Mon intérêt croissant pour les mécanismes d'oncogenèse a alors motivé un second stage post-doctoral (Stanford, 2001-2004, CCSR, Dir : Dr D. Felsher) dans un laboratoire spécialisé dans l'étude des mécanismes d' « addiction oncogénique », de par l'utilisation de différents modèles murins conditionnels de tumorigenèse. Mes travaux ont mis en évidence : (i) le rôle clé du microenvironnement tumoral, et notamment de l'angiogenèse, dans la survenue de rechutes tumorales après inactivation de l'oncogène MYC dans un modèle de lymphome dépendant de cet oncogène ; (ii) l'efficacité de la combinaison thérapeutique : inactivation de l'oncogène MYC et blocage de l'angiogenèse en terme de prévention de ces rechutes.

À mon retour en France (Toulouse, 2004-2008, INSERM U563, Dir : Pr G. Delsol), j'ai mis à profit mon expérience américaine pour développer et caractériser des modèles cellulaires et murins conditionnels pour l'expression de l'oncogène ALK (pour Anaplastic Lymphoma Kinase), ceci afin de compléter la grande spécialisation de mon laboratoire d'accueil sur l'étude des lymphomes anaplasiques à grandes cellules (LAGC) ALK positifs.

Depuis mon recrutement à l'INSERM, en 2008, en tant que CR1, j'ai utilisé ces modèles cellulaires et animaux pour démontrer (i) que ces lymphomes ALK-positif présentent une addiction pour l'oncogène ALK ; (ii) que l'angiogenèse, et notamment le VEGF (régulé en partie par le microARN 16), participe au développement tumoral et représente donc une cible thérapeutique potentielle; et enfin (iii), que l'inhibition de l'autophagie cytoprotectrice, activée sous traitement Crizotinib, améliorait l'efficacité des thérapies ciblant l'oncogène ALK.

Les projets de recherche que je souhaite développer aujourd'hui s'articulent autour de deux mots-clefs : les lymphomes anaplasiques à grandes cellules ALK-positif et l'autophagie. Ils se subdivisent en trois grands axes de recherche : (i) le rôle, (ii) la régulation et (iii) la modulation thérapeutique de l'autophagie dans ces lymphomes ALK positif. Le premier axe consiste à définir le rôle cytoprotecteur ou cytotoxique de l'autophagie sous diverses thérapies ou combinaisons thérapeutiques actuellement proposées pour améliorer le traitement des patients; le second vise à identifier les mécanismes de régulation post-transcriptionnelle de l'autophagie (notamment via les microARNs) ; et le troisième porte sur le développement d'une nouvelle formulation vaccinale anti-ALK, à base d'autophagosomes, pour compléter les thérapies ciblant l'oncogène ALK, et prévenir, sur le long terme, l'apparition de rechutes tumorales.